5th FISC

SECTION 4

TRANSPORTATION AND DEPOSITION

Page

PREDICTING DEPOSITION PATTERNS IN SMALL BASINS --
D. Michael Gee..... 4-1
BEDLOAD SHOALS IN A DEEP-DRAFT NAVIGATION CHANNEL --
Karl W. Eriksen and Fong J. Grey..... 4-8
RESPONSE OF LOWER MISSISSIPPI RIVER LOW-FLOW STAGES --
Charles M. Elliott, Robert E. Rentschler and John H. Brooks..... 4-16
EXAMINATION OF RED RIVER DYNAMIC LOOP RATING CURVE --
Phil G. Combs..... 4-24
DELTAIC DEPOSITION IN THE ATCHAFALAYA BASIN --
Billy J. Garrett and Nancy Powell..... 4-32
DENDROGEOMORPHIC ANALYSIS OF WETLAND SEDIMENTATION --
Cliff R. Hupp and David E. Bazemore..... 4-40
BOTTOMLAND SEDIMENTATION NEAR HIGHWAY CROSSINGS --
David E. Bazemore and Cliff R. Hupp..... 4-48
FLOW AND SEDIMENT TRANSPORT IN ROUGH CHANNELS --
Jonathan M. Nelson, William W. Emmett and J. Dungan Smith..... 4-55
LOW-FLOW SEDIMENT TRANSPORT IN THE COLORADO RIVER --
J. R. Grey, R. H. Webb and D. W. Hyndman..... 4-63
CONSTRUCTION EFFECTS ON SEDIMENT FOR TWO BASINS IN PUERTO RICO --
Allen Gellis..... 4-72
SEDIMENT TRANSPORT IN THE LOWER MISSISSIPPI RIVER, 1983-1985 --
Charles R. Demas, D. K. Demchek and P. B. Curwick..... 4-79
SEDIMENT DEPOSITION IN A FIXED BED CHANNEL --
Yeemeng Chiew..... 4-87
PREDICTION OF BEDLOAD IN SANDBED CHANNELS --
K. Mahmood and M. H. Mehrdad..... 4-94
DEPOSITION ON REVETMENTS ALONG THE SACRAMENTO RIVER, CA --
Karin J. Fischer, M. D. Harvey and D. B. Pridal..... 4-102
SIZE DISTRIBUTION OF NONUNIFORM BED MATERIAL IN TRANSPORT --
Chih Ted Yang and Shenggan Wan..... 4-109
CASE HISTORY: CHANNEL AGGRADATION ABOVE A RESERVOIR --
Christopher A. Gorbach and Drew C. Baird..... 4-115
MODELING SETTLING BASIN DEPOSITION AND SLUICING --
Ernest L. Pemberton and Curtis J. Orvis..... 4-123
SAND TRANSPORT IN GOODWIN CREEK --
Joe C. Willis..... 4-131
BED LOAD TRANSPORT ON TWO SMALL STREAMS --
Roger A. Kuhnle..... 4-139
SEDIMENT TRACING IN STEP POOL IN GRANITE STREAMS IN IDAHO --
Gary Ketcheson and Walter F. Megahan..... 4-147
SEDIMENT TRANSPORT IN HEADWATER CHANNELS IN IDAHO --
Kent R. Johnejack and Walter F. Megahan..... 4-155
TRANSPORT OF UNIFORM AND NON-UNIFORM SEDIMENT SIZES --
Hsieh-Wen Shen and Chris Xudong Rao..... 4-162

Page

METHODS OF MEASURING INCIPIENT MOTION OF BED LOAD IN MOUNTAIN RIVERS --
Wojciech Bartnik..... 4-170
POSTFIRE SUSPENDED SEDIMENT IN YELLOWSTONE PARK --
Jana Mohrman and Roy Ewing..... 4-175
MOVEMENT OF BED MATERIAL CLASTS IN MOUNTAIN STREAMS --
Luna B. Leopold and David C. Rosgen..... 4-183

PREDICTING DEPOSITION PATTERNS IN SMALL BASINS

By D. Michael Gee, Research Hydraulic Engineer, Hydrologic Engineering Center, Davis, CA.

ABSTRACT

A technique for estimating sediment depositional patterns based upon flow patterns is described. Flow patterns are computed using a finite element model for two-dimensional, vertically averaged flow. Once the velocity and depth fields are computed, the bed shear stress distribution can be found. If the annual volume and approximate particle size of the inflowing load is known, anticipated depositional locations and quantities can then be estimated. Use of this technique to forecast the temporal development of the deposits by computing the velocity fields for several steady flow conditions is described. The resulting graphical displays of velocity fields and shear stress contours are very useful to the design engineer. This procedure avoids the complexity associated with use of a two-dimensional sediment transport and dispersion model. Application of the technique to the design of a basin 180 ft. (55 m.) wide by 610 ft. (186 m.) long is described.

INTRODUCTION

Conventional sediment basin design procedures rely on volumetric relationships to determine flow through times, estimated trap efficiency, and average annual deposition rates. Design guidance has been prepared by USACE (1989). These approaches do not necessarily reflect the interaction between changes in bed topography due to scour and/or deposition and the influence of these changes on velocity and shear stress distributions. Some designs have been approached using one-dimensional numerical modeling of flow and sediment such as HEC-6 (USACE-HEC, 1990). Some concerns with these approaches are that complex velocity patterns such as recirculation and short circuiting may not be properly described. These flow patterns may result in uneven distributions of sediment concentration and, therefore, an uneven distribution of sediment deposits (Montgomery, et al. 1983). The use of a fully two-dimensional model for both flow and sediment distribution such as TABS-2 (McAnally et al. 1984) is an attractive approach to improve the prediction of the distribution of sediment deposits. The use of such a model, however, may involve more effort and data acquisition than can be justified for small basin design. The technique described herein represents a midway approach that includes the velocity and shear stress fields in detail, from which the sediment deposition distribution and rates can be inferred. A brief description of this approach was presented by Deering and Larock (1989).

MODEL SELECTION

It is assumed that the salient flow features of small basins can be described in the two horizontal directions and that the variance of velocity in the vertical is the traditional logarithmic velocity distribution for turbulent flow in open channels (French 1985). A widely used model that is suitable for this condition is RMA-2 (King & Norton 1978). RMA-2 has been applied to a wide variety of problems including floodplain analysis (Gee et al. 1990), marsh flooding (MacArthur et al. 1990), sediment basin design (Deering & Larock 1989), has been adapted for bridge design (FHWA 1989), and serves as the hydrodynamic module of the TABS-2 system (McAnally et al. 1984). This model solves the depth integrated Reynolds equations for two-dimensional free-surface flow in the horizontal plane using the finite element method for both steady and unsteady flows. The finite element formulation of RMA-2 allows boundary roughness and geometric resolution to vary spatially to accurately depict topography. It also provides a wide variety of boundary conditions. Wetting and drying of portions of the solution domain is allowed. The two-dimensional approach relieves the engineer from having to construct cross sections that are perpendicular to the flow for all flows, as is required in a one-dimensional analysis.

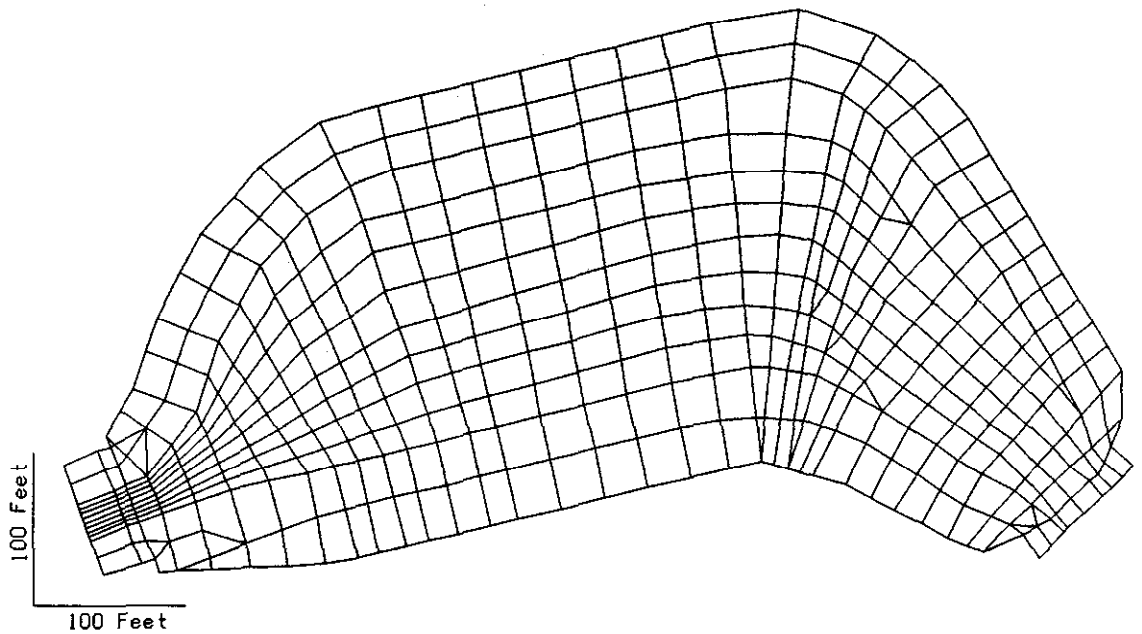

Figure 1. Example Finite Element Mesh, Wildcat Creek Basin.

APPROACH

An example finite element mesh is shown in Fig. 1. Note that the elements are both quadrilateral and triangular. Computational nodes exist at the corners and mid-sides of each element. The bottom elevation is given at each corner node and linearly interpolated for the mid-side nodes. Bed roughness and turbulent exchange coefficients are assigned to groups of elements (not necessarily neighbors) by the user. Solution of the two-dimensional flow equations provides the x- and y-components of the velocity, and the depth, at each computational node. The local shear stress can be calculated from these variables if one assumes that the relation for average shear in a cross section can be applied locally as follows.

$$\tau = \gamma RS \tag{1}$$

Where τ is the bed shear stress, γ is the unit weight of water, R is the hydraulic radius (taken here as the local nodal depth) and S is the friction slope. Now, rewriting Manning's equation in terms of S, we have:

$$S = \frac{n^2u^2}{2.22R^{4/3}} \tag{2}$$

Where u is the resultant of the calculated x and y nodal velocity components, as shown in equation (3) and n is Manning's roughness coefficient.

$$u^2 = u_x^2 + u_y^2 \tag{3}$$

Combining, we can solve for the shear stress:

$$\tau = \gamma \frac{n^2 u^2}{2.22 R^{1/3}} \tag{4}$$

One must now relate the n-values, which are associated with elements, with the computed values for u and R (depth) which are located at nodes. For this study, the n-value associated with a node was computed as the arithmetic average of the n-values for all elements connected to that node. We have placed these computations in the vector plotting program (VECTOR) which is a post-processor for RMA-2. VECTOR also prepares files of water surface elevation and velocity magnitude for contouring.

AN EXAMPLE

Introduction

The Wildcat Creek sediment basin was designed to trap sediment that potentially could cause excess scour or deposition in a downstream flood control channel. Right-of-way considerations and environmental concerns dictated the bent alignment shown in Fig. 1 (flow is from right to left). Based on cross section average velocity and settling lengths computed from the particle fall velocity, it was estimated that the basin would trap 100% of the sediment larger than fine sand (0.125 mm). A hydrodynamic analysis was performed to ascertain whether the bent alignment would indeed trap the size range and volume of sediment needed and whether high velocities would impinge on the banks requiring some form of bank protection.

Sediment Basin Description

The Wildcat Creek sediment basin was designed to have a maximum width of 180 ft. (55 m.) and length of 610 ft. (186 m.). The bottom slope is 0.0005 and the side slopes 1V:3H. The maximum depth is about 12 ft. (3.7 m.).

Hydraulics

As Wildcat Creek is ephemeral, continuous simulation was not necessary. Therefore, several hydraulic scenarios were studied to verify that the basin would perform as designed. It was planned that deposits would most likely have to be removed from the basin on an annual basis. This led to simplification in the number of conditions to be analyzed because the problem was reduced to evaluation of the interactions between average annual deposition and the occurrence of the design (1% exceedance) event. The results presented here are only for the design event; refer to Deering and Larock (1989) for information on other scenarios. Furthermore, as the basin volume is small relative to the hydrograph volume, the analysis could be performed assuming steady flow. The 1% chance exceedance event is 2300 cfs (65 cms). The drainage area is about 7.8 mi^2 (2000 hectares).

Scenario

The situation presented herein represents the condition of the basin after several years' average annual deposition (not removed). The flow evaluated is that of the design (1% chance exceedance) event. The distribution of the deposits shown in Fig. 2 was created based on simulation of the shear stress distribution in the empty basin and observation of other flood control projects having similar flow and sediment transport conditions. The bar deposits are formed from flows expanding into open areas. Initial deposits will form in the lower velocity areas causing the flow to redistribute, expanding again and reinitiating the bar formation process. This results in bar formation on the left and right

Figure 2. Bottom Elevations (ft).

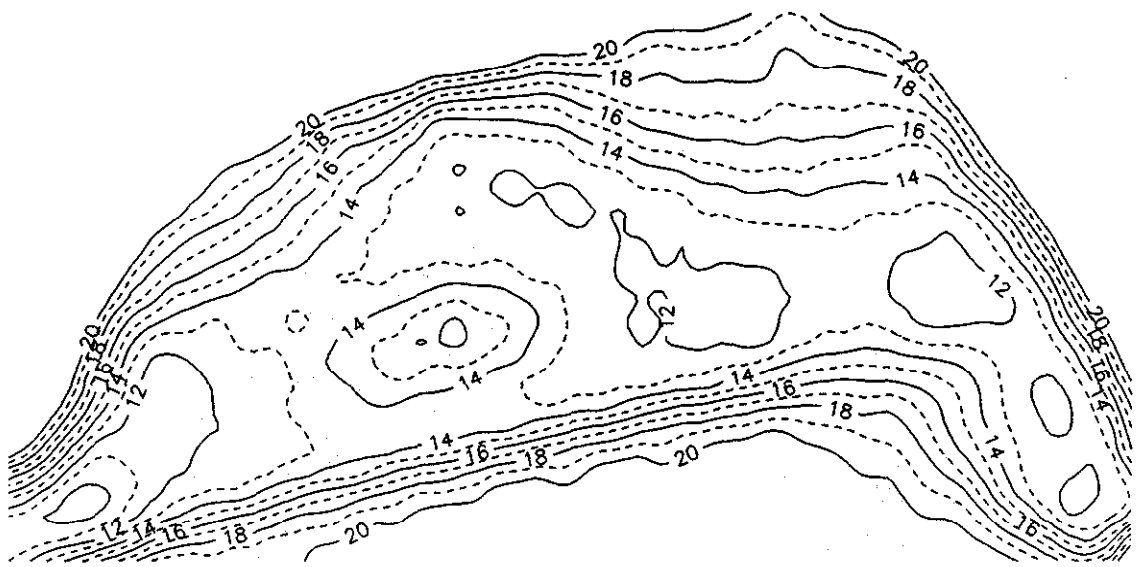

banks, immediately downstream of the entrance, and a central bar further downstream. The assumed deposition pattern has a volume equivalent to that of the average annual deposits for the time period selected. The nodal elevations of the finite element mesh that was developed for the design (empty) basin were modified to reflect this hypothetical deposition pattern.

Modeling parameters

The Manning's n-values were set to 0.03 for most of the basin based on it being maintained as smooth earth. The values for one portion of the left bank were set to 0.06 based on maintaining the native heavy vegetation there. The sensitivity of the results to these values, assuming the project is not well maintained should be checked and may be significant to the design event water surface elevation. The turbulent exchange coefficients were uniformly set to 10 lb-sec/ft^2 (480 N-sec/m^2) for all elements. This was based on prior experience with finite element meshes of this scale. The sensitivity of the results to variation of these values within reasonable ranges was checked and found to be insignificant.

Boundary conditions

This is a simple 2-D problem in that it is analogous to traditional 1-D backwater computations with regard to boundary conditions. A discharge was specified at the upstream (right) end of the model. In 2-D, however, the direction of the discharge must be given which was selected to be perpendicular to the inflow boundary line (see Fig. 3). The downstream boundary condition was specified as a water surface elevation appropriate for the discharge being analyzed based on design studies of the downstream reach. A rating curve could have been used for the downstream boundary if appropriate. Along all other boundaries, the flow direction is parallel to the boundary.

Modeling results

The flow field for the design event is depicted on Figure 3. The flow enters the basin as a plume of

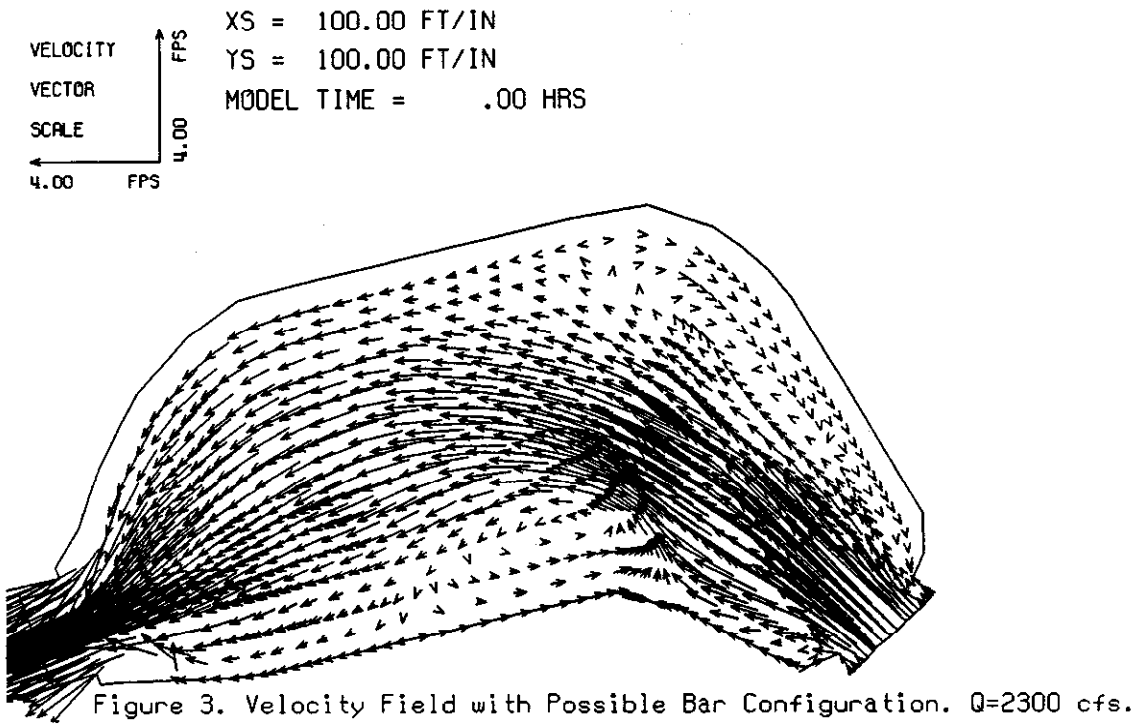

Figure 3. Velocity Field with Possible Bar Configuration. Q=2300 cfs.

relatively high velocity. Recirculation zones are seen on each side of the inflow plume. This is obviously not a one-dimensional situation. The hypothetical bar formations do not appear to force the higher velocity jet against either of the banks as originally suspected. The associated shear stress field for this flow and bottom condition is shown in Figure 4.

The shear stress is low enough that sediments of the size of interest will be trapped in the basin. Note particularly the zones of near zero shear that correspond to the recirculation cells near the left and right banks. The clustering of contours near the banks is an artifact of the contouring process.

CONCLUSIONS

The technique presented herein represents a midway approach to the prediction of spatially complex sediment transport processes. Much can be inferred from viewing the velocity and shear stress distributions. Once the velocity field has been computed, the computation of the shear stress distribution is trivial. If, at this stage, one determines that simulation of the full two-dimensional transport and dispersion of sediment is necessary, the hydrodynamic analysis already performed can be used directly in the sediment transport simulation.

COMPUTATIONAL ASPECTS

The finite element mesh used for this study contains about 550 elements and 1370 nodes. This produces about 2300 simultaneous equations. To solve this system for steady flow using six iterations takes about 15 minutes on a 25 MHz 386 computer. The system can be run within the DOS 640K limitation.

ACKNOWLEDGEMENTS

This study was performed for the U. S. Army Corps of Engineers District, Sacramento with the

Figure 4. Shear Stress (lb/sq ft).

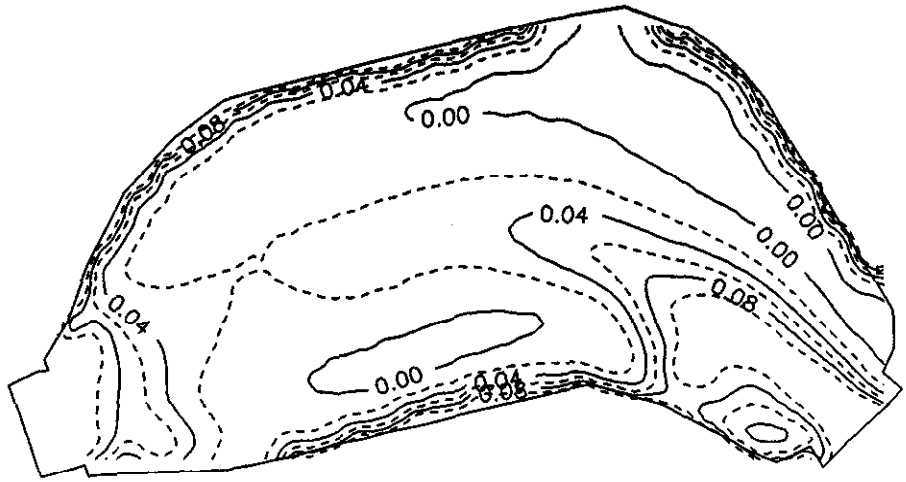

assistance of the U. S. Army Corps of Engineers Waterways Experiment Station. The opinions expressed herein are those of the author and not necessarily those of the U. S. Army Corps of Engineers.

REFERENCES

Deering, M. K. and Larock, B. E. (1989) "The Design of Sediment Basins Using Two-Dimensional Hydrodynamic Techniques," Proceedings of the 1989 ASCE National Conference on Hydraulic Engineering, New Orleans, LA.

Federal Highway Administration (1989) "FESWMS-2DH Finite Element Surface-Water Modeling System: Two-Dimensional Flow in a Horizontal Plane," Pub. No. FHWA-RD-88-177.

French, R. H. (1985) "Open-Channel Hydraulics," McGraw-Hill.

Gee, D. M., et al. (1990) "Two-Dimensional Floodplain Modeling," Proceedings of the 1990 ASCE National Conference on Hydraulic Engineering and the International Symposium on the Hydraulics/Hydrology of Arid Lands, San Diego, CA.

King, I. P. and Norton, W. R. (1978) "Recent Application of RMA's Finite Element Models for Two-Dimensional Hydrodynamics and Water Quality," Proceedings of the 2nd. Int. Conf. on Finite Elements in Water Resources, Pentech Press, London.

MacArthur, R. C., et al. (1990) "Two-Dimensional Finite Element Simulation of the Flooding Characteristics in Kawainui Marsh, Hawaii, "Proceedings of the 1990 ASCE National Conference on Hydraulic Engineering and the International Symposium on the Hydraulics/Hydrology of Arid Lands, San Diego, CA.

McAnally, W. H., et al. (1984) "Application of Columbia Hybrid Modeling System," Jour. Hyd. Engr., ASCE Vol. 110, No. 5, Paper 18796.

Montgomery, R. L., et al. (1983) " Dredged Material Sedimentation Basin Design," Jour. Env. Engineering, ASCE, Vol 109, No. 2.

U. S. Army Corps of Engineers (1989) "Sedimentation Investigations of Rivers and Reservoirs," Engineer Manual 1110-2-4000.

U. S. Army Corps of Engineers Hydrologic Engineering Center (1990) "HEC-6 Scour and Deposition in Rivers and Reservoirs," Users Manual.

BEDLOAD SHOALS IN A DEEP-DRAFT NAVIGATION CHANNEL

By Karl W. Eriksen and Fong J. Grey, Hydraulic Engineers, U. S. Army Corps of Engineers, Portland, Oregon

ABSTRACT

Shoaling has been a persistent problem in the Columbia River since the first deep-draft navigation channel was constructed in the early 1900's. Channel modifications and upstream reservoirs have changed the sediment transport regime, but have had little impact on the overall shoaling rates. The continual reoccurrence of shoals is reflected in the annual volume of dredging the Corps of Engineers must do to maintain the navigation channel. Both the historic and recent maintenance dredging averages are approximately six million cubic yards per year.

The shoaling patterns indicate two distinct types of shoals in the Columbia River: 1) small, isolated sand waves shoals across the navigation channel; and 2) large cutline shoals parallel to the channel. The smaller shoals result from bedload transport causing sand waves to form and move along the river bed. Repeated bathymetric surveys have shown sand wave movement of several hundred feet per year and wave heights of up to 12 feet. The largest shoals in the Columbia River occur along the navigation channel cutlines. Cutline shoals grow from the outside edge of a dredge cut, toward the center of the channel and can be over a mile long. It appears that bedload transport on the river bed outside the channel is deflected towards the cutline to form these shoals. It appears that gravity and the transverse bed-slope combine to cause the deflection.

INTRODUCTION

It is important to understand the shoaling processes of a river in order to properly design and maintain a navigation channel. The selection of channel alignment, hydraulic control structure locations, advance maintenance dredging depths and disposal methods are all influenced by the causes of shoaling. As part of the Corps of Engineers efforts to reduce operation and maintenance (O&M) dredging in the Columbia River deep-draft navigation channel, recent studies have examined sediment movement, sediment supply, and shoal formation in the navigation channel. A sediment budget was developed to determine the source and availability of shoal material. Bathymetric surveys from the early 1900's up to the present were reviewed to study sediment movement and shoal formation.

DESCRIPTION OF STUDY AREA

Morphology.

The Columbia River deep-draft navigation channel extends from the mouth to the Portland, Oregon/Vancouver, Washington area, about River Mile (RM) 107. The general planform of this reach is shown in Figure 1. The estuary is 4-5 miles wide and extends upstream to around RM 25. Upstream of RM 25, the main river channel varies from 1700 ft to 3000 ft wide, with minor bifurcations. The river bends tend to have very long radii, typically over 15,000 ft. Sharper bends only occur where basalt cliffs control the river's alignment. The bed

of the main channel is composed of deep deposits of mostly fine and medium sand (0.125-0.50 mm). The natural riverbanks consist of basalt or erosion resistant silt and clay deposits. These overbank silt-clay deposits range from 20 ft to 150 ft thick and overly much deeper sand deposits. Sandy beaches occur only where dredged material has been placed along the shore. There has been little change in the river's location in the last 6,000 years (USACE, 1986).

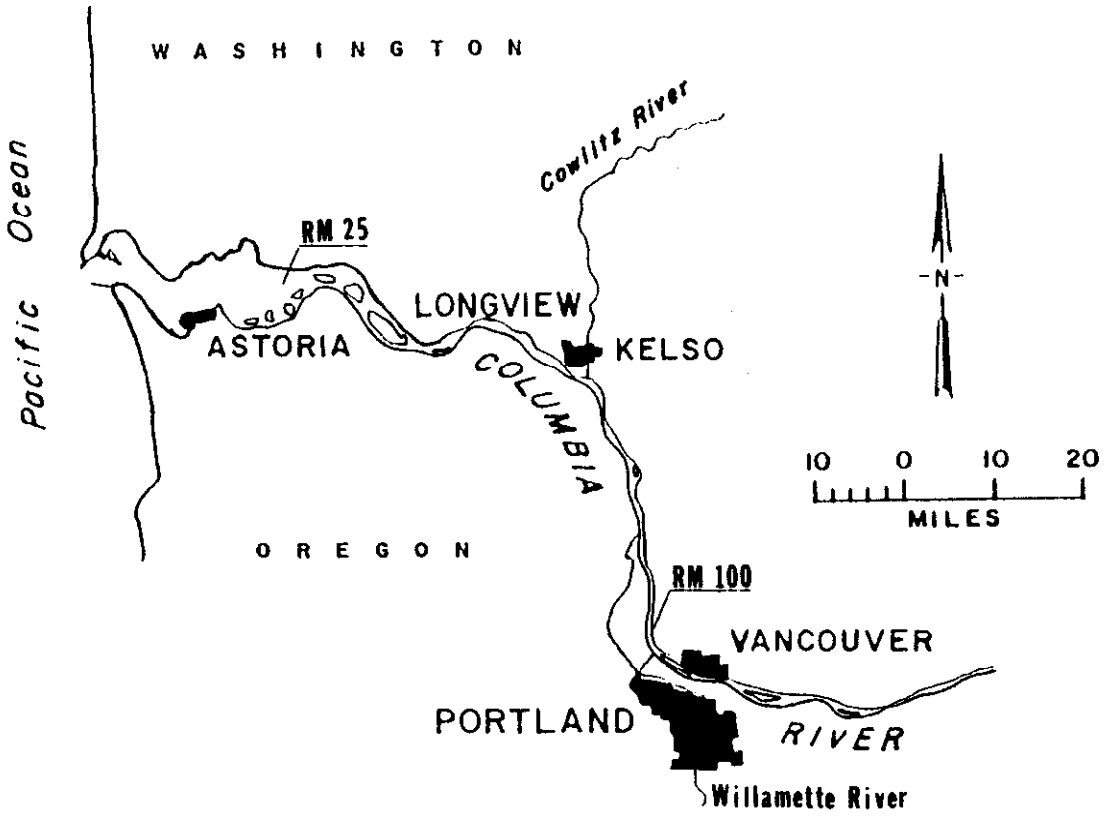

Figure 1 - Study Area Map

The Navigation Channel

The Columbia River navigation channel was originally authorized in 1899 with a 25-ft minimum depth. The authorized depth was increased to 30-ft in 1912, 35-ft in 1930, and 40-ft in 1962. Many pile dikes and several large sand fills were constructed prior to 1940 to constrict flow and control channel alignment at the river's shallowest reaches. Some of these shallow reaches were naturally less than 20 ft deep and over 5,000 ft wide. Additional pile dikes were built during the 40-ft deepening to further constrict flow and reduce erosion at dredged material disposal sites. The annual dredging required to construct and maintain the navigation channel are shown in Figure 2. The O&M dredging varies from year to year, but has averaged around 6-7 million cubic yards (mcy) per year since the 1920's, despite the increases in depth and construction of hydraulic control structures.

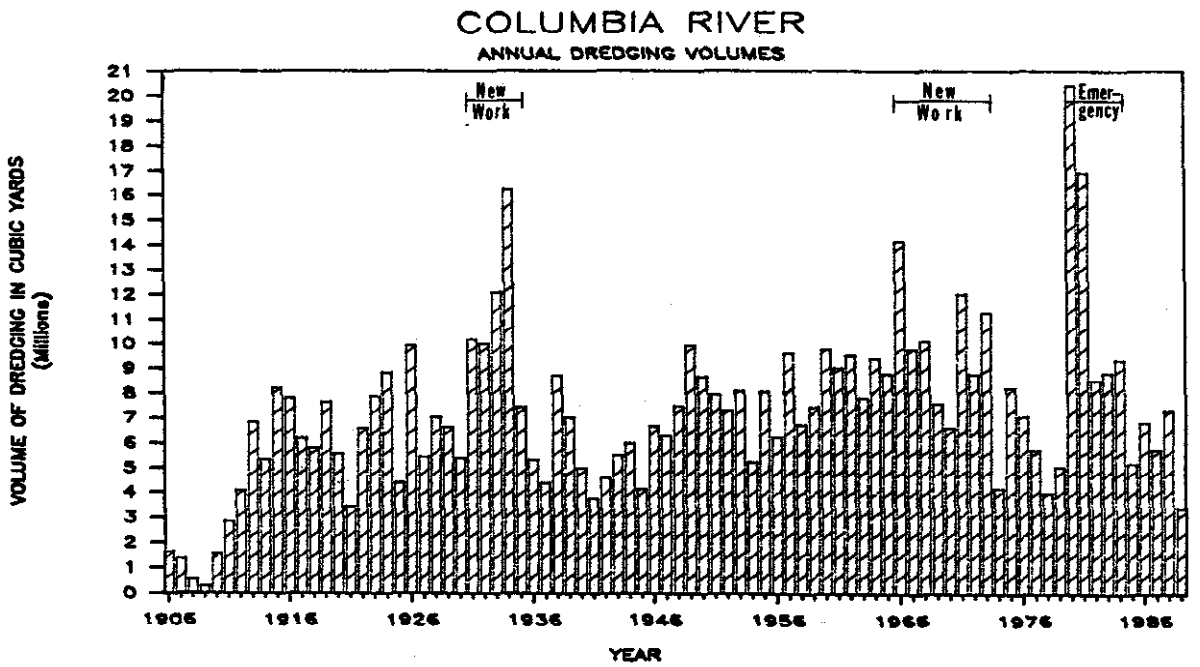

Figure 2 - Annual Dredging Volumes

The current navigation channel is maintained to minimum dimensions of 40-ft deep and 600-ft wide. It generally follows the river's thalweg and much of the channel is deeper than the required 40 ft. Shoals tend to form in reaches of the channel where the depths prior to construction were less than 40 ft. Hopper and pipeline dredges annually remove about 6.5 mcy of sand from the shoals in the navigation channel. Material from hopper dredges is disposed of in deep water outside the navigation channel. The most common practices for pipeline dredges are upland and shoreline disposal. Occasionally, a pipeline will end-dump material in-water alongside the channel. Five feet of advance maintenance dredging is used to make possible an annual dredging cycle.

Hydrology.

Concurrent with the navigation channel development, upstream reservoir storage was being increased. Upstream reservoirs now store water during the spring snowmelt freshet. After completion of the large Canadian storage reservoirs in the early 1970's, the 2-yr flood peak at The Dalles, Oregon., was reduced from 580,000 cfs under natural conditions to 360,000 cfs with regulation (USACE North Pacific, 1987). The stored water is then released during the fall low flow period to increase hydro-electric power generation.

The instantaneous discharge in the study reach changes constantly due to the effects of ocean tides. The instantaneous discharge can range from negative values during the flood tide, to twice the mean daily value at peak ebb flow. The tidal effects are much greater during low river flows than during high flows.

SEDIMENT BUDGET

A sediment budget was developed to identify the source of shoaling material. Annual transport quantities were estimated for both suspended sediment and bedload. Pre- and post-regulation sediment budgets were developed and compared to the corresponding O&M dredging to see if the reduction in sediment yield had reduced shoaling by a like amount.

Suspended Sediment.

The suspended sediment concentrations in the Columbia River are quite low. Measurements taken during the spring freshet in 1922, before any large dams were built, found an average suspended sediment concentration of 130 ppm downstream of the Willamette River (Hickson, 1961). Measurements taken in 1959 and 1960 (USACE Portland, 1961) and in the 1980's (USGS, 1980-1986) found similar concentrations. Based on observed concentrations and appropriate flow-durations curves, the Corps estimated that the average annual suspended sediment yield at Vancouver, Washington, has been reduced from 12 mcy/yr pre-regulation to only 2 mcy/yr post-regulation (USACE Portland, 1986). Bed material is generally less than 15% of the suspended load, and increases to over 30% only when the discharge exceeds 400,000 cfs. This indicates the average suspended bed material transport in the study area is between 0.2 and 0.6 mcy/yr.

Bedload.

No attempt has been made to directly measure the bedload transport of the Columbia River. Bedload estimates were made using two independent methods. An empirical equation developed by the USGS was used to estimate unmeasured load for pre- and post-regulation conditions. That equation is based on the modified Einstein equation and relates unmeasured load to river discharge (USACE Portland, 1986). Applying this equation to the pre- and post-regulation flow-duration curves resulted in bedload estimates of 1.5 mcy/yr pre-regulation and 0.2 mcy/yr post-regulation.

The second estimate was made by equating bedload transport to the movement of the sand waves present on the bed. Sequential surveys were made of two sets of sand waves, one during high flow conditions and the second during average discharge conditions. The analyses of those surveys and flow conditions resulted in bedload estimates ranging from 0.1 mcy/yr to 0.4 mcy/yr.

Shoal Material Source.

Operation and maintenance dredging have been relatively constant despite a reduction in total bed material transport from 5.1 mcy/yr pre-regulation to 1.0 mcy/yr post-regulation. Comparing the average O&M dredging volume of 6.5 mcy/yr to an average total bed material transport rate of 1.0 mcy/yr indicates less material is now being transport into the study area than is dredged from the navigation channel. Therefore, the main source of shoal material must be within the study area. Bathymetric surveys (USACE Portland, 1800's-1990) indicate that there has been significant bed degradation in areas adjacent to the most commonly dredged reaches. The volume of bed degradation is not enough to account for all the dredging. Experience has shown that beach erosion occurs at most shoreline disposal sites. These sandy shorelines are

much more easily eroded than the natural silt/clay banks. Given the stability of the natural banks, the most likely sources of shoal material are riverbed degradation and erosion from dredge material disposal sites. Material from these sources is transported as bedload into the navigation channel.

SHOAL FORMATION

The vast majority of the Columbia River navigation channel shoaling is the direct result of bedload transport. The two dominant shoal forms are large sand waves and cutline shoals. Sand waves are present throughout the river channel and cause shoals across the channel where wave crests rise above -40 ft Columbia River Datum (CRD). Cutline shoals are much larger and run parallel to the channel. Cutline shoals develop at the same locations year after year.

Sand Wave Shoals.

Sand waves have long been recognized as a shoaling problem in the Columbia River. Hickson (1930) noted 8- to 10-ft sand waves forming ridges across the 30-ft deep channel. Sand waves create similar shoals in today's 40-ft channel. Figure 3 shows the variation in size and shape that is typical of this type of shoaling. The volume of an individual sand wave shoal is small, generally less than 30,000 cy, but they are numerous enough to represent a significant amount of the annual O&M dredging.

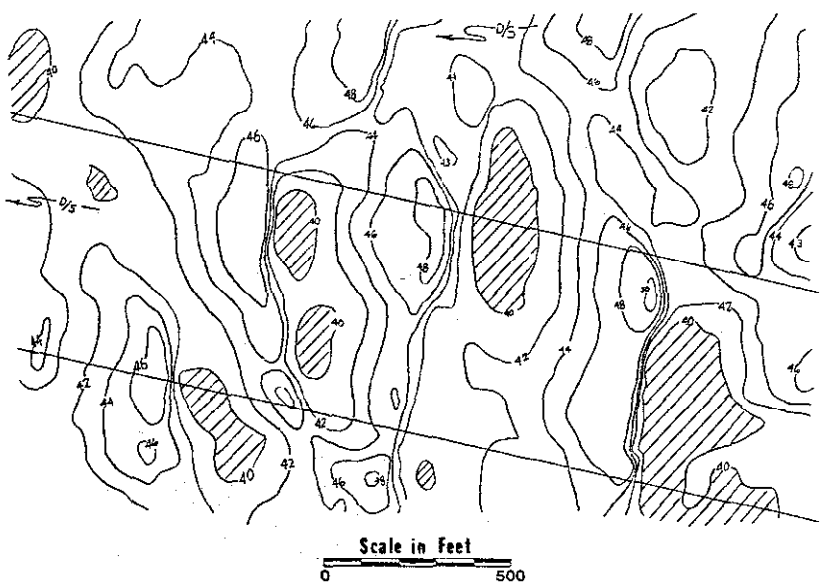

Figure 3. Sand Wave Shoal Pattern

Sand wave shoals do not appear at the same location each year because of the time required for the waves to form and grow. The 5-ft of advance maintenance dredging utilized in the Columbia River, means the sand waves must grow to 8- to 10-ft high before they become shoals. The main source of material for sand waves is the bed of the navigation channel. Dredging leaves a fairly flat channel bottom on which the waves will form. The wave troughs are scoured from below the dredged surface, with material from the trough then forming the

wave crest. Because the maximum wave height seldom exceeds 12 ft, sand waves shoals do not occur where the channel bottom is much deeper than 45-ft CRD. The average rate of movement and change in crest height of a series of large sand waves near RM 66, under varying discharge conditions are listed in Table 1. Initially these waves averaged 650-ft in length and 9.5-ft high. The surveys indicate the rate of downstream migration is related to river discharge, but the relationship of discharge to height changes is not as clear. The rate of migration was near 18 ft/day when the discharge was over 370,000 cfs, but averaged only 3 ft/day for discharges of 310,000 cfs or less. Wave crest elevations decreased during the high discharge period, but rose and fell during the lower discharges. Other observations of Columbia River sand wave behavior suggest that crest elevations increase during lower discharges. The crest elevations of the shoals shown on Figure 3 increased gradually during an 8 month period when discharges were in the 150,000 to 200,000 cfs range. The fact that sand wave shoals develop somewhere in the Columbia River every year also suggests that height increases may occur during low discharges.

TABLE 1. SUMMARY OF SAND WAVE MOVEMENT AND CREST ELEVATION CHANGES IN THE VICINITY OF RIVER MILE 66

TIME PERIOD DURING 1986	AVERAGE DAILY DISCHARGE (CFS)	AVERAGE DOWNSTREAM MOVEMENT (FT/DAY)	AVERAGE CHANGE IN HEIGHT (FT)
Feb. 27 - Mar. 10	410,000	18	-2
Mar. 10 - Mar. 17	370,000	17	-1
Mar. 17 - Mar. 25	290,000	6	0
Mar. 25 - Apr. 07	310,000	0	-0.5
Apr. 07 - Apr. 16	280,000	3	+1
Apr. 16 - Jun. 04	300,000	4	0

Cutline Shoals.

Cutline shoals form along the navigation channel dredging cutline, parallel to flow, and can extend several thousand feet along the channel. The primary cause of cutline shoals is gravity pulling bedload down the side-slopes and into the navigation channel. As river currents move bedload over a bed with a transverse slope, gravity will give the sediment a transverse velocity component independent of the water (Fredsoe, 1978). The steeper the transverse slope, the greater the deflective force on the bedload. Bedload on or near the 1V:3H cutline would therefore be deflected sharply toward the navigation channel. The bedload within the dredged channel would have a very slight, or no, transverse velocity component because of the flat surface of the cut. Along the cutline there would be a convergence of bedload moving downstream in the navigation channel and transversely on the side-slope, resulting in the formation of a shoal. Figure 4 shows the theoretical bedload movement caused by a combination of hydraulic and gravitational forces. This process would cause the side-slopes to erode until an equilibrium transverse slope is reached for the deeper channel. In the Columbia River, these shoals occur on the inside of long bends and on straight river reaches. They are especially severe in areas of the river that were less than 40-ft deep prior to construction of the existing channel. Cutline shoals are much larger than

sand wave shoals, the 12 largest of these shoals account for nearly half of the annual 6.5 mcy of O&M dredging. Grishanin and Lavygin (1987) concluded that this mechanism is also the main cause of shoaling of dredge cuts in Russian rivers with sandy beds.

The mechanics of cutline shoals have only recently been examined in the Columbia River. Beeman (1985b) noted that in the river entrance and at some estuary locations, the side-slopes adjusted to channel deepening by maintaining the pre-deepening transverse slope and degrading to a lower elevation. It was concluded that the side-slopes were supplying sediment to the shoals. The Corps (1988) found the same side-slope response adjacent to cutline shoals in riverine portions of the navigation channel. The Corps further concluded that the sediment removed from the side-slopes was being transported directly into the navigation channel as bedload. Prior to those studies, the cutline shoal areas were generally treated as low sediment transport reaches and low river velocities were considered to be the main cause of shoaling (Hickson, 1961; Dodge, 1976; and Beeman, 1985a). Channel constrictions were built at many of these sites to improve hydraulic conditions and reduce deposition. This practice has been successful where adequate bank protection has been provided. But in some cases, disposal sites have been located near the top of degrading side-slopes and have aggravated the shoaling. With the new insight into the cutline shoaling process, dredging and disposal practices will be modified to better maintain these large shoals.

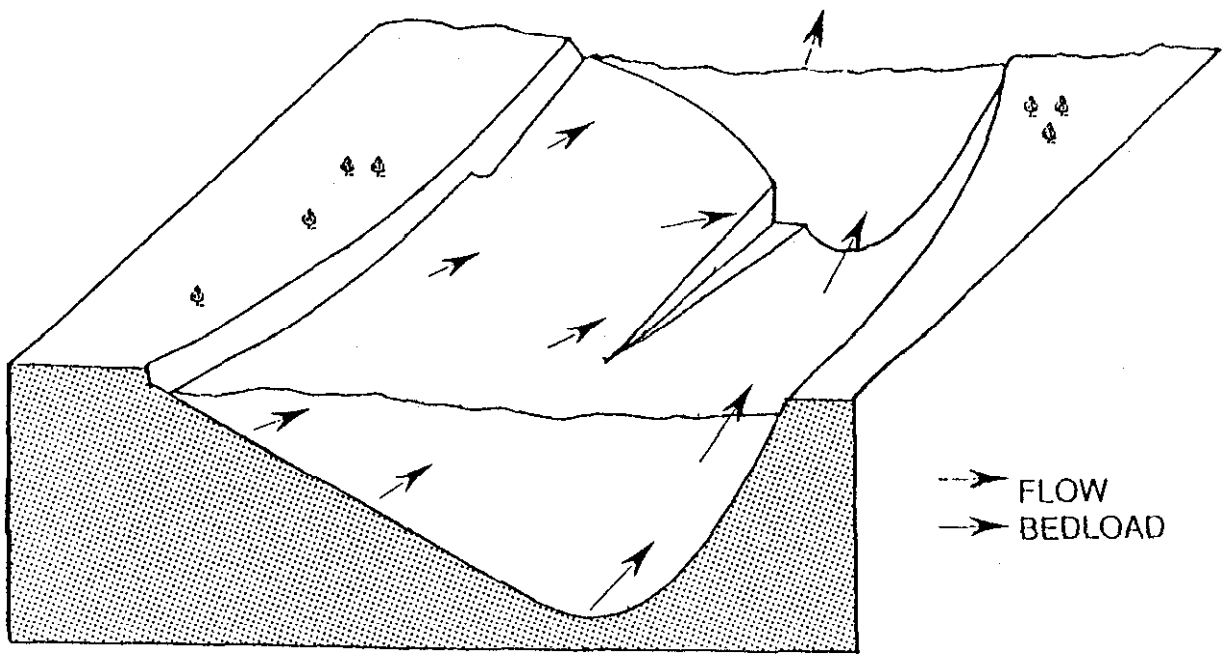

Figure 4. Bedload transport paths under a gravitational influence.

CONCLUSION

The majority of shoaling in the Columbia River navigation channel is the direct result of bedload transport processes. Sand waves have long been recognized as a cause of shoaling and dredging methods have been developed to minimize their interference with navigation. Cutline shoaling processes have only recently been identified and proper O&M practices are yet to be developed. Both these processes are significant in the deep-draft channel because of the close proximity of the channel design depth and the riverbed. The insights gained from this investigation highlight the value of periodically reviewing theories about expected river behavior and comparing them to actual river behavior.

REFERENCES

Beeman, Ogden, Associates, 1985a, Studies to Control Shoaling of the Navigation Channel, Lower Columbia River, U.S. Army, Corps of Engineers, Portland District, Portland, Oregon

Beeman, Ogden, & Associates, 1985b, Studies to Control Shoaling of the Navigation Channel, Lower Columbia River and Estuary, U.S. Army, Corps of Engineers, Portland District, Portland, Oregon

Dodge, R. O., 1976, Construction of the 40-Foot Channel in Columbia River, "Rivers '76", ASCE, Vol. 1, pp 259-279

Fredsoe, J., 1978, Sedimentation of River Navigation Channels, Journal of the Hydraulics Division, ASCE, Vol. 104, No. HY2

Grishanin, K. V. and A. M. Lavygin, 1987, Sedimentation of Dredging Cuts in Sand Bottom Rivers, Bulletin of the Permanent International Association of Navigation Congresses, Bulletin 1987, No. 59

Hickson, R. E., 1930, Shoaling on the Lower Columbia River, The Military Engineer, Vol. XXII, No. 123

Hickson, R. E., 1961, Columbia River Ship Channel Improvement and Maintenance, Journal of the Waterways and Harbors Division, ASCE, Vol. 87, No. WW2, pp 71-93

U.S. Army Corps of Engineers, North Pacific Division, 1987, Columbia River Basin, Cumulative Frequency Curve, Maximum Annual Daily Discharge, Columbia River at The Dalles, Oregon

U.S. Army Corps of Engineers, Portland District, 1961, Sedimentation Investigation, Lower Columbia and Willamette Rivers, July 1959-August 1960

U.S. Army Corps of Engineers, Portland District, 1986, Investigation of Bank Erosion at Sauvies Island, Oregon

U.S. Army Corps of Engineers, Portland District, 1988, Operational Plan FY88, Lower Columbia River, Maintenance Improvement Review

U.S. Geological Survey, 1980-1986, Water Resources Data, Oregon

RESPONSE OF LOWER MISSISSIPPI RIVER LOW-FLOW STAGES

by Charles M. Elliott, Supervisory Hydraulic Engineer; Robert E. Rentschler, Potamologist; and John H. Brooks, Civil Engineering Technician; U.S. Army Corps of Engineers, Mississippi River Commission, River Engineering Branch, Vicksburg, Mississippi

ABSTRACT

Changes in stage-discharge relationship at low flow between the mouth of the Ohio River and Old River, Louisiana are described and the possible causes are discussed. The difference in stage from 1962 to 1988 for comparable low flows ranges from a lowering of 11 feet to an increase of 3 feet. The lowering has occurred in the upstream and middle parts of the reach, and the increase in the downstream part. The following factors are believed to influence the changes: Cutoffs, channel training dikes, revetments, dredging, levees, changes in flow and sediment load due to basin development, tectonic activity (i.e. New Madrid earthquake of 1812), and other natural longterm geomorphic adjustments.

INTRODUCTION

Great distress accompanied the Drought of 1988. Withered crops and parched riverbeds made international headlines. The drought also let us examine changes in the relationship of low flow to river stage on the lower Mississippi River. Some aspects of the changes that we will describe resemble the behavior of the lower Missouri River (Harrison, 1953, and U.S. Army, 1976); others mirror the behavior of tiny rivers which are similar to the Mississippi only in that they also transport water and sediment.

DESCRIPTION OF CHANGES IN LOW-FLOW STAGE/DISCHARGE RELATION

The Lower Mississippi River extends from the confluence of the Ohio and Mississippi Rivers to the Gulf of Mexico, a distance of about 960 river miles. This paper focuses on that portion of the river between the Ohio confluence and the Old River Control Structures in Louisiana, 315 miles above the Gulf, where about 30 per cent of the flow diverts into the Atchafalaya, and low water is only about 10 feet above sea level (Figure 1).

Figure 2 shows profile data and the location of major gaging stations. The profiles show the classic concavity upward except for the slight concavity downward at the upstream end, which may be the result of tectonic activity, especially the New Madrid Earthquake of 1811-12. Figure 3 shows 1962 and 1988 low water profiles in the study reach. In the "big picture", the difference in them is slight, but a closer look (Figures 4 and 5) shows significant changes in some reaches. The most change is between miles 780 and 580. Transitions to relative stability are made upstream and downstream from this reach. Local anomalies may be caused by variations in bed material and river channel hydraulic properties. A few "blips" are likely caused by survey errors or very localized flow anomalies. The flow corresponding to the 1962 profile was about 144,000 cubic feet per second in the upper part of the study reach, and about 172,000 in the lower part. Corresponding flows for the 1988 profile were about 131,000 cfs and 160,000 cfs. The difference of about 8% only accounts for about one foot of stage lowering. Obviously, other factors are involved.

The profiles show the locations of changes, but the timing must be derived from stage-discharge data. Good data since about 1930 is available. However, earlier data is too limited to reliably define trends. Figure 6 shows specific gage plots for six stations. The lowest discharge displayed, 200,000 cubic feet per second, is the lowest discharge with adequate data for annual rating curves. It is about 30% greater than for the 1962 and 1988 profiles, but should reliably reflect trends for low flows.

The changes vary significantly from station to station. To display this, the data for 200,000 cfs are superimposed in Figure 7. The upstream station, Cairo,

shows equilibrium since 1950, while the downstream station, Natchez, shows an increase in stage since 1945. The stations in between show a wide range in magnitude, direction, timing, and rate of change. However, the dominant process is a lowering of low-flow stages. Figure 8 compares daily minimum, maximum, and 1988 flows at Memphis. Although the record for daily low flows was only broken on 41 days in 1988, the record for daily low stages was broken on 201 days, dramatizing the changes in the relationship between low flows and low stages.

CAUSES OF CHANGES IN LOW-FLOW STAGE/DISCHARGE RELATION

The probable causes of these changes (or longterm trends), as distinguished from causes of variations (or short term fluctuations), are:

- Cutoffs
- Channel training dikes
- Revetments
- Dredging
- Levees
- Changes in flow and sediment load due to basin development
- Tectonic activity (i.e. New Madrid earthquake of 1812)
- Continuing longterm natural geomorphic adjustments

A factor which does not cause changes, but may be a stabilizing influence, is erosion resistant bed material. This may be non-alluvial material, or may be gravel, either with a local source or relict from the braided regime following the last glacial period (Queen, Rentschler, and Nordin, 1991).

Other factors, which only cause variations in the stage-discharge relation, include precedent flows, bed roughness (including water temperature), episodic bed material movement, and changes in channel alignment. These factors, likely to have temporary and/or local effects, were documented by Webb (1981) for the station at Memphis, and will not be addressed in this paper.

Cutoffs, channel training dikes, revetments, channel maintenance dredging, and levees are components of the project being implemented by the U.S. Army Corps of Engineers for flood control and navigation (Mississippi River Commission, 1972). Levees in their present form date from about 1930, cutoffs from about 1930, revetments and maintenance dredging from about 1950, and dikes from about 1960. Work continues on revetments, dikes, and dredging, with a project completion date of about 2010.

The **cutoffs** shown on Figure 9 likely affect flowlines the most. The work of Lane (1955) lets us illustrate this qualitatively (Figure 10). The centroid of length reduction from the cutoffs is at Greenville. An oversimplified, but conceptually helpful representation of Lane's model for the Lower Mississippi is shown by Figure 11, which treats the aggregate of cutoffs as one long cutoff. This "model" resembles the classic case of lower flowlines upstream and higher flowlines downstream with time, but in our case upstream lowering is the dominant process. A hypothesis for this imbalance is presented below.

This hypothesis is that **channel training dikes**, in conjunction with **revetments**, may transpose the "hinge point" of cutoffs downstream, thus accenting the upstream lowering effect while dampening the downstream raising effect. Channel training changes the geometry of crossings, increasing low flow conveyance, which infers a flattening of energy slope and lowering of flowline. The greatest geometry change usually occurs where the pre-trained channel is shallowest and least efficient at low flow. Revetments often develop a deeper and narrower cross section at low flow in bends. Conveyance at low flow is likely to increase, thus having an effect similar to that of dikes. There is only one dike downstream of the study reach, but revetments and cohesive bank material maintain an even narrower and deeper channel than in the study reach.

A causal relationship can also be inferred from Figure 12, which compares 1962 and 1988 low water profiles and the highest thalweg elevation for the same time

periods over each crossing between Miles 750 and 650. A lowering of the elevations of the crossings was accompanied by a lowering of the low flow profiles. Crossing elevations are of course influenced by the flow at time of survey, and the channel surveys are not precisely synoptic with the low water profiles, but the changes shown are verified by numerous surveys made over that time period at various flows.

Channel maintenance dredging for navigation is performed during the low water season in crossings which have not yet been adequately improved by training works. The dredged material is usually deposited a short distance away and remains in the channel. The quantity of material moved is insignificant compared to the material transported by the river. However, since the dredging is done at the shallowest locations, the effect on flowlines is to make the broad-crested weir effect of shallow crossings less pronounced. Dredging therefore extends the effect of dikes, but is to a degree a local short term factor.

Another type of dredging, mining of gravel from the river, may have a longterm effect on channel form (Lagasse, Winkley, and Simons, 1980). In our case, if it reduces armoring of the bed of the main channel, the tendency might be to allow more bed and flowline lowering, thus accenting the effect of dikes, revetments, and maintenance dredging. If gravel is removed outside the main low flow channel, a wider, shallower, perhaps even divided, less efficient channel might ultimately result, thus reducing the effects of dikes and maintenance dredging. The complex interaction between bed material size, bed form, depth of flow, and roughness, as described by Simons and Senturk (1976), make any general hypothesis tenuous.

A debate raged among early river engineers about the effects of **levees** on flowlines. Walters (1975), Watson (1982 and 1984), and Walters and Simons (1984) hypothesized that early levees produced changes in channel geometry even before the present non-overtopping system was completed. However, the complex combinations of changes in other variables and their interaction make it impossible for us to confidently assess the longterm effects on low flowlines. It can be hypothesized that confinement of more flood flow to the main channel would increase channel size, with the residual effect of a more efficient channel at low flows. In fact, the same hypothesis was used to justify some early levee construction to improve navigation. However, the studies cited above present evidence that the accompanying increase in sediment transport may cause aggradation in some reaches, thus frustrating firm conclusions. Also, it is difficult to separate stage increases at high flows due to less floodplain conveyance and storage from stage increases due to a decrease in in-channel conveyance caused by aggradation.

Changes in flow and sediment load is also a complex factor because of the interaction with changes due to other factors. Flow augmentation by reservoirs raises minimum stages, thus "mitigating" flowline lowering, but the effect on channel-forming discharges is small, and the longterm effect on low-flow stage-discharge relation is nebulous.

At the downstream end of the study reach, flows from the Mississippi River into the Atchafalaya Basin through Old River were increasing rapidly prior to completion of the Control Structure 30 years ago, but Figure 6 does not reveal any obvious effect on low flowlines upstream at Natchez. Neither has there been any significant change since the flow diversion was stabilized. Watson (1982) discusses this complex situation in detail.

The suspended sediment input to the study reach has declined (Keown, Dardeau, and Causey, 1986), which would infer eventual bed and flowline lowering, but the net effect after interaction with other factors is unknown. Preliminary results of a study indicate that the bed material may be slightly finer now than in 1932 (Queen, Rentschler, and Nordin, 1991).

Tectonic activity in the form of earthquake potential has recently become a concern of the general public in the Lower Mississippi Valley . Geomorphologists

are aware that more subtle activity may also have effects on the river (Watson 1984). However, in the absence of a dramatic event such as the New Madrid Earthquake, it is difficult to prove that a particular aspect of river behavior is being affected by tectonics. Since the river bed at low flow is usually recently deposited material, flowlines should adjust to gradual tectonic movement, thus obscuring the effects.

Continuing longterm natural geomorphic adjustments in slope and geometry, predating stage-discharge records, may be defining the "base" condition that the other adjustments are superimposed on. The scanty data from pre-cutoffs hint at an aggradational trend, but this may be a case of a little data being a dangerous thing. Walters (1975) states that possible aggradation may have been the result of the New Madrid Earthquake and/or early partial confinement by levees. Since we cannot confidently define this base trend in low-flow stage/discharge relations, we will only state that the Lower Mississippi may not have been in equilibrium even before the Earthquake or man's works. Fisk (1944) stated that the River had shown no tendency to aggrade or degrade since its diversion through Thebes Gap near Cairo, which Saucier (1974) estimates to have occurred about 6,000 years ago. However, an engineering definition of equilibrium must be more restrictive than a geologic definition, hence our caution in hypothesizing.

The contents of this paper do not necessarily reflect the official views and policies of the Corps of Engineers.

REFERENCES

Fisk, H.N., 1944, "Geological Investigation of the Alluvial Valley of the Lower Mississippi River", Mississippi River Commission, Vicksburg, Mississippi

Harrison, Alfred S., 1953, "Study of Effects of Channel Stabilization and Navigation Project on Missouri Levels", MRD Sediment Series No. 32 (Nov. 1983), U.S. Army Corps of Engineers, Missouri River Division, Omaha, Nebraska

Keown, Malcolm P., Dardeau, Elba A., and Causey, Etta M., 1986, "Historic Trends in the Sediment Flow Regime of the Mississippi River", Water Resources Research, Vol. 22, No. 11 (October)

Lagasse, P.F., Winkley, B.R., and Simons, D.B., 1980, "Impact of Gravel Mining on River System Stability", Proceedings of the Waterways, Port, Coastal and Ocean Division, American Society of Civil Engineers, Vol 106, No. WW3, Proc. Paper 15643, pp. 389-404

Mississippi River Commission, 1972, "Improvement of the Lower Mississppi River and Tributaries, 1931-1972", Vicksburg, Mississippi

Queen, B.S., Rentschler, R.E., and Nordin, C.F., 1991, "Bed Sediment Size Changes of the Mississippi River, 1932 to 1989", Proc. of the Fifth Federal Interagency Sedimentation Conference

Rentschler, R.E., and Smith, L.M., 1989, "Response of the Lower Mississippi River to River Engineering", Presented at Geological Society of America Conference, St. Louis, Missouri

Saucier, R.T., 1974, "Quaternary Geology of the Lower Mississippi River Valley", Research Series No. 6, Arkansas Archaeological Survey, Fayetteville, Arkansas

Simons, D.B., and Senturk, F., 1976, Sediment Transport Technology, Water Resources Publications, Fort Collins, Colorado

U.S. Army Corps of Engineers, Omaha District, 1976, "A Study of the Shift in the Stage-Discharge Relationship of the Missouri River at Sioux City, Iowa", Omaha, Nebraska

Walters, Wallace H. Jr., 1975, "Regime Changes of the Lower Mississippi River", MSc. Thesis, Colorado State University, Fort Collins, Colorado

Walters, Wallace H. Jr., and Simons, D.B., 1984, "Longterm Changes of Lower Mississippi River Meander Geometry", River Meandering, p. 318-329, American Society of Civil Engineers, New York

Watson, Chester C., 1982, "An Assessment of the Lower Mississippi River Below Natchez, Mississippi", PhD. Dissertation, Colorado State University, Fort Collins, Colorado

Watson, Chester C., Schumm, Stanley A., and Harvey, Michael D., 1984, "Neotectonic Effects on River Pattern", River Meandering, pp. 55-66, American Society of Civil Engineers, New York

Webb, Jerry W., 1987, "Low Water Conditions on the Lower Mississippi River", Presented at Workshop on Rigid Boundary Hydraulic Problems of Flood Control Projects, Ansted, West Virginia, April 1987

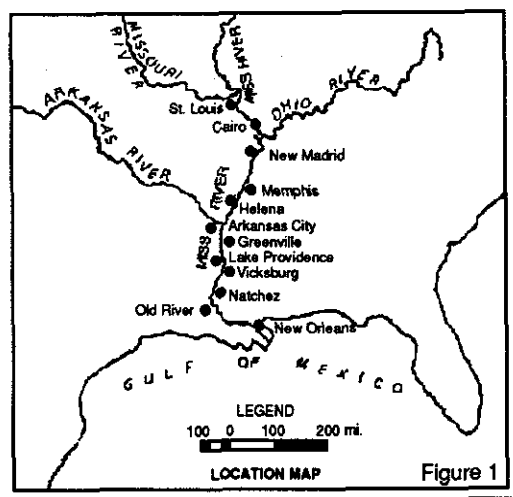

Figure 1

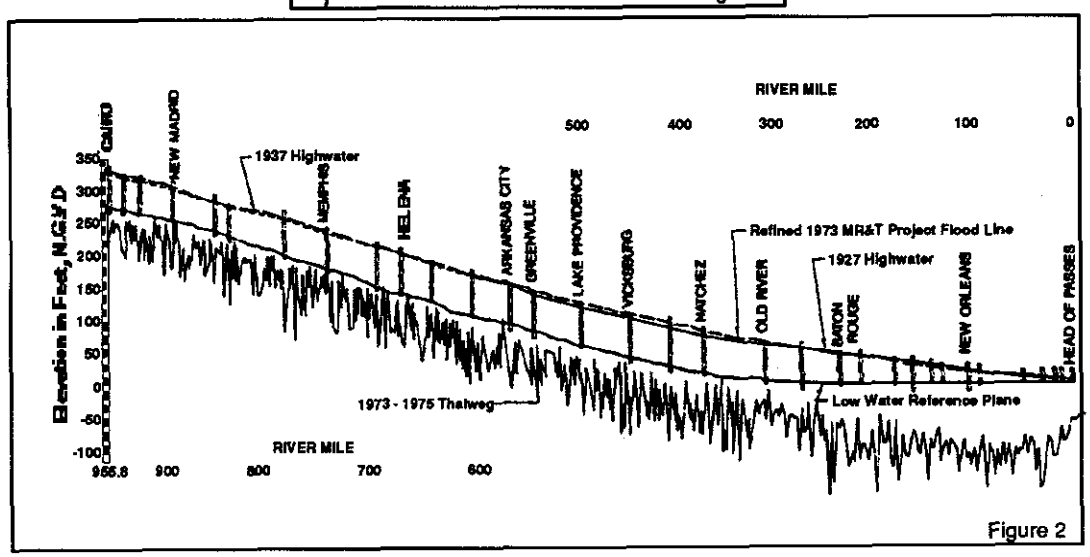

Figure 2

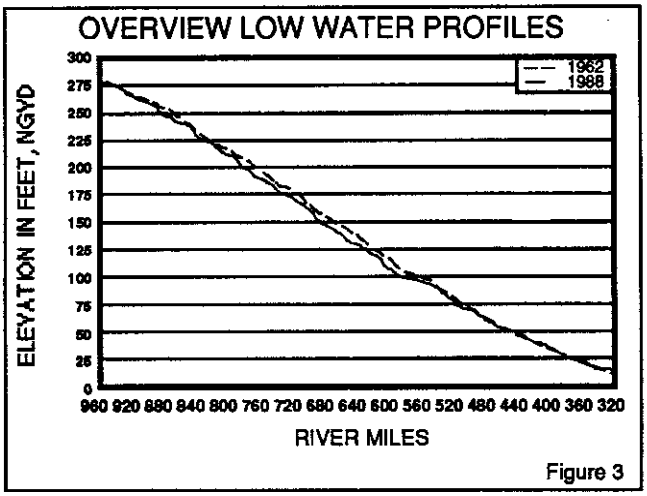

Figure 3

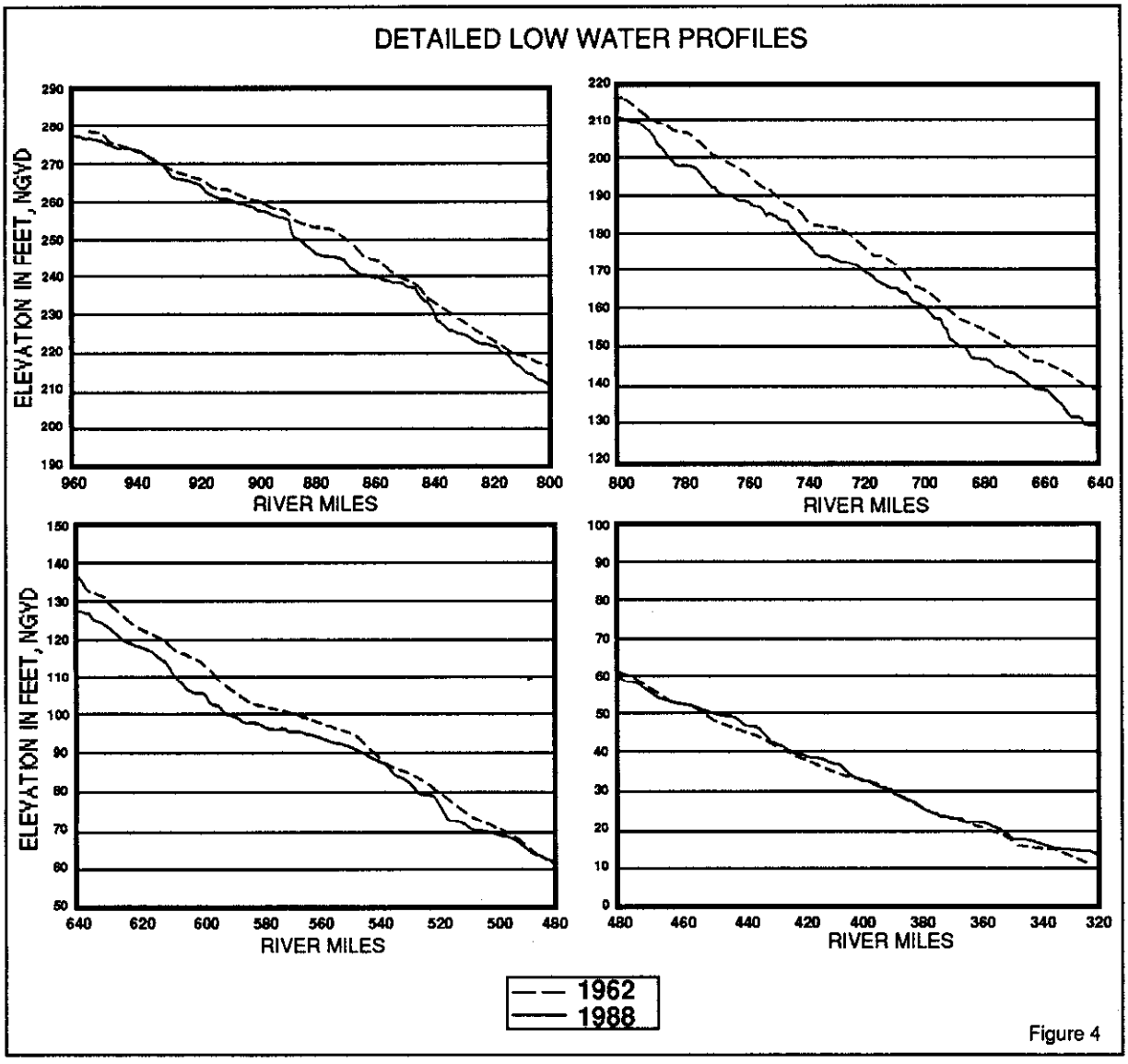

Figure 4

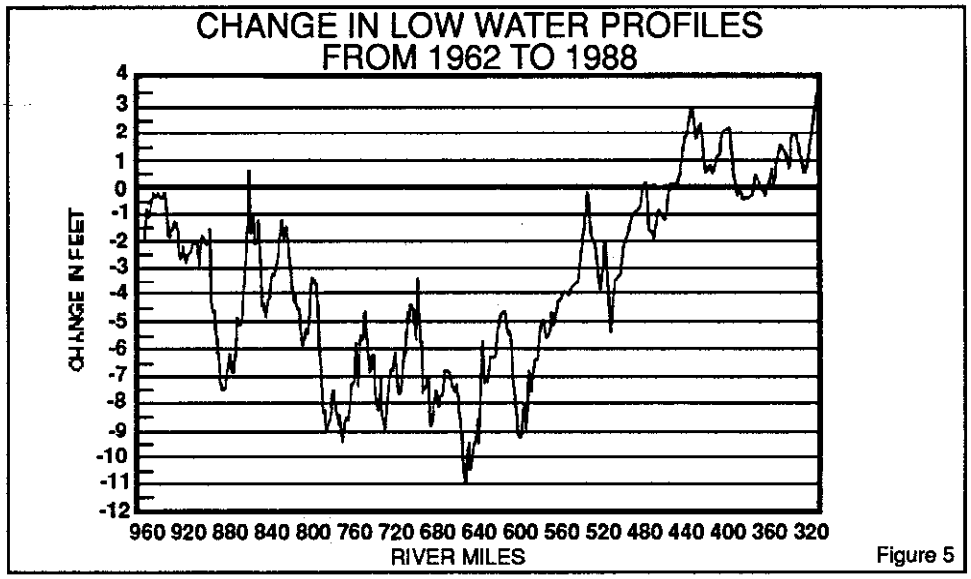

Figure 5

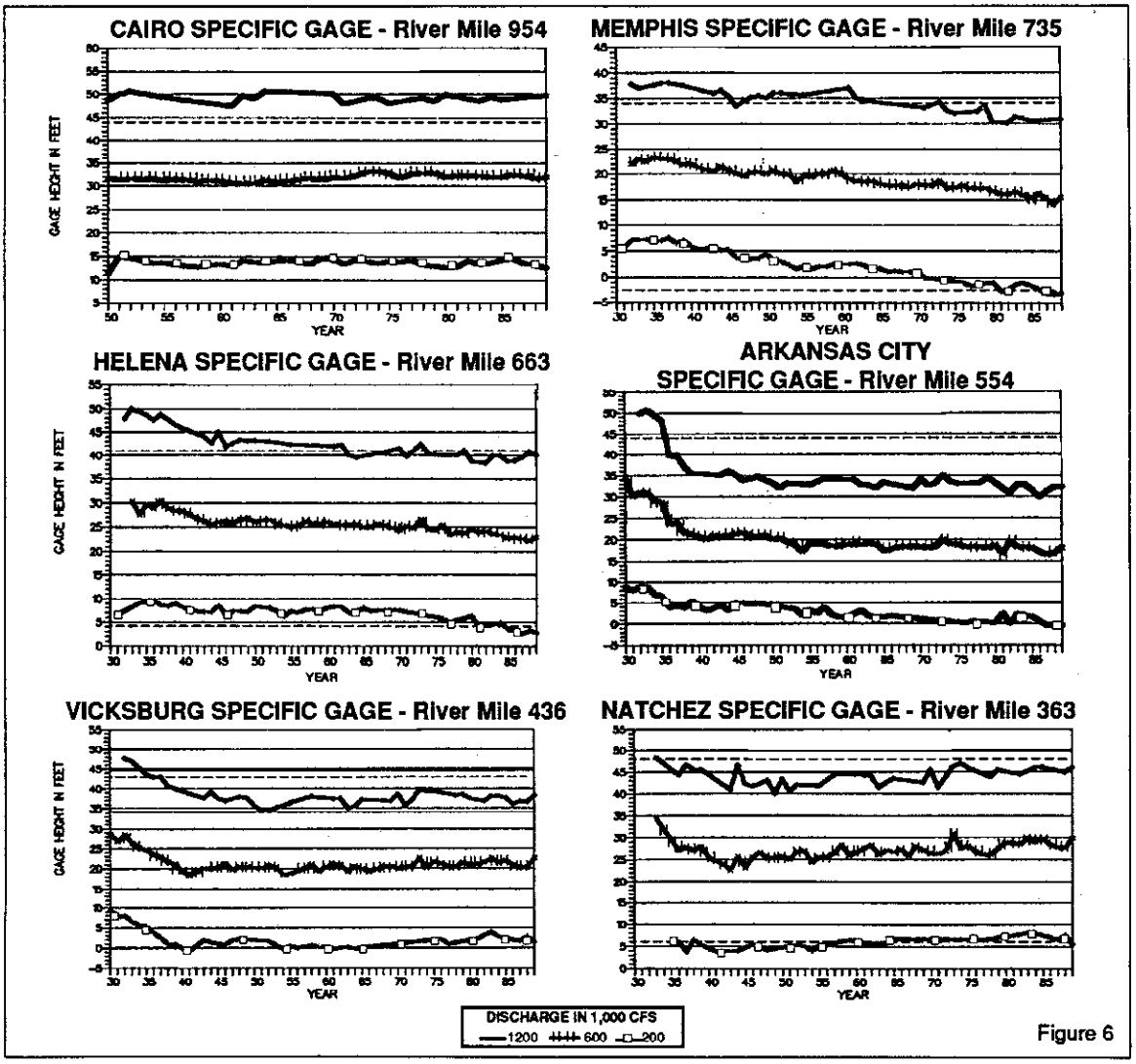

Figure 6

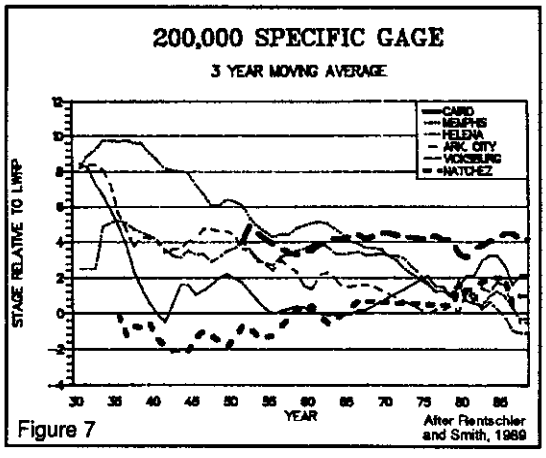

Figure 7

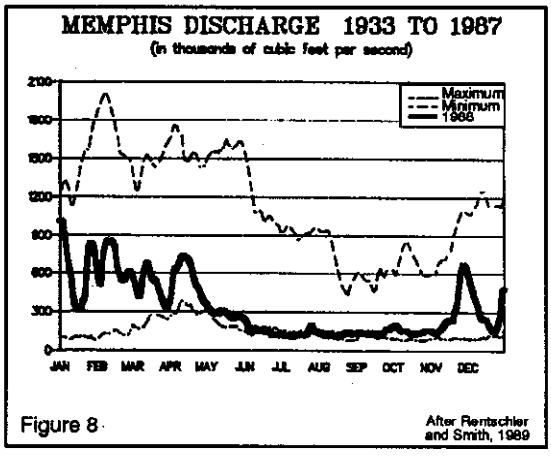

Figure 8

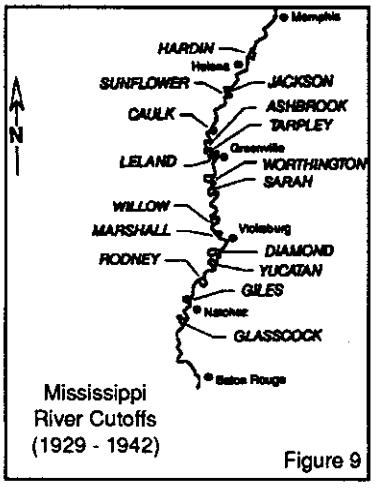

Mississippi River Cutoffs (1929 - 1942)

Figure 9

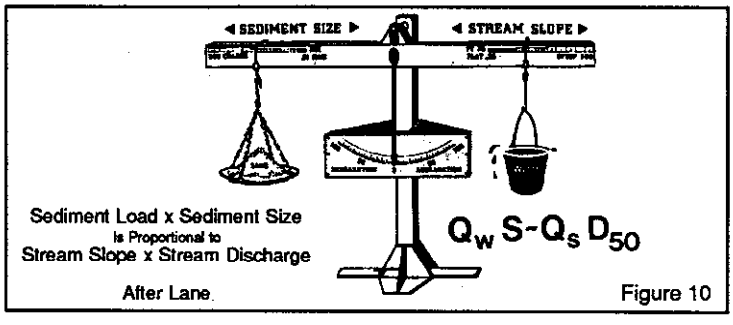

Figure 10

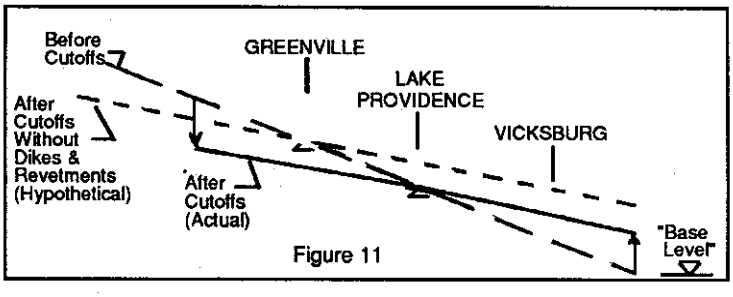

Figure 11

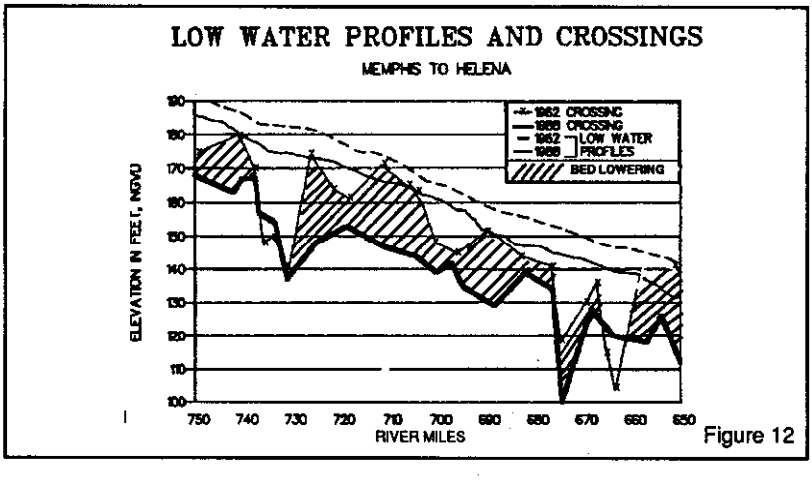

Figure 12

EXAMINATION OF RED RIVER DYNAMIC LOOP RATING CURVE

By Phil G. Combs, Hydraulic Engineer, U.S. Army Corps of Engineers, Vicksburg District, Vicksburg, Mississippi

INTRODUCTION

The relationship between stage and discharge is one of the most important hydraulic characteristics which is used by engineers, planners, designers, farmers, and the general public. The conceptual rating curve presented in Figure 1 represents the idealized relationship between stage and discharge; a single valued unique curve. The rating curve may be viewed as a snapshot of the channel reach, hopefully a representative snapshot. It reflects the required stage to pass a particular flow through the channel which implicitly reflects the channel conveyance of the channel reach. However, in alluvial channels the curve depicted in Figure 1 is generally not representative. More common to the alluvial channels is the loop or hysteresis curve, which is the subject of the this paper. The loop rating curve depicted in Figure 2 represents the more common type rating curve experienced in alluvial channels. No complete analysis has been conducted to determine the causative factors and influences which generate the loop rating curve.

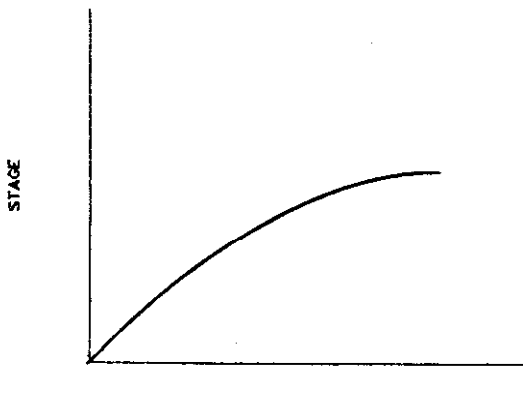

Figure 1. Typical single valued rating curve

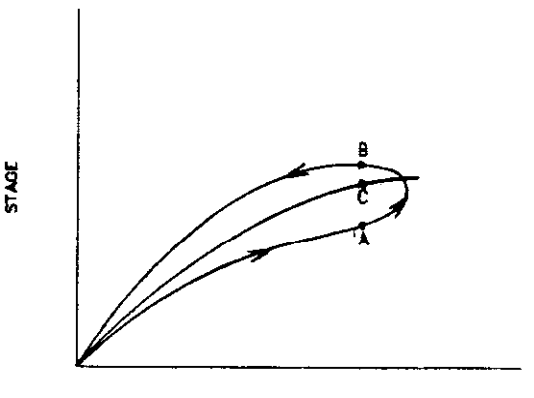

Figure 2. Typical loop rating curve

LITERATURE REVIEW

In evaluating the causative factors of the loop rating curve in alluvial channels it becomes readily apparent that there are at least four principal factors which must be addressed; (1) dynamic effects, (2) bedform changes and Manning's n changes, (3) temperature effects, and (4) aggradation and degradation of the channel. Even though temperature is known to affect the stage discharge relationship by changing the kinematic viscosity, it will not be specifically addressed in the paper.

Henderson (6), Jansen (7), Cunge (4), and others have attributed the loop rating curve to be the result of the dynamic effects of a flood hydrograph. However, none of these writers has included flume or field data to evaluate the completeness of the assumptions for the dynamic control of the rating curve. These three writers utilize the dynamic terms within the St. Venant equation to explain the loop effect. An order of

magnitude analysis of the terms of the St. Venant equation reveals that the flatter the bed slope, the more impact the dynamic terms will have on the friction slope and correspondingly the more influence it will have on the loop rating curve. This paper is addressing the Red and Mississippi Rivers which have bed slopes flat enough to allow the dynamic terms to be dominant. By considering only the dynamic terms in a rigid boundary channel, there are three different depths which can occur in a channel for a given flow: rising limb depth, falling limb depth, and uniform flow depth. This is demonstrated in Figure 2 by points A, B, and C.

Figure 3 represents observed rating curves for the Mississippi River at Vicksburg, Miss. These observed curves clearly show that the conceptual curve considered by Henderson, Jansen, and Cunge is much more simplistic than the rating curves which occur in nature. The observed curves imply that there are more factors to be considered than just the dynamic effects.

Combs and Flowers conducted extensive studies in 1975-1977 evaluating the loop rating curve on the Mississippi River with a fully dynamic wave numerical model (3,11). These studies were conducted to determine whether the loop effect could be simulated numerically. These studies found that the Manning's n value decreased as the stage increased, decreasing from .028 to .016. As the 1973 hydrograph was routed through the numerical model, it computed a rating curve at Vicksburg which reproduced the observed rating curve on the rising limb of the hydrograph but fell below the observed rating curve on the recession of the hydrograph, as demonstrated on Figure 4. In order to reproduce the rising and falling limbs of the hydrograph two sets of n values had to be used, Figures 5-6. It should be noted that the loop rating curve produced by using the rising limb n values was generally about one half the size of the observed loop (computed loop was about 1.0-1.2 ft. and the observed loop was about 2.0-2.5 ft.). Thus in addition to the dynamic effects which were fully reproduced, there were other factors influencing the loop effect. The higher n values on the recession limb of the hydrograph implied that the greater roughness was due to a combination of increased roughness due to bed forms and/or channel geometry changes. Combs and Flowers did not attempt to identify the causative factors influencing the loop rating curve besides the dynamic effects.

The effect which the resistance to flow has on the loop rating curve in alluvial channels will not be considered. Several writers (1,8,9,13) have investigated the grain and form roughness of alluvial channels and the relationship of velocity, depth, and slope to the form of roughness. We will turn our attention to the findings of Simons and Richardson (8,9), Simons, Richardson, and Haushild (10), Colby (2), and Dawdy (5). These works are representative of the state-of-the-knowledge of the relationship of the stage-dicharge curve to resistance to flow.

The bed form roughness in alluvial channels is a function of the sediment characteristics and the flow characteristics. The bed configuration can be changed by altering either the discharge (which affects the depth), slope, temperature, or the bed material size distribution (9).

In considering the case of a hysteresis effect reflected in the stage-discharge curve, Simons and Richardson (8) stated that "... the

magnitude of resistance to flow lags the actual discharge, that is, the change of bed roughness lags the change of discharge. This results in a smaller resistance to flow and smaller depth than would normally occur for equilibrium flow. The reverse occurs on the falling stage."

It has been shown for gentle bed sloped alluvial channels that the loop rating curve is significantly influenced by the dynamic terms in the St. Venant equation and by the bed forms and channel roughness. Unfortunately the only known dynamic studies on a natural channel is the work of Combs and Flowers. Similarly there is not an extensive amount of information or published literature on alluvial channel bed forms and channel roughness.

Another important factor influencing the loop rating curve is the change in channel geometry throughout a hydrograph. There is no known literature which addresses specifically the aggradation and degradation which occurs throughout a channel reach within a hydrograph. However, it is known that generally the bends scour in high flow and the crossings aggrade, while in low flow this trend is reversed. The data which follows from the Red River provides definitive evidence that the aggradation/degradation processes are more complex than this broad generalization.

DATA COLLECTION AND ANALYSIS

Analysis of stream gaging data collected on the Red River was conducted to aid in evaluating the causative factors of the loop rating curve. The study reach of the Red River is located in central Louisiana in the vicinity of Alexandria, realigned miles 43-90. Discharge and suspended sediment samples are collected on a regular basis at Alexandria, La.

Discharge and Channel Profile Data Collection

The 1989 flow on the Red River was high which was reason to intensify the stream gaging data collection. During the high flow periods, discharge was measured on a daily basis in order to accurately determine the flow rate. Additionally, during 1989 longitudinal thalweg profiles were obtained for reaches along the Red River from Alexandria downstream to Lock and Dam 1, approximately 47 miles. These profiles were conducted from a moving boat profiling the thalweg continuously along the reach. The profiles reflect depth of flow and by inspection and interpretation the type and magnitude of bed forms present throughout the reach may be determined. The boat profiles are uncontrolled surveys, but location can be determined relatively accurately by markings made on the profile scrolls by the technicians indicating land markings or river mile markers.

Rating Curve Analysis

The 1989 flow hydrograph, Figure 7, was quite unusual in that there were three highwater events experienced at Alexandria, LA, all of which closely approximated the 10 year frequency flow of 145,000 cfs. Note that the first event occurred in February, while the second event occurred at the end of May and the third event occurred at the beginning of July. The second event was clearly independent of the first while the third event occurred before the river had returned to base flow from the second event. Figure 8 represents the rating curve reflecting the 1989 flow conditions.

The lower loop represents the first flood event, while the second and third flood events are represented by the two higher loops, respectively. The first rise had a loop of approximately 1.5 feet while the second and third flood events had loops of 1.6 and 3.0 feet, respectively. Each of the successive flood events is shifted higher than the previous loop rating curve. As seen from analysis of Figure 8, the second flood event peaked 3.5 feet above the first peak and the third peak occurred 4.0 feet above the second peak or a total of 7.5 feet above the first peak. None of the literature has ever addressed this phenomenon of rating curve shifting during a hydrograph. An analysis of the stream gaging data will be conducted in order to gain insight into the channel processes.

It has been shown that the dynamic effects and the bed form roughness changes influence the magnitude of the loop rating curve. It would require development of a dynamic routing model to clearly identify the portion of the loop effects experienced at Alexandria, La in 1989 and to make judgements on the change in the bed form roughness. However, considerable insight will be gained by analysis of the stream gaging as well as the sediment and longitudinal profile data gathered throughout the highwater period on the Red River.

Area vs. Discharge

Evaluation of the discharge and the corresponding cross sectional area for each measurement provides evidence whether there is a constant or variable relationship between the two variables. Figure 9 gives a clear indication that the Q vs. Area relationship remains virtually constant throughout the hydrograph, while the Q vs. Stage (Figure 8) varies as much as 7.5 feet. This data implies that if the Q vs. Area is constant and the Q vs. Stage is rising then the channel must be aggrading to compensate for the rise in stage.

Bed Elevation vs. Q

An analysis was then conducted to determine how the bed elevation varied with discharge. The analysis consisted of evaluating the bed elevation derived from the gaging station at Alexandria and evaluation of the longitudinal profiles. Both data sets indicated a similar relationship. There is a clear indication that the bed is higher for each successive flood event.

The longitudinal profiles were begun on 26 May 1989 and continued throughout the remainder of 1989. The typical reach selected is located at river miles 55-59.5, realigned mileage. This reach was selected since it has a gage located on the Moncla Bridge at the upper end of the reach, thus water surface elevation and slope could be easily determined. Additionally, the reach is considered to be a typical reach of the lower Red River. Figures 10-13 are copies of the longitudinal profiles in the general vicinity of the typical reach. From review of the profiles for the sample dates, it becomes obvious that the boat traversed the reach at different speeds. This was due primarily to the channel velocity. Examination of the profiles indicates the following:

Date of Survey	Representative Bed Elevation, NGVD
26 May 1989	18
7 Jul 1989	29
22 Jul 1989	27
10 Oct 1989	21

The representative bed elevation was determined by visually recognizing an elevation which represents the reach. As is clearly obvious, these profiles reflect the same aggradation trends as indicated in Figures 8-9. The bed aggrades approximately 11 feet from the second flood event to the third event and thereafter degrades back to an elevation of about 20 feet, NGVD. Therefore, the data derived from the cross sections at the gaging station were representative of the channel reach. This conclusion verifies one of the assumptions in the introduction that the rating curve is representative of the channel reach.

Bed Forms

These profiles may also be used to study the channel bed forms. Review of Figure 10, which is the longitudinal profile for 26 May, reveals that the bed is composed of small dunes in the range of 2-4 feet in height. Whereas, Figure 11, representing 7 July, indicates dunes ranging in height from 5-8 feet and similarly for 22 July, Figure 12, indicated dunes varying in height from 3-10 feet. The vast majority of the latter dunes are more than 5 feet in height. Finally, Figure 13 for 10 October shows ripples or dunes being about 2-2.5 feet in height. It is difficult to discern whether the latter profile indicate ripples, dunes or a combination. It is noteworthy that the bed forms do not diminish in magnitude with increasing flow, as found by Simons and Richardson in flumes and some channels which have steeper slopes than the Red River. At this time it is difficult to determine what influence the bed forms had on the rating curve. Additional study would be necessary with a numerical model to differentiate the effects caused by the bed form changes.

SUMMARY

It has been shown that the loop rating curve for the alluvial channels considered in this paper is sensitive to the dynamic effects of the hydrograph, the bed form and grain roughness changes, and also to the aggradation/degradation changes in the channel bed. As a result it is more appropriate to refer to the loop rating curve as the dynamic loop rating curve. This more closely identifies that it is dynamic in nature. There is no known literature that has identified the aggradational processes which have been shown to occur on the Red River.

REFERENCES

Brooks, Norman H. (1955), Mechanics of Streams with Movable Beds of Fine Sand, with discussion, Transactions of the American Society of Civil Engineers, vol. 123, 1958, p. 526-594

Colby, Bruce R. (1960), Discontinuous Rating Curves, for Pigeon Roost and Cuffawa Creeks, Mississippi, U.S. Dept. Agriculture, Agriculture Research Service 41-36, p.31.

Combs, Phil G. and Flowers, Don (1977), A Study of the Dynamic Rating Curve of the Mississippi River, Proceedings of the Mississippi Water Resources Conference, Mississippi Water Resource Research Institute, Miss. State, Miss.

Cunge, Jean A. (1975), Applied Mathematical Modeling of Open Channel Flow, in Mahmood,K and Yevjevich, V. (Ed.), Unsteady Flow in Open Channels, Ch. 10, Water Resource Publications, Ft. Collins, Co.

Dawdy, David R. (1961), Depth-Discharge Relations of Alluvial Streams-Discontinuous Rating Curves, U.S. Geological Survey Water Supply Paper 1498-C, p.16.

Henderson, F.M. (1966), Open Channel Flow , p. 391-394, Macmillan Company, New York.

Jansen, P.Ph., Bendegom, L. van, Berg, J. vanden, deVries,M., and Zanen, A. (Ed.) (1979), Principles of River Engineering, The Non-Tidal Alluvial River, Pittman Publishing, London.

Simons, D.B., and Richardson, E.V. (1961), Forms of Bed Roughness in Alluvial Channels, Journal of Hyd Div, American Society of Civil Engineers, No. HY3, May 1961, p. 87-105.

Simons, D.B., and Richardson, E.V. (1960), Resistance to Flow in Alluvial Channels, Journal of Hyd Div, American Society of Civil Engineers, HY5, May 1960, p. 73-99.

Simons,D.B., Richardson, E.V. and Haushild, W.L. (1962), Depth-Discharge Relations in Alluvial Channels, Journal of Hyd Div, American Society of Civil Engineers, HY5, Sep 1962, p. 57-73.

U.S. Army Corps of Engineers, Vicksburg District (1977), Dynamic Loop Study.

Vanoni, Vito A. (Ed.) (1975), Sedimentation Engineering, Manual No. 54, American Society of Civil Engineers, New York, New York.

Vanoni, Vito A. and Brooks, Norman H. (1957), Laboratory Studies of the Roughness and Suspended Load of Alluvial Streams, Report No. E-68, Sedimentation Laboratory California Institute of Technology.

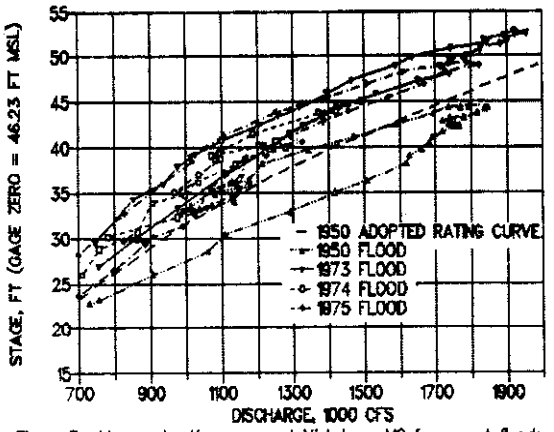

Figure 3. Measured rating curves at Vicksburg, MS for recent floods

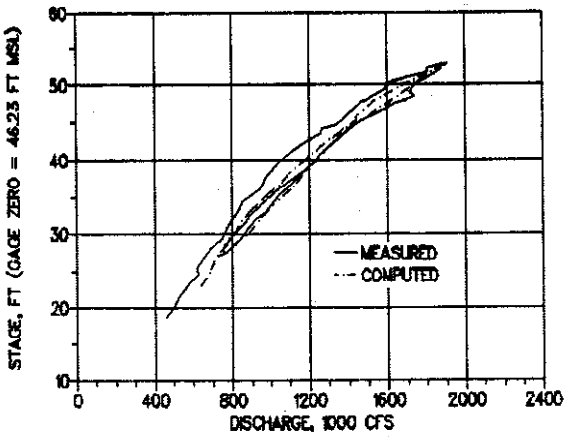

Figure 4. 1973 rating curve at Vicksburg, MS using single valued Manning's n

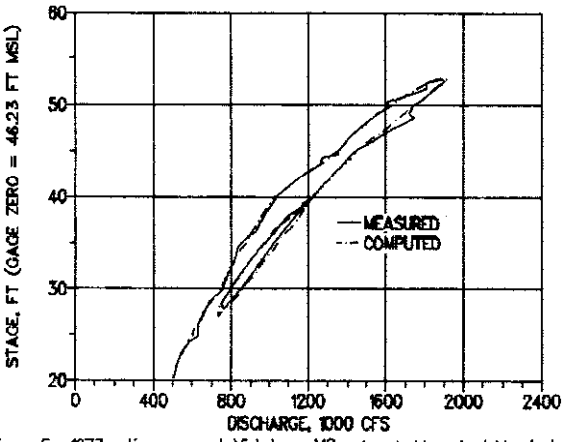

Figure 5. 1973 rating curve at Vicksburg, MS using double valued Manning's n

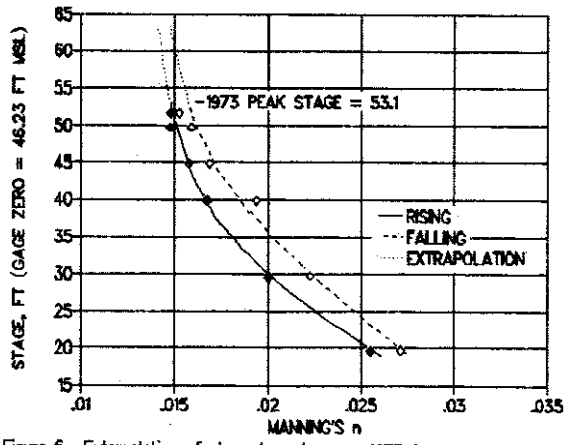

Figure 6. Extrapolation of channel roughness – 1973 flood at Vicksburg, MS

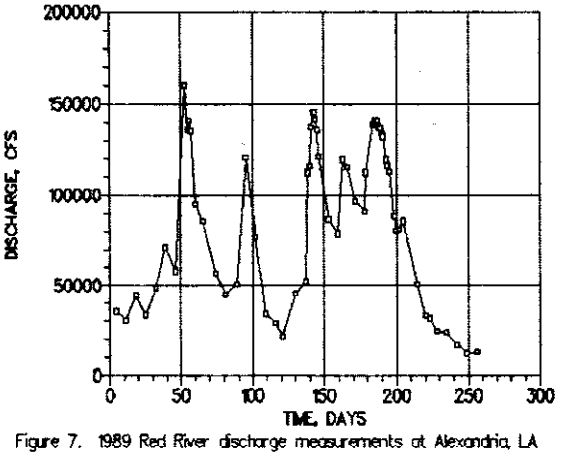

Figure 7. 1989 Red River discharge measurements at Alexandria, LA

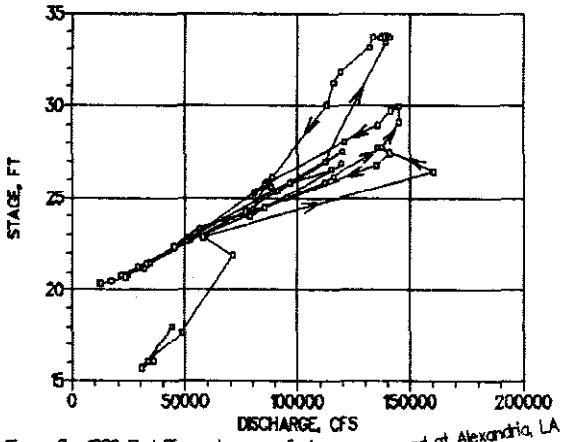

Figure 8. 1989 Red River stage vs discharge measured at Alexandria, LA

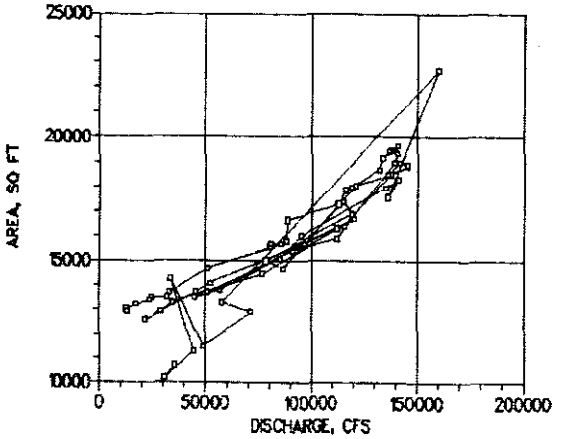

Figure 9. 1989 Red River flow area vs measured discharge at Alexandria, LA

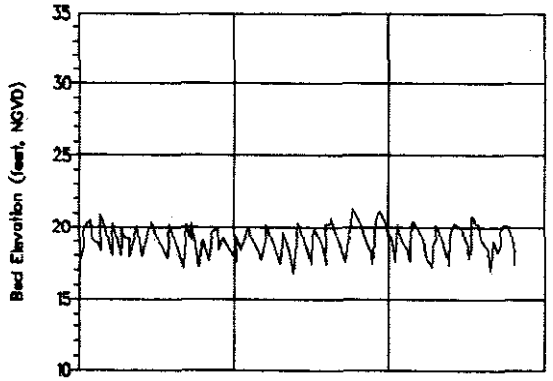

Figure 10. Channel Profile near Moncla, LA (26 May 1989)

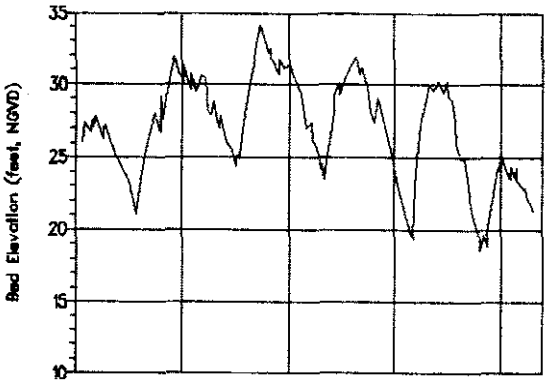

Figure 11. Channel Profile near Moncla, LA (7 July 1989)

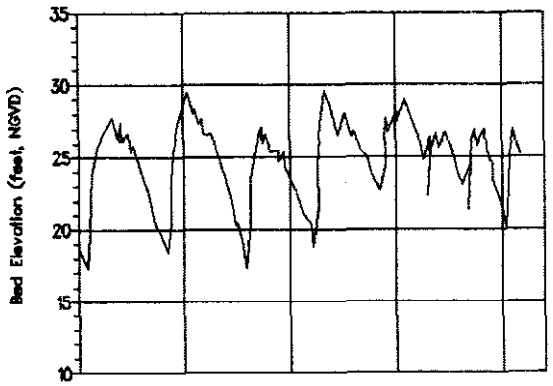

Figure 12. Channel Profile near Moncla, LA (22 July 1989)

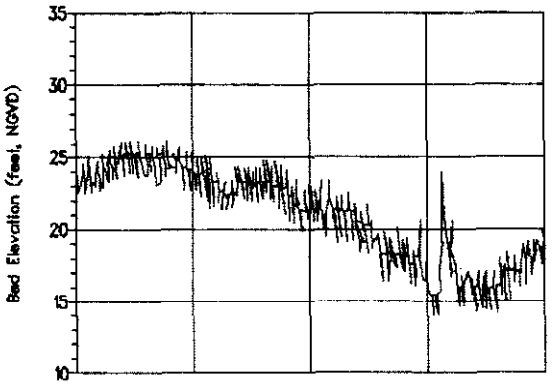

Figure 13. Channel Profile near Moncla, LA (10 Oct 1989)

DELTAIC DEPOSITION IN THE ATCHAFALAYA BASIN

by Billy J. Garrett, Hydraulic Engineer, Headquarters, US Army Corps of Engineers, and Nancy Powell, Hydraulic Engineer, US Army Corps of Engineers, New Orleans District

ABSTRACT

By the mid 1800's, the Atchafalaya River was firmly established as a distributary of the Mississippi River. Removal of a debris raft and construction of levees along the upper reach of the Atchafalaya produced rapid enlargement of the channel with resultant increase in flow and sediment. As the Atchafalaya captured an increasing percentage of Mississippi River flow, the forces of flow and sediment began to generate rapid changes in the river and its basin.

Sediments were transported to an area of tidal lakes above Morgan City, connected to the Gulf of Mexico by the Lower Atchafalaya River. Deltas formed in these lakes as the river pushed its channel to the Gulf. As the lakes rapidly filled with alluvial deposits, the tidal interchanges decreased and then ceased; the Lower Atchafalaya River began to decrease in size. By the mid 1900's, the lake area above Morgan City had reached enough of a sediment filled state that a subaqueous delta began to form at the mouth of the Lower Atchafalaya River. Subaerial deltas for the Lower Atchafalaya River and Wax Lake Outlet appeared after the 1973 flood.

The deposition in the lakes area north of Morgan City, the subsequent reduction of the outlet capacity of the Lower Atchafalaya River, and the development of the deltas in the Atchafalaya Bay have impacted the ability of the Atchafalaya floodway to convey flood flows and have affected the Corps of Engineers' flood control program. This paper will address the impacts of the deltaic deposition on stages and flows within the Atchafalaya Basin and Bay and the solutions implemented and proposed by the Corps.

ATCHAFALAYA BASIN

The Atchafalaya River is not a river but a distributary of the Red and Mississippi Rivers. It carries all of the flow of the Red and a substantial portion of the Mississippi southward through the upper Atchafalaya Basin in a well defined leveed channel. The channel meanders in the middle basin through many interconnecting bayous, enters the lower basin through Grand and Six Mile lakes, and then empties via Wax Lake Outlet and the Lower Atchafalaya River into Atchafalaya Bay and the Gulf of Mexico.

The Atchafalaya River is a relatively young river. About 500 years ago an enlarged loop in the Mississippi River meandered westward and captured the

Red River in vicinity of Turnbull Island. The meander loop, one arm of which is now known as Old River, cut into an ancient channel of the Mississippi River. The flood waters of the Red and Mississippi Rivers entered this new outlet and began excavating the old waterway to form the present Atchafalaya River. The upper end of the channel soon filled with debris, forming an impenetrable raft of logs which continued to grow until, in 1831, Henry Shreve isolated the Atchafalaya from the Mississippi by means of a cutoff at the narrow neck of the Old River loop. The raft, cut off from its major source of debris, ceased to grow. Various groups made unsuccessful attempts to clear the river for navigation between 1839 and 1855. Upon removal of the raft in 1855, by the State of Louisiana, the river enlarged its channel, threatening capture of the Mississippi by 1975.

The great flood of 1927 resulted in the Flood Control Act of 1928. Under this act, and subsequent amendments, the U.S. Army Corps of Engineers began development of a flood control plan for the lower Mississippi River and its tributaries. This plan provides for the control of the maximum probable flood that may occur in the Lower Mississippi Valley. With the features of the flood control plan in place the maximum probable flood at the latitude of Old River is 3,000,000 cfs. This project flood is to be routed to the sea by the Atchafalaya Floodway and Mississippi River. Distribution of the project flood is shown on Figure 1.

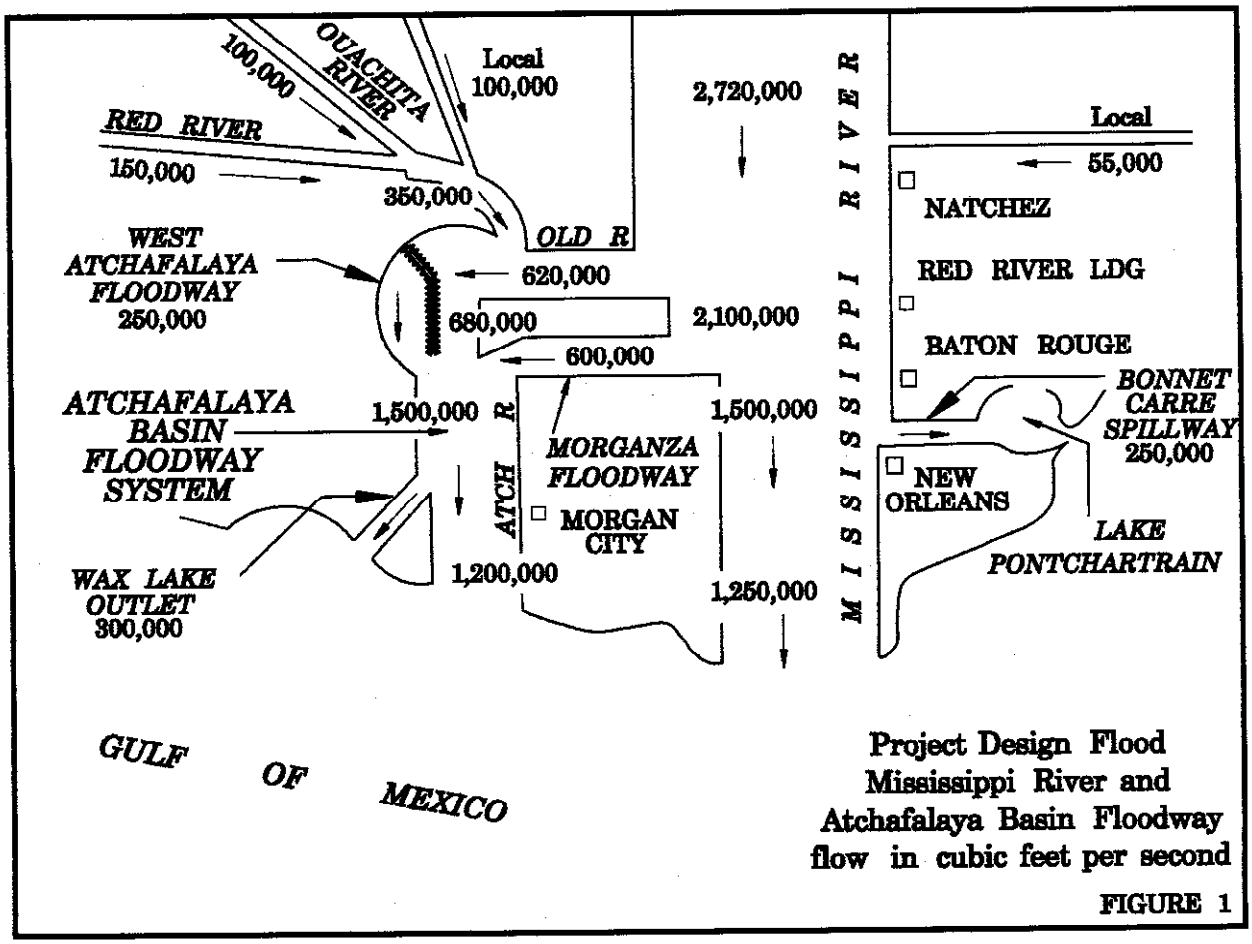

Project Design Flood
Mississippi River and
Atchafalaya Basin Floodway
flow in cubic feet per second

FIGURE 1

Flood control features of the Atchafalaya Basin, shown on Figure 2, consist of the following:

1. Old River Control Structures (Low Sill, Auxiliary, Overbank) These structures regulate the amount of Mississippi River flow entering the Atchafalaya River.
2. East and West Atchafalaya Basin Protection Levees
3. Levees along the upper 55 miles of the Atchafalaya River
4. West Atchafalaya Floodway
5. Morganza Floodway
6. Center channel/Training works
7. Wax Lake Outlet
8. Wax Lake Outlet Control Structure
9. Avoca Island Levee
10. Levees West of Berwick
11. Floodgates, locks, and pumping stations

DELTAIC DEPOSITION

Deposition in the Atchafalaya Basin commences below the lower limit of influence of the Atchafalaya River levees. The construction of the levees, along with the removal of the raft in the Atchafalaya River, resulted in rapid enlargement of the channel and marked increase in the velocity and discharge. The efficiency of the river as a sediment carrier has increased also, contributing not only material carried in suspension from the Red, Mississippi and Old Rivers but providing Atchafalaya River material which is carried down into the lower basin.

The sedimentation process in Grand and Six Mile Lakes has taken place in two phases. These phases are due, at least in part, to the original configuration of Grand Lake; ten miles wide at its upper end, tapering to two miles at Cypress Island. Deltaic accretions formed in Grand Lake above mile 100, in a fan pattern until about 1940. The delta developed at a relatively uniform rate into the lake in all directions. Beginning in 1937 a central channel was implemented through the delta, after which time flow through the delta was confined primarily to this channel and the other distributaries were effectively cut off. Delta growth was subsequently confined to the distal end of the main channel. The main channel discharged directly into Grand Lake and, because there was no longer a gradual decrease in current velocity through a network of distributaries, sediment was transported farther out into the lake and deposited over a larger area of the lake bottom. The main channel extended itself into Grand Lake by the growth of its natural banks. The natural banks were emergent during low flow periods and quickly became vegetated so the subsequent high flow eroded them only with difficulty, except by local crevassing. These natural banks had the effect of restricting the flow through the main channel even during periods of high discharge. The natural banks thus formed by the main channel, and the smaller channels to the east and west of it, combined to form a continuous emergent bar. This bar enlarged until, by 1950, it had formed a large body of land almost completely filling the portion of Grand Lake north of Willow Cove. Grand and Six Mile Lakes were essentially filled by 1978,

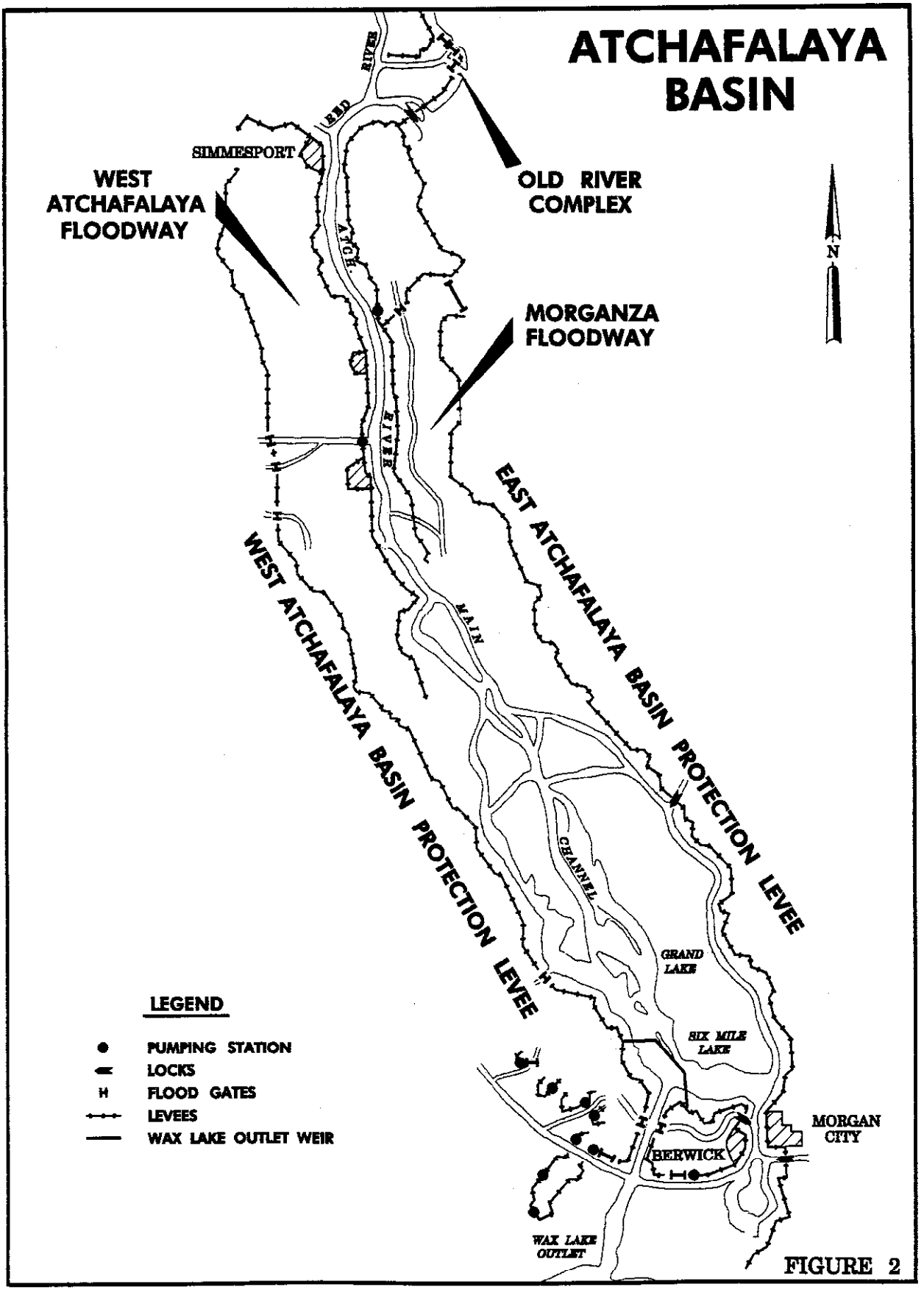
ATCHAFALAYA BASIN
SIMMESPORT
WEST ATCHAFALAYA FLOODWAY
OLD RIVER COMPLEX
MORGANZA FLOODWAY
N
RED RIVER
ATCH. RIVER
MAIN CHANNEL
EAST ATCHAFALAYA BASIN PROTECTION LEVEE
WEST ATCHAFALAYA BASIN PROTECTION LEVEE
GRAND LAKE
SIX MILE LAKE
MORGAN CITY
BERWICK
WAX LAKE OUTLET
LEGEND
PUMPING STATION
LOCKS
FLOOD GATES
LEVEES
WAX LAKE OUTLET WEIR

FIGURE 2

Figure 3. These back swamp areas are still expected to receive 5 to 9 feet of deposition over the next 50 years without man's intervention.

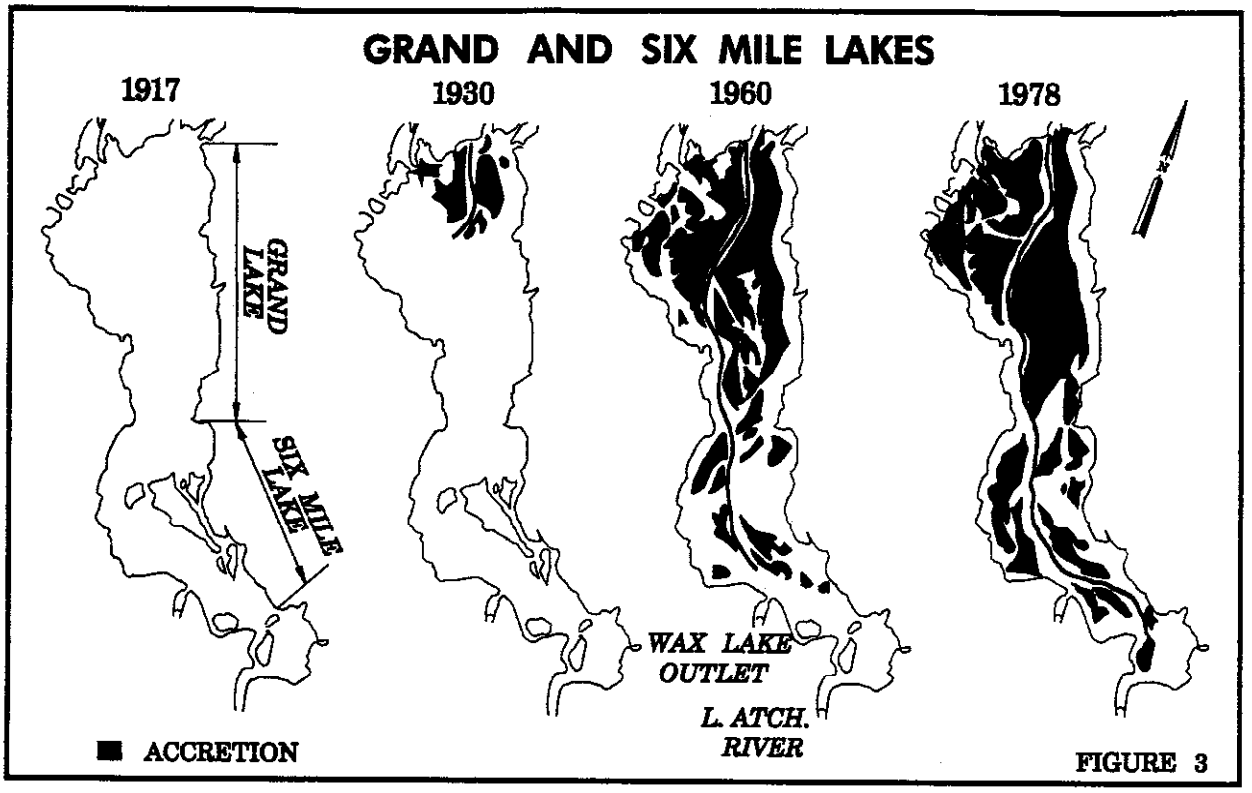

The natural outlet for the Atchafalaya River system is below Morgan City. Dredging of a flood control channel through Wax Lake Outlet shortened the distance from the lakes to the bay by 13 miles in 1942. Since the high water year of 1950, the high water flow through Wax Lake Outlet has increased from 20 to 30 percent of the total flow at Simmesport. The increase in flow resulted in enlargement of the channel from 18,000 square feet below bankfull in 1945 to 40,000 square feet in 1985. The Lower Atchafalaya River lost channel capacity. This resulted in an overall decrease in channel capacity for the two outlets , as shown on Figure 4, and an increase in flood elevations.

Periodic sampling of suspended sediment in the outlets, beginning in January 1965, indicated a yearly rate of 16 million cubic yards per year entering Wax Lake Outlet and 42 million cubic yards per year entering the Lower Atchafalaya River. Since 1978, the bulk of the sediments have been moving past Morgan City into the Atchafalaya Bay. The Atchafalaya Bay is receiving an estimated + 40 million cubic yards of suspended sediment per year, and it is anticipated that by 2030 Atchafalaya Bay will be filled beyond Point Au Fer Reef.

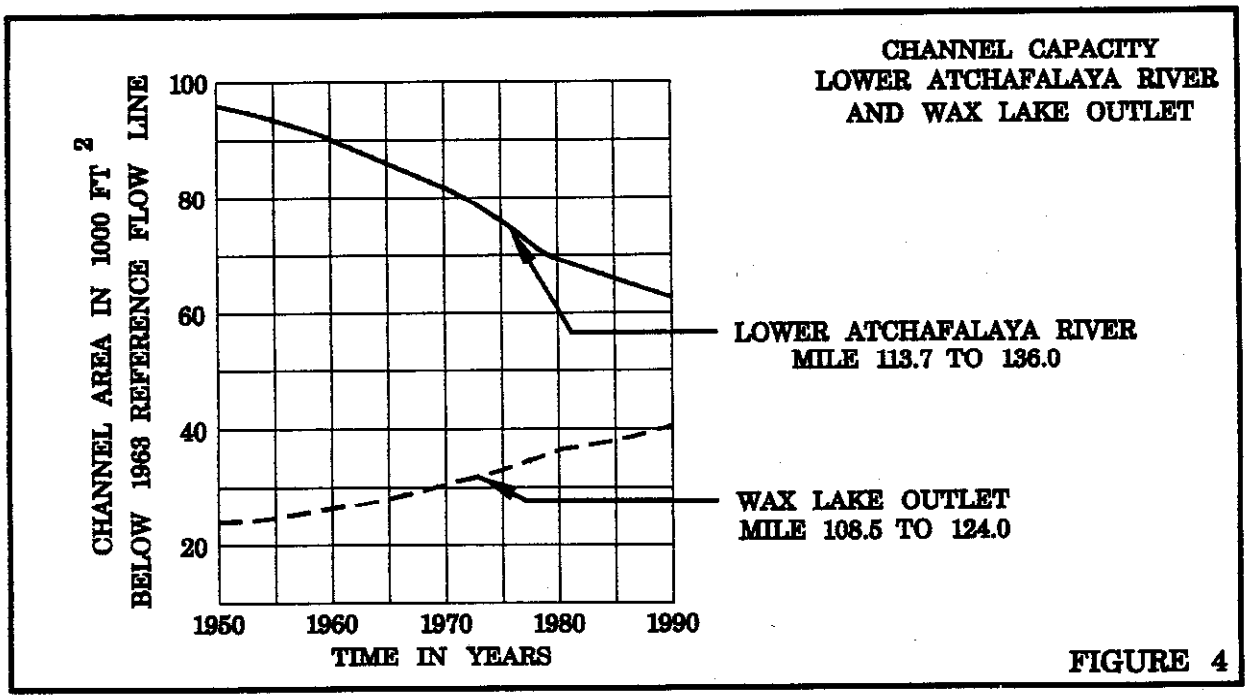

FIGURE 4

IMPACT AND SOLUTIONS

So, what are the consequences of all this deltaic activity? The most visible impact is the conversion of open water bodies such as Grand and Six Mile Lakes to land mass. The impact of the most concern to the Corps Mississippi River and Tributaries Project (MR&T) is the loss of flood flow capacity of the floodway and the resulting increase in the Project Design flowline and levee elevations. As an example of this increase due to sedimentation, Table 1 shows the design flood elevation at 3 points; Morgan City, LA, Myette Point and Bayou Sorrel Lock.

TABLE 1
Design Flood Elevations

	Morgan City			Myette Point			Bayou Sorrel Lock		
Year	1957	1963	1973	1957	1963	1973	1957	1963	1973
Stage ft. NGVD	13.0	14.1	17.4	19.4	22.4	25.5	23.0	25.2	27.7

As you can see there is a substantial rise in the flowline resulting in the protection levee having to be raised; a very costly item of work.

In addition to increasing the federal government costs to provide flood protection, sedimentation also results in the normal flow stages to be higher, particularly in the lower floodway basin and Morgan City area. As Figure 5 shows, the stages at Morgan City have risen several feet over time

for a flow of 240,000 cfs. This, in recent time, 1980's and into the 90's, is having a detrimental effect on the local economy. Many of the businesses that exist on the batture side of the levee/floodwall in Morgan City are now experiencing high water problems and lost revenues on a annual basis.

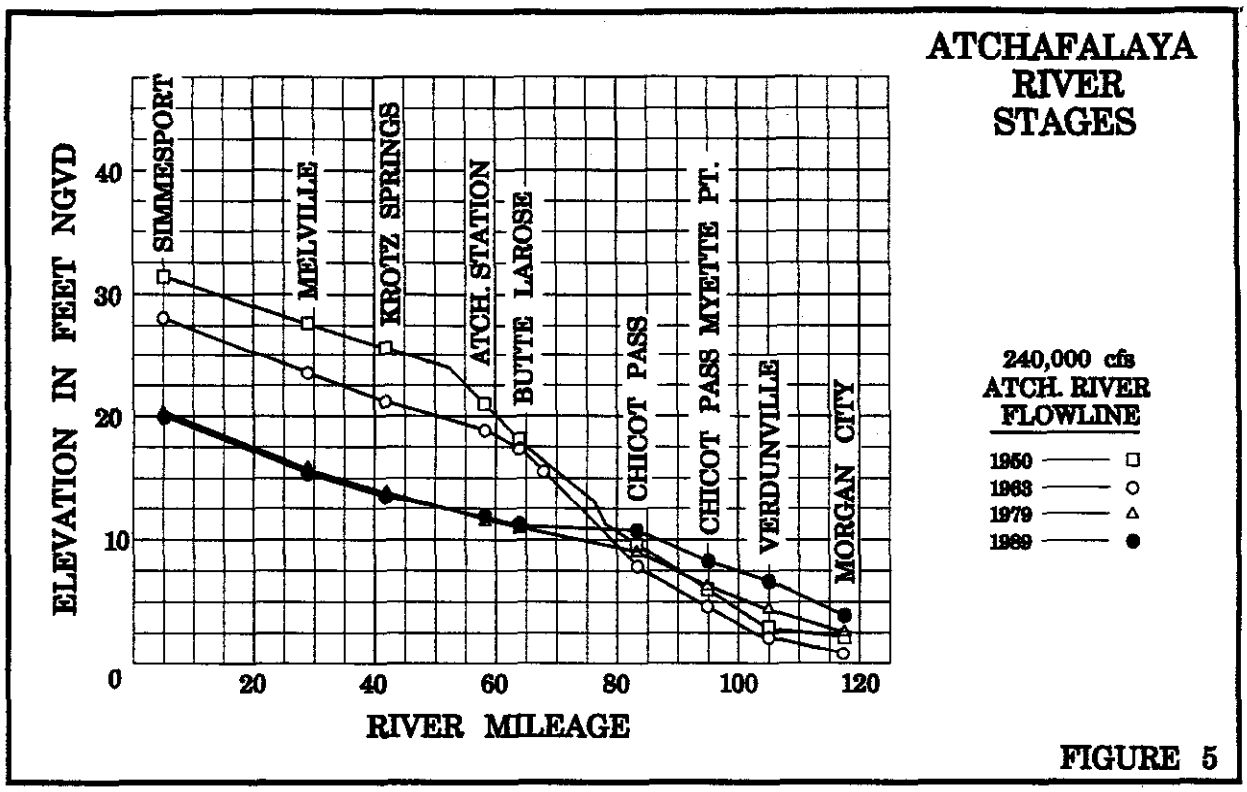

FIGURE 5

The increase in flood stages is one problem addressed by the Corps in the study, "Atchafalaya Basin Floodway System, Louisiana Feasibility Study", completed in 1982. The Corps recommended the following solutions:

1. Construct training works for the main channel from the end of the river levees to Myette Point. The training works would simulate the development of natural ridges, confining low to average flows to the main channel. This would accelerate the development of the main channel and reduce the amount of future overbank deposition. Construction of these training works commenced in 1990.

2. Construct a control structure at the head of Grand Lake to control the distribution of low to average flows between the Lower Atchafalaya River and Wax Lake Outlet. The Wax Lake Outlet Structure, completed in 1987, will prevent the increase in the capacity of Wax Lake Outlet at the expense of flood flow capacity of the Lower Atchafalaya River.

3. Realign major distributary channels in the middle basin to reduce the amount of sediment entering and depositing in the backswamps via these channels. Construction should commence in 1991.

CONCLUSION

1. The rapid acceleration of sedimentation in the lower basin is attributed to channel enlargement in the upper basin and transport of sediments normally deposited in the middle basin to the lower basin. The Atchafalaya River has filled the lakes in the lower basin, Grand and Six Mile Lakes, and is now building a delta in Atchafalaya Bay as it moves its channel into the Gulf of Mexico.

2. It is estimated that the Atchafalaya Bay will be filled beyond Point Au Fer Shell Reef by 2030.

3. The flow line for Project Flood should continue its upward migration for the next 50 years. The solutions proposed by the Corps will reduce some but not all of the increase in project flood stage.

4. Levees and floodwalls will need continual maintenance and improvement to offset the changes in elevation resulting from the delta deposits that have occurred and will continue to occur in the lower Basin and Atchafalaya Bay area.

REFERENCES

Latimer, Rodney A. and Schweizer, Chas. W., US Army Corps of Engineers, Mississippi River Commission, 1951, The Atchafalaya River Study.

US Army Corps of Engineers, New Orleans District, 1982, Atchafalaya Basin Floodway System, Louisiana Feasibility Study.

US Army Corps of Engineers, New Orleans District, 1985, Mississippi River and Tributaries, Atchafalaya Basin Floodway, LA, Design Memorandum No. 40, Wax Lake Outlet Control, General Design Memorandum.

US Army Corps of Engineers, New Orleans District 1988, Mississippi River and Tributaries, Atchafalaya Basin Floodway, LA, Design Memorandum No. 41, Channel Training above the Latitude of Morgan City, General Design Memorandum.

US Army Corps of Engineers, New Orleans District, 1989, Mississippi River and Tributaries, Atchafalaya Basin Floodway, LA, Design Memorandum No. 43, Cross Basin Channel Realignment, General Design Memorandum.

DENDROGEOMORPHIC ANALYSIS OF WETLAND SEDIMENTATION

By Cliff R. Hupp, U.S. Geological Survey, Water Resources Division, Reston, Virginia and David E. Bazemore, U.S. Geological Survey, Nashville, Tennessee

ABSTRACT

Dendrogeomorphic techniques were used to describe and interpret patterns of sedimentation rates at two forested wetland sites in West Tennessee. Over 50 sampling stations were established along transects up- and downstream from bridge structures, and 515 trees were examined for depth of sediment accretion and cored for age determination. Temporal variation in sedimentation rate may be related more to stream channelization and agricultural activity than to bridge and causeway construction. Sedimentation rates have increased substantially in the last 28 years, although channelized streams may have overall lower rates than unchannelized streams. Comparisons of sedimentation rates based on deposition over artificial markers (short term) to those determined from tree-ring analysis (long-term) indicate that rates and trends are similar where hydrogeomorphic conditions have not been altered substantially. Mean overall rates of sedimentation (between 0.24 and 0.28 centimeters per year) determined dendrogeomorphically are comparable to other published rates. Dendrogeomorphic techniques allow for the estimation of sedimentation over relatively long periods of time, and are reasonably accurate, simple, and provide information that is otherwise unobtainable.

INTRODUCTION

Relatively little quantitative information is available concerning sedimentation rates in forested wetlands, even though the sediment-trapping function of wetlands is commonly acknowledged. Quantitative studies on the fate of sediment, sediment budgets, and sediment routing in riverine and palustrine wetlands (Cowardin et al. 1979) are likewise rare. Sedimentation dynamics has been studied in relation to rising water levels in coastal Louisiana forests (Conner and Day 1988), and Boto and Patrick (1979) indicate that most studies have been of tidal marshes or aquatic beds and not in forested-freshwater wetlands. Furthermore, water-budget data are difficult to obtain and frequently contain substantial error (Winter 1981), and, as suggested by LaBaugh (1986), even the more comprehensive studies (Crisp 1966, Mitsch et al. 1979, Hemmond 1980, Verry and Timmons 1982) differ greatly in their hydrologic methods, assumptions, and interpretations. This lack of consistent mass-balance studies poses a substantial barrier to understanding the influence wetlands exert on water quality (LaBaugh 1986), including suspended-sediment transport and storage.

Rivers in the Mississippi embayment of the Gulf Coastal Plain transport generally high concentrations of suspended sediment due to channel instability and erodible uplands (Simon and Hupp 1987). Floods, extensive channelization, and long hydroperiods increase the likelihood of deposition of suspended sediments on flood plains and forested wetlands. Hupp and Morris (1990) have documented mean-annual sedimentation rates from 0.01 cm/yr on elevated parts of a wetland to 0.60 cm/yr in a slough adjacent to the Cache River in Arkansas.

The dual purposes of this paper are to present dendrogeomorphic analyses of the temporal variation in sedimentation rates in the vicinity of two selected causeway-bridge crossings in forested West Tennessee wetlands (Figure 1) and to demonstrate the utility of dendrogeomorphic evidence of sedimentation dynamics. From a larger study conducted to assess the effects of bridge crossings on wetland sedimentation, two sites were selected for presentation in this paper. The sites reported here are the largely unchannelized Hatchie River near State Route 54 and the channelized Big Sandy River near State Route 69 (Figure 1). These two rivers represent channelized and unchannelized rivers of West Tennessee, and together they reflect the overall sedimentation trends of this area (Bazemore and Hupp, this volume). This paper also serves a companion paper (Bazemore and Hupp, this volume) on the spatial aspects of sedimentation related to bridge construction.

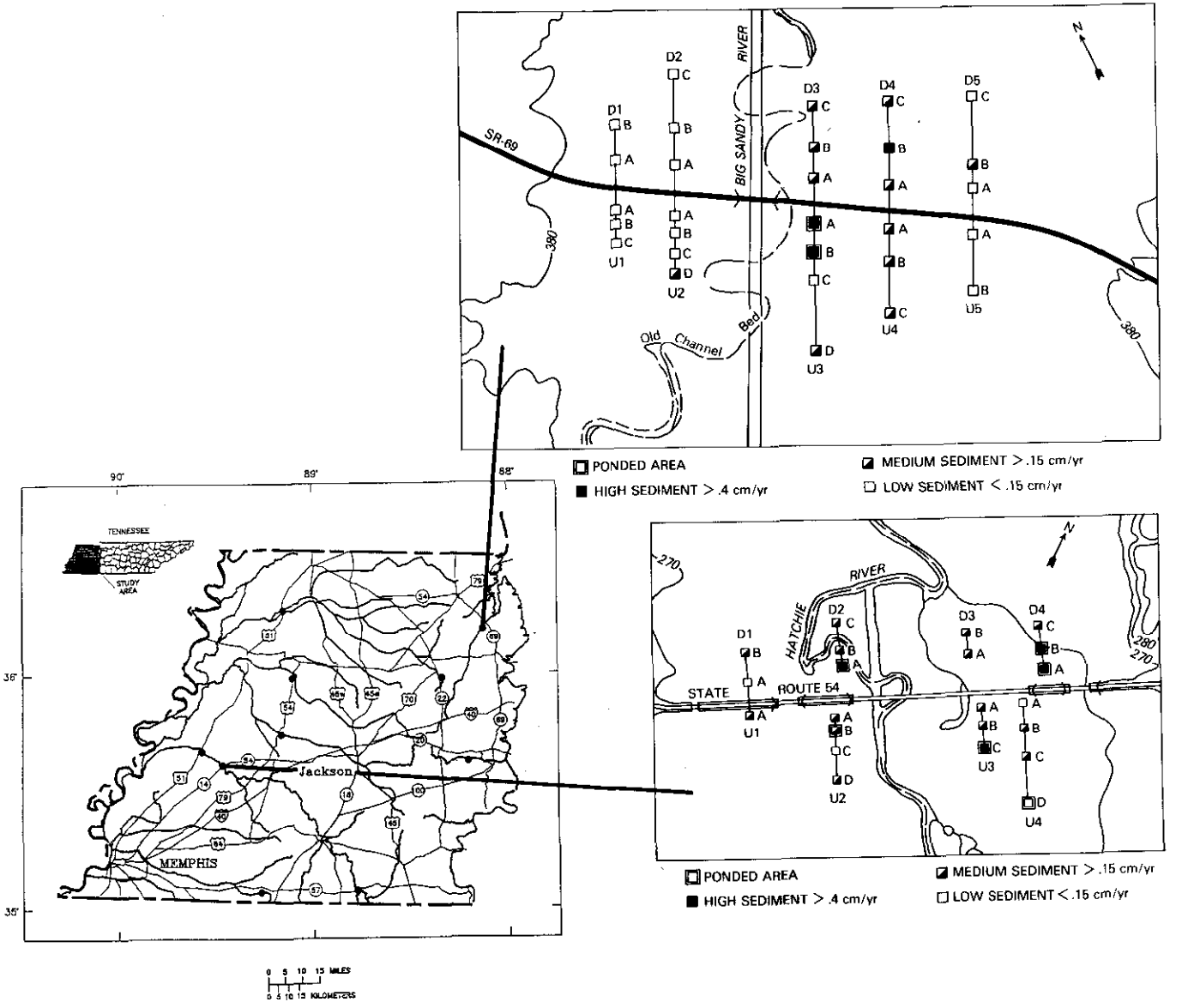

Figure 1. Location of study sites in West Tennessee and transects and stops at each site. General sedimentation rate is indicated at each stop.

Tree-ring analyses in wetlands are largely devoted to responses to frequency and magnitude of flooding (Mitsch and Rust 1984), long-term trends in runoff (Cleaveland and Stahle, 1989), species distribution in relation to hydroperiod (Bedinger 1971), nutrient cycling (Mitsch et al. 1979), or tree-growth models (Phipps 1979). Several studies have related tree growth (basal area increment) to nutrient enrichment (Brown 1981, Marois and Ewel 1983, Brown and van Peer 1989). Sigafoos (1964) and Everitt (1968) showed that point-sedimentation depths and rates on flood plains could be estimated by excavating "buried" trees and determining their age. This technique has been used extensively on the banks of channelized West Tennessee streams to estimate bank-accretion rates (Hupp 1987, 1988). These rates agree closely with those determined from cross-sectional analyses (Simon and Hupp 1987). Hupp and Morris (1990) used dendrogeomorphic techniques to estimate sedimentation rates in forested southeastern wetlands, and determined that rates were significantly related to local elevation, presence of sloughs or back swamps, and the timing of intensified agricultural production within the basin.

METHODS

Transects parallel to the stream and across the flood plain were established at the two study sites; four upstream and four downstream from State Route 54 on the Hatchie River, and six upstream and five downstream from State Route 69 on the Big Sandy River. Sampling stations along these transects provided sedimentation-rate information relative to distance from channel, distance from bridge structures, elevation, and topographic variation; 22 and 33 stations were sampled at the Hatchie and Big Sandy sites, respectively (Figure 1). Results of the spatial aspects are reported in Bazemore and Hupp (this volume).

Buried stems are the principal form of botanical evidence from which to estimate sedimentation rates. Initial tree roots grow just below the ground surface and eventually form the major root trunks that radiate from the germination point. The basal flare, or root collar and initial root zone are thus a distinctive marker of the original ground surface (Figure 2). A tree trunk subjected to substantial accretion typically has the appearance of a telephone pole (Figure 2).

Age determinations were made by extracting an increment core from the base of each tree. Ring counts made from the biological center (first year of growth) to the outside ring provide the tree age at the height of the coring. Depending on the difficulty of ring boundary determination, counts may be made in the field or the core may be returned to the laboratory for microscopic examination and crossdating (Cleaveland 1980, Phipps 1985). Duever and McCollom (1987) provide a thorough discussion on the use of ring counting as an alternative to more laborious dendrochronological techniques (Cleaveland and Stahle, 1989) that may be unnecessary in some cases. Most cores in the present study were crossdated.

Increment cores were taken from 6 to 13 trees at each sampling station. These cores were surfaced (sanded), cross-dated, and measured in the laboratory (Phipps, 1985). Each tree was excavated to its major radiating roots (Figure 2) and the depth of burial was measured. The depth of burial was divided by the tree age to obtain an estimated sedimentation rate (Figure 2). These values were averaged for each sampling station. Whenever possible, trees of various ages were sampled to determine temporal variation in sedimentation rates and to reduce the potentially disproportionate contribution of young trees to sedimentation rate determination.

Several schemes were used in an attempt to reduce tree-age data relative to mean sedimentation rate, including the subtraction of deposition depths of younger from older trees. The best method, however, was the simple separation of mean sedimentation rates determined from trees in various age classes. Although these dendrogeomorphic techniques have limitations, no other methodology provides long-term sedimentation-rate data in this detail.

Short-term rates of sedimentation were measured at most stations by placing a clay pad on the ground surface (Baumann, and others, 1984; Kleiss, and others, 1989). White powdered clay was poured onto a cleared 0.5 meter area to a depth of about 4 centimeters. This clay becomes a fixed plastic marker after absorption of moisture from the ground. All clay pads were left in place for at least one year and were subjected to several inundation events. These pads were subsequently examined to determine the depth of sediment over the marker layer. These data were compared to the long-term estimates from dendrogeomorphic analysis.

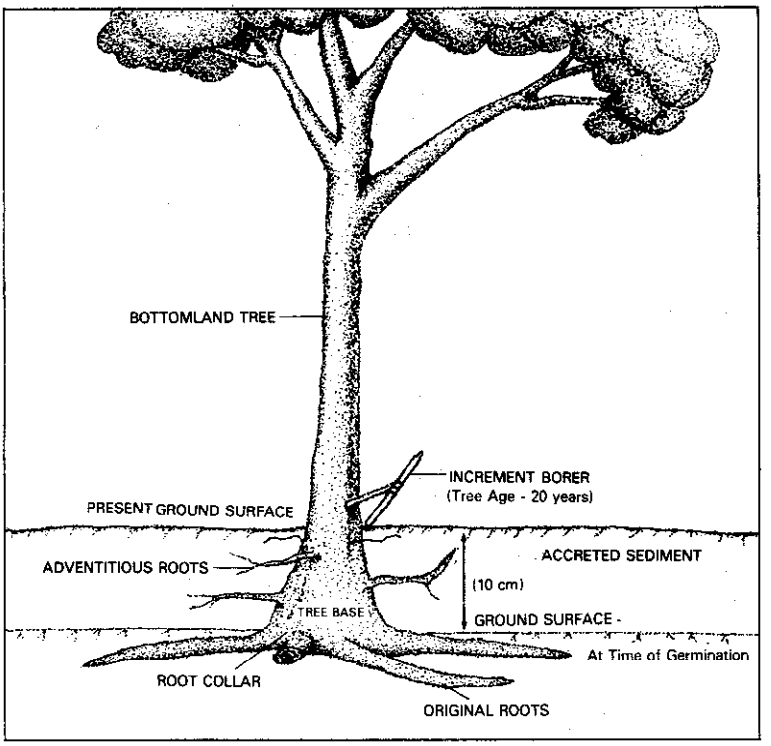

Figure 2. Generalized "buried" bottomland tree. As an example, excavation to original roots measures 10 cm of net deposition since germination, and tree-ring counting indicates tree is 20 years old. Therefore, estimated sedimentation rate in the general vicinity of the tree is approximately 0.5 cm/yr.

RESULTS AND DISCUSSION

Sedimentation rates along the Big Sandy River were generally lower than along the Hatchie River (Figure 1). Channelization typically reduces flood duration and would be expected to result in decreased deposition. Additionally, increased sedimentation was not observed upstream from the study sites, where backwater effects may increase sedimentation. Highest sedimentation rates on the Hatchie River (Figure 1) were nearest the channel or in old sloughs, while the highest sedimentation rates on the Big Sandy River occur on the right-bank flood plain in the general pre-channelization direction of flow (Figure 1). At both sites, sedimentation rate is strongly correlated with elevation, hydroperiod, topographic form, and degree of ponding (Bazemore and Hupp, this volume). Spatial aspects of wetland sedimentation are discussed more fully by Hupp and Morris (1990) and Bazemore and Hupp (this volume).

Temporal variation in sedimentation rate was observed at each site (Figure 3). In total, 515 variously aged trees were sampled, 237 and 278 at the Hatchie and Big Sandy sites, respectively. Tennessee Department of Transportation records indicate that a bridge was in place at the Big Sandy River site in 1922. However, the bed of a substantially older road crossing is about 100 meters downstream of the present structure; the fill of that bed is only 1.5 to 2 meters above the flood-plain surface. Channel work here was originally completed in 1918 with subsequent enlargement and drainage improvement in 1945. Two rather distinct drops in sedimentation rate (Figure 3) in the 1900-10 decade and the 1940-49 decade may be attributable to these two periods of channel work. The sharp rise in rates over the past 28 years may have resulted from agricultural increases in the basin or post-channelization system recovery (Simon and Hupp, 1987).

Tennessee Department of Transportation records indicate the present bridge and roadway were built in the early 1940's, at which time a loop cut off was constructed where the channel approaches the bridge. Apparently the bridge has had little influence upon subsequent sedimentation rates (Figure 3). Rates are relatively constant until about 1960 but increase thereafter, which coincides with the channelization of many Hatchie River tributaries and increased agriculture in the basin. This sharp increase in sedimentation rate (Figure 3) at both sites since about 1960 is likewise seen in several other streams in West Tennessee and Arkansas (Hupp and Morris, 1990).

The long-term dendrogeomorphic results and short-term clay-pad results (Figure 4) indicate that sedimentation rates are higher along the Hatchie River than along channelized reaches of the Big Sandy River. If there has been minor hydrologic alteration through dendrogeomorphic time, it is expected that these two techniques will yield roughly similar results, and this is the case for the Hatchie River site (Figure 4b). However, because the Big Sandy River site (Figure 4a) has experienced channelization, flood-plain ditching, and downstream dam construction, a wider disparity in the two techniques is expected at this site.

Mean overall rates of sedimentation were 0.24 cm/yr and 0.28 cm/yr for the Big Sandy and Hatchie Rivers, respectively. These values fall within the range of published sedimentation rates for bottomland-hardwood swamps (Boto and Patrick, 1978; Delaune and others, 1978; Mitsch and others, 1979; Johnson and others, 1984; Cooper and others, 1987). Studies conducted in Arkansas (Kleiss and others, 1989; Hupp and Morris, 1990) compared dendrogeomorphic techniques to artificial-marker techniques and also found close agreement. The direct measurement of sediment over markers provides precise, although short-term, values of local deposition. Although the precision of dendrogeomorphic techniques may still need testing and calibration, they provide a valuable, time-saving method for interpretation of relative differences in long-term sedimentation processes.

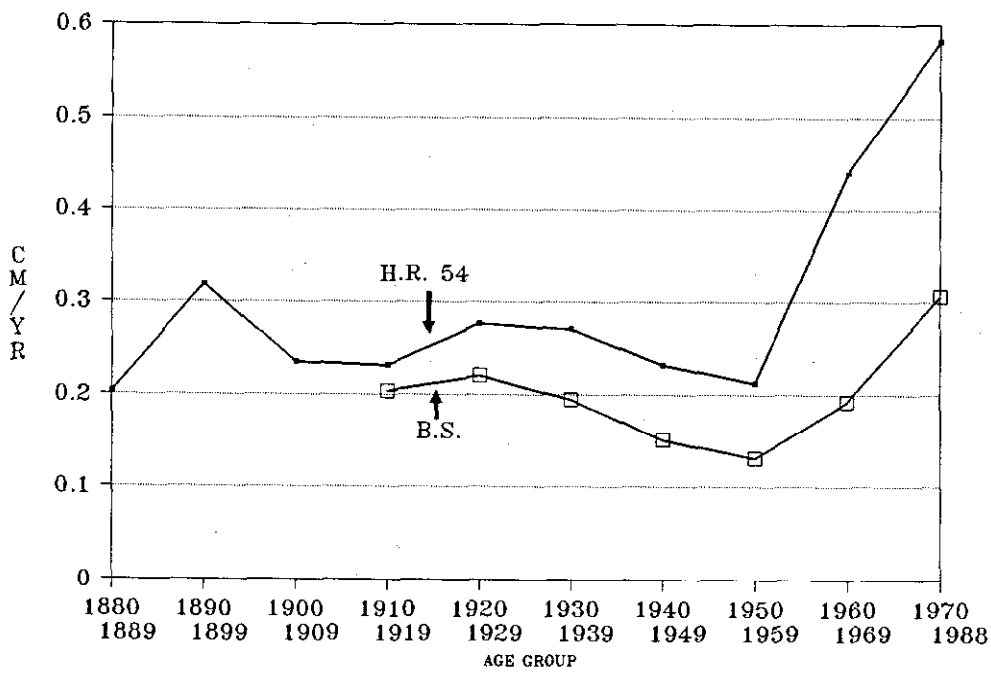

Figure 3. Sedimentation rates in centimeters per year by age group at the Hatchie and Big Sandy Rivers. H.R. 54 and B.S. refer to the Hatchie and Big Sandy Rivers respectively.

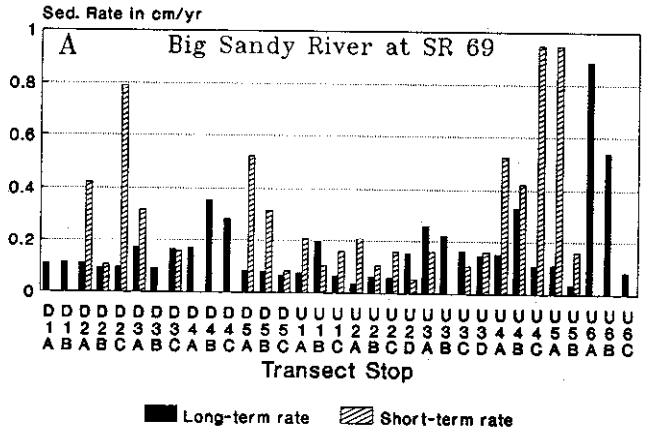

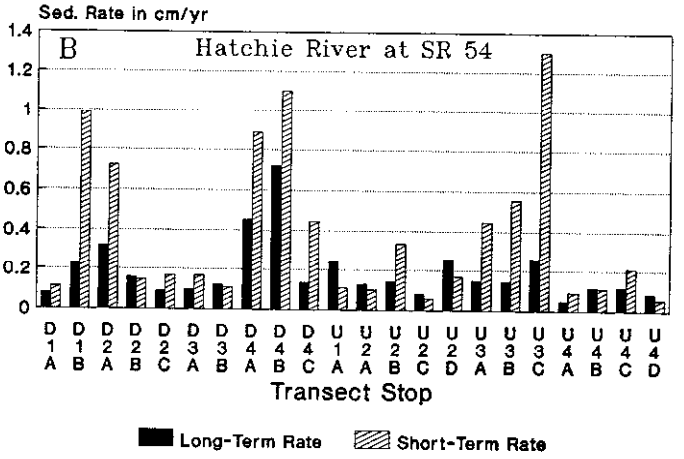

Figure 4. Long- and short-term sedimentation rates in centimeters per year by transect stop at the Big Sandy River (A) and at the Hatchie River (B).

REFERENCES

Baumann, R.H., J.W. Day, Jr, and C.A. Miller. 1984. Mississippi deltaic wetland survival: Sedimentation versus coastal submergence. Science 224:1093-1095.

Bedinger, M.S. 1971. Forest species as indicators of flooding in the lower White River Valley, Arkansas. U. S. Geological Survey Professional Paper 750-C, Washington, DC, USA.

Boto, K.G. and W.H. Patrick, Jr. 1979. Role of wetlands in the removal of suspended sediments. p. 479-489. In P. E. Greeson et al. (eds.) Wetland Functions and Values: State of Our Understanding, , American Water Resources Association, Minneapolis, MN, USA.

Brown, S. 1981. A comparison of the structure, primary productivity, and transpiration of cypress ecosystems in Florida. Ecological Monographs 51:403-427.

Brown, S. and R. van Peer. 1989. Response of pondcypress growth rates to sewage effluent application. Wetlands Ecology and Management 1:13-20.

Cleaveland, M.K. 1980. Dating tree rings in eastern United States, Dendrology in the Eastern Deciduous Forest Biome. Virginia Polytechnic Institute and State University, Blacksburg, VA, USA. Pub. FWS-2-80, p. 110-124.

Cleaveland, M.K. and D.W. Stahle. 1989. Tree-ring analysis of surplus and deficit runoff in the White River, Arkansas. Water Resources Research 25:1391-1401.

Cooper, J.R., J.W. Gilliam, R.B. Daniels, and W.P. Robarge. 1987. Riparian areas as filters for agricultural sediment. Soil Science Society of America Journal 51:416-420.

Conner, W.H. and J.W. Day, Jr. 1988. Rising water levels in coastal Louisiana: Implications for two coastal forested wetland areas in Louisiana. Journal of Coastal Research 4:589-596.

Cowardin, L.M., V. Carter, F.C. Golet, and E.T. LaRoe. 1979. Classification of wetlands and deepwater habitats of the United States. U.S. Fish and Wildlife Service, Washington, DC, USA. FWS/OBS-79/31.

Crisp, D.T. 1966. Input and output of minerals for an area of Pennine Moorland: The importance of precipitation, drainage, peat erosion, and animals. Journal of Applied Ecology 3:327-348.

DeLaune, R.D., R.J. Buresh, and W.H. Patrick, Jr. 1978. Sedimentation rates determined by 137 Cs dating in a rapidly accreting salt marsh. Nature (London) 275:532-533.

Duever, M.J. and J.M. McCollom. 1987. Trade-offs between the use of tree-counting and dendrochronology in ecological studies. p. 611-621, Proceedings of the International Symposium on Ecological Aspects of Tree-Ring Analysis, U.S. Department of Energy, Washington, DC, USA. CONF-8608144.

Everitt, B.L. 1968. Use of cottonwood in an investigation of the recent history of a flood plain. American Journal of Science 266:417-439.

Hemmond, H.F. 1980. Biogeochemistry of Thoreau's Bog, Concord, Massachusetts. Ecological Monographs 50:507-526.

Hupp, C.R. 1987. Determination of bank widening and accretion rates and vegetation recovery along modified West Tennessee streams. p. 224-233, Proceedings of the International Symposium on Ecological Aspects of Tree-Ring Analysis, U.S. Department of Energy, Washington, DC, USA. CONF-8608144.

Hupp, C.R. 1988. Plant ecological aspects of flood geomorphology and paleoflood history. p. 335-356. In V.R. Baker et al. (Eds.) Flood Geomorphology. John Wiley and Sons, Inc., New York, NY, USA.

Hupp, C.R., and E.E. Morris. 1990. A dendrogeomorphic approach to measurement of sedimentation in a forested wetland, Black Swamp, Arkansas. Wetlands, 10, 107-124.

Johnston, C.A., G.D. Bubenzer, G.B. Lee, F.W. Madison, and J.R. McHenry. 1984. Nutrient trapping by sediment deposition in a seasonally flooded lakeside wetland. Journal of Environmental Quality 13:283-290.

Kleiss, B.A., E.E. Morris, J.F. Nix, and J.W. Barko. 1989. Modification of riverine water quality by an adjacent bottomland hardwood wetland. p. 429-438. In D.W. Fisk (ed.) Wetlands: Concerns and Successes. American Water Resources Association Proceedings, Bethesda, MD, USA.

LaBaugh, J.W. 1986. Wetland ecosystem studies from a hydrologic perspective. Water Resources Bulletin 22:1-10.

Marois, K.C. and K.C. Ewel. 1983. Natural and management-related variation in cypress domes. Forest Science 29:627-640.

Mitsch, W.J., G.L. Dorge, and J.R. Wiemhoff. 1979. Ecosystem dynamics and a phosphorus budget of an alluvial swamp in southern Illinois. Ecology 60:1116-1124.

Mitsch, W.J. and W.G. Rust. 1984. Tree growth responses to flooding in a bottomland forest in northeastern Illinois. Forest Science 30:499-510.

Phipps, R.L. 1979. Simulation of wetlands forest vegetation dynamics. Ecological Modeling 7:257-288.

Phipps, R.L. 1985. Collecting, preparing, crossdating, and measuring tree-increment cores. U.S. Geological Survey Water Resources Investigations Report 85-4148, Washington, DC, USA.

Sigafoos, R.S. 1964. Botanical evidence of floods and flood-plain deposition. U.S. Geological Survey Professional Paper 485-A, Washington, DC, USA.

Simon, A. and C.R. Hupp. 1987. Geomorphic and vegetative recovery processes along modified Tennessee streams: An interdisciplinary approach to disturbed fluvial systems. p. 251-262. In International Association of Hydrological Sciences (IAHS) Publication No. 167.

Verry, E.S. and D.R. Timmons. 1982. Waterborne nutrient flow through an upland-peatland watershed in Minnesota. Ecology 63:1456-1467.

Winter, T.C. 1981. Uncertainties in estimating the water balance of lakes. Water Resources Bulletin 17:82-115.

BOTTOMLAND SEDIMENTATION NEAR HIGHWAY CROSSINGS

By David E. Bazemore, Hydrologist, U.S. Geological Survey, Nashville, Tennessee and Cliff R. Hupp, Botanist, U.S. Geological Survey, Reston, Virginia

ABSTRACT

Highway crossings have been suggested to cause increased rates of sedimentation upstream of bridge and causeway structures. Comparisons between fine-grained deposition rates upstream and downstream from bridge and causeway structures at 11 bottomland sites in West Tennessee did not indicate higher upstream sedimentation rates. At seven sites, upstream deposition rates were not significantly different from downstream rates, and downstream rates were higher at the remaining four study sites. Silt and clay deposition rates were correlated with surface elevation at four sites and with flood-plain ponding at five sites. Channelization history may also affect rates of bottomland sedimentation. No evidence was found to support the suggestion that higher sedimentation rates occur upstream because of backwater created by highway crossings. Sand splays, which were typically observed downstream from bridges and along downstream channels, appeared related to flow constrictions by highway causeways, constructed levees, and spoil banks.

INTRODUCTION

This report describes sedimentation rates on eleven bottomland study sites in West Tennessee. The purpose is to test the hypothesis that sediment-deposition rates are higher upstream from highway crossings than downstream. Higher rates upstream would be expected if backwaters from highway crossings trap sediments. Accelerated sediment deposition rates are of concern because of the possible harmful effects on bottomland (wetland) environments.

The eleven study sites are in West Tennessee, which is in the Mississippi embayment and part of the Gulf Coastal Plain province (Fig. 1). Unchannelized rivers in West Tennessee generally have low gradients, with meandering, alluvial channels and broad, relatively flat flood plains and terraces. Bottomlands in this region typically support bottomland-hardwood forests, cypress-tupelo swamps, and marshes. Three of the study sites are on the Hatchie River (Fig. 1), which is mostly unchannelized although some reaches near bridges have been straightened, as have most tributaries. The remaining study sites are on rivers channelized in the early 1900's and dredged periodically since then (Fig. 1).

Highway crossings at the study sites include causeways (embankments) that transverse flood plains and bridge structures that cross river channels. Roadway embankments at eight of the study sites have been in place since the early 1900's. Two study sites, Beaver Creek at State Route 1 and Obion River at State Route 3, are the only sites with recently constructed roadway embankments, completed in 1988 and in 1978 respectively.

Rivers in West Tennessee transport some of the highest concentrations of suspended sediment in the United States (Milliman and Meade, 1983; Trimble and Carey 1984). Suspended-sediment concentrations and, by extension, availability of sediment for deposition, are nevertheless highly variable for West Tennessee streams. Variation is greatest on adjusting, channelized streams. Sediment discharges vary systematically with the stages of channel evolution, and vary by as much as a factor of ten (Simon, 1989); a six-stage model of channel evolution following channelization was developed by Simon and Hupp (1987).

Few investigators have reported rates of sediment deposition within bottomland wetlands (Boto and Patrick, 1979). Mitsch and others (1979), using sediment traps, estimated an average rate of less than 0.2 centimeters per year in a cypress tupelo swamp in southern Illinois. Johnston and others (1984) reported natural levee deposition rates of 2.62 centimeters per year for a stream in Wisconsin, based on ^{137}Cs dating, but did not estimate deposition rates over a broad extent of the wetland. Cooper and others (1987) used ^{137}Cs dating techniques to estimate deposition rates of less than 0.26 centimeters per year for a flood-plain swamp in North Carolina. Hupp and Morris (1990) report mean deposition rates of 0.34 centimeters per year for sloughs and 0.07

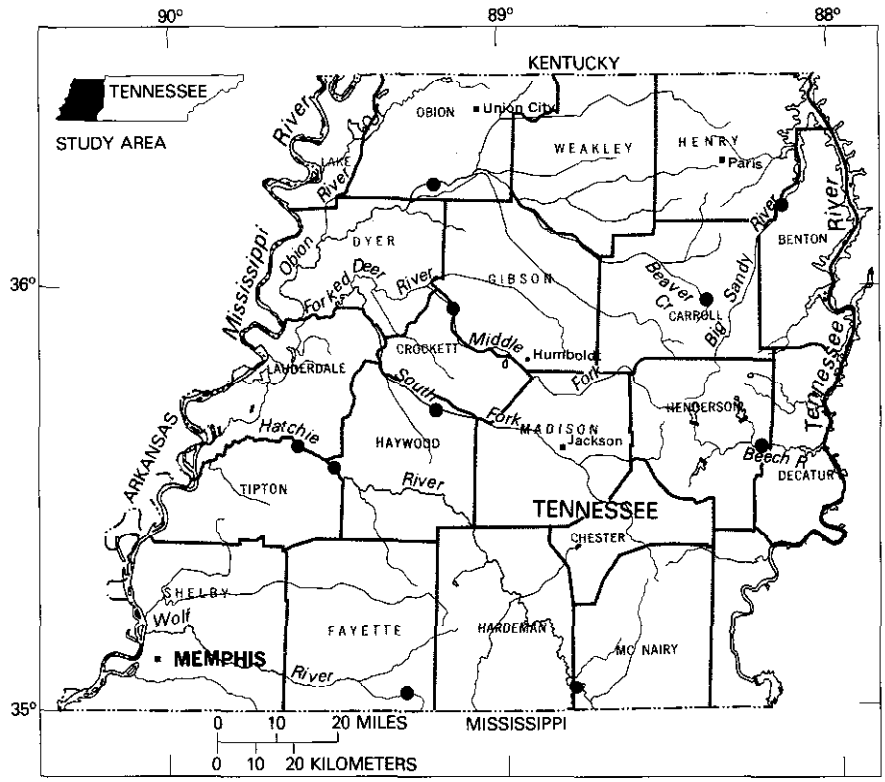

Figure 1. Location of wetland study sites in West Tennessee.

centimeters per year for "islands" (elevated portions of the flood plain) in a forested wetland on the Cache River, Arkansas. Average rates of deposition for the present study fall within the above published ranges.

APPROACH

Rates of fine-grained deposition were measured on flood plains upstream and downstream from highway crossings using the geomorphic and tree-ring techniques described by Hupp and Bazemore (this volume). Sampling transects were established over the broad extent of flood plains but were not typically located within 100 meters of stream channels (Hupp and Bazemore, this volume). This sampling design was used to determine the spatial distribution of fine grained (silt, clay, and very fine sand) sediments. Sand splays were observed on most flood plains downstream of the highway crossing; several areas were sampled for rate of sand deposition. Sand deposition was not included in the upstream and downstream comparisons.

Several factors determine sediment concentrations available for deposition: drainage area, drainage density, geology of the source area, land use above the site, and channelization. These factors were assumed to be constant among sampling stations at a given study site. However, surface elevations and ponding characteristics are distinctly variable among sampling stations at a given study site and these variables were considered in the evaluation of sedimentation rates. Elevation data were adjusted for down-valley slope.

Deposition rates upstream from highway crossings were compared to downstream rates (H_0 = there is no difference between upstream and downstream sedimentation rates) in the following ways: 1) T-tests were preformed on the ranks of the deposition data sorted by location upstream or downstream from highway crossings at each site. 2) At sites in which deposition rates correlated with elevation above the stream channel, data were sorted by elevation groups (equal increments) before upstream-downstream comparison tests were preformed (two-way factorial analysis of variance on ranks of deposition rates). 3) At sites where high rates of deposition were measured in locally ponded areas, data were sorted by ponding category (ponded or well drained) before upstream-downstream comparison test were preformed (two-way factorial analysis of variance on ranks of deposition rates).

RESULTS AND DISCUSSION

Simple comparisons show no tendency (alpha = 0.05) for higher deposition rates of fine-grained material upstream from highway crossings (Fig. 2). Four of the 11 study sites have significantly higher downstream rates (alpha = 0.05). This comparison does not take into account variation in deposition rates that may be associated with variation in flood-plain elevation above the stream channel or with flood-plain ponding. The lack of evidence for higher deposition rates upstream of highway crossings suggest no substantial sediment trapping results from backwater. Hydraulic modelling conducted at these sites (T. H. Diehl, written communication, 1990) suggests that there is minor backwater created by the highway crossings.

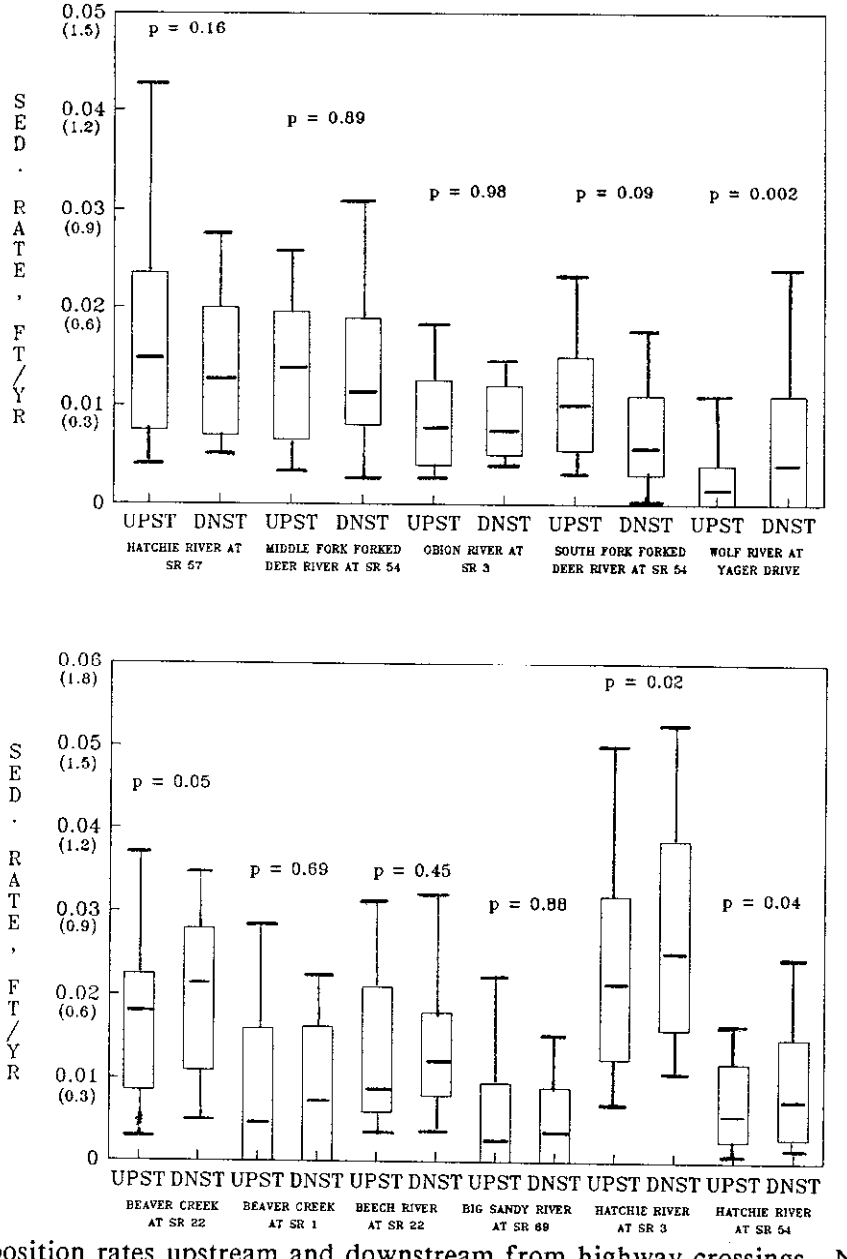

Figure 2. Deposition rates upstream and downstream from highway crossings. Numbers in parentheses on Y axis are centimeters per year. Significance levels of difference between rates are indicated by p-values from t-tests on ranks of deposition rates. * Indicate significant (alpha = 0.05) differences in deposition rate. From top of box plots, the 90, 75, 50 (median), 25, and 10 percentiles are shown.

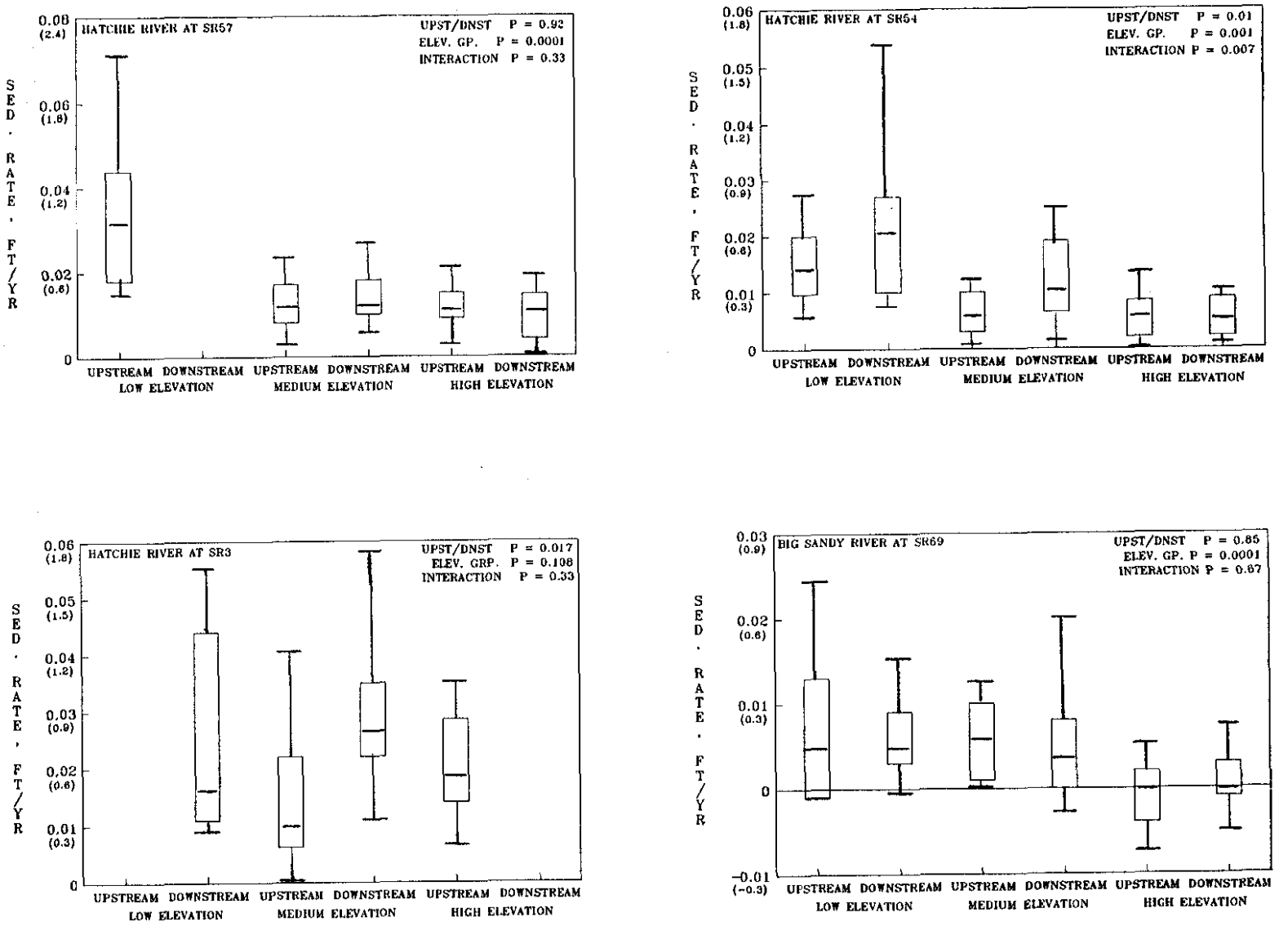

Figure 3. Rates of sediment deposition upstream and downstream from highway crossings by elevation groups; p-values indicate significance levels.

Four of the study sites show a significant inverse correlation (alpha = 0.05) between sediment deposition rates and elevation of the flood plain (Fig. 3). No sites show a tendency for higher upstream deposition rates within the elevation categories. Two of the four sites have significantly higher downstream rates (alpha = 0.05) within the elevation categories (Fig. 3).

High deposition rates are positively correlated with flood-plain ponding (alpha = 0.05) at five of the study sites, but upstream-downstream differences within ponding categories are observed at only two of the sites (Fig. 4). Downstream rates are significantly higher at the Wolf River site (alpha = 0.05) and higher downstream rates at the Hatchie River site are nearly significant (p = 0.055). In general, high rates of sedimentation are associated with low locally ponded areas. In particular, sloughs and back swamps may experience the highest sedimentation rates.

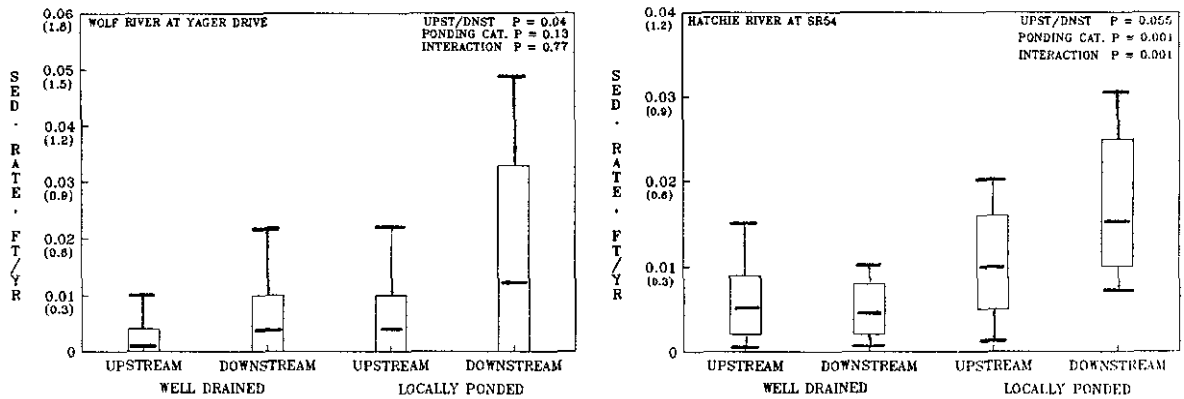

Figure 4. Rates of sediment deposition upstream and downstream from highway crossings by localized ponding category; p-values indicate significance levels.

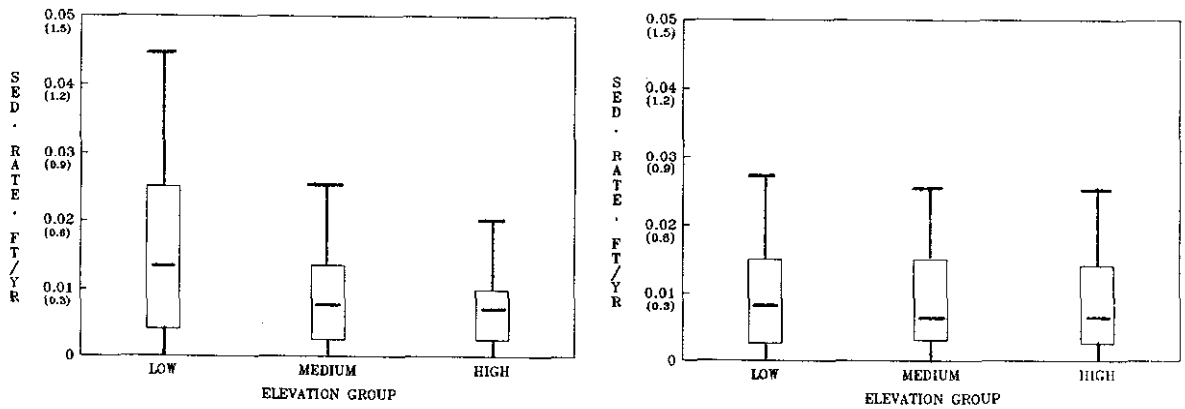

Figure 5. Rates of sediment deposition by elevation group for (A) sites on unchannelized rivers and (B) sites on channelized rivers. Differences among elevation groups are significant (p = 0.0001) on unchannelized sites (A), whereas they are insignificant (p = 0.38) on channelized sites (B).

Highway crossings may have opposite or variable effects on the upstream and downstream flood plains that mask trends for higher rates in either direction. Accelerated velocities near the upstream bridge openings increases erosion locally. Flows downstream from bridge openings may transport increased concentrations of fine-grained sediments for flood-plain deposition. Increased sediment concentrations may result in the slightly higher downstream rates observed at some study sites (Fig. 2).

Deposition rates are more spatially consistent along unchannelized streams than on channelized streams. For example, deposition rate and flood-plain elevations are more strongly correlated for the unchannelized streams (Fig 5). Stronger correlations on the unchannelized streams may be prevented by localized channel work and ditches. Additionally, sedimentation rates may vary substantially depending on stage of channel evolution (Simon and Hupp, 1987) following stream modifications. Beaver dams may complicate the understanding of sedimentation variation, regardless of channelization history.

Deposition of sand splays on flood plains was typically observed downstream from bridge crossings. Rates of deposition were measured at four sampling stations in sand-deposition areas at two of the study sites. Average rates of sand deposition ranged from 1.97 centimeters per year to 2.30 centimeters per year. At the study site on Big Sandy River sand splays one to two feet in height were observed as far as 650 meters downstream from the bridge opening, extending as far as 45 meters from the channel. Flows are constricted at the Big Sandy site by the highway crossing and by spoil banks parallel to the channel.

Increased velocity and turbulence due to flow constrictions by highway crossings, levees, and spoil banks locally increase the capability of the resulting flows to transport sand. Levees or spoil banks parallel to channels create a flow gradient between the channel and flood plain. This effect can extend much farther downstream than the effect of the constricted opening at the highway crossing.

CONCLUSIONS

Deposition rates of fine-grained sediments were not significantly greater along reaches upstream than downstream reaches from highway crossings. Four of the 11 study sites had higher rates downstream. Rates of deposition are inversely correlated with flood-plain elevation at four of the nine study sites. At five sites, high deposition rates were found in ponded areas. Unchannelized streams may experience less spatial variation in deposition than channelized streams. Sand splays downstream from bridge openings at most sites may be related to flow constrictions in turn caused by a combination of highway embankments and spoil banks (or levees) parallel to channels.

REFERENCES

Boto, K.G., and Patrick, W.H., Jr.. 1979, Role of wetlands in the removal of suspended sediments. p. 479-489. In P. E. Greeson and others (eds.) Wetland Functions and Values: State of Our Understanding, American Water Resources Association, Minneapolis, MN, USA.

Cooper, J.R., Gilliam, J. W., Daniels, R. B., and Robarge, W.P.. 1987, Riparian areas as filters for agricultural sediment. Soil Science Society of America Journal 51, 416-420.

Hupp, C.R., and Morris, E.E., 1990, A dendrogeomorphic approach to measurement of sedimentation in a forested wetland, Black Swamp, Arkansas. Wetlands 10, 1-18.

Hupp, C.R., and Bazemore, D.E., 1991, Dendrogeomorphic analysis of wetland sedimentation. This Volume.

Johnston, C.A., Bubenzer, G. D., Lee, G. B., Madison, R. W., and McHenry, J. R., 1984, Nutrient trapping by sediment deposition in a seasonally flooded lakeside wetland. Journal of Environmental Quality 13, 283-290.

Milliman, J. D. and Meade, R. H., 1983, World-wide delivery of river sediment to the oceans. Journal of Geology 91, 1-21.

Mitsch, W. J., Dorge, G. L., and Wiemhoff, J. R., 1979, Ecosystem dynamics and a phosphorus budget of an alluvial swamp in southern Illinois. Ecology 60, 1116-1124.

Simon, A., 1989, A model of channel response in disturbed alluvial channels. Earth Surface Processes and Landforms 14, 11-26.

Simon, A., and Hupp, C. R.. 1987, Geomorphic and vegetative recovery processes along modified Tennessee streams: An interdisciplinary approach to disturbed fluvial systems. IAHS-AISH Pub. No. 167, 251-262.

Trimble, S. W. and Carey, W. P., 1984, Sediment characteristics of Tennessee streams and reservoirs. U. S. Geological Survey Open-File Report 84-749, pp. 32.

FLOW AND SEDIMENT TRANSPORT IN ROUGH CHANNELS

By Jonathan M. Nelson, William W. Emmett, and J. Dungan Smith, Hydrologists, U.S. Geological Survey, Water Resources Division, Lakewood, Colorado

ABSTRACT

A theoretical method for relating stage and sediment discharge to flow discharge in streams with large relative roughness is tested using a comprehensive set of data from a small stream in Wyoming. The method is composed of two elements. First, a stage-discharge relation is determined for a given channel geometry. This requires that the variation in the hydraulic roughness be calculated as a function of discharge. This is accomplished by using measured sediment sizes in conjunction with a simple model for the extraction of momentum associated with flow around and over sediment particles on the bed. The technique is developed herein for the case where grain roughness is the dominant part of the total channel drag, although the approach may be combined with other roughness models for channels where other sources of drag are important. The computed variation in the velocity profile with stage is used with a steady, uniform flow model to compute a stage-discharge relation and a boundary shear-stress distribution in the study reach. The second element consists of the computation of sediment discharge from known particle-size distributions and the calculated boundary shear stress. This is accomplished using existing models for the critical shear stress and transport rate of sediment on poorly sorted beds.

The method is tested using channel geometry and sediment size information from a reach of Little Granite Creek, a small stream located in the Bridger-Teton Forest about 40 km southeast of Jackson, Wyoming. Little Granite Creek is a tributary to Granite Creek, which flows into the Hoback River, a tributary to the Snake River. The availability of extensive flow and sediment-transport measurements in this channel provides an excellent opportunity to test the above-described technique. The study reach is about 100 m long, 7 m wide, and has a bed slope of 0.0175. The median bed sediment size, D_{50}, is about 10 cm and D_{84} is about 20 cm. The depth at bankfull discharge determined from a field survey of channel geometry is approximately 1 m, so even at the highest flows, many of the sediment particles on the bed are a large fraction of the flow depth in size. Computed flow and sediment transport rating curves show good agreement with measured data. Although further verification is necessary, the approach appears promising, especially considering that all the information necessary to apply the model to a channel like Little Granite Creek could be collected in a single day (a pebble count, a survey of the cross-section at the gage, and a survey of channel slope).

INTRODUCTION

River and stream channels often have beds consisting of particle sizes that are a significant fraction of the flow depth, particularly in steep, mountainous regions. Most of the present understanding of the vertical structure of turbulent flow over hydraulically rough channel beds, however, proceeds from the initial work of Nikuradse [1933] and is valid relatively far from the roughness elements on the boundary. In this situation, roughness can be adequately treated using a representative roughness length in conjunction with a quasi-logarithmic velocity profile. This approach is not valid in regions of the flow where momentum fluxes and pressure forces associated with obstacles on the bed play a significant role in the local momentum balance. Thus, the vertical flow structure and the relation between bottom stress and velocity are not well predicted in channels with high relative roughness and, as a result, several important problems related to the flow and sediment transport in these streams are poorly characterized.

The purpose of this paper is to present results from a test of a predictive model for computing flow and bedload sediment transport rating curves in high-roughness channels. Although this information can be developed empirically, doing so accurately requires an extensive data set gathered over a relatively long period, so the value of a predictive model is clear. Furthermore, the results of a carefully tested model can be extrapolated to examine the impacts of relatively rare events or to evaluate the long-term effects of natural or manmade changes in streamflows (e.g., dams and diversions).

The goals of the modeling approach used herein are to provide two essential relations, one beween stage and

flow discharge and the other between flow discharge and sediment discharge. The stage-discharge relation is determined for a given channel geometry and bed particle-size distribution. For channels with beds composed of sediment with sizes that are a significant fraction of the flow depth (more than about 5%), the vertical structure of the flow must be calculated in a manner that includes the extraction of momentum associated with flow around and over sediment particles on the bed. Because the relative protrusion of the particles into the flow varies significantly with flow depth, the computed vertical structure also will vary with flow depth. As the flow becomes very deep, the vertical structure over most of the flow depth will asymptotically approach a quasi-logarithmic profile. At shallower depths, the flow structure will vary in a relatively complicated manner as a function of the grain geometry on the bed. This means that approaches using constant friction or Manning coefficients cannot yield valid predictions of the stage-discharge relation. In addition, even for situations where the roughness variation is relatively small over the range of discharges observed, it is typically difficult to make visual estimates of Manning coefficients, as discussed by Jarrett [1989]. Using the method described below, the variation in velocity structure is computed and a relation between the velocity profile and the depth is found using information that is relatively easy to measure. This, in turn, is used along with the stream geometry to obtain a stage-discharge relation. The computation also provides a link between discharge and the boundary shear stress distribution on the channel bed. That relation is used to fulfill the second objective, which is to compute the bedload flux for each flow discharge. This is accomplished using existing equations for bedload fluxes and critical shear stresses on poorly sorted gravel beds. Preliminary testing of this technique is carried out using a comprehensive data set from Little Granite Creek, Wyoming.

DEVELOPMENT OF THE MODEL

The Flow Model

The local momentum balance in flows over rough beds is typically dominated by large convective accelerations and complex turbulence fields. As a result, there is at present no computational flow model capable of making accurate predictions of local flow characteristics (e.g., velocity or Reynolds stress at a point) in channels with beds made up of particles that are large relative to flow depth. However, for practical purposes, local flow characteristics usually are not of interest, and the real goal of a model must be to reduce the complexity of the local, highly stochastic problem to some simpler, spatially averaged characterization. In a spatially averaged sense, the momentum balance in rough channels is between gravitational force (or, equivalently, pressure gradient) acting to accelerate the flow and drag on the bed tending to decelerate the flow. Thus, in a channel of uniform cross section and average bed slope, but with a highly irregular bed in a local sense, the spatially averaged momentum balance is between the stress divergence and the pressure gradient. This leads to the following expression for the vertical distribution of the spatially averaged stress [Tennekes and Lumley, 1972, p. 150, and Middleton and Southard, 1984, pp. 97-118]:

$$\tau_{xz}(z) = \tau_b \left(1 - \frac{z}{H}\right) \tag{1}$$

where τ_{xz} is the stress on a horizontal plane acting to transfer momentum in the vertical, z is the vertical coordinate, and H is the flow depth. The boundary shear stress ($\tau_{xz}(0)$), is given by

$$\tau_b = \rho g H S \tag{2}$$

where ρ is fluid density, g is gravitational acceleration, and S is the magnitude of the water-surface slope.

Following the technique developed by Wiberg and Smith [1987a, 1990], the total stress is divided into two components: the actual fluid stress τ_f, and a surrogate stress associated with the drag on sediment particles acting as obstacles to the flow. If the drag stress is denoted τ_d, the fact that the water surface is unstressed can be used to rewrite τ_{xz} as follows:

$$\tau_{xz}(z) = \tau_f(z) + \left(\tau_d(z) - \left(\tau_d\right)_s\right) \tag{3}$$

where $\left(\tau_d\right)_s$ is the drag at the surface produced by particles protruding through the water surface. The drag on particles in the flow can be calculated using a simple drag law in conjunction with empirical drag coefficients

using the following expression:

$$\tau_d(z) = \sum_i \frac{1}{2} \rho C_d U_r^2 \frac{A_i}{A_b} \tag{4}$$

where the reference velocity U_r is given by

$$U_r = \frac{1}{A_i} \int_{A_i} u(z)\, dA \quad . \tag{5}$$

In the above equations, A_i is the cross-sectional area of a particle perpendicular to the flow, A_b is the area of the bed occupied by the particle, and the sum is over all particles comprising the bed. The spatially averaged vertical profile of streamwise velocity is given by u(z), and the drag coefficient, C_d, is determined as a function of Reynolds number for spheres [Schlicting, 1979; Flammer et al., 1970]. While the approximation that sediment particles have drag coefficients of spheres may not be ideal, drag coefficient in the Reynolds similarity range vary from about 0.5 for spheres to 1.0 for cylinders, and sensitivity analyses indicate that the model predictions are not sensitive to this range of values.

To close the set of equations above, the shear is related to the stress profile by using an eddy viscosity K_t:

$$\tau_{xz}(z) = \rho K_t \frac{\partial u}{\partial z} \quad . \tag{6}$$

The eddy viscosity is composed of a velocity scale U_t and a length scale L_t for the turbulence acting to exchange momentum in the vertical direction:

$$K_t = U_t L_t \tag{7}$$

In boundary-layer flows with roughness elements very small compared to the flow depth, Rattray and Mitsuda [1974] found that the best-fit eddy viscosity was given by

$$K_t = \begin{cases} k u_* z \left(1 - z/H\right) & z \le 0.2H \\ k u_* H / 6.24 & z > 0.2H \end{cases} \tag{8}$$

where $u_* = (\tau_b/\rho)^{1/2}$ and k is von Karman's constant (=0.40). In their original development of this approach for rough beds, Wiberg and Smith [1987a] hypothesized that the velocity scale for the turbulence should be given by a local fluid shear velocity:

$$U_t = \left(\frac{\tau_f}{\rho}\right)^{1/2} \quad . \tag{9}$$

At depths well above the sediment particles on the bed, $\tau_d = 0$ and the eddy viscosity of equation (8) is valid. Near the bed, U_t can be calculated by solving equation (3) for the fluid stress and using equation (9). Determining the length scale of the turbulence near the particles requires a separate assumption. Wiberg and Smith [1987a, 1990] used a concentration-weighted average of the length scale from the Rattray-Mitsuda [1974] eddy viscosity (eq. 8) and 0.40 times the average particle diameter at that level. Because this combination of length scales was weighted by the concentration of various particle sizes at different levels in the flow, the result of that approach is that the turbulent length scale returns to the smooth bed profile at the top of the grains on the bed. Because τ_d also goes to zero above the bed particles, the eddy viscosity will follow the Rattray-Mitsuda profile from the top of the particles to the water surface, and the vertical velocity profile in this region will be unaffected by the particles. Flume measurements made by J. Nelson and P. Whiting [pers. comm.] indicate that the spatially averaged vertical velocity profiles are altered by the bed roughness to a height of 2 to 4 grain diameters above the largest particles on the bed surface. In view of this observation, the results presented herein use a modified turbulent length scale from the average zero-level of the bed up to a height of 3 D_{84}. In this region, the turbulence is primarily associated with the wakes of particles, so the length scale can be set using results from wake theory and measurement. Schlicting [1979, p. 739-743] demonstrated that the turbulent length scale in a wake is proportional to the wake height, b:

$$L_t = 0.18\,b \quad . \tag{10}$$

Relating the wake height to the characteristic particle diameter precisely in a complex situation with interacting wakes is beyond our present understanding of these flows. Ultimately, the relation between near-bed turbulent length scales and particle-size distributions must be determined with careful experiments, and work of this nature is ongoing [J. Nelson and P. Whiting, pers. comm.]. The wake heights, however, must scale roughly with particle size, and this assumption is used herein. Because larger particles are more effective at producing turbulence, one can expect the momentum-defect weighted average of length scales to be skewed toward the larger sizes on the bed. Given the crude present understanding of this problem, it is probably appropriate to assume that the turbulent length scale near the bed is given by

$$L_t = 0.18\,D_{84} \qquad z \leq 3\,D_{84} \quad . \tag{11}$$

This assumption is used herein to set the turbulent length scale below $2D_{84}$. Above $4D_{84}$, the length scale associated with equation (8) is used. The length scales are matched smoothly between $2D_{84}$ and $4D_{84}$. In channels with low roughness, where equation (8) is valid, a logarithmic profile can be expected to occur only up to about 20% of the flow depth. Thus, if the influence of bed particles is felt to a height of $3D_{84}$ (or $4D_{84}$ for the smoothly matched length scale), logarithmic segments of velocity profiles can be expected to occur only in flows deeper than about $15D_{84}$.

Although the length of this paper precludes a detailed description of the numerical solution of equations (1) through (11), the basic idea can be understood as follows. One begins by estimating some initial vertical velocity profile. This profile is used in equations (4) and (5) with measured grain size information to compute τ_d. This profile is used in equation (3) with (1) and (2) to calculate a profile of τ_f. The τ_f profile is used in equation (8) to obtain the turbulent velocity scale, and equations (9) and (11) are used to compute the turbulent length scale [note that equation (9) provides a turbulent length scale when divided by the square root of equation (1), because τ_d is zero in the region above the particles]. These quantities provide an eddy viscosity profile using equation (7), and then (6) is integrated to determine a new velocity profile. This process is continued iteratively until convergence of the velocity profile is obtained. In practice, the use of relaxation greatly improves the convergence characteristics, especially if the initial guess for the velocity profile is poor. To compute the discharge for a given stage, the computed velocity profiles for various depths are integrated vertically and across the channel using the surveyed cross section at the gage.

The Sediment-Transport Model

For the computation of bedload fluxes, the method developed by Parker et al. [1982] is used. This technique allows computation of the sediment flux in a gravel-bed channel using mean grain size by applying a similarity argument for the fluxes in various grain-size classes.

Using the following definitions,

$$\tau_B^* = \frac{\tau_b}{(\rho_s - \rho)gD} \tag{12}$$

$$q_B^* = \frac{q_B}{\left[\left(\frac{\rho_s - \rho}{\rho}\right)gD^3\right]^{1/2}} \tag{13}$$

$$W^* = \frac{q_B^*}{\left(\tau_B^*\right)^{3/2}} \tag{14}$$

where q_B is the bedload flux per unit width, ρ and ρ_s are water and sediment density, respectively, and D is the mean grain size of the surface layer, the Parker equation for total bedload flux over a poorly sorted gravel bed is given by

$$W^* = \begin{cases} 0.0025 \exp\left[14.2(\phi_{50} - 1) - 9.28(\phi_{50} - 1)^2\right] & 0.95 < \phi_{50} < 1.65 \\ 11.2\left(1 - \dfrac{0.822}{\phi_{50}}\right) & \phi_{50} > 1.65 \end{cases} \tag{15}$$

In equation (15), ϕ_{50} is defined in terms of the boundary shear stress and the critical shear stress. Using the nondimensionalization defined in equation (12), ϕ_{50} is given by

$$\phi_{50} = \frac{\tau_B^*}{1.18\tau_c^*} \tag{16}$$

The value of τ_c^* was set using the model for critical shear stress developed by Wiberg and Smith [1987b] with a pocket angle, ϕ, of 30°. This yields the critical stress for first motion rather than significant motion (see Wiberg and Smith [1987b] for a more detailed discussion), as required for use in the Parker equation if surface particle sizes are used. The Wiberg-Smith model yields a value of about 0.028 for τ_c^*, in good agreement with the value of 0.0299 reported by Parker [1982].

The volumetric bedload fluxes per unit width calculated from the Parker equation are multiplied by sediment density and integrated across the channel width for each discharge using the surveyed channel cross section. This yields the total mass of bedload discharge as a function of flow discharge.

STUDY SITE AND DATA COLLECTION

The approach described above was tested using channel geometry and sediment-size information from a reach of Little Granite Creek, a small stream located in the Bridger-Teton Forest about 40 km southeast of Jackson, Wyoming. Little Granite Creek is a tributary to Granite Creek, which flows into the Hoback River, a tributary to the Snake River. The study reach is located at U.S. Geological Survey gaging station 13019438 and is about 100 m long, 7 m wide, and has a slope of 0.0175. The D_{50} of the bed particles is about 10 cm and D_{84} is about 20 cm. The depth at bankfull discharge is about one meter, so even at the highest flows, many of the sediment particles on the bed are a large fraction of the flow depth. The reach is relatively uniform in width and depth, so the theory described above was applied using the fact that the spatially averaged flow is uniform. It is worth noting here that even for cases where bars and width variation are present, equation (1) is approximately valid [Nelson and Smith, 1989] and the vertical structure computed from the model can be used in a quasi-three-dimensional flow model to compute the variation of stage, stress, and bedload sediment flux with flow discharge.

The availability of extensive flow and sediment-transport measurements in Little Granite Creek provides an excellent opportunity to test the described technique. Flow and bedload discharge were measured at this site during regular visits from water year 1982 through 1989. Flow discharge was measured at each visit using a Price current meter and procedures described by Buchanan and Somers [1965]. Through water year 1989, 141 discharge measurements had been made. The data used in this paper for testing the predicted stage-discharge relation are the 60 ice-free wading measurements made at the gage in the 4-year period from water year 1986 through water year 1989. Bedload during the 8-year period from water years 1982 through 1989 was measured with a Helley-Smith bedload sampler [Helley and Smith, 1971]. Bedload was sampled at about 20 equally-spaced cross-channel locations as suggested by Emmett [1980]. A total of 113 traverses of the stream constitutes the bedload data used in the comparison between measured and predicted bedload fluxes discussed below.

Particle-size distributions were found using a modified version of the Wolman [1954] sampling technique. Particles were measured every 0.15 m along the channel centerline for 100 m. Downstream, cross-stream, and vertical axes were measured and the vertical protrusion of the particle into the flow was also determined [as required for the computation of A_i and A_b in equation (4); see Wiberg and Smith, 1990]. The particles were divided into size classes by vertical protrusion, and the average A_i and A_b for each size class were used to calculate the value of τ_d for each size class. The vertical extent of τ_d for each size class is simply the vertical

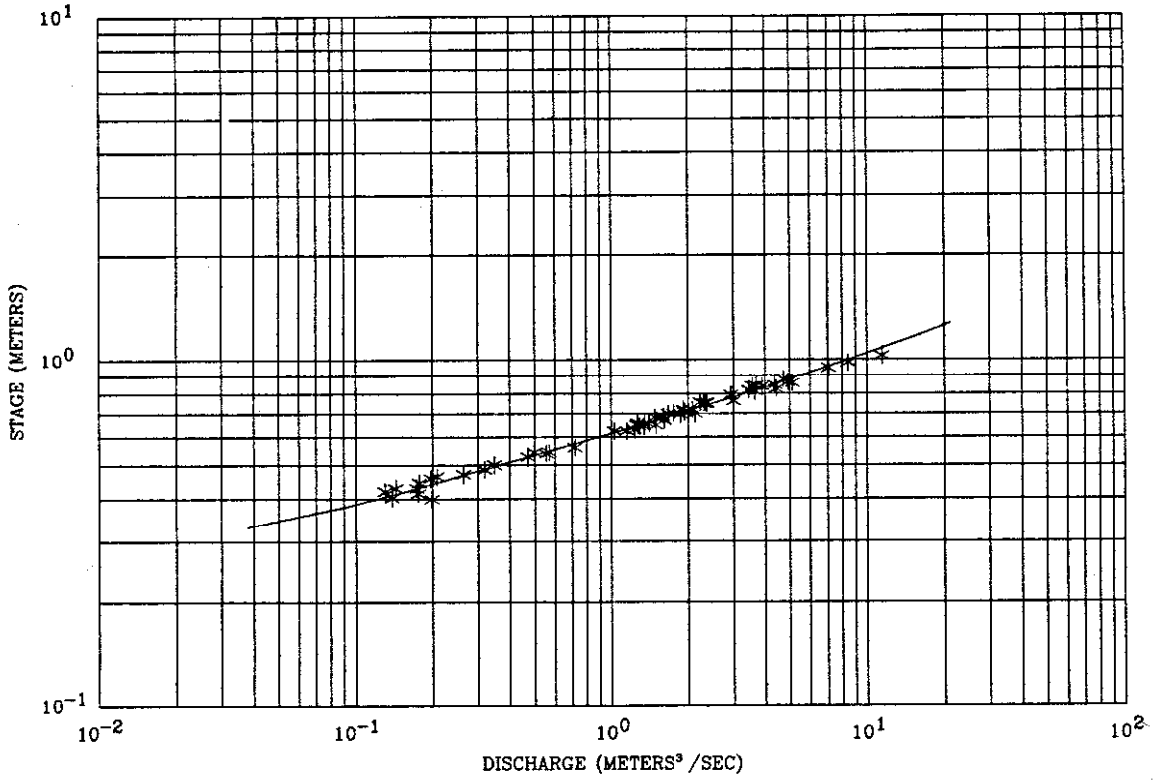

Figure 2. Measured and predicted stage-discharge relation for Little Granite Creek, Wyoming.

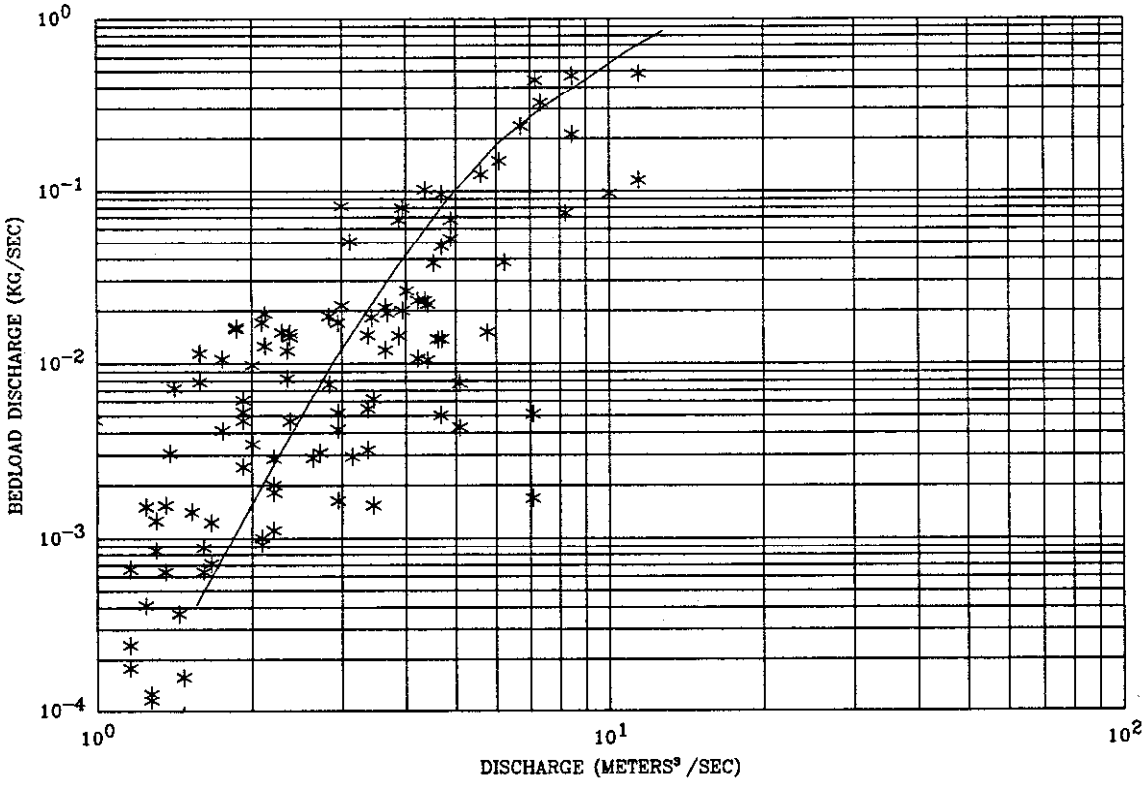

Figure 3. Measured and predicted bedload discharge-flow discharge relation for Little Granite Creek, Wyoming.

protrusion associated with that size class. The total τ_d profile used in the computations is obtained by summing τ_d over all size classes. Channel cross-section geometry was determined by doing a level survey.

RESULTS AND DISCUSSION

In Figure 1, calculated vertical-velocity profiles for Little Granite Creek are shown in linear and log-linear form for several flow depths. In reality, stream depths above about 1 m would result in overbank flows and the depths greater than about 1.5 m shown in the figure probably would not be attained; but the purpose here is to show the variation in velocity profile shape for various ratios of particle size to flow depth typical for mountain rivers. For the greatest depth at which the velocity profile was calculated, the depth is about 50 times D_{84}, and the profile is essentially logarithmic, except very near the bed. At the shallowest depths, the flow is dominated by the form drag on the bed particles and the velocity profile is nearly linear. For a channel like Little Granite Creek, the velocity profile at physically realizable depths is approximated much more accurately by a linear profile than by a logarithmic one. This agrees with the velocity profile measurements made by Jarrett [1989] in rough channels. The curvature in the upper 80% of the flow depth in the log-linear plot of velocity at the largest flow depth is associated with the structure of the Rattray-Mitsuda [1974] eddy viscosity. Even in this case, a truly logarithmic profile only occurs between about $z/H = 4D_{84}/H = 0.085$ and $z/H = 0.2$.

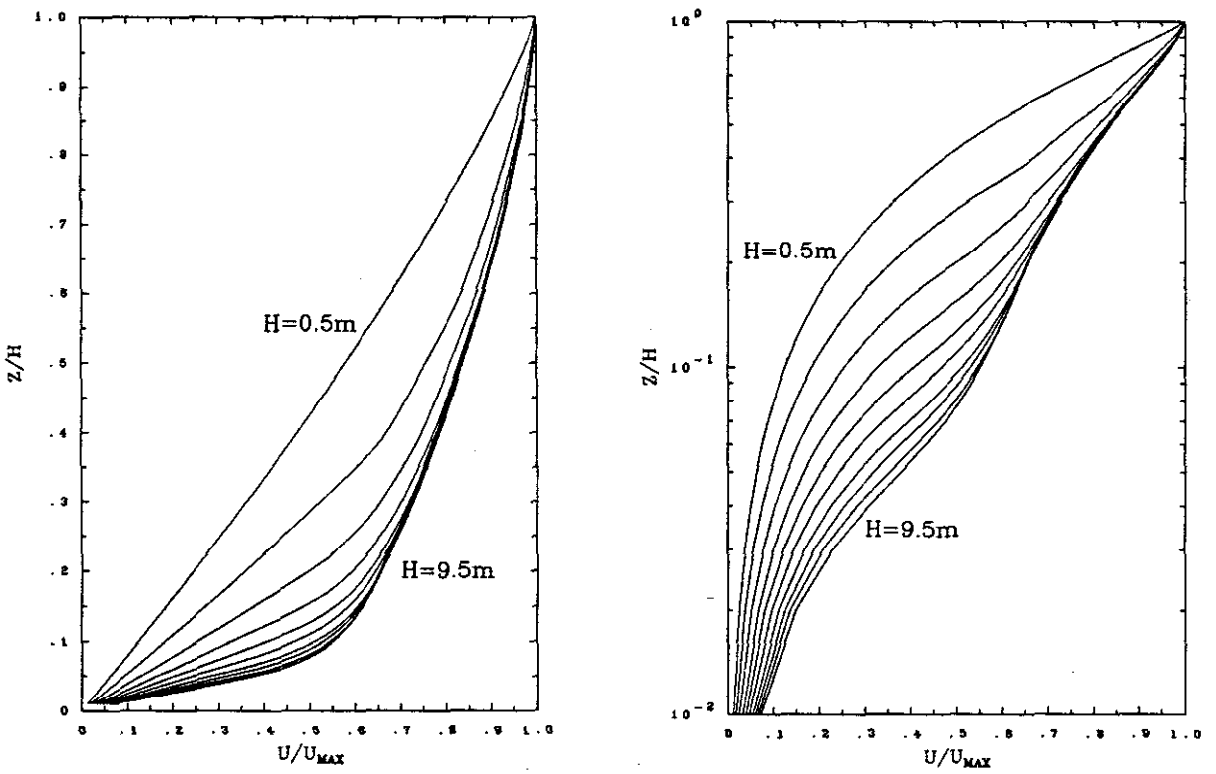

Figure 1. Linear and semi-logarithmic plots of velocity profiles for the grain-size distribution in Little Granite Creek. Depths vary from 0.5 to 9.5 meters by 1 meter increments.

In Figure 2, the computed stage-discharge curve is shown along with measured data. It is important to note that the model above was applied without adjustment in order to make this prediction. Sensitivity analyses indicate that the result is relatively insensitive to the drag coefficient and the eddy viscosity well above the bed (the Rattray-Mitsuda profile was employed, as discussed above). As expected, however, the solution is relatively sensitive to the turbulent length scale used in the near-bed region. The wake scaling used herein was applied without modification for the prediction shown in Figure 2, but varying the magnitude of the length scale near the bed by a factor of only 2 results in a poorer fit to the data. Further experimental verification of the length scale is needed to increase confidence in the generality of the approach. Nevertheless, considering this and other types of uncertainty, both in the model and the data, it is clear that the prediction does a reasonable job of reproducing the measurements, especially considering that all the information that went into applying the model at this site could easily be collected in a single day (a pebble count, a survey of the cross-section at the gage, and

a survey of channel slope).

The comparison between measured and computed bedload discharges is shown in Figure 3. Although the scatter in the measured values is considerable due to the actual variability of bedload transport rates and to the inherent difficulty in making bedload flux measurements in a channel like Little Granite Creek, it appears that the predictions of the Parker equation, when combined with channel geometry and a model relating flow discharge to boundary shear stress, can provide good predictions of total bedload discharge in gravel-bed channels. In some sense, the success of the Parker equation is associated with some general similarities in particle-size distributions in gravel-bedded channels in that it allows prediction of the total flux of sediment in the channel based on information about a single grain size in the bed surface layer. The actual flux of material of the size used in the equation is often negligible. In the case at hand, the D_{50} of the surface layer cannot even enter the nozzle of a Helley-Smith sampler, but when the actual flux of this class is computed, one finds that the probability of a particle of that size encountering the sampler is small.

The approach described herein is a reasonable way to predict stage-discharge and bedload discharge to flow discharge relations in situations where measurements are not available as a result of logistical or economic constraints. Developing more confidence in the technique will require a more complete understanding of the near-bed turbulence field and verification of the general approach at other sites where field data are available.

REFERENCES

Buchanan, T.J., and Somers, W.P., 1965, Discharge measurements at gaging stations. U.S. Geological Survey Techniques of Water Resources Investigations, Book 3, Chapter A8, 65p.

Emmett, W.W., 1980, A field calibration of the sediment-trapping characteristics of the Helley-Smith bedload sampler. U.S. Geological Survey Professional Paper 1139, 44p.

Flammer, G.H., Tullis, J.P., and Mason, E.S., 1970, Free surface, velocity gradient flow past spheres. J. Hydraul. Div. ASCE, 96(HY7), 1485-1502.

Helley, E.J. and Smith, W. 1971, Development and calibration of a pressure-difference bedload sampler. U.S. Geological Survey Open-File Report, 18p.

Jarrett, R.D., 1989, Hydraulics Research in Mountain Rivers, In: B.C. Yen (ed.), Proceedings of the International Conference on Channel Flow and Catchment Runoff, pp. 599-608.

Middleton, G.V. and Southard, J.B., 1984, Mechanics of Sediment Movement. Society of Economic Paleontologists and Mineralogists Short Course No. 3, 2nd edition, S.E.P.M., Tulsa, 401p.

Nelson, J.M., and Smith, J.D., 1989, Flow in meandering channels with natural topography. In: S. Ikeda and G. Parker (eds), River Meandering, AGU Water Res. Mono. 12, Washington, D.C., 69-102.

Nikuradse, J., 1933, Stromungsgesetze in rauhen rohrne. VDI-Forshungsheft 361. (English translation: 1950, Laws of flow in rough pipes. NACA Tech. Memo. 1292, Natl. Advis. Comm. for Aeron., Washington, D.C.)

Parker, G., Klingeman, P.C., and McLean, D.G., 1982, Bedload and size distribution in paved gravel bed streams. J. Hydraul. Div. ASCE, 108(HY4), 544-571.

Rattray, M., and Mitsuda, E., 1974, Theoretical analysis of conditions in a salt wedge. Estuarine and Coastal Marine Science, 2, 373-394.

Schlicting, H., 1979, Boundary Layer Theory. McGraw-Hill, New York, 817p.

Tennekes, H. and Lumley, J.L., 1972, A First Course in Turbulence. MIT Press, Cambridge, 300p.

Wiberg, P.L., and Smith, J.D., 1987a, Initial motion of coarse sediment in streams of high gradient. In: Erosion and Sedimentation in the Pacific Rim, Proc. of Corvallis Symp., IAHS Publ. 165, 299-308.

Wiberg, P. L. and Smith, J.D., 1987b, Calculations of the critical shear stress for motion of uniform and heterogeneous sediments. Water Resources Research, 23(8), 1471-1480.

Wiberg, P.L., and Smith, J.D., 1990, Velocity distribution and bed roughness in steep streams. Water Resources Research, in press.

Wolman, M.G., 1954, A method of sampling coarse river-bed material. Trans. Amer. Geophys. Union, 35(6), 951-956.

LOW-FLOW SEDIMENT TRANSPORT IN THE COLORADO RIVER

By John R. Gray, Supervisory Hydrologist, U.S. Geological Survey, 300 W. Congress Street, Tucson, Arizona 85701-1393; Robert H. Webb, Research Hydrologist, U.S. Geological Survey, 1675 W. Anklam Road, Tucson, Arizona 85705; and David W. Hyndman, Department of Earth Sciences, Stanford, California 94305

ABSTRACT

In support of beach-stability research, bedload and suspended sediment were measured during a steady flow of 5,880 ft^3/s and receding flows from 12,100 to 5,660 ft^3/s in the Colorado River above National Canyon, near Supai, Arizona, October 7-12, 1989. During steady flows, 75 percent of the mean total-sediment discharge of 138 t/d was in suspension and about half the total-sediment load was finer than 0.062 mm. Median grain sizes of bedload and bed material were 0.43 and 0.40 mm, respectively. Although steady-flow bedload transport varied from the mean by about 45 percent, suspended-sediment discharge remained constant within sampling error. Statistical analyses indicate that mean and median rates measured concurrently using the Helley-Smith and BL-86-3 bedload samplers were not significantly different. At larger transport rates, however, the rates measured by the Helley-Smith exceeded those measured by the BL-86-3. Transport rates from bedload samples collected with Helley-Smith and BL-86-3 bedload samplers in sections 8 ft apart demonstrate no consistent autocorrelation or cross correlation. Cross-sectional bedload-transport rates measured concurrently or consecutively with the bedload samplers showed good agreement indicating that bedload varied by at least a factor of 2.4 during the steady-flow period. Ninety-five percent of bedload transport during low flow occurred in the center one-third of the channel.

INTRODUCTION

Operation of Glen Canyon Dam since 1963 has significantly altered flow and sedimentation characteristics of the Colorado River in Grand Canyon National Park. Before 1963, the Colorado River carried a large suspended-sediment load through Grand Canyon National Park. Most of the sediment from the drainage area above the dam is now deposited in Lake Powell. Suspended-sediment concentrations in the Colorado River in Grand Canyon typically are less than 200 mg/L, whereas concentrations commonly exceeded 10,000 mg/L between 1928 and 1959.

Sand banks and bars used for camping beaches by rafters are composed of sand that was both deposited and eroded by the river. The riverbed serves as a reservoir of sand that is available to be transported to the beaches (Wilson, 1986, p. 5-133). The combination of daily flow variability, sediment-trapping characteristics at the dam, and fluvial sediment-transport mechanics has led to public concern over the long-term stability of the beaches on which rafters camp in Grand Canyon (Schmidt and Graf, 1987, p. 2-3).

In an effort to evaluate the future of beaches in Grand Canyon National Park, a series of studies of hydrologic characteristics of the Colorado River called the Glen Canyon Environmental Studies took place from 1983 to 1986. A continuation of these studies started in October 1989 and is hereafter referred to as "October Studies." The October Studies were conducted during flows resulting from a constant release of 6,000 ft^3/s at Glen Canyon Dam during October 6-9, 1989.

This paper describes results of one aspect of the October Studies—research of sediment-transport characteristics at the gaging station, 09404120 Colorado River above National Canyon, near Supai, Arizona, from October 7 through October 12, 1989.

CHARACTERISTICS IN GAGE REACH

The gaging station is at river mile 166, about one-quarter mile upstream from the mouth of National Canyon (fig. 1) in Grand Canyon National Park. National Rapid, at the mouth of National Canyon, controls the stage-discharge relation at the gage. For 2/3 mi upstream and 1/3 mi downstream from the gage, the channel is relatively straight. A cableway from which all flow and sediment data are collected spans the river 250 ft upstream from the gage. The cross section at the cableway generally is trapezoidal with a surface width, mean depth, and mean cross-sectional velocity of 250 ft, 13 ft, and 1.8 ft/s, respectively, at flows near 5,900 ft^3/s. Near 12,000 ft^3/s, these values increase to 270 ft, 16 ft, and 2.7 ft/s, respectively. Eddies occur within about 20 ft of each bank at these discharges. The discharge hydrograph for the gage for October 7-12, 1989, is shown in figure 2. Discharges from 8:00 a.m. October 8 through 2:00 p.m. October 11 receded gradually from about 6,050 ft^3/s to about 5,800 ft^3/s and are hereafter referred to as steady flow of 5,880 ft^3/s.

This site was selected for sediment-transport research for three reasons. First, the stage-discharge relation is well defined and stable, permitting accurate estimates of discharge from the stage-discharge relation when discharge was not measured. Second, the relatively straight channel reach upstream from the gage theoretically minimized effects of secondary flow induced by bends on the spatial distribution of bedload. Third, previous knowledge of the site indicated that physical characteristics, primarily flow, bed configuration, and bed material, would be amenable for use with pressure-difference-type bedload samplers (Graf and others, 1986, p. 5-61 to 5-70; W.B. Garrett, hydrologic technician, U.S. Geological Survey, oral commun., 1989). Potentially unique morphological and local hydraulic characteristics at this site preclude extrapolation of results described herein to other sites even under similar discharges.

METHODS OF STUDY

Suspended-sediment and bedload-transport data were collected to define temporal and spatial variability. Temporal and spatial variability of sediment transport, and particularly of bedload, can be large. Discharge was measured and bed material was sampled in support of sediment-transport measurements.

Bed-material data were collected with a BM-54 bottom-material sampler (Edwards and Glysson, 1988, p. 28-30) and the equal-width-increment method. The sampler was used once at a vertical unless no sediments were trapped, whereupon a second attempt was made to collect a sample. One bag per vertical was used to hold sediments for determinations of dry weight and grain-size distributions. Fifteen analyses of grain-size distributions were determined from bed-material samples collected during the October Studies.

Bedload samples were collected with two pressure-differential bedload samplers that have 3-inch-square intakes. The two samplers were a 90-pound Helley-Smith bedload sampler with a 3.22 flare-to-throat-area (expansion) ratio and a BL-86-3 bedload sampler with a 1.4 expansion ratio.

The Helley-Smith bedload sampler has been used extensively by the U.S. Geological Survey. This was the first field test of the BL-86-3 that bears the nozzle-flare dimensions tentatively adapted as a standard for bedload samplers by the Federal Interagency Sedimentation Project. Collection bags of 250-micron mesh were used with both samplers. Samplers were left on the bottom for recorded periods that ranged from 120 to 190 seconds. Bedload-transport rates at a point were computed from samples using methods described by Edwards and Glysson (1988, p. 103). Grain-size distributions were determined from 61 bedload samples. A total of 390

determinations of bedload-transport rate per foot of width were made using cross-sectional-transit and repetitive fixed-vertical measurements.

The unequal-width increment method was used to collect bedload samples in transits for eight of ten determinations of bedload discharge (Edwards and Glysson, 1988, p. 99-107). Bedload discharge during the third and fourth transits were obtained using the a variation of the equal-width-increment method; five consecutive measurements per vertical were made at each of six verticals, and a single measurement was made at a seventh vertical nearest the right bank. Simultaneous transits with both samplers were made with the BL-86-3 sampler about 8 ft to the right of the Helley-Smith sampler. The BL-86-3 was used exclusively when a single transit was made.

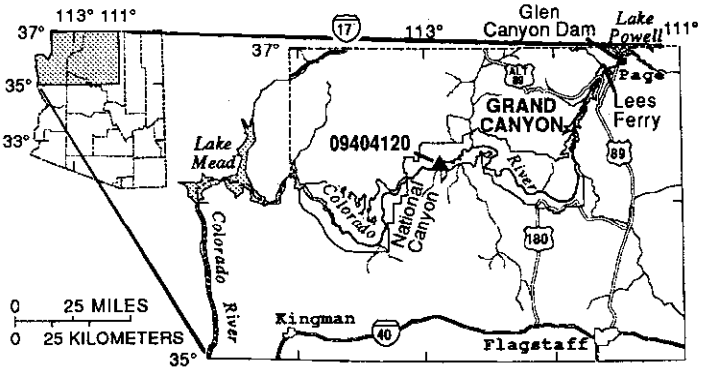

Figure 1.—*Location of study area and the Colorado River gaging station and number above National Canyon, near Supai, Arizona.*

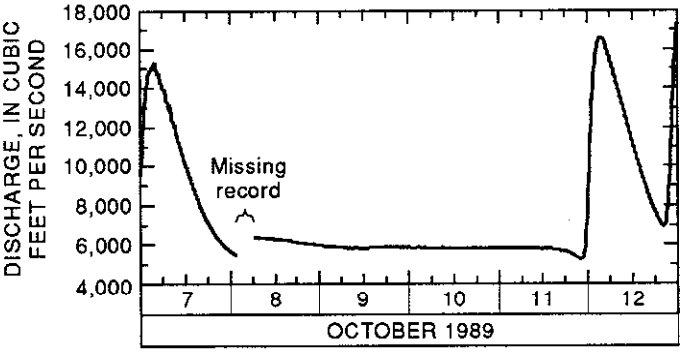

Figure 2.—*Discharge hydrograph for Colorado River above National Canyon, near Supai, Arizona, October 7-12, 1989.*

Evaluations of temporal bedload variability at fixed verticals in the measuring section were made on three separate days. Samples were collected simultaneously with the BL-86-3 sampler about 8 ft to the right of the Helley-Smith sampler. Repetitive sampling produced bedload data pairs of 50, 30, and 15 observations. Bedload-transport rates for fixed verticals were determined from samples collected by this method.

Differences in sampling efficiency between samplers with expansion ratios of 1.4 and 3.22 have not been completely quantified but are likely to be small compared with potential errors inherent in bedload sampling (Harvey Jobson, hydrologist, U.S. Geological Survey, written commun., 1990). An analysis of results from samples collected concurrently during transits and fixed-vertical sampling with the Helley-Smith and BL-86-3 samplers was made to evaluate the effect of different samplers on calculated bedload-transport rates. Bedload-transport rates calculated from repetitive sampling in fixed verticals can be biased if bedload transport at sites 8 ft apart differ significantly. Paired samples collected during transits presumably would be less susceptible to this type of bias unless the distribution of bedload transport over the cross section was markedly asymmetrical.

Six suspended-sediment discharge measurements were made with a D-74 depth-integrating sampler at flows ranging from 5,880 ft^3/s to 11,200 ft^3/s. The equal-discharge-increment method (Edwards and Glysson, 1988, p. 54-61) with five verticals per transit was used. Suspended-sediment samples were analyzed for concentrations and for percentage of sediments finer than 0.062 mm in diameter.

BEDLOAD

Of the 390 bedload samples collected, 155 were paired samples collected with the Helley-Smith and BL-86-3 bedload samplers. Ninety-five pairs were obtained by repetitive sampling from fixed verticals (table 1), and 60 were collected during all or parts of transit numbers 1-10 (table 2). The median grain size of bedload from 61 randomly selected samples from both samplers was 0.43 mm in diameter, and about 90 percent of bedload was between 0.25 and 1.0 mm

Table 1.—*Results of repetitive sampling from fixed verticals from three data-collection periods at Colorado River above National Canyon, near Supai, Arizona*

Date	Time		Mean discharge, in cubic feet per second	Flow regime	Sampler type	Station	Number of samples	Bedload transport, in tons per day per foot				
	Start	End						Mean	Median	Standard deviation	Maximum	Minimum
10-09-89	1045	1544	5,880	Steady	Helley-Smith	[1]141	50	0.76	0.56	0.61	2.20	0.03
					BL-86-3	[1]149	50	0.70	0.65	0.48	2.02	0.07
10-11-89	1126	1427	5,880	Steady	Helley-Smith	130	30	0.56	0.47	0.50	1.79	0.01
					BL-86-3	138	30	0.46	0.41	0.31	1.19	0.03
10-12-89	1606	1710	7,950	Falling	Helley-Smith	130	15	0.85	0.72	0.68	2.11	0.07
					BL-86-3	138	15	0.59	0.46	0.46	1.87	0.09

[1]The first four samples were collected several feet left of these stations.

Table 2.—*Summary of bedload-transit data and associated characteristics at Colorado River above National Canyon, near Supai, Arizona*

Transit number	Date	Time		Mean discharge, in cubic feet per second	Flow regime	Sampler type	Summary of individual verticals[1]			
		Start	End				Number of samples	Sum[2], in tons per day	Maximum, in tons per day per foot	Standard deviation, in tons per day per foot
1	10-08-89	0806	1008	5,880	Steady	BL-86-3	14	39.5	1.02	0.36
2	10-08-89	1014	1133	5,880	Steady	BL-86-3	13	33.5	1.34	0.43
3	10-10-89	0741	1049	5,880	Steady	Helley-Smith	[3]7	[3]23.1	[4]1.79	
4	10-10-89	0741	1049	5,880	Steady	Bl-86-3	[3]7	[3]21.0	[4]0.97	
5	10-10-89	1054	1206	5,880	Steady	Helley-Smith	12	33.3	1.86	0.54
6	10-10-89	1054	1206	5,880	Steady	BL-86-3	12	34.4	0.98	0.35
7	10-11-89	1626	1755	5,880	Steady	BL-86-3	14	42.9	1.18	0.42
8	10-11-89	1635	1755	5,880	Steady	Helley-Smith	13	50.9	1.04	0.41
9	10-11-89	1801	1829	5,880	Steady	BL-86-3	[5]6			
10	10-11-89	1801	1829	5,880	Steady	Helley-Smith	[5]6			
11	10-12-89	0912	1028	11,700	Receding	BL-86-3	19	41.3	1.61	0.40
12	10-12-89	1033	1147	10,900	Receding	BL-86-3	19	33.1	1.35	0.31

[1]Zero bedload transport was measured in at least one vertical of each transit.
[2]Summed bedload from individual verticals is weighted for subsection width.
[3]Five consecutive samples were collected in each of the left six verticals. A single sample was collected at the seventh vertical.
[4]Maximum value is for a single measurement within a vertical.
[5]Cross-sectional transits were not completed due to darkness.

in diameter (medium to coarse sand). Although a mean of about 4 percent of bedload collected was finer than 0.25 mm in diameter, this value should represent a minimum because the 250-micron mesh collection bag is designed to pass material finer than 0.25 mm in diameter. Median bed-material grain-size diameter was 0.40 mm. Grain-size data and the fact that flow was subcritical indicate that sand dunes or ripples formed the bed of the river.

Table 3.—*Combined results from fixed-vertical and cross-sectional bedload measurements during stready flow from 155 paired samples at Colorado River above National Canyon, near Supai, Arizona, October 8-11, 1989*

	Bedload transport, in tons per day per foot				
Sampler	Mean	Median	Standard deviation	Maximum	Minimum
Helley-Smith	0.53	0.30	0.57	2.20	0
Bl-86-3	.46	.38	.44	2.02	0

Sampler Comparison

The relative efficiency of the Helley-Smith and BL-86-3 samplers was compared using the 155 paired bedload-transport rates. Mean and median bedload-transport rates measured by the BL-86-3 were 88 and 126 percent, respectively, of those measured by the Helley-Smith sampler (table 3).

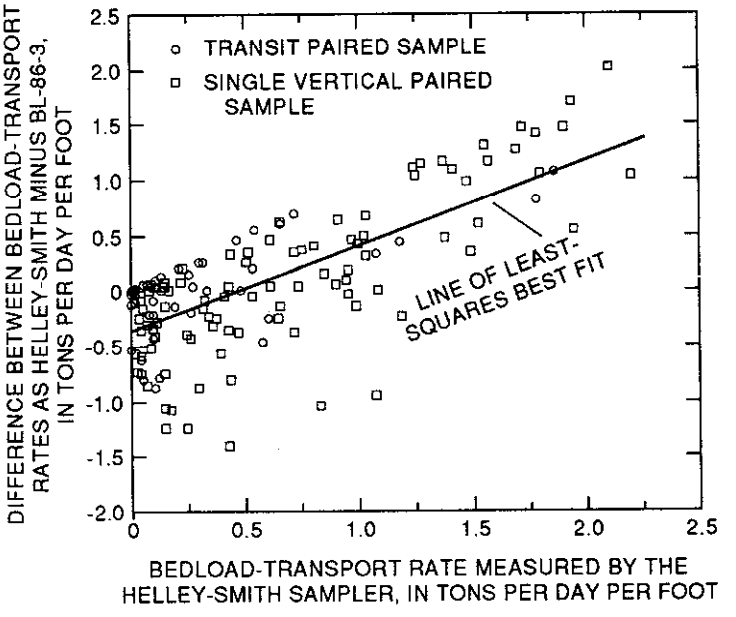

Figure 3.—*Relation of differences in bedload-transport rates consecutively measured with the Helley-Smith and BL-86-3 samplers to those measured with the Helley-Smith sampler at Colorado River above National Canyon, near Supai, Arizona.*

A t-test accepted the null hypothesis that the mean of the differences was equal to zero, and the Wilcoxon test found no significant differences in median values ($T<0.05$). However, a review of differences determined from concurrent bedload measurements plotted against Helley-Smith transport rates in figure 3 shows that the Helley-Smith sampler tended to collect less bedload than the BL-86-3 at smaller transport rates and more bedload at larger transport rates. This trend is evident from data obtained by fixed-vertical and transit methods. The linear regression equation using all 155 paired data that best describes this trend is

$$BL = 0.24HS + 0.33,$$

where BL and HS are bedload-transport rates measured in tons per day per foot of width for the BL-86-3 and Helley-Smith bedload samplers, respectively. The coefficient of determination for this equation equals 52 percent.

If larger bedload-transport rates correspond to larger flow velocities during fluctuations within 0.25 ft of the streambed, the different expansion ratios associated with each sampler could be responsible for the disparity in rates measured by the samplers. The larger expansion

ratio of the Helley-Smith may result in larger negative pressures induced by larger flow velocities past the nozzle flare with respect to that occurring under similar conditions with the BL-86-3. At lower local-flow velocities, effects of reduced negative pressures may be masked by other differences in sampler characteristics. This could result in the Helley-Smith being more efficient at larger local-flow velocities (a "vacuuming" effect) and less efficient at smaller local-flow velocities, with respect to the BL-86-3. The sand-size bed material would presumably be more susceptible to "vacuuming" than would the coarser-grained material.

Uncertainties related to the absolute sampling efficiency of both samplers under the conditions used precluded the application of coefficients to transport rates measured by either sampler. Hence, no adjustments based on relative sampler performance were made to transport rates in ensuing analyses.

Transport

Bedload-transport rates generally vary considerably with time in a cyclic manner at all points of transport in a stream cross section, even during steady-flow conditions (Hubbell and Stevens, 1986, p. 4-20; Carey, 1986, p. 4-131 to 4-140). This inherent variability affects the accuracy of bedload measurements, particularly when few samples are collected. To characterize bedload variability, a combination of temporal (fixed-vertical) and spatial (cross-sectional) sampling was used.

Temporal Variability

Bedload-transport rates from individual samples collected with both samplers from fixed verticals are shown in figure 4. Results from each sampler were evaluated without adjustments for variations in sampling interval, which averaged about 6 minutes. Lag-1 autocorrelation and lag-zero cross-correlation analyses were performed on consecutively and concurrently measured bedload-transport rates, respectively, to evaluate temporal trends.

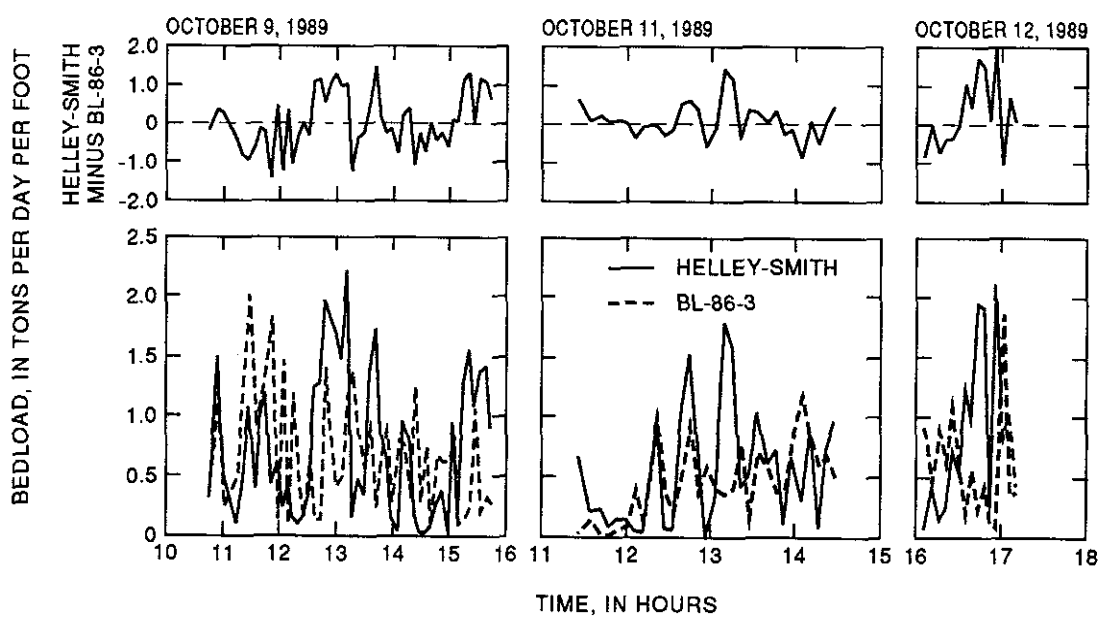

Figure 4.—*Temporal variability in bedload-transport rates between the Helley-Smith and BL-86-3 samplers at Colorado River above National Canyon, near Supai, Arizona.*

Lag-1 autocorrelation values for the 50 and 30 fixed-vertical steady-flow sample sets collected using the Helley-Smith sampler (table 1) were 0.49 and 0.25, respectively. For the BL-86-3 sampler, these values were 0.03 and 0.35, respectively. Lag-1 autocorrelations for paired data collected during receding flow on October 12 had values of -0.19 and 0.13, with the larger value obtained from the Helley-Smith. These results indicate an inconsistent lag-1 autocorrelation in the three time series for both samplers. Similar results from fixed-vertical bedload studies have been expressed qualitatively by other researchers (Carey, 1986; Edwards and Glysson, 1988; Hubbell and Stevens, 1986).

Lag-zero cross correlations were performed on data obtained concurrently by each sampler for the three fixed-vertical data sets (table 1). Lag-zero cross correlation values of 0.05 and 0.36 were calculated from the first and second steady-flow fixed-vertical measurements, respectively. A cross-correlation value of -0.35 was calculated for the receding flow measurements on October 12. The data show a lack of a consistent cross correlation in bedload-transport rates measured consecutively at points 8 ft apart.

Data collected during transits 1-10 (table 2) made during steady flow are available to define temporal variability in steady-flow bedload transport. Low-flow bedload-transport rates at the gage averaged 35 t/d and ranged from 21 to 51 t/d. Although the maximum value exceeded the minimum by 240 percent, rates measured concurrently by the BL-86-3 varied from those measured by the Helley-Smith by -10, 3, and -19 percent for transits 3 and 4, 5 and 6, and 7 and 8, respectively. Consecutively measured mean rates using the BL-86-3 sampler varied by 17 and 53 percent during steady flow and by 25 percent during receding flow. The close agreement between results from concurrently collected bedload transits suggests that the rate measured approximated the actual bedload rate during the sampling period.

Disparities between consecutively collected bedload transits indicate that bedload rates were changing over the sampling period. The total range measured might be a crude measure of variability in bedload transport during steady flows of 5,880 ft^3/s at this site.

Spatial Variability

According to Edwards and Glysson (1988, p. 94), there is little basis for predicting the cross-sectional distribution of bedload transport, even during steady flow. Cross-sectional bedload rates varied considerably within each transit during the October Studies. All bedload data collected during the steady-flow period were used to evaluate spatial variability of bedload over 4 days.

Results from 155 paired steady-flow bedload samples were combined in even 10-foot intervals in the cross section (referenced to zero feet at a point landward of the left bank and referred to as "stations") for analysis. Box and whisker plots were generated for all transport-rate values within the 10-foot intervals (fig. 5). Effectively all steady-flow-bedload transport occurred between stations 80 and 200, or in about half the 250-foot river width. Ninety-five percent of transport occurred in an 80-foot section between stations 100 and 180. Mean and median transport in these eight 10-foot intervals were 0.44 and 0.51 (t/d)/ft, respectively, with a standard deviation of 0.19 (t/d)/ft. Mean and median transport rates for adjacent 10-foot sections show lag-1 autocorrelations of 0.85 and 0.81, respectively. The data indicate that, in spite of large temporal and spatial variations between individual bedload measurements, even during steady flow, the spatial distribution of bedload transport was relatively continuous and mostly confined to the center one-third of the river width.

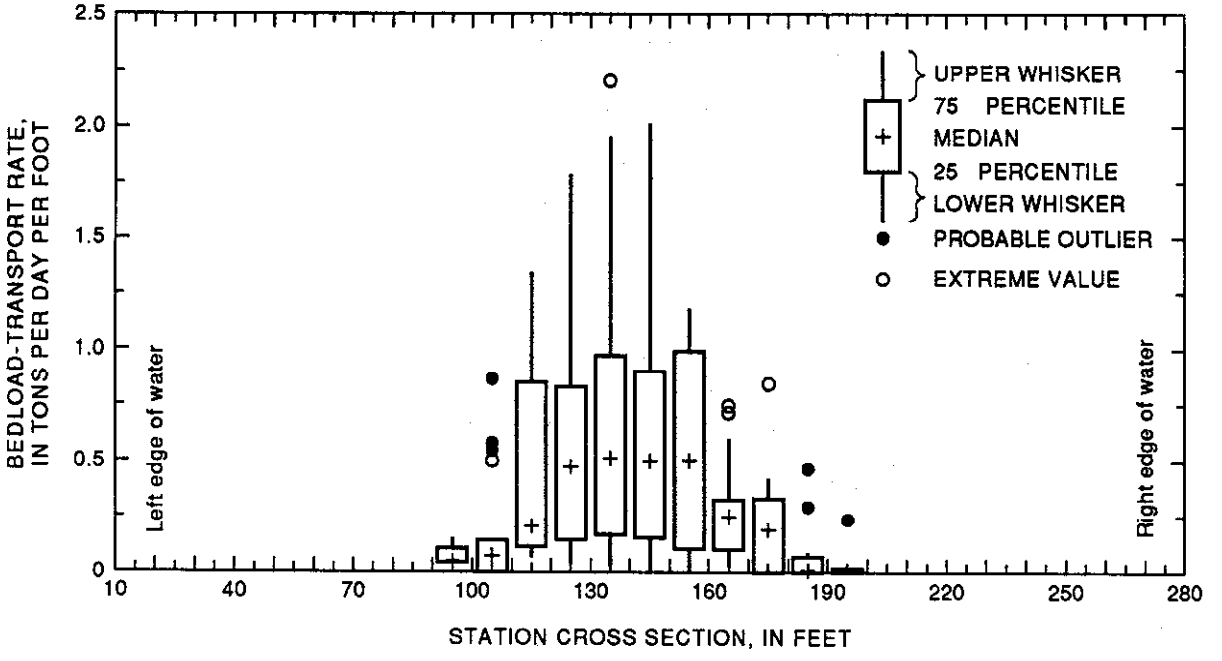

Figure 5.—*Box and whisker plots showing distribution of bedload over cross section during steady flow of 5,880 cubic feet per second at Colorado River above National Canyon, near Supai, Arizona, October 8-11, 1989.*

Table 4.—*Summary of suspended-sediment data and associated characteristics at Colorado River above National Canyon, near Supai, Arizona*

				Suspended sediment		
Date	Time	Mean discharge, in cubic feet per second	Flow regime	Mean concentration, in milligrams per liter	Instantaneous discharge, in tons per day	Grain size finer than 0.062 mm, in percent
10-07-89	1215	11,200	Receding	39	1,180	54
10-08-89	1100	5,880	Steady	7	110	77
10-09-89	0900	5,880	Steady	7	110	75
10-10-89	1800	5,880	Steady	7	110	65
10-11-89	0930	5,880	Steady	5	79	58
10-12-89	1140	10,600	Receding	363	10,400	92

SUSPENDED SEDIMENT

Mean cross-sectional values for suspended-sediment concentration, suspended-sediment discharge, and the fraction of sediments finer than 0.062 mm in diameter are given in table 4. Mean concentration values ranged from 5 to 363 mg/L. Instantaneous suspended-sediment discharges ranged from 79 to 10,400 t/d. Median particle-size values ranged from 54 to 92 percent material finer than 0.062 mm. Largest mean concentration, instantaneous suspended-sediment discharge, and the largest percentage of fine material were associated with the October 12 measurement, which followed tributary stormflows to the Colorado River. The mean concentration of 6.5 mg/L based on four steady-flow measurements corresponds to a mean suspended-sediment discharge of 103 t/d. Suspended-sediment concentrations remained essentially constant during

the low-flow period, with a standard deviation of 1 mg/L from the four concentration values. One milligram per liter is within sampling, analytical, and rounding errors.

TOTAL LOAD

Total sediment discharge is the sum of suspended-sediment discharge and bedload discharge, although true "bedload" might be underestimated or overestimated based on bedload samples. Errors in bedload estimation are minimized when sampling depths exceed 3 ft (W.P. Carey and D.W. Hubbell, hydrologists, U.S. Geological Survey, written commun., 1990) and therefore were not considered to be significant during the October Studies.

During the steady-flow period, the mean suspended-sediment discharge was 103 t/d, and mean bedload-transport rate was 35 t/d. Addition of these values yields a mean total-sediment discharge of 138 t/d based on measurements during the low-flow period. Suspended-sediment discharge composed 75 percent of total-sediment discharge. Seventy percent of suspended sediments transported were finer than 0.062 mm. Therefore, about half the total-sediment discharge during the low-flow period was finer than sand-size material.

CONCLUSIONS

Bedload and suspended sediment were measured during a steady flow of 5,880 ft^3/s and receding flows from 12,100 and 5,660 ft^3/s in the Colorado River above National Canyon near Supai, Arizona, October 7-12, 1989. Relative efficiencies of the Helley-Smith and BL-86-3 bedload samplers were not consistent over the range of transport rates during the steady-flow period and likely introduced some bias in the results. However, results of hypotheses testing failed to show that mean and median rates measured by the bedload samplers were significantly different. Transport rates from bedload samples collected with Helley-Smith and BL-86-3 samplers in sections 8 ft apart showed no consistent lag-1 autocorrelation or cross correlation. Cross-sectional bedload-transport rates measured concurrently or consecutively with the bedload samplers, however, showed good agreement, suggesting that bedload cross-sectional sampling techniques may yield acceptable results in spite of local spatial and temporal variability. The distribution of median values of bedload-transport rates in 10-foot intervals during steady flow, which resembles a bell-shaped curve, indicates general spatial stability in large-scale bedload-transport rates under the conditions measured in contrast to large variability typically associated with individual measurements.

REFERENCES

Carey, W.P., 1986, Probability distributions for bedload transport. Proceedings of the Fourth Interagency Sedimentation Conference, March 24-27, Las Vegas, v. 1, p. 4-131 to 4-140.

Edwards, T.K., and Glysson, G.D., 1988, Field methods for measurement of fluvial sediment. U.S. Geological Survey Open-File Report 86-531, 117 p.

Graf, J.B., Pemberton, E.L., and Schmidt, J.C., 1986, Sediment studies in Grand Canyon, Arizona. Proceedings of the Fourth Interagency Sedimentation Conference, March 24-27, Las Vegas, v. 2, p. 5-61 to 5-70.

Hubbell, D.W., and Stevens, H.H., 1986, Factors affecting accuracy of bedload sampling. Proceedings of the Fourth Interagency Sedimentation Conference, March 24-27, Las Vegas, v. 1, p. 4-20 to 4-29.

Schmidt, J.C. and Graf, J.B., 1987, Aggradation and degradation of alluvial sand deposits, 1965 to 1986, Colorado River, Grand Canyon National Park, Arizona. U.S. Geological Survey Professional Paper 1493, 74 p.

Wilson, R.P., 1986, Sonar patterns of Colorado River bed, Grand Canyon. Proceedings of the Fourth Interagency Sedimentation Conference, March 24-27, Las Vegas, v. 2, p. 5-133 to 5-142.

CONSTRUCTION EFFECTS ON SEDIMENT FOR TWO BASINS IN PUERTO RICO

Allen Gellis, U.S. Geological Survey, PO Box 364424, San Juan, PR 00936

ABSTRACT

Construction activities in expanding urban areas may produce large quantities of sediment. Construction in the Río Piedras basin, which drains part of San Juan, the main urban center of Puerto Rico, is proceeding rapidly. It is estimated that in the year 2000 the basin will be completely urbanized. Suspended-sediment data collected near construction areas in the Río Piedras basin, Puerto Rico, indicate suspended-sediment concentrations as high as 50,000 to 80,000 milligrams per liter and sediment yields from 21,600 to 33,200 tons per square mile per year.

The contribution of sediment from one construction site was documented during a small runoff event in a tributary to the Río Grande de Loíza. During the event, suspended-sediment concentrations were much higher downstream of the construction site than upstream, and about a ton of sediment was delivered to the stream from the construction site.

The Río Grande de Loíza basin, which borders the Río Piedras basin, contains San Juan's major water-supply reservoir, Lago Loíza. Since impoundment in 1954, sediment has been accumulating in the reservoir at an exponential rate. Land development in the basin over the last 25 years may be the major factor affecting the reservoir's sedimentation rate. Sediment supplied from development of the Caguas area could have significantly contributed to the loss of capacity of the reservoir.

INTRODUCTION

The San Juan metropolitan area has experienced rapid growth over the last twenty years. The number of housing units in the Metropolitan area increased from 134,000 in 1970 to 156,000 in 1980 (U.S. Department of Commerce, 1982). This represents a shift in population to the suburban areas from the central city, which grew more slowly. For example, in the suburban area of Cupey, the population increased 44 percent between 1970 and 1980 (U.S. Department of Commerce, 1982). As a result of this population shift, developers are building in remaining areas that are largely rural. The Río Piedras basin (fig. 1), which drains an area of 26 square miles into the San Juan Harbor has been heavily affected by the expansion of metropolitan San Juan. About 75 percent of the basin is developed and the remaining 25 percent is expected to be developed by the year 2000 (U.S. Army Corps of Engineers, 1984).

The proximity of the Lago Loíza basin, which has a drainage area of 209 mi (square miles), to metropolitan San Juan (fig. 1) has also made it susceptible to development. Changes in land use have radically transformed the basin in the last 60 years. The amount of land devoted to agriculture in the basin peaked in the 1950's (Brockman, 1952). Since then, large quantities of agricultural land have been taken out of production or developed. The population in Caguas, the major urban area in the basin, grew from 48,000 in 1930 to 188,000 in 1980, a 292 percent increase. The Caguas urban area nearly doubled in size between 1964 and 1982. Construction of housing developments is continuing in Caguas and other municipalities in the Lago Loíza basin. Associated with this increase in urban development has been an increase in sand and gravel mining operations in

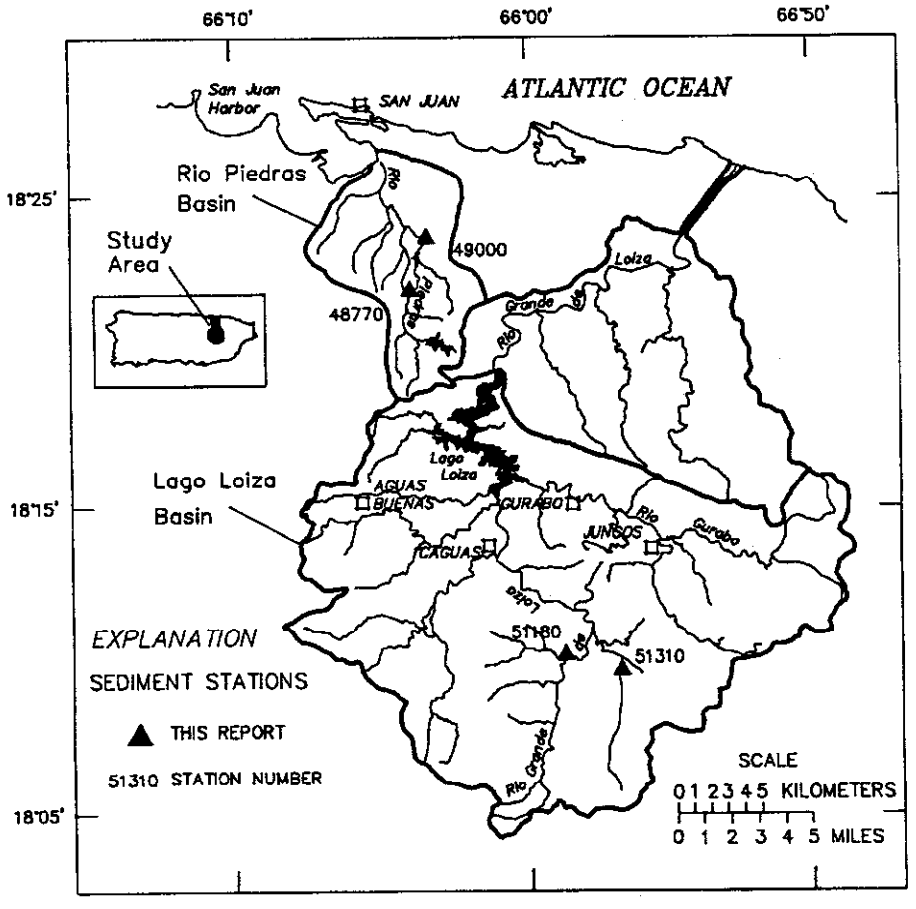

Figure 1. Map showing locations of sediment stations in the Río Piedras and Río Grande de Loíza basins.

the basin that are needed to supply developers with construction materials (Puerto Rico Environmental Quality Board, 1978).

Steep slopes, high annual rainfall, and thick weathered soils in the Río Piedras and Lago Loíza basins provide a high natural level of sediment production (Nevares and Dunlap, 1948; Arnow and Bogart, 1959; Simon and Guzmán-Ríos, 1990). The expansion and development associated with urban growth in these basins add to this already high level of sediment production and may cause serious problems. One of the most critical problems being reservoir sedimentation.

The major water-supply reservoir for San Juan, Lago Loíza (fig. 1), has lost 70 percent of its capacity in the last 36 years and may be rendered useless as early as 2000 (Quiñones and others, 1989; Collar and Guzmán-Ríos, 1991). It is believed that urban development in the basin may have contributed to the rapid rate of sedimentation in Lago Loíza.

Although the problem of sedimentation in Lago Loíza was recognized in the past (Quiñones and others, 1989), the problem has become a major concern for the Puerto Rico Aqueduct and Sewer Authority, which has recently initiated several sediment mitigation strategies.

SUSPENDED SEDIMENT FROM CONSTRUCTION SITES

Suspended-sediment samples were collected near sites that have been cleared for development in the Río Piedras basin (fig. 1) and in Quebrada Salvatierra, a tributary to the Río Grande de Loíza (station 51180 in fig. 1). These samples were collected using depth-integrated bridge samplers, hand-held samplers, and automatic suspended-sediment sampling devices.

Río Piedras

Two sediment data-collection stations were established in the Río Piedras basin in water year 1988 (fig. 1). The farthest upstream station, Río Piedras at El Señorial (station 48770 in fig. 1), is located adjacent to a housing development that increased in size from 400 to 700 acres during 1986 to 1988. Comparison of the suspended-sediment rating curves (fig. 2) for El Señorial and Río Piedras at Río Piedras (station 49000 in fig. 1), may be made using an equal runoff value, referred to as a normalized discharge. At a normalized discharge of 100 ft3/s/mi2, the suspended-sediment concentration at El Señorial is 28,000 mg/L (milligrams per liter) (fig. 2). At this same normalized discharge the suspended-sediment concentration at Río Piedras at Río Piedras is 12,000 mg/L. At higher flows the suspended-sediment concentration at El Señorial has been as high as 80,000 mg/L (fig. 2).

For purposes of comparison to the Río Piedras basin, a suspended-sediment curve for a station draining a largely rural area, Río Cayaguas at Cerro Gordo (station 51310 in fig. 1) is included in figure 2. The Río Cayaguas basin is about 77 percent pasture, 22 percent forest, and 1 percent urban. At the same normalized discharge selected in the Río Piedras basin, (100 ft3/s/mi2), the suspended-sediment concentration is much lower, 3,200 mg/L (fig. 2). The highest concentration recorded at Río Cayaguas was 9,000 mg/L (fig. 2). Therefore, at the same normalized discharge, the station in largely urban Río Piedras basin, had sediment concentrations about 4 to over 8 times higher than those at the station in the rural Río Cayaguas basin.

For a 18-month period in 1988-89 the total sediment load at Río Piedras at El Señorial was 372,600 tons or 33,200 t/mi/yr (tons per square mile per year). At Río Piedras at Río Piedras for a two year period, 1988-89, the total load was 540,000 tons or 21,600 t/mi/yr. At Río Cayaguas the sediment yield for water years 1984 through 1986 was 6,880 t/mi/yr. Therefore, the sediment yields in the Río Piedras basin in 1988-89 were 3 to 5 time greater than the sediment yield in Río Cayaguas during 1984-86. The difference in sediment yields between Río Piedras at Río Piedras and Río Cayaguas for these two periods is 26,280 t/mi/yr. Assuming that the two periods are hydrologically equivalent in repect to sediment production and there were no substantial upstream sediment sources at El Señorial, and that the sediment yield from Río Cayaguas represents a background level, then depending on the area of the construction site (400 to 700 acres), it may have supplied between 24,000 and 42,000 t/mi/yr. This is similar to the range of 25,000 to 50,000 t/mi/yr, reported by Guy and Ferguson (1962) for construction areas near Washington, D.C.

Quebrada Salvatierra

In Quebrada Salvatierra (drainage area of 3.74 mi2), a tributary to the Río Grande de Loíza (station 51180 in fig. 1), the effects of runoff from a cleared area on suspended-sediment concentrations was documented in April 1990. Eighty

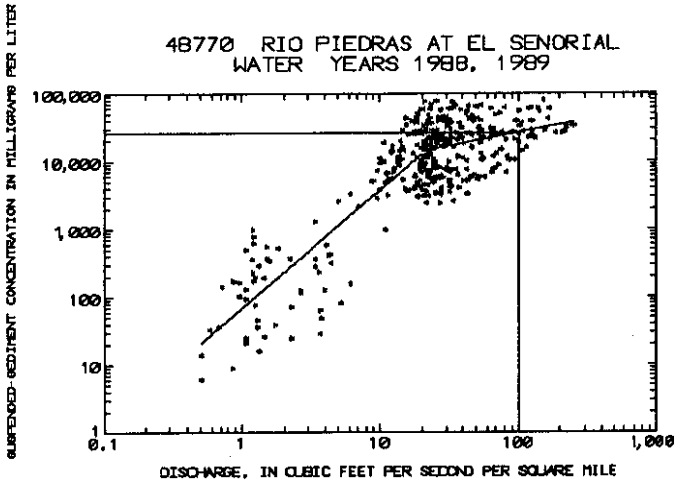

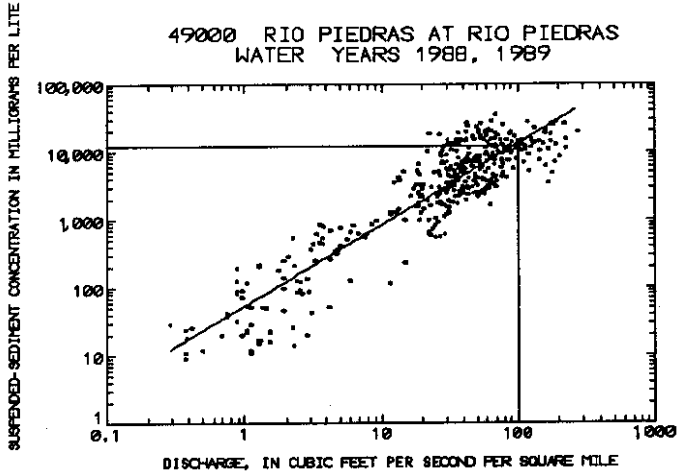

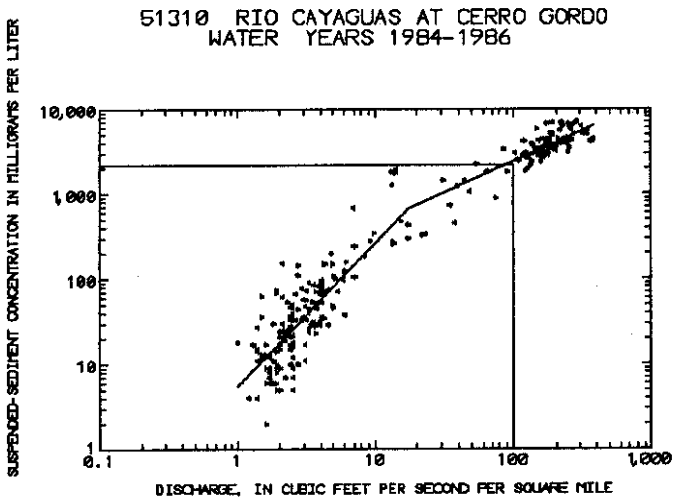

Figure 2. Normalized suspended-sediment rating curves for, a) Río Piedras at El Señorial, b) Río Piedras at Río Piedras, and c) Río Cayaguas.

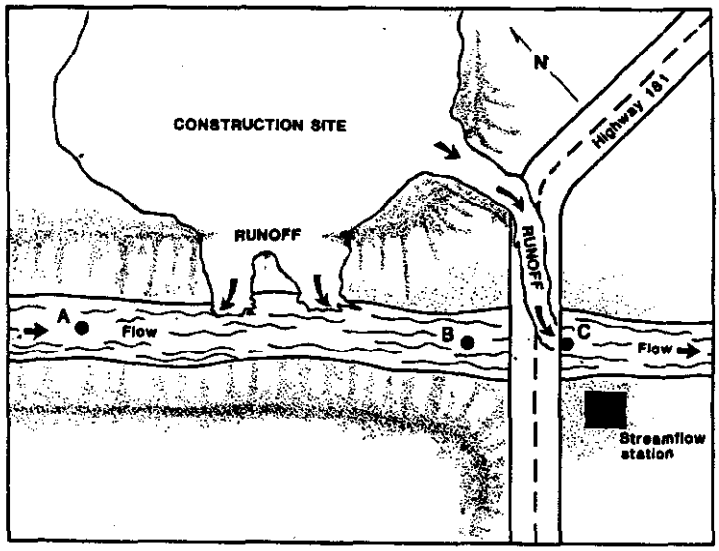

Figure 3. Suspended-sediment sampling sites during a runoff event at Quebrada Salvatierra, April 19, 1990.

feet upstream of the sediment station, 10 acres had been cleared for development (fig. 3). During a localized rainstorm on April 19, 1990, 0.5 inch of rain fell in 30 minutes near the station. Highly turbid water was observed flowing into the channel from the construction site. Suspended-sediment samples were collected at two locations, upstream (site A in fig. 3) and downstream of the construction area (site B in fig. 3). Two samples also were collected from runoff that flowed onto the road from the construction area (site C in fig. 3).

A plot of suspended-sediment concentrations with time at sites A and B is shown in figure 4. The rain ceased at 11:45 a.m. Suspended-sediment concentrations in samples collected between 11:15 and 11:30 am, when considerable runoff was still occurring, indicate that suspended-sediment concentrations downstream of the development (site B) were as high as 10,000 mg/L. Suspended-sediment concentrations were between 100 and 200 mg/L upstream of the construction site (site A). Runoff ceased around 12:00 noon, after which the upstream and downstream suspended-sediment concentrations were both about 600 mg/L. The total contribution of sediment from the construction site during this event was approximately a ton.

One runoff sample collected at each site was analyzed for particle size (table 1). All three stations had small percentages of sand in suspension. However, striking differences in percentages of fines was apparent. Upstream of the construction site, 70 percent of the sediment was finer than 0.002 mm (millimeters) and was mostly very fine clay and colloid particles. Only 19 percent of the sediment had particle sizes in this range downstream of the cosntruction (site B). As a result of construction activities, suspended-sediment concentrations downstream from the construction site were much higher than those upstream of the construction site and suspended-sediment particles generally were much larger, in the silt and clay ranges. The size of

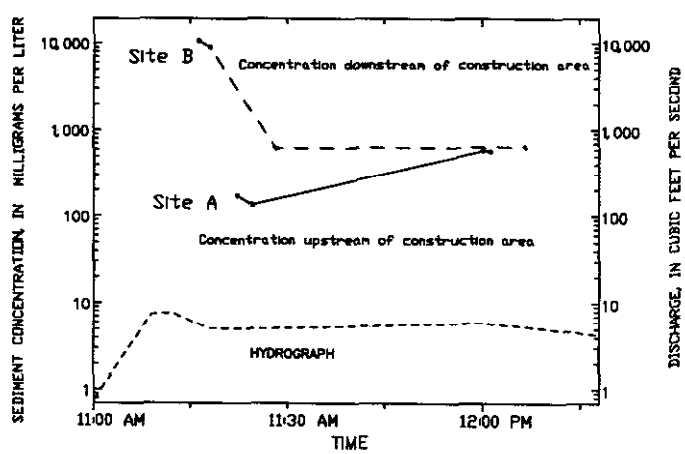

Figure 4. Suspended-sediment concentrations and discharge in a stream receiving runoff from a construction site at Quebrada Salvatierra, April 19, 1990.

Table 1.--Particle-size analysis of suspended-sediment in runoff at sites A, B, and C

Site	Percent finer than indicated, size in millimeters										Suspended-sediment concentration (milligrams per liter)
	Sand					Fines					
	1.0	0.5	0.25	0.125	0.062	0.031	0.016	0.008	0.004	0.002	
A Upstream from construction site	100	99	99	99	98	96	92	91	80	70	582
B Downstream from construction site	100	100	100	100	99	97	83	56	34	19	10,770
C From road runoff	100	100	100	99	96	86	64	39	22	11	24,700

this construction site was small (3 acres) but the large construction sites related to urbanization projects in Caguas and Gurabo (100 acres) might be expected to produce suspended-sediment concentrations comparable to those at this site or the site on Río Piedras (fig. 2).

SEDIMENTATION OF LAGO LOIZA

Lago Loíza, which provides about 50 percent of the public water supply for San Juan, has lost 70 percent of its storage capacity (21,700 acre-feet) since completion in 1953 (Quiñones and others, 1989; Collar and Guzmán-Ríos, 1991). An evaluation of past bathymetric surveys by Collar and Guzmán-Ríos (1991) has shown that the reservoir is filling at an exponential rate and will probably be filled with sediment before the year 2000.

A possible explanation for the exponential increase in the sedimentation rate of Lago Loíza may be the increasing rate of land development in the basin. An increases in the sedimentation rate from 3.68 to 10.42 acre-feet per year occurred at Lake Barcroft, Virginia, when the drainage basin became developed (Guy and Ferguson, 1962). Total area of development in the Caguas area was estimated from topographic maps to be 1,200 acres between 1964 to 1982. Using the highest sediment yields calculated from the construction area at Río Piedras at El Señorial, 42,000 t/mi/yr, and assuming similar sediment delivery occurred during construction in Caguas if all the area were under development, then an estimated 79,000 t/mi/yr of sediment might have been produced from the 1,200 acres. This development in Caguas could have reduced the capacity of Lago Loíza by 76 acre-feet or 0.4 percent of the original capacity of 21,700 acre-feet per year during this period. If these estimates are accurate, the contribution of sediment from Caguas would represent about 17 percent of the yearly average rate of sedimentation for Lago Loíza of 439 acre-feet per year (Quiñones and others, 1989). While it is obviously not possible for all the 1,200 acres to have been under construction for the period 1964 to 1982, and probably not even in 1 year, it can be seen that the contribution from this area to sediment of the reservoir might be significant.

Other anthropogenic sediment sources in the Lago Loíza basin are sand and gravel mining operations and agriculture. Sand and gravel, important commodities in Puerto Rico, are mined from stream channels, on floodplains, and on hillslopes. Although there is little agriculture in the basin, sediment may be introduced when steep slopes are farmed or grazed, and when vegetation is burned for clearing.

CONCLUSION

Puerto Rico's largest city, San Juan, has experienced major urban growth in recent years. Two stations affected by this development, Río Piedras at El Señorial and Río Piedras at Río Piedras, had sediment yields in 1988-89 ranging from 21,600 to 33,160 t/mi/yr. This rate is 3 to 5 times greater than the sediment yield from a largely rural basin, Río Cayaguas. In a stream in the Lago Loíza watershed, suspended-sediment concentrations collected below a construction site during one runoff event were much greater than the suspended-sediment concentrations collected upstream of the site.

The rapid rate of sedimentation of Lago Loíza may be attributable in large part to runoff from construction sites related to urban development which has increased in the last 25 years in the basin. Construction sites in Puerto Rico have been shown to produce much larger concentrations of suspended-sediment in runoff than non-construction areas. The need for documenting the effect of construction and other land use practices on reservoir sedimentation has prompted the Puerto Rico Aqueduct and Sewer Authority to fund additional research.

REFERENCES

Arnow, T. and Bogart, D.B., 1959, Water problems of Puerto Rico and a program of water-resources investigations: Transactions of the Second Caribbean Geological Conference, p. 120-129.

Brockman, V., 1952, Land utilization in Caguas-San Lorenzo. In Rural land classification program of Puerto Rico, Northwestern University Studies in Geography, no.1. Northwestern University, Evanston, Illinois, p. 115-160.

Collar, P.D. and Guzman-Ríos, S., 1991, Sedimentation in Lago Loíza, Puerto Rico and sediment mitigation alternatives: This volume.

Guy, H.P. and Ferguson, G.E., 1962, Sedimentation in small reservoirs due to urbanization: Jour. Hydraul. Div., ASCE, v. 88, no. HY2, Proc. Paper 3070, p. 27-37.

Nevares, R., Jr. and Dunlap, J.C., 1948, Some engineering and geological data on reservoir sedimentation in Puerto Rico: U.S. Geological Survey Unpublished Report, 24 p.

Puerto Rico Environmental Quality Board, 1978, Draft report on mining pollution control study. Water quality management plan for the Island of Puerto Rico, P-138, 68 p.

Quiñones, F., Green, B., and Santiago, L., 1989, Sedimentation survey of Lago Loíza, Puerto Rico, July 1985: U.S. Geological Survey Water-Resources Investigations Report 87-4019, 17 p.

Simon, A. and Guzman-Ríos, S., 1990, Sediment discharge from a montane basin, Puerto Rico: Implications of erosion processes and rates in the humid tropics: In Research Needs and Application to Reduce Erosion and Sedimentation in Tropical Steeplands. International Association of Hydrological Sciences Special Publication, 192, p. 35-47.

U.S. Army Corps of Engineers, 1984, Río Puerto Nuevo survey report. Main report and environmental impact statement, 34 p.

U.S. Department of Commerce, 1982, 1980 census of population and housing: Puerto Rico. U.S. Department of Commerce, Bureau of Census, PHC80-V-53, p. 53-1 - 53-11. 1991

SEDIMENT TRANSPORT IN THE LOWER MISSISSIPPI RIVER, 1983-85

By C.R. Demas and D.K. Demcheck, U.S. Geological Survey, Baton Rouge, Louisiana; and Philip B. Curwick, Ecotech, Baton Rouge, Louisiana

ABSTRACT

An intensive suspended-sediment study was conducted from November 1983 to February 1985 along a 475.6 kilometer reach of the lower Mississippi River from near the mouth at Venice, Louisiana, to Tarbert Landing, Mississippi. Samples were collected during steady-flow conditions of the river to describe steady-state suspended-sediment transport characteristics.

In a downstream direction, total suspended-sediment concentrations decreased by as much as 85 percent at flows less than 14,200 m^3/s (cubic meters per second) and increased as much as 44 percent at flows greater than 19,800 m^3/s. Total suspended-sediment concentrations decreased at flows less than 14,200 m^3/s with as much as 84,000 Mg/d (megagrams per day) of sediment being deposited in the river, but increased at flows greater than 19,800 m^3/s with as much as 168,000 Mg/d of sediment being resuspended from the riverbed. Generally, deposition and resuspension were caused by the fines fraction ($\leq$0.063 mm, millimeter) of the total suspended sediment.

Suspended sand (>0.063 mm), in contrast, indicated no increase in a downstream direction during any of the flow conditions measured. Downstream changes in total suspended-sediment concentrations indicate that the bed of the lower Mississippi River serves as a sink for sediments during flows less than 14,200 m^3/s and a source during flows greater than 14,200 m^3/s.

INTRODUCTION

Interest in the use of Mississippi River water and sediment to mitigate coastal erosion and minimize the effects of sedimentation on navigation prompted the study of suspended-sediment transport (SST) characteristics of the lower Mississippi River in Louisiana. Studies by Everett [1971] and Wells [1980] indicated that concentrations of total suspended-sediment (TSS) decreased in a downstream direction in the lower Mississippi River at flows less than 17,000 m^3/s and increased in a downstream direction at flows greater than 17,000 m^3/s. However, Wells [1980] had no information on SST at flows greater than 17,000 m^3/s, and both studies were based on a small number of samples.

In an attempt to verify Everett's [1971] original findings, an intensive suspended-sediment (SS) study to define steady-flow SST characteristics of the lower Mississippi River was conducted from November 1983 to February 1985. This report verifies Everett's [1971] findings and describes SST characteristics during steady-flow conditions. Previous investigations have only considered transport characteristics of total SS. However, this report addresses total suspended sediment (TSS), suspended sand, (SSD) and suspended fines (SF) which consist primarily of silt and clay.

STUDY REACH

The study area of the lower Mississippi River extends from Tarbert Landing, Miss., to near the mouth at Venice, La., (fig. 1) encompassing a total of 475.6

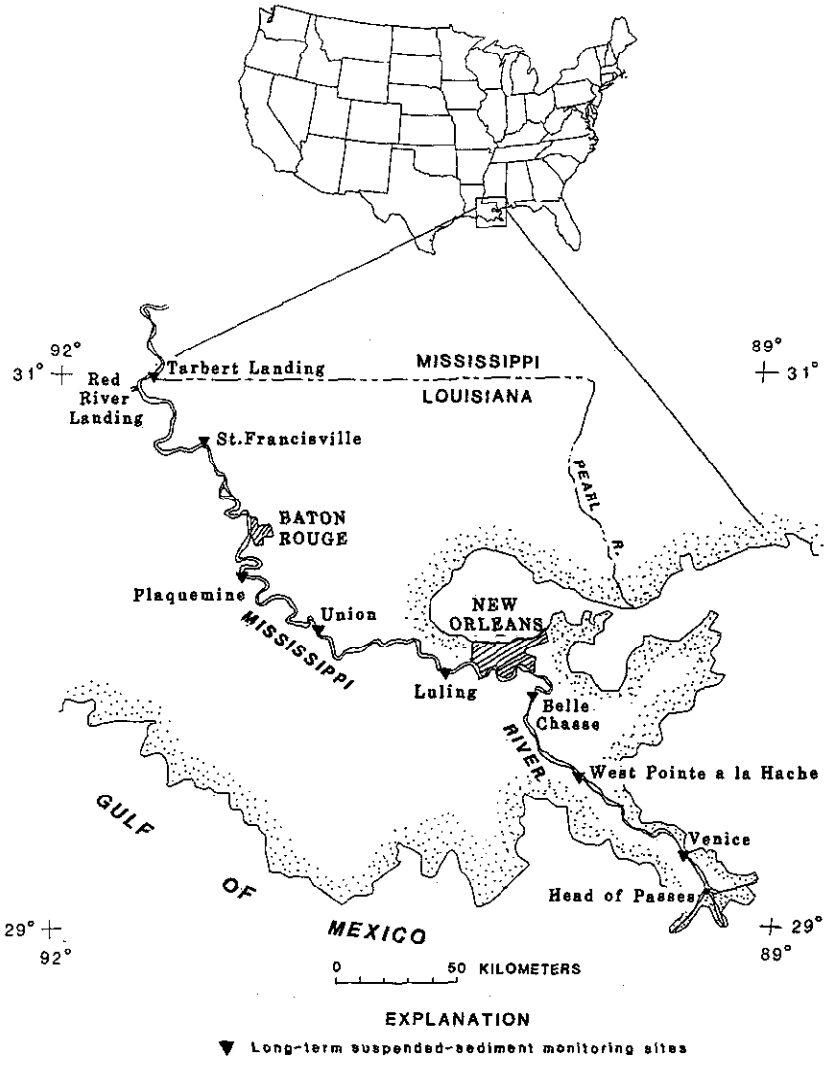

Figure 1.-- Location of study reach.

river kilometers (km). This reach of the river is bordered with levees for almost the entire length. Also, no tributaries or distributaries of any significance enter or leave the river in this reach. River channel depths are maintained at 3.7 m (meters) from Tarbert Landing to Baton Rouge and 12.9 m from Baton Rouge to Venice for navigation. Depths exceeding 30 m are common along many of the bends throughout the entire study reach. Stream velocities range from less than 0.6 m/s (meter per second) to greater than 2.4 m/s, depending on stage and location; average velocity is approximately 0.7 m/s.

The lower Mississippi River generally rises in late fall or early winter and in early spring. The spring rise generally has a higher peak discharge, and the high water may last until midsummer. A period of low water then follows until late fall, and the cycle is repeated. Steady flow occurs many times during the year because the river channel acts as a reservoir and can store significant amounts of water that buffer stage changes. Steady flow is indicated by the following data that were recorded at Red River Landing, La.:

Date of sampling trip	Mississippi River stage (meters) Initial	Final	Percent change
November 14-18, 1983	6.22	6.37	2.4
October 15-19, 1984	5.67	5.73	1.1
November 5-9, 1984	10.79	11.49	6.5
December 3-7, 1984	12.04	12.01	.2
May 1-5, 1984	15.85	15.58	1.7
January 7-10, 1985	13.75	14.36	4.4

MATERIALS AND METHODS

Samples for the analysis of SS were collected at eight long-term monitoring sites and numerous miscellaneous sites along the study reach. Long-term monitoring sites were the lower Mississippi River at or near Tarbert Landing, St. Francisville, Plaquemine, Union, Luling, Belle Chasse, West Pointe a la Hache, and Venice (fig. 1). Five equal-width increment depth-integrated SS samples were collected in the cross section at each site and analyzed individually for sand and fines concentrations and particle-size distribution.

Samples from miscellaneous sites also were collected as frequently as every 8 km and analyzed for only sand and fines concentrations. Three depth-integrated SS samples were collected in the centroid of flow, bracketing the thalweg of the channel. No SS samples were collected in areas of saltwater because this indicated the upstream flow of seawater.

All SS samples were collected with an 8-liter collapsible-bag sampler similar to the one used by Stevens and others [1980], Nordin and others [1983], and Richey and others [1986]. In the field, samples were separated into sand (>0.063 mm) and fines ($\leq$0.063 mm) fractions by wet sieving through a 20-centimeter brass U.S. Standard No. 230 sieve. Samples were analyzed at a U.S. Geological Survey sediment laboratory according to methods described by Guy [1969] and the U.S. Army Corps of Engineers [1970].

Stream discharge was measured using the moving-boat technique [Smoot and Novak, 1969] at the beginning of every sampling trip at Tarbert Landing and at the end of the trip at Belle Chasse and West Pointe a la Hache to determine average trip flow conditions for the study reach. Measurements also were made at intermediate sites, depending upon time available and river stage. The discharge data presented are the arithmetic averages of measured discharges for the sampling trip. Detailed discussions of data collection are presented by Demas and Curwick [1987].

RESULTS

The downstream variations in the concentration of TSS, suspended fines (SF), and suspended sand (SSD) for three ranges in flow conditions of the lower Mississippi River are shown in figures 2-4. Flows were divided into low (<14,200 m^3/s), medium (14,200-19,800 m^3/s), and high (>19,800 m^3/s) flow conditions on the basis of the discharge-duration curve presented by Wells [1980, p. 7].

Concentrations of TSS decreased significantly in a downstream direction at flows less than 14,200 m^3/s (fig. 2). For example, concentrations decreased in

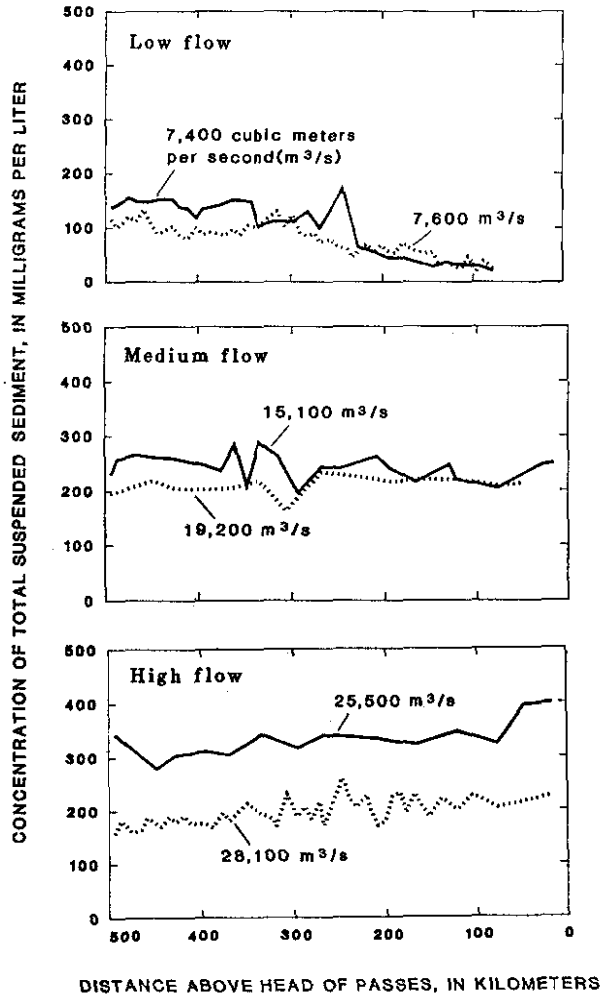

Figure 2.--Downstream variation in the concentration of total suspended sediment in the lower Mississippi River at low, medium, and high steady-flow conditions.

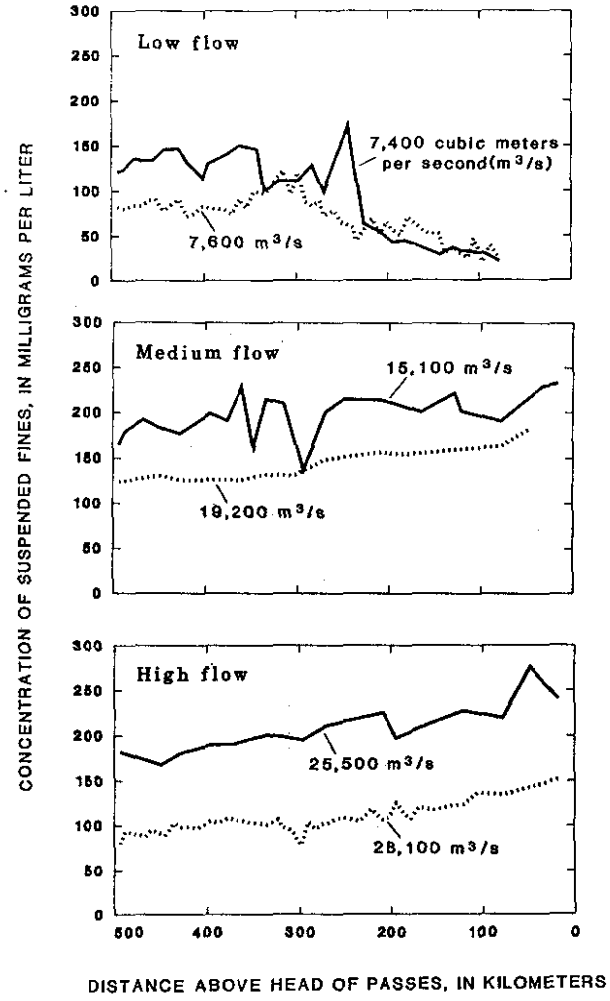

Figure 3.--Downstream variation in the concentration of suspended fines (<0.063) millimeter in lower Mississippi River at low, medium, and high steady-flow conditions.

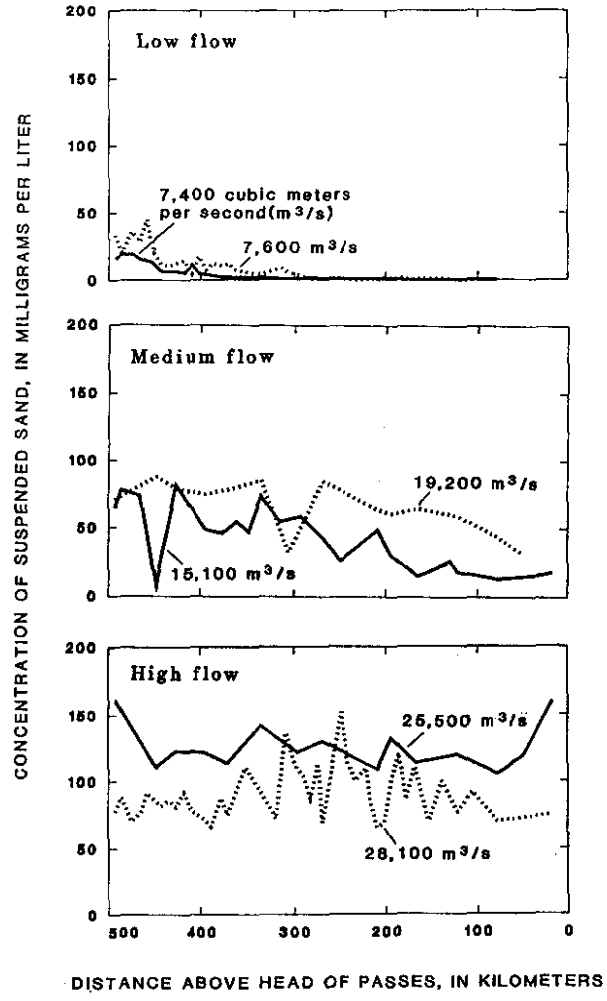

Figure 4.--Downstream variation in the concentration of suspended sand (<0.063) millimeter in lower Mississippi River at low, medium, and high steady-flow conditions.

a downstream direction by 79 and 85 percent at flows of 7,600 and 7,400 m^3/s. This converts to 58,000 and 84,000 Mg/d of SS being deposited between Tarbert Landing and West Pointe a la Hache during these two low flow conditions.

Concentrations of TSS increased slightly in a downstream direction during medium flow conditions (fig. 2). Increases of about 9 percent were observed during flows of 15,100 and 19,200 m^3/s. Sediment was resuspended at a rate of 40,000 and 29,000 Mg/d between Tarbert Landing and Venice during these two medium flow conditions.

At high flows, concentrations of TSS increased significantly in a downstream direction (fig. 2). Concentrations of TSS increased between Tarbert Landing and Venice by 17 and 44 percent at flows of 25,500 and 28,100 m^3/s. Sediment was resuspended at a rate of 124,000 and 168,000 Mg/d during these two high flow conditions.

Table 1 lists the net downstream change in suspended-sediment concentrations observed during the six steady-flow conditions (fig. 2-4). Variations in concentrations of suspended fines (SF) caused the major changes observed in concentrations of TSS that occurred in the entire study reach. At high flows, net differences in concentrations of SF were responsible for 98 percent (25,500 m^3/s) and 96 percent (28,100 m^3/s) of the net downstream change in concentrations of TSS observed. Changes in concentrations of SF accounted for 60 percent (19,200 m^3/s) and 62 percent (15,100 m^3/s) of net downstream change in TSS concentrations observed during medium flow, and 88 percent (7,400 m^3/s) and 64 percent (7,600 m^3/s) of the net downstream change in TSS concentrations observed during low flow.

Table 1.--Net downstream change in suspended-sediment concentrations observed during six steady-flow conditions of the lower Mississippi River, Louisiana

[Minus sign (-) indicates a net loss in suspended sediment; plus sign (+) indicates a net gain in suspended sediment]

Discharge (cubic meters per second)	Date	Number of samples	Net change (milligrams per liter)		
			Sand	Fines	Total sediment
		Low flow			
7,600	November 1983	50	-32	-58	-90
7,400	October 1984	30	-16	-116	-132
		Medium flow			
15,100	November 1984	22	-47	+78	+31
19,200	December 1984	14	-40	+58	+18
		High flow			
28,100	May 1984	42	-3	+72	+69
25,500	January 1985	15	-1	+58	+57

Concentrations of SF decreased in a downstream direction during low flows and increased during medium and high flows (fig. 3). For example, the concentration of SF decreased with flows of 7,600 m^3/s from 91 mg/L (milligrams per liter) at km 451.3 to 24 mg/L at West Pointe a la Hache. Net decrease was 58 mg/L in SF concentrations for the study reach (table 1).

Concentrations of SF increased in a downstream direction during medium flow (15,100 m^3/s) from 165 mg/L at Tarbert Landing to 233 mg/L at Venice. This also was observed at high flow (25,500 m^3/s) when SF concentrations increased from 182 mg/L at Tarbert Landing to 240 mg/L at Venice. Net increases of 78 and 58 mg/L in the concentration of SF were observed during these medium and high flows.

Median particle size, d_{50}, of SF decreased in a downstream direction during low flows and remained relatively constant during medium and high flows. The d_{50} of SF ranged from 0.004 mm at St. Francisville to 0.001 mm at West Pointe a la Hache with an average of 0.002 and 0.003 mm during flows of 7,600 and 7,400 m^3/s. The D_{50} of SF during medium flows ranged from 0.007 mm at Union to 0.003 mm at Luling with averages of 0.006 and 0.004 mm during flows of 15,100 and 19,200 m^3/s. During high flows d_{50} of SF ranged from 0.007 mm at Plaquemine to 0.001 mm at Tarbert Landing with an average of 0.002 and 0.005 mm during flows of 28,100 and 25,500 m^3/s. The SF data from the sites at low, medium, and high flows show that there is very little downstream variation in median particle-size of SF transported by the lower Mississippi River in Louisiana.

Concentrations of suspended sand (SSD) (table 1) indicated no net increase in the downstream direction during any of the steady-flow conditions. Concentrations of SSD decreased about 100 percent between Tarbert Landing and West Pointe a la Hache during flows of 7,400 and 7,600 m^3/s (fig. 4); net losses of 16 and 32 mg/L of SSD from the water column were observed. Initial concentrations of SSD were 16 and 33 mg/L during these two flow conditions. Significantly, 64 percent of the sand in suspension at Tarbert Landing had settled out in the reach between Tarbert Landing and St. Francisville (a distance of 65.8 km) and an additional 24 percent in the reach between St. Francisville and Plaquemine (a distance of 92.4 km). This converts to 14,000 and 15,000 Mg/d of SSD being deposited between Tarbert Landing and St. Francisville, and St. Francisville and Plaquemine. Concentrations of SSD never exceeded 2.0 mg/L in samples collected downstream from km 282.2 (initial concentration of SSD was 33 mg/L at Tarbert Landing) and averaged 1.1 mg/L downstream from this location. Similar percent reductions in SSD also were observed between Tarbert Landing and St. Francisville, and Tarbert Landing and Plaquemine during flows of 7,400 m^3/s.

The d_{50} of the SSD decreased in the downstream direction during these two low-flow conditions. The d_{50} of SSD decreased from 0.160 mm at Tarbert Landing to 0.103 mm at West Pointe a la Hache during the flow of 7,400 m^3/s. Similar decreases in d_{50} of SSD were observed during the flow of 7,600 m^3/s. Average d_{50} of SSD was 0.137 and 0.122 mm for flows of 7,400 and 7,600 m^3/s.

Concentrations of SSD decreased by 72 and 56 percent between Tarbert Landing and Venice during flows of 15,100 and 19,200 m^3/s. Sand remained in suspension much longer with these flows. During flows of 15,100 m^3/s, there was no significant change in SSD concentration at long-term sites until km 194.0, where a decrease of 54 percent was measured. During a flow of 19,200 m^3/s, a similar decrease in concentrations of SSD was not observed until km 48.3. In

both instances, no decrease in SSD concentrations was observed at either St. Francisville or Plaquemine. Concentrations of SSD ranged from 78 mg/L at km 486.6 to 13 mg/L at km 78.4 during a flow of 15,100 m^3/s and from 88 mg/L at km 447.9 to 31 mg/L at km 48.3 at a flow of 19,200 m^3/s.

The d_{50} of SSD decreased in a downstream direction during two measurements at medium flows; however, major differences in the d_{50} were not observed until km 122.3. The d_{50} for SSD ranged from 0.138 mm at Tarbert Landing to 0.102 mm at Venice at a flow of 15,100 m^3/s and from 0.157 mm at St. Francisville to 0.120 mm at West Pointe a la Hache at a flow of 19,200 m^3/s. Average d_{50} for SSD were 0.124 and 0.140 mm for flows of 15,100 and 19,200 m^3/s.

Concentrations of SSD also decreased in a downstream direction during high flows of 25,500 and 28,100 m^3/s. For example, SSD concentrations ranged from 161 mg/L at Tarbert Landing to 105 mg/L at km 78.4 during a flow of 25,500 m^3/s and from 137 mg/L at km 308.1 to 65 mg/L at km 209.2 during a flow of 28,100 m^3/s.

The d_{50} of SSD decreased steadily over the study reach at both high flow conditions. The d_{50} of SSD ranged from 0.144 mm at St. Francisville to 0.103 mm at Venice during a flow of 25,500 m^3/s and from 0.177 mm at Tarbert Landing to 0.105 mm at West Pointe a la Hache during a flow of 28,100 m^3/s. Average d_{50} for SSD were 0.118 and 0.135 mm flows of 25,500 and 28,100 m^3/s.

No relation was observed between average particle-size distributions of TSS and different flow conditions. The d_{50} of both SSD and SF were often observed to be larger during low flow than high flow. For example, the average d_{50} of SSD samples collected during low-flow of 7,400 m^3/s (0.137 mm) was greater than the average d_{50} of SSD samples collected during a medium flow of 15,100 m^3/s (0.124 mm) and a high flow of 25,500 m^3/s (0.118 mm). The reason for this apparent lack of relation between increasing discharge and average particle size is probably related to antecedent hydrologic conditions which determine the source and, therefore, the size of the material transported.

Downstream changes in concentrations of TSS indicate that the bed of the lower Mississippi River serves as a sink for sediments during low flows and a source of sediment during medium and high flows. For example, in a downstream direction TSS concentration decreases during low flow with as much as 84,000 Mg/d of sediment being deposited in the study reach, but TSS concentration increases during high flows with as much as 168,000 Mg/d of sediment being resuspended from the riverbed. Resuspension of sediment from the riverbed is the only possible source of this material because: (1) the river is bordered by levees along the entire study reach, thereby excluding sediment contributions by overland runoff, and (2) no significant tributaries enter the river in the study reach to contribute additional sediment loads from other watersheds.

CONCLUSIONS

Analysis of SS data verified the initial findings by Everett [1971] on the movement of SS in the lower Mississippi River during steady-flow conditions. Concentrations of TSS decreased as much as 85 percent in a downstream direction at flows less than 14,200 m^3/s and increased as much as 44 percent at flows greater than 19,800 m^3/s. The variation in concentration of TSS was caused primarily by changes in concentrations of SF. Concentrations of SSD, in

contrast, never increased during any of the steady-flow conditions. Particle-size distributions of both the sand and the fines fractions showed no apparent relation to discharge and are probably determined by antecedent hydrologic conditions which determine the source of the material available. Data indicate that the bed of the lower Mississippi River serves as a sink for SS during flows less than about 14,200 m^3/s and a source during flows greater than 14,200 m^3/s.

REFERENCES

Demas, C.R., and Curwick, P.B., 1987, Suspended-sediment, bottom-material, and associated chemical data from the lower Mississippi River, Louisiana: Louisiana Department of Transportation and Development Water Resources Basic Records Report No. 14, 117 p.

Everett, D.E., 1971, Hydrologic and quality characteristics of the lower Mississippi River: Louisiana Department of Public Works Technical Report No. 5, 48 p.

Guy, H.P., 1969, Laboratory theory and methods for sediment analysis: U.S. Geological Survey Techniques of Water-Resources Investigations, book 5, chap. C1, 58 p.

Nordin, C.F., Jr., Cranston, C.C., and Mejia-B., Abel, 1983, New technology for measuring water and sediment discharge in large rivers: Proceedings of Second International Symposium on River Sedimentation, October 11-16, 1983, Nanjing, China, Beijing, Water Resources and Electric Power Press, p. 1145-1158.

Richey, J.E., Meade, R.H., Salati, E., Devol, A.H., Nordin, C.F., and dos Santos, U., 1986, Water discharge and suspended sediment concentrations in the Amazon River: Water Resources Research, American Geophysical Union, v. 22, no. 5, p. 756-764.

Smoot, G.F., and Novak, C.E., 1969, Measurement of discharge by the moving-boat method: U.S. Geological Survey Techniques of Water-Resources Investigations, book 3, chap. A11, 22 p.

Stevens, H.H., Lutz, G.A., and Hubbell, D.W., 1980, Collapsible-bag suspended-sediment sampler: Journal of Hydraulic Engineering, American Society of Civil Engineers, v. 106, no. 4, p. 611-616.

U.S. Army Corps of Engineers, 1970, Engineer manual: Laboratory soils testing, engineering and design: Appendix V, Grain-size analysis: EM 1110-2-1906, 27 p.

Wells, F.C., 1980, Hydrology and water quality of the lower Mississippi River: Louisiana Department of Transportation and Development, Office of Public Works Water Resources Technical Report No. 21, 83 p.

SEDIMENT DEPOSITION IN A FIXED BED CHANNEL

By Yee-Meng Chiew, Lecturer, Nanyang Technological Institute, Singapore 2263, Republic of Singapore. (CYMCHIEW@NTIVAX.BITNET)

ABSTRACT

This study compares computed results from three published models for evaluating incipient condition for sediment deposition in a fixed bed channel with experimental results. The results show that the model proposed by Novak and Nalluri (1975) may form an upper limit, whereas that proposed by Arora et al. (1984) may form a lower limit for the criterion for sediment deposition in a fixed bed channel.

INTRODUCTION

In the last two decades, Singapore had experienced rapid development leading to intensive urbanization of her drainage catchments. The Drainage Department had carried out extensive works all over the island republic to cater for the increased flood peak because of the large paved areas created within the drainage basins. One of their works was to concrete-line all major waterways in the country. Today, almost all major drains or canals in the country are concrete-lined and thus, have rigid boundaries. As a result, excessive discharge of sediment, from construction sites for example, invariably leads to undesirable sediment deposition along the canals.

In general, deposition of sediments occurs when the sediment transporting capacity of the channel is less than the rate at which sediment enters the channel. Sediment deposition has been well studied in alluvial channel. Numerical models, such as HEC-6, has been designed for use under such a condition. However, the transporting capacity of a fixed bed channel is likely to differ from that of a loose-bed channel. Thus, the equations governing sediment deposition in one type of channel cannot be conveniently "transferred" to the other. Additional works are necessary to investigate the factors governing the transport and deposition of sediments in fixed-bed channel.

The objective of this study is to investigate the incipient condition for sediment deposition in a fixed bed channel. Published studies in this area are presented. The computed results using three existing models for evaluating the limiting rate of sediment input are compared to experimental results obtained from this study.

RESULTS FROM PREVIOUS STUDIES

From the vast amount of literature on sediment transport, comparatively little information can be found for sediment transport on a fixed bed channel. This is probably because fixed bed accounts for lesser economical and environmental importance.

Novak and Nalluri (1975) studied sediment transport in smooth fixed bed channels. They studied the maximum rate of sediment input to a channel

without sediment deposition. For channels with a circular cross section, they found that this condition can be defined by

$$\frac{\tau^{5/4} g^{1/4}}{\gamma_s^{5/4} d^{1/2} \nu^{1/2}} = 0.017 + 0.69 \times 10^{-5} \left(\frac{G_s g^{1/3}}{\gamma_s \nu^{5/3}}\right) \qquad (1)$$

where G_s = total bed load in N/s;
g = gravitational acceleration, = 9.81 m/s^2;
d = diameter of sediment particles in m;
γ_s = specific weight of sediment in N/m^3;
τ = bed shear stress in N/m^2; and
ν = kinematic viscosity in m^2/s.

The equation implies that when $G_s = 0$, the resulting τ value defines the incipient condition for sediment entrainment for given sediment and fluid properties. However, the critical shear stress computed using eqn. 1 is much lower than that predicted using the Shields Entrainment Function.

Pullaiah (1978) used very fine sediments, ranging from 0.006 - 0.027 mm in size, to investigate the threshold value for suspended sediment deposition in a smooth rectangular channel. He found that the limiting concentration is a function of $\psi u^*_b/w_o$, where ψ is a correction factor which depends on the flow Reynolds Number; u^*_b = mean bed shear velocity and w_o = fall velocity of sediment.

Itakura and Kishi (1980) investigated the critical condition for the initiation of deposition of suspended sediment in an open channel flow with a rough bed where the bed roughness, k_s = 0.3 mm. They related the critical deposition condition to a flux Richardson Number and stated that this condition occurred when the critical flux Richardson Number, R_{fc} = 0.02, where

$$R_{fc} = \frac{y_o}{L}\left(1 + \alpha\frac{y_o}{L}\right)^{-1} = 0.02 \qquad (2)$$

and

$$\frac{1}{L} = \frac{\kappa g (S_s - 1) w_o c}{u^*_b{}^3} \qquad (3)$$

where κ = 0.4 = von Karman constant;
S_s = specific gravity of sediment;
c = average volumetric sediment concentration;
w_o = fall velocity;
y_o = average depth of flow;
α = 7.0 = Monin-Obukhov constant; and
L = Monin-Obukhov length.

Arora et al. (1984) conducted flume experiments to determine the criterion for deposition of sediment transported in rigid boundary

channels. The authors used experimental data obtained from six different sediments (one of which was coal dust with a particle size = 0.164mm) transported in both smooth and rough rectangular channels. This data set includes experimental data obtained by Pullaiah (1978). They plotted the limiting sediment concentration, C_L to a rather complicated function which included the sediment, flow and channel effects. For a given flow condition, C_L is the sediment concentration above which deposition occurs. They reported that they were able to collapse all experimental points onto one unique curve. The equation of this curve is

$$C_L = \frac{qS_c^{2.5}}{\nu f_b^2 (w_o d/\nu)^{0.6}} \qquad (4)$$

where C_L = limiting volumetric concentration in ppm;
S_c = bed slope/(S_s-1);
f_b = bed friction factor; and
q = unit flow rate.

When the effect of channel shape is taken into consideration, i.e., for non-rectangular channels, the authors merely suggest to append an additional term, $(D/y_o)^2$, where D = hydraulic depth of flow and y_o = flow depth, at the end of the function in eqn (4). Fig. 1 contains the function proposed by Arora et al. (1984) and they reported that Fig. 1 may be used to determine the maximum concentration which can be transport in flows on rigid channels without objectionable deposition on the bed.

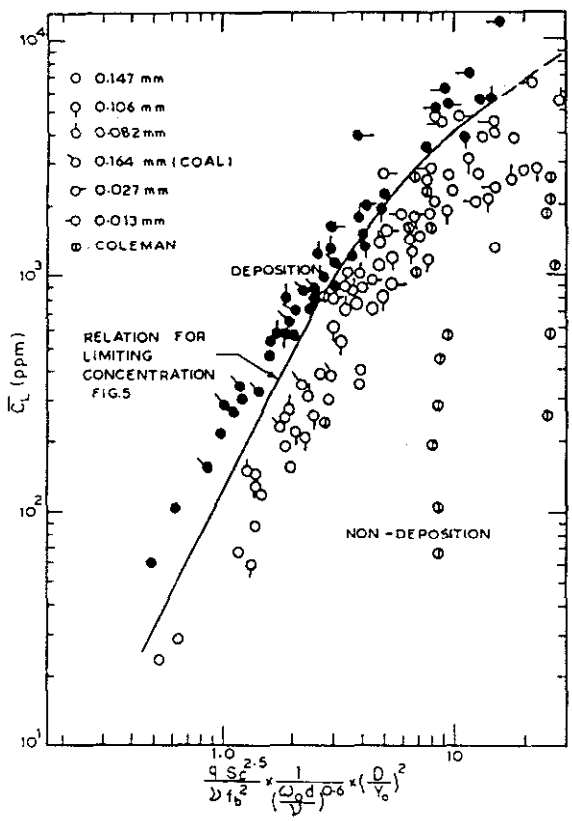

Fig. 1. Criterion for sediment deposition - Arora et al. (1984)

EXPERIMENTAL SET-UP AND PROCEDURE

The experiments of this study were conducted in a rectangular glass flume that was 8 m long, 0.25 m wide and 0.25 m deep at the Nanyang Technological Institute. A uniform flow was first established before adding sediments to the flow. The flow depth of all the tests was fixed at 100 mm and four bed shear velocities were used. They were 0.015, 0.018, 0.031 and 0.06 m/s, respectively. The bed shear velocity was determined from the velocity profile of the flow, which was measured using a 10 mm diameter propeller. Measurement of the velocity profiles was conducted before input of sediment to the flow. The bed slope was adjusted to ensure a uniform flow condition in all the tests.

Once the predetermined flow was obtained, sediment with a known rate was introduced at the upstream end of the flume and observations were made on the pattern of transport and deposition of the sediments. The sediment input rate was varied systematically in order to examine its influence on the deposition pattern. Altogether four uniform sediments were used and Table 1 contains summary of their properties.

Table 1. Properties of sediments used in experiments

Mean Particle Size, mm	Specific Gravity	Geometric Standard Deviation
0.23	2.65	1.22
0.33	2.65	1.19
0.50	2.65	1.20
0.80	2.65	1.23

As the sediment particles enter the flow, they tend to settle under their own weight. The upward component of the turbulent velocities, on the other hand, prevents them from falling. Deposition of sediment will be prevented if the turbulence of the flow can offset the weight force of the sediment particles in transport.

Observations from the study showed that, when the sediment input rate was low, sediment particles traveled a long distance before settling onto the channel bed. In cases when the applied bed shear stress was high and the particle size was small and input rate low, no settlement was observed within the length of the flume. As the input rate increased, the sediment particles took a shorter time to settle. For very high sediment input rate, the sediment particles virtually dropped vertically.

In the experiment, the settled sediment particles would still move as bed load and no stationary bed composed of the sediment particles was formed. During the test, the horizontal distance traveled by the sediment particles, l_h, before settlement onto the channel bed was measured and the sediment input rate was plotted as a function of l_h. Fig. 2 contains one of these curve (for $u^*_b = 0.06$ m/s). The critical or limiting rate of sediment input is taken as the rate when $l_h \rightarrow \infty$.

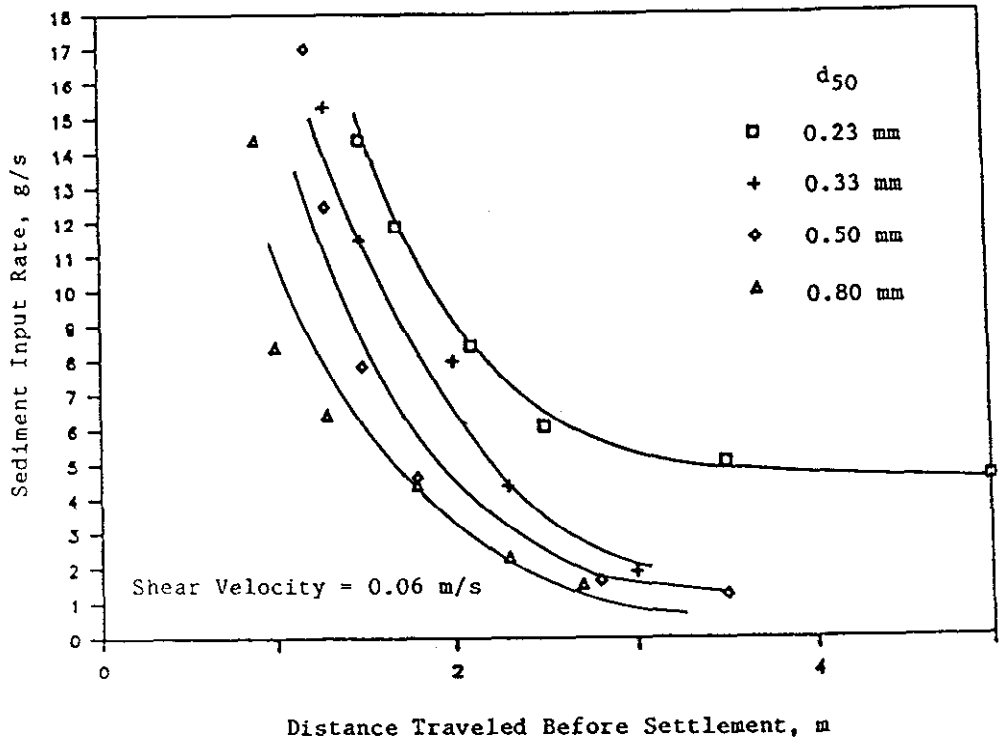

Fig. 2. Sediment input rate versus distance traveled before settlement

The definition of limiting concentration or limiting sediment input rate must be understood clearly in this type of study. For example, the limiting condition in the results published by Novak and Nalluri (1975) may be completely different from that reported by the other researchers. Their definition is the maximum sediment input rate to a channel without the tendency of the sediment to deposit, i.e., under no circumstances was a loose stationary bed allowed to form on the channel bed. Arora et al. (1984), on the other hand, stated that every channel has an upper limit of concentration beyond which objectionable deposition occurs. Surely this definition is rather arbitrary and subject to different interpretation of the word "objectionable". Thus one has to be careful when attempting to compare published results in this type of study. The definition of the incipient deposition of sediment is even more subjective than that of the threshold condition for sediment entrainment. Literatures relating to the threshold conditions for initiation of sediment transport reported variations of the results and one of the reasons for such variations has been attributed to the different definition of threshold conditions. Therefore, similar, if not worse problems would exist for the determination of threshold condition for sediment deposition.

COMPARISONS OF RESULTS

Table 2 contains the experimental results from this study and the computed results using the three methods discussed earlier. It must be pointed out that the volumetric concentration (in terms of m^3 of sediment per m^3 of water) obtained from both the equations proposed by Itakura and Kishi (1980) and Arora et al (1984) has been converted to N/s by multiplying the volumetric concentration by the volume flow rate and the bulk density of the sediment. The weight density of the sediment is assumed to be equal to 1400 kg/m^3 x 9.81 m/s^2.

The results show that the method proposed by Novak and Nalluri (1975) overestimates the limiting sediment input rate when compared with the experimental results from this study and that obtained from using the other two methods. The results are not surprising if one is clear of the definition of deposition used by Novak and Nalluri (1975). As was discussed earlier, the bed load (G_s in eqn. 1) is the maximum possible

Table 2. Limiting Sediment Input Rate

Test No.	d_{50} (mm)	Measured Rate, N/s	Computed Rate, N/s		
			Novak & Nalluri	Itakura & Kishi	Arora et al.
1	0.23	0.0451	0.1426	0.1041	5.76×10^{-4}
2	0.33	0.0185	0.1190	0.0707	3.68×10^{-4}
3	0.50	0.0122	0.0967	0.0459	2.21×10^{-4}
4	0.80	0.0098	0.0764	0.0283	1.25×10^{-4}
5	0.33	0.0065	0.0227	0.0064	1.51×10^{-5}
6	0.50	0.0049	0.0184	0.0042	9.06×10^{-6}
7	0.80	0.0039	0.0145	0.0026	5.11×10^{-6}
8	0.23	0.0046	0.0068	0.0013	1.46×10^{-6}
9	0.33	0.0028	0.0056	0.0009	9.36×10^{-7}
10	0.50	0.0019	0.0045	0.0006	5.62×10^{-7}
11	0.80	0.0018	0.0035	0.0003	3.17×10^{-7}
12	0.33	0.0025	0.0038	0.0005	6.32×10^{-7}
13	0.50	0.0017	0.0031	0.0003	3.80×10^{-7}
14	0.80	0.0016	0.0024	0.0002	2.14×10^{-7}

rate of transport along the channel bed without deposition. The limit of this transport is the cessation of sediment transport altogether. The limiting condition used in this study is somewhat different from that defined by Novak and Nalluri (1975). Hence the computed results using eqn. 1 are expected to be higher than the experimental results.

For $u^*_b = 0.06$ m/s, the computed results using eqns. 2 and 3 proposed by Itakura and Kishi (1980) are much higher than the experimental results (tests 1-4) whereas the former are lower than the latter for $u^*_b = 0.018$ and 0.015 m/s (test 8-14). For $u^*_b = 0.031$ m/s, the computed and experimental results compare very well indeed (test 5-7). The ratio of the computed over measured rate of sediment ranges from 0.13 - 3.82. It appears that the magnitude of the shear velocity has not been adequately accounted for in the equations proposed by Itakura and Kishi (1980).

The values of the computed results using eqn. 4 proposed by Arora et al. (1984) are very small, much smaller than both the experimental results form this study and that computed using the other two methods. The discrepancy is attributed to the definition of the limiting condition defined by the authors. As was discussed previously, the definition of

"objectionable" deposition is at best vague and the criterion is subject to different interpretation. The writer suspects that the limiting criterion proposed by Arora et al (1984) applies to the slightest sediment deposition.

CONCLUSIONS

The study shows that the definition of sediment deposition is very important in studying the criterion for sediment deposition along rigid boundary channels. Comparisons of published data confirm its importance. The equation proposed by Novak and Nalluri (1975) may be used as the upper limit for sediment deposition, and excessive siltation can be expected if their method is adopted for design. On the other hand, the equation proposed by Arora et al. (1984) provides a very stringent criterion for sediment deposition along a fixed bed channel.

ACKNOWLEDGMENTS

The writer wishes to express his appreciation to C.W. Mak for conducting the experimental works in the laboratory.

REFERENCES

Arora, A.K., Ranga Raju, K.G., and Garde, R.J., 1984, Criterion for Deposition of Sediment Transported in Rigid Boundary Channels. Channels and Channel Control Structures, Proc. 1st Int. Conf. on Hydraulic Design in Water Resources Engineering, Southampton, England, 3.45 - 4.56.

Itakura, T., and Kishi, T., 1980, Open Channel Flow With Suspended Sediments. J. Hyd. Div., ASCE, 106(8), 1325-1343.

Novak, P., and Nalluri, C., 1975, Sediment Transport in Smooth Fixed Bed Channels. J. Hyd. Div., ASCE, 101(9), 1139-1154.

Pullaiah, V., 1978, Transport of Fine Suspended Sediment in Smooth Rigid Bed Channels, Ph.D Thesis submitted to University of Roorkee, Roorkee, India.

PREDICTION OF BEDLOAD IN SANDBED CHANNELS

By K. Mahmood, Professor and Director and M.H. Mehrdad, Research Associate, International Water Resources Institute, The George Washington University, Washington D.C. 20052

ABSTRACT

Bedload is an important fraction of sediment load in field channels mainly because it plays a direct role in the bed forming phenomena. Measurement of bedload in sandbed field channel, which is required for validation of theoretical methods of prediction, is nearly impossible. Indirect measurement of bedload in these channels can be carried out by the analysis of sequential bed profiles provided that the theoretical considerations that relate "wave form" and "sediment mass" transport are satisfied. It is shown that the two can be related for ripple and dune type of bedform. Experimental data from sandbed field channels and laboratory flumes is used to show that both Meyer-Peter Muller and Einstein Bedload Function provide reasonably accurate prediction of bedload. Experience with Missouri River, near Omaha and ACOP Canal data show that sequential profiles can also be used to measure the space and time variation of bedload in channels.

INTRODUCTION

The earlier equations for prediction of sediment load in channels, e.g., DuBoys, were bedload equations. It was later, during the 30's through 50's, that concepts of bedload, suspended load and wash load were evolved and theoretical methods for the prediction of bed material load were developed. Of these methods, Einstein's bedload function (1950) is theoretically the most profound and it permits the computation of bedload and suspended bed material load separately. Many of the later sediment transport functions, e.g., Colby (1964), however, imply that bedload is a part of the bed material load computed by them but do not permit separate computation of bedload.

In the case of sandbed field channels, bedload is a small proportion of bed material load. For example in Missouri River near Omaha and Pakistan Canals (Mahmood, et al., 1987), bedload varies upto about 10% of bed material load. However, bedload is an important fraction of sediment load in field channels because it play a direct role in the evolution of bedforms, channel bed transients and other bed forming phenomena. It is also theoretically important as it provides the link between channel bed, the source of bed material load, and the rest of the flow field.

Testing the accuracy of bedload prediction in field channels is one of the more difficult tasks in sedimentation engineering -- more so, in sand bed channels. The reason is that sand beds are highly susceptible to disturbance of flow field caused by the sampler and in the case of mass accumulation methods, it is difficult to separate the bedload from suspended bed material load that is carried close to the bed.

Sequential (time-lapse) bed profiles in field channels provide a convenient non-invasive method of measuring bedload. The concept of relating bedload with the migration of bedforms is fairly old (Hubbell, 1964), and a number of

attempts have been reported in literature to correlate bedload with the volume and celerity of bedforms both in laboratory and field channels. However, theoretical considerations that would relate the transport rate of "wave form" and "sediment mass" have not always been clear and numerical methods required for bedload calculations have not been standardized.

This paper describes the theoretical justification for measurement of bedload through sequential bed profiles in ripple-dune bed regime and presents the comparison of measured and predicted bedload. Space and time variation of bedload in Missouri River and ACOP Canals is also described.

MEASUREMENT OF BEDLOAD THROUGH SEQUENTIAL PROFILES

Theoretical Considerations

In the case of two dimensional bedforms (no variation across the channel width), the relationship between the spatial variation of bedload and time variation of bed level can be written by Exner's equation as

$$\frac{\partial g_b}{\partial x} = - \frac{\partial z}{\partial t} , \tag{1}$$

where the variation of suspended load along the bedform has been ignored; g_b= bedload in volume of bed material per unit width; x = abscissa measured parallel to the average bed; z = bed elevation above a reference datum and t = time. In ripple and dune type of bedform, sediment particles are eroded from the stoss side, roll over the crest and are deposited on the lee side so that the bedform moves downstream, say, with a celerity C.

Introducing a moving coordinate system

$$z' = z \quad ; \quad x' = x - C \cdot t , \tag{2}$$

and using the chain rule Eq. (1) can be written as

$$\frac{\partial g_b}{\partial x'} + \frac{1}{C} \cdot \frac{\partial g_b}{\partial t} = C \frac{\partial z'}{\partial x'} - \frac{\partial z'}{\partial t} . \tag{3}$$

If the bedform shape is invariant during downstream migration, i.e., $\partial z'/\partial t = 0$, and the sediment discharge is in a state of equilibrium, i.e., $\partial g_b/\partial t = 0$, Eq. (3) can be integrated as

$$g_b(x) = C \left[z(x) - z_o \right] \tag{4}$$

where g_b = zero at $z = z_o$, (See Figure 1). Equations similar to (4) have been derived by Mercer and Haque (1973) and Mahmood (1980) among others. Equation (4) shows that at any instant of time the bedload along a bedform varies in proportion to the elevation of bed above a datum at $z = z_o$. The location of this datum is determined by the mode in which the bedload transport affects

the bedform migration. If the eddy on the lee side of bedform is weak and bedload movement is in positive x direction all along the bedform, z_o lies in the trough of the dune. More commonly, in a region upstream of the reattachment point, A in Figure 1, the bedload is actually moving upstream so that z_o lies at or near A. In plane bed regime z_o lies in the channel bed and in antidunes, z_o lies above the bedform crest. In the two latter cases, bedload can not be computed from the measurement of bedforms. Integration of Eq. (4) along a bedform train gives

$$\bar{g}_b = \frac{1}{L} \int_0^L C \left[z(x) - z_o \right] dx \ , \tag{5}$$

where $\bar{g}_b$ is the spatially averaged bedload in units of volume of bed sediment per unit width and unit of time over length L. Computation of bedload from Eq. (5) requires measurement of z(x) for the interval $0 \le x \le L$, celerity of the bedform C and evaluation of z_o.

For ripples and dunes, the ratio of z_o to the wave amplitude H depends on the ratio of eddy length to bedform wavelength L_e/L, ripple index L/H and angle of repose of the bed material ϕ. For dunes in Missouri River near Omaha, this ratio has been estimated by Mahmood (1980) to be 0.2 and the spatially averaged bedload has been estimated by

$$\bar{g}_b = \frac{0.6}{L} \int_0^L C \left[z(x) - z_t \right] dx \ , \tag{6}$$

where z_t is the elevation of trough.

Values of z(x) and C in a channel can be measured by sonic profiles taken along a line parallel to mean flow direction at times t and t+Δt. Obviously, the lapse time interval Δt should be much smaller than the time taken by prevalent bedform to travel its own length. Two numerical schemes to compute bedload from sequential profiles have been developed by Mahmood (1980). These are the Downcrossing and Cross Spectral methods. Experience with Missouri River (Mahmood, 1985) and Pakistan Canals (Mehrdad, 1989) data shows that the two methods yield consistent results. It is pointed out that alternate method for the computation of bedload would be to measure z(t) at a given location in the channel and to evaluate the bedload through cross spectral analysis (Willis and Kennedy, 1977). However, in field sandbed channels this method requires rather long duration of measurement. For example in ACOP Canals, a measurement of z(t) would be required for about 300 hrs to obtain $\bar{g}_b$ averaged over 5 bedform lengths and it is better to use sequential profiles. Further, in sequential profiles, it is essential that the longitudinal location and scaling of bed profiles be accurately measured (Mahmood et al., 1988, Mehrdad, 1989). Lateral shifting of bed profile also needs to be controlled but is less critical.

EVALUATION OF BEDLOAD EQUATIONS

Three bedload equations have been selected to evaluate their accuracy of prediction. These are: 1) Meyer-Peter Muller (MPM), 2) Einstein Bed-Load Function (EBLF) and 3) Toffaleti. Bed profiles data used in this evaluation are Missouri River near Omaha (Mahmood, 1985), ACOP Canals (Mehrdad, 1989), flume data of Crickmore (1967), Willis and Kennedy (1977), and Engel and Lam Lau (1980). In each case the theoretical bedload by the selected function has been calculated by a computer program similar to ODSET package of USACE Omaha District (Mahmood, 1983). Measured bedload from sequential profiles has been calculated by the above investigators. The results for MPM and EBLF are shown in Figures 2 and 3. It is seen that over 3 log cycles of bedload coverage both of these result methods fairly accurate results. If any thing, EBLF appears to underestimate at low and overestimate at high concentrations. Toffaleti method generally gives large underestimation of bedload and is not judged suitable for this purpose.

SPACE-TIME VARIATION OF BEDLOAD

Sequential profiles have been used in Missouri River and ACOP Canals studies to measure the space and time variation of bedload in the study reaches. Spatial variation for Jamrao canal (Run JM2), averaged over four pairs of runs, is shown in Figure 4. The maximum bedload, about twice the average is measured near the channel centerline. The cyclical variation across the channel width is most probably related to the secondary circulation cells identified in the isovels and boundary shear stress measurements. The Missouri River data, Figure 5 are in a mildly curved left handed channel bend and show an interesting result. The channel cross-section in the upstream Segment 3 is skewed towards the right bank due to the effect of preceding left-handed bend. The cross-section in middle Segment 2 is symmetrical and that in the downstream is mildly skewed towards the left bank. The middle segment comprises the crossing between the bends preceding and following the study reach.

The space and time variation in figures 5a, 5b and 5c is related to the geometry of channel. The temporal shift in the distribution of bedload in the middle segment, is due to the shifting nature of flow through crossings and the accentuation of bedload towards the left bank in Segment 1 is related to the left-handed curvature of the study reach. The reasons for temporal variation of bedload in Segment 3 are not readily apparent. For the prevalent flow of 37,000 cfs, the water surface width in this part of Missouri River is about 36 percent larger than the stable (regime) width. The temporal variation in bedload may, therefore, be caused by the lateral oscillations of maximum velocity thread in a "wide" channel. On the other hand, the temporal variation of bedload across the section may be normal behavior of long radius alluvial rivers bends, wherein the band of maximum bedload follows an oscillating path. Data from other near-straight and sharply curved bends can clarify this point.

CONCLUSIONS

Presently, there is no practical method available to directly measure bedload in large sandbed channels. In view of the experience reported herein, it is concluded that the method of sequential profiles is a viable procedure for

measuring bedload when dune bedforms exist. Recent technological progress in the development of multichannel narrow beam ultrasonic sounder, positioning equipment and digital recording under field conditions has made it possible to implement sequential profiling conveniently and economically. The method is especially attractive because it can, also, measure spatio-temporal variation of bedload and, thus, provide a better understanding of the dynamics of alluvial channels. The comparison of measured bedload with Meyer-Peter Muller Formula and Einstein's Bedload Function shows that they provide fairly accurate prediction.

ACKNOWLEDGMENTS

Financial support for the analysis reported herein has been provided by National Science Foundation Grant Nos: INT-8612851 to The George Washington University and INT-8019241 to Pakistan Water and Power Development Authority (WAPDA).

REFERENCES

Crickmore, M. J., "Measurement of Sand Transport in Rivers with Special Reference to Tracer Methods." Sedimentology, Vol. 8, 1967.

Colby, B.R., "Discharge of Sands and Mean-velocity Relationships in Sand-bed Streams." USGS Prof. Paper 462-A, 1964.

Einstein, H. A., "Bed Load Function for Sediment Transportation in Open Channels." Technical Bulletin 1026, United States Department of Agriculture, Soil Conservation Service, Washington, D.C., 1950.

Engels, P., and Lam Lau, Y., "Computation of Bed Load Using Bathymetric Data." Journal of the Hydraulics Division, ASCE, Vol. 106, HY3, 1980.

Hubbell, D.W., "Apparatus and Techniques for Measuring Bedload." USGS Water-Supply Paper 1748, 1964.

Mahmood, K., "Verification of Sediment Transport Functions - Missouri River." MRD Sediment Series No. 19, U.S. Army Corps of Engineers, Omaha District, Omaha, NE, September 1980.

Mahmood, K., "Missouri River - Programmer's Manual, Sediment Transport Program ODSET." MRD Sediment Series No. 27, U.S. Army Corps of Engineers, Missouri River Division, Omaha, NE, August 1983.

Mahmood, K., "Analysis of Multi-Channel Sequential Profile Data - Missouri River Near Omaha, NE." MRD Sediment Series No. 36, U.S. Army Corps of Engineers, Omaha District, Omaha, NE, September 1985.

Mahmood, K., Choudri, A. Masud, Haque, M.I. and Mehrdad, M. Hamid, "ACOP Canals - Equilibrium Runs Computerized Data Base." Technical Report No.IWRI-87-4, International Water Resources Institute, School of Engineering and Applied Science, The George Washington University, Washington, D.C., November 1987.

Mahmood, K., Haque, M.I. and Mehrdad, H., "Measurement and Analysis of Bedforms." Mechanics of Alluvial Channels, Water Resources Publications, Littleton, CO, 1988.

Mehrdad, M.H., "Bedforms - Their Measurement, Analysis And Application." D.Sc.Thesis, The George Washington University, Washington, D.C., July 1989.

Mercer, A.G. and Haque, M.I., "Ripple Profiles Modeled Mathematically." Journal of the Hydraulic Division, ASCE, Vol. 99, No. HY3, March 1973.

Willis, J. C., and Kennedy, J.F., "Sediment Discharge of Alluvial Streams Calculated from Bed Form Statistics." IIHR Report No. 202, Iowa Institute of Hydraulic Research, The University of Iowa, Iowa City, Iowa, June 1977.

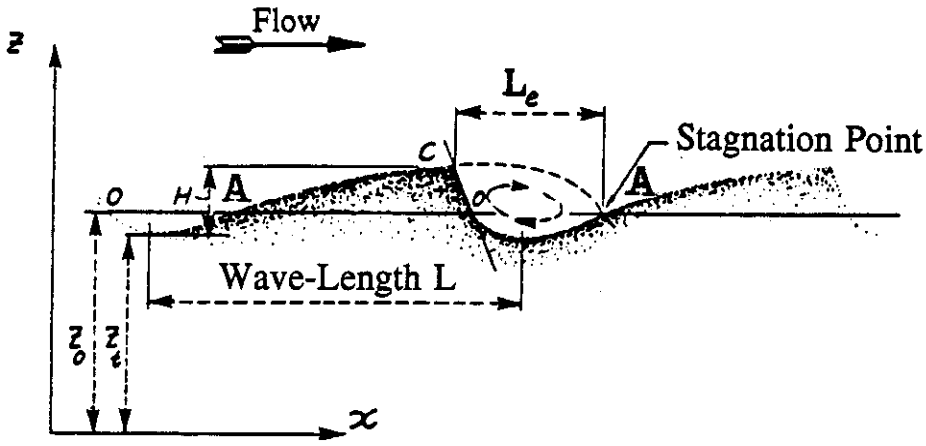

Figure 1 Definition Sketch

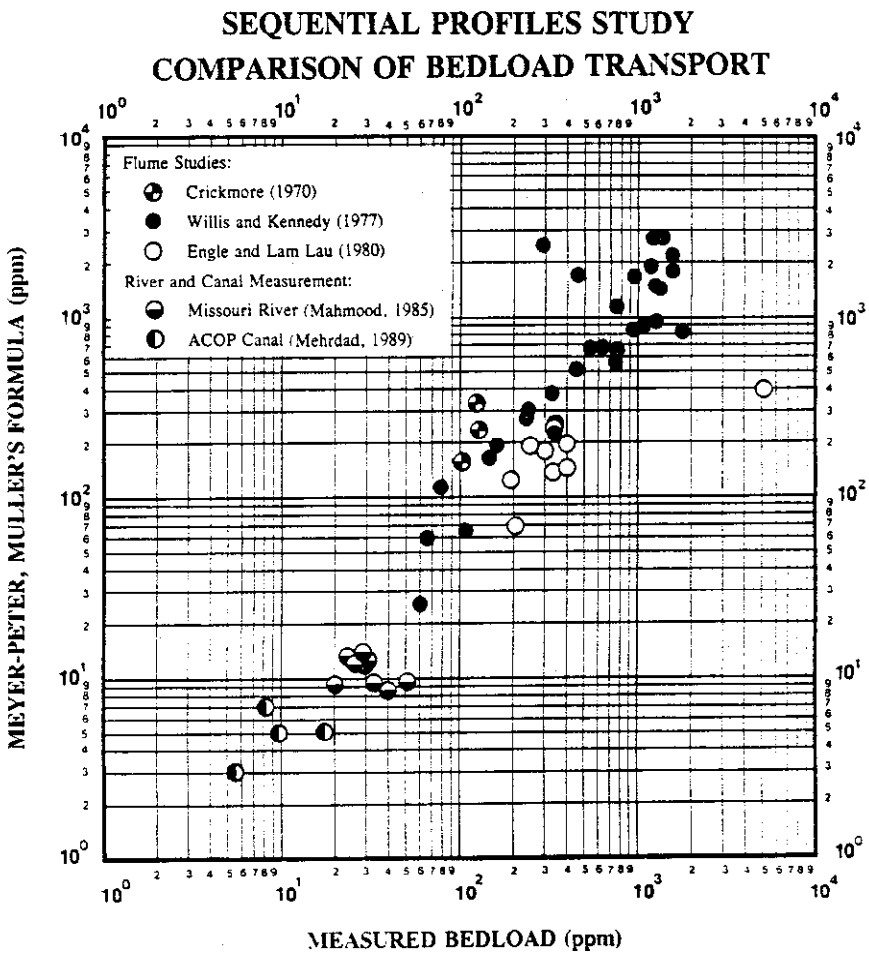

Figure 2 Comparison of Bedload Concentration Measured by Sequential Profiles and Computed by Meyer-Peter, Muller Formula.

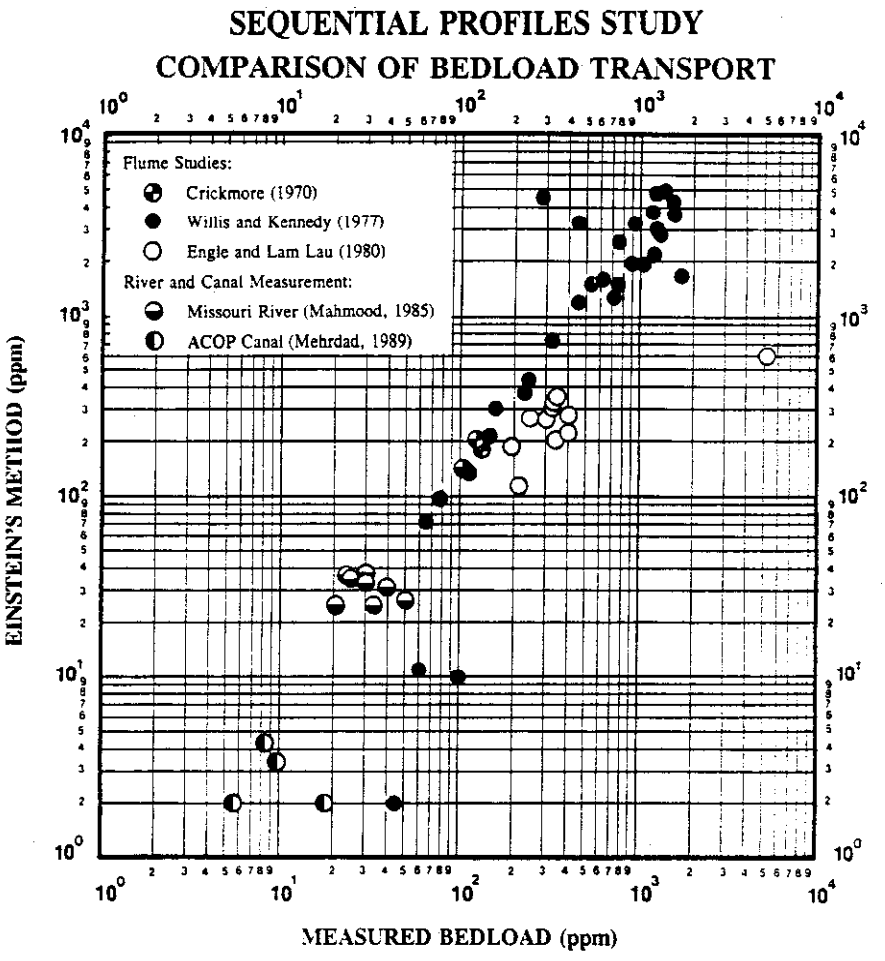

Figure 3 Comparison of Bedload Concentration Measured by Sequential Profiles and Computed by Einstein Bed-Load Function.

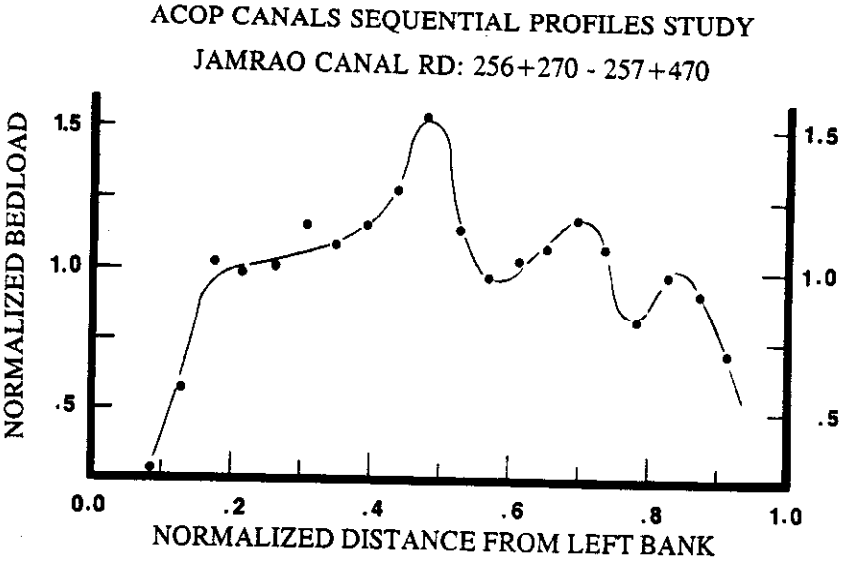

Figure 4 Spatial Variation of Bedload Across Channel Width. Jamrao Canal; Date: 07-31-84 thru 08-01-84.

SEQUENTIAL PROFILES STUDY

MISSOURI RIVER

Date: 07-27-82

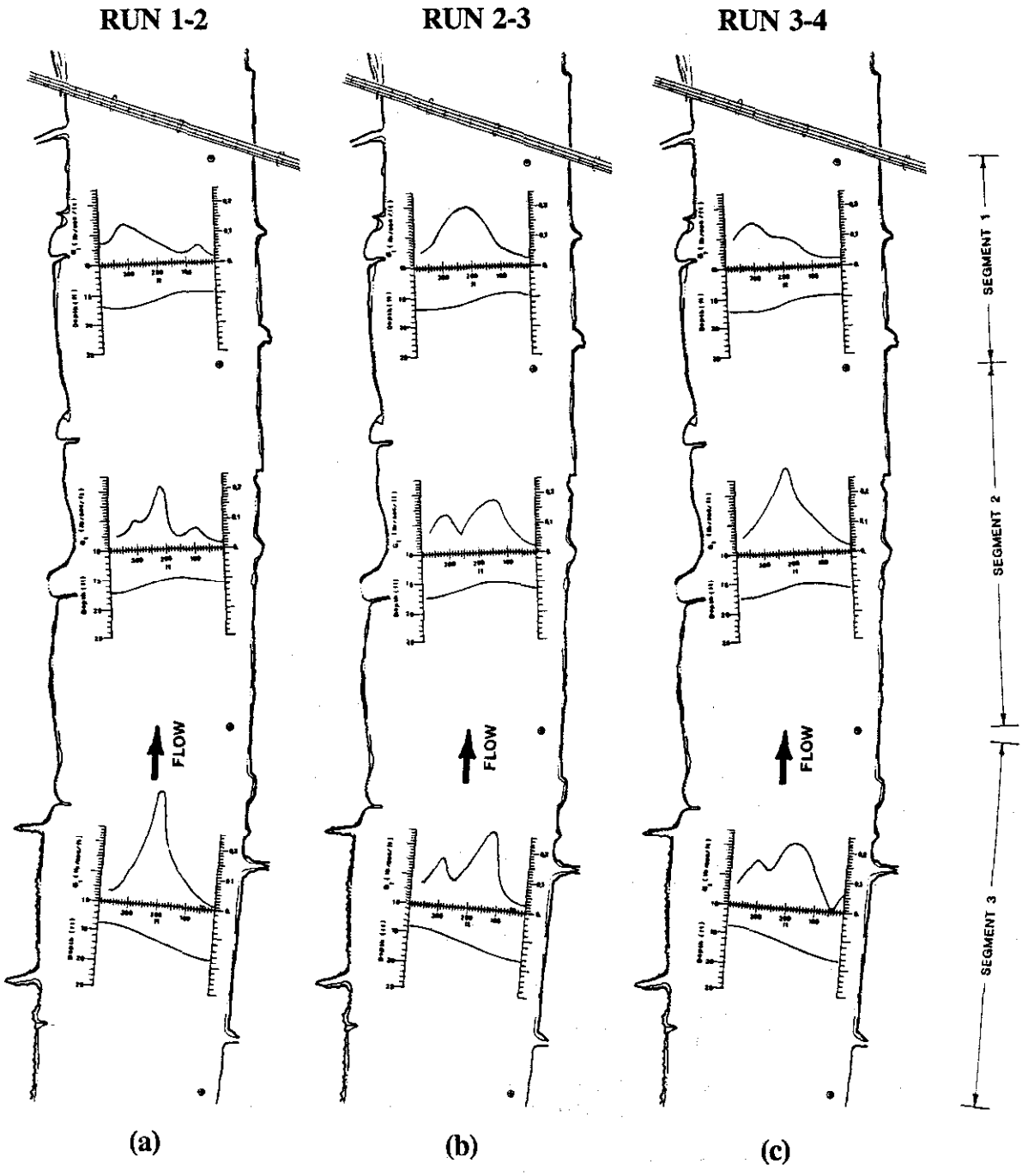

Figure 5 Spatio-temporal Variation of Bedload in Missouri River.

DEPOSITION ON REVETMENTS ALONG THE SACRAMENTO RIVER, CA

By K.J. Fischer[1], M.D. Harvey[2] and D.B. Pridal[3]

ABSTRACT

Between Verona (RM 78) and Colusa (RM 144) on the Sacramento River, approximately 52 percent of the total bank length (both banks) has been revetted to protect the flood control levees that are part of the Sacramento River Flood Control Project. Within this reach of the river, bank revetments include river cobble riprap (RCRR) that was emplaced at a bank angle of 3H:1V and quarry rock riprap (RXRR) that was emplaced at a bank angle of 2H:1V. In general RCRR was used before 1970 and RXRR was used after 1970. At almost all locations where RCRR was used to protect the banks, thick, berm-shaped sedimentary deposits have formed on top of the revetments. The sediments are composed of fine sand (50 percent) and silt and clay (50 percent). In contrast, very little sediment has been deposited on the RXRR sites.

Two cross sections were surveyed - one 50 feet upstream, and the other 50 feet downstream of the Wilkens Slough gaging station (RM 117.7) and the cross section elevations were tied into the gage datum. At the upstream cross section, the right bank was revetted with RXRR in 1986 and the left bank was revetted with RCRR in 1970. At the downstream cross section, both banks were revetted with RCRR in 1966. Between 6 and 7 feet of deposition were measured on the RCRR and less than 1 foot was measured on the RXRR. Deposition on the RCRR increased the bank angle from 3H:1V to 2H:1V. Deposition on the revetments is dependent on the original bank angle and is independent of age of the revetment and the presence or absence of vegetation.

HEC-2 analysis showed that the top of the berm was correlated with a discharge of 29,500 cfs (2 percent duration), the crest of the berm was correlated with a discharge of 18,700 cfs (22 percent duration) and the base of the berm was correlated with a discharge of 5,200 cfs (84 percent duration). Deposition has reduced cross section area by about 3 percent and appears to reduce channel conveyance at low flows. At higher flows, reduced channel roughness appears to compensate for the reduced cross section area.

[1,2]Water Engineering and Technology Inc., 419 Canyon, Suite 225, Fort Collins, Colorado 80521
[3]U.S. Army Corps of Engineers, Sacramento District, Sacramento, California

INTRODUCTION

The Sacramento River Bank Protection Project is a continuing construction project designed to provide protection for the existing levees and flood control facilities of the Sacramento River Flood Control Project. It consists of 977 miles of levees plus overflow weirs, pumping plants and bypass channels along the Sacramento River from RM 0 near Collinsville to RM 194 near Chico, including several sloughs and the lower reaches of major tributaries. The study reach discussed in this paper extends from Verona (RM 79.5 to Colusa (RM 144) (Fig. 1).

Although the process of lateral accretion within stream channels and its effect on channel morphology have been studied by numerous workers (Taylor and Miall, 1978; Harvey and Watson, 1988; Schumm, 1960), lateral deposition onto rock revetments has not been evaluated in detail. On the Sacramento River, the general bank protection strategy between Verona (RM 79.5) and Colusa (RM 144.5) has been to riprap remaining berms to the top of bank where levee erosion is imminent. Approximately 52 percent of the bankline between Verona and Colusa is revetted. Bank protection along the study reach consists of rock riprap, river cobble riprap and concrete rubble riprap. Extensive deposition onto revetment was observed between Colusa and Verona (WET, 1990). Analysis of the location, extent, depth, morphology, depositional history and stage dependency of the deposition allows evaluation of revetment emplacement criteria and maintenance standards for riparian vegetation in the revetments.

CHARACTER OF DEPOSITION

Sediment deposition onto riprap extends almost continuously on revetted banks from Verona to Colusa. Two cross sections were surveyed at RM 117.7 where extensive deposition is present atop revetment. These cross sections were tied into the elevation of a USGS gaging station at Wilkens Slough. The cross sections were surveyed approximately 100 feet apart from one another - one upstream (Cross Section 5) and one downstream (Cross Section 4) of the gage. Each section reflects different revetment histories.

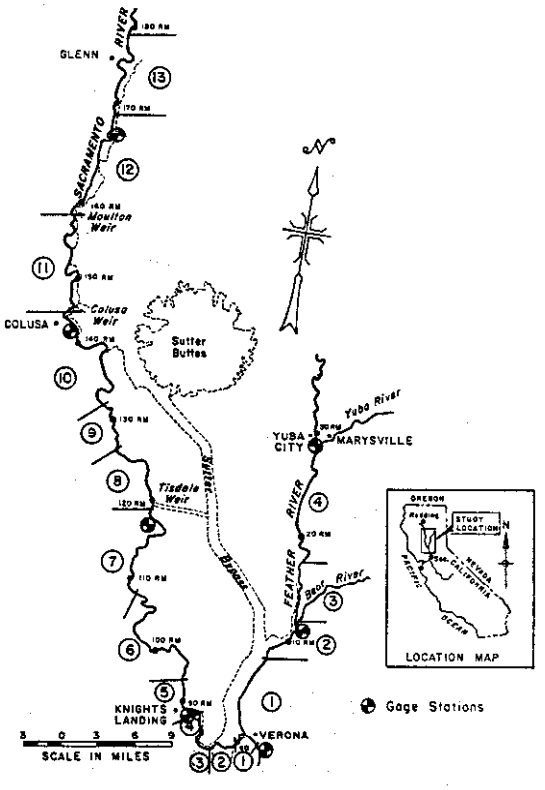

Figure 1. Location map of study reach showing subreach delineations.

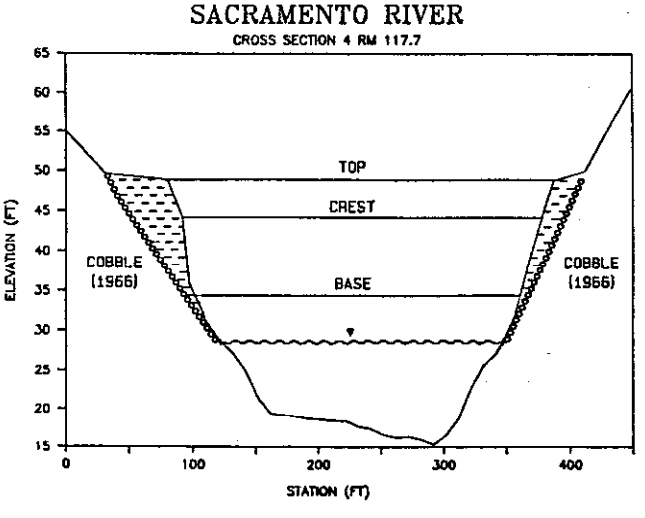

Figure 2. Cross Section 4, RM 117.7

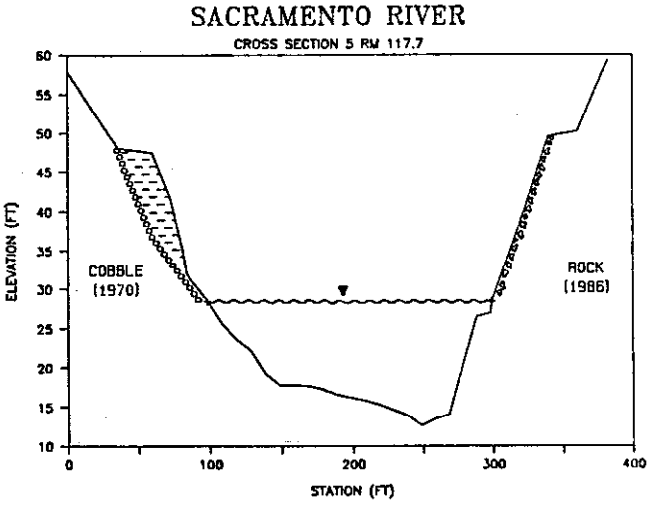

Figure 3. Cross Section 5, RM 117.7.

The detailed surveys document the characteristic berm shape of the deposition atop the riprap (Figs. 2 and 3). Both sites have been colonized only by young grasses, probably due to defoliation of vegetation as a standard maintenance practice. Both the right and left banks of Cross Section 4 were revetted with river cobble in 1966; Cross Section 5 was revetted on the right bank with rock in 1986 and on the left bank with river cobble in 1970 (Figs. 2 and 3). The exposure of river cobble both above and below the deposition at a constant angle allowed the determination of the approximate thickness of the berm.

Figures 4 and 5 show enlarged views of the berms present at each cross section. The river cobble riprap was emplaced at Cross Section 4 at an angle of 2.9H:1V (Fig. 4). Subsequent deposition has steepened that angle on the right bank to 1.7H:1V (Fig. 4). The maximum vertical thickness of sediment is 7 feet on the true right bank and 8 feet on the true left bank. At Cross Section 5, a similar berm is present on the true left bank (Fig. 5). On the right bank, rock riprap was emplaced at a bank angle of 2H:1V in 1986; subsequent deposition onto the bank has been minimal (Fig. 3). The true right bank at both cross sections reflects a bank angle that is slightly steeper than 2H:1V; in fact, looking down the bank, no distinct bank angle change is observable at the contact between the river cobble and rock revetment.

The survey results suggest that the extent of deposition onto riprap is dependent on original bank angle and perhaps revetment age. The older sites that were revetted with river cobble at a bank angle of 3H:1V contain consistently more deposition than younger revetment that was constructed at a 2H:1V angle. Further observations at other localities indicate that bank angle, not time, ultimately controls the quantity of sediment deposited. Regardless of age of emplacement, revetted banks are capped by deposition which has steepened the bank angle to approximately 2H:1V. Consequently, riprap emplaced at an original bank angle of 2H:1V is not conducive to subsequent sediment accumulation of substantial volume. The exceedence of a stable bank angle through continued deposition results in mass failure of the berm. Failure of the berm generally does not involve underlying revetment. The stability of the berm appears to be dependent on sediment cohesion; the cohesiveness of the deposited sediment at the sites studied allows bank angle steepening to approximately 2H:1V.

Between Verona and Colusa, approximately 140,000 tons of sediment are stored on river cobble revetment. This number is based on the berm dimensions surveyed at Wilkens Slough and the lateral extent of 3H:1V-emplaced river cobble riprap along the channel bank. Over 25 years, this equates to 4,600 tons/year sediment storage on the revetment. Grain size analysis results show that the berm sediment consists of 50 percent sand- 29 percent silt- and 21 percent clay-sized material.

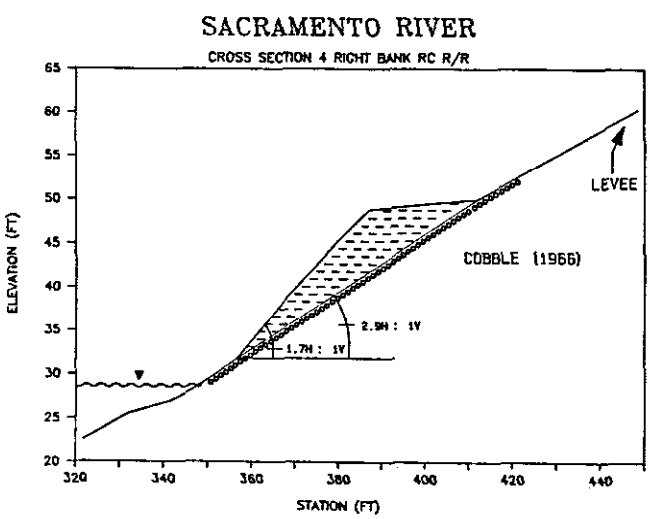

Figure 4. Plotted right bank of Cross Section 4, RM 117.7.

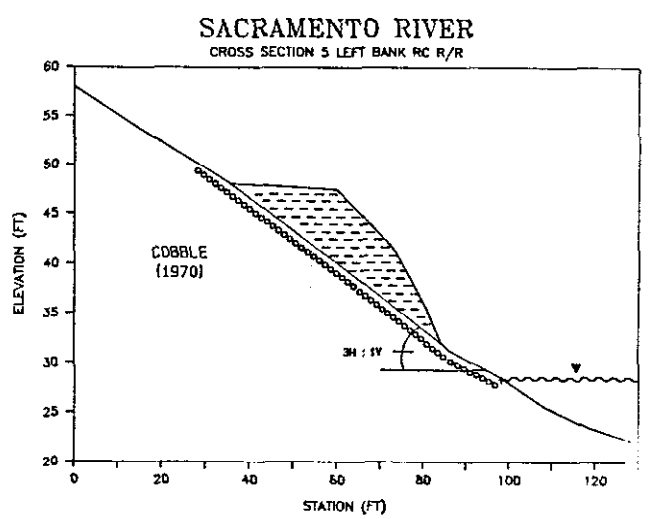

Figure 5. Plotted left bank of Cross Section 5, RM 117.7.

HYDRAULIC EVALUATION

As the two cross sections were tied into true elevations at the USGS Wilkens Slough gaging station, it was possible to insert the sections into a HEC-2 data file made available by the Sacramento District Corps of Engineers. With these cross sections in the data file, HEC-2 was run and a rating curve generated for the sections. The elevations of the top, crest and base of the deposition were placed onto the rating curve and a discharge value for each geomorphic horizon on the berm was determined (Fig. 6).

These discharges then were evaluated in terms of flow duration. The elevation of the top of the berm is correlative to a discharge of approximately 29,500 cfs, which is equaled or exceeded 2 percent of the time; the crest of the berm is correlative to 18,700 cfs, which is equaled or exceeded 22 percent of the time; and the base of the deposition reflects a discharge of 5,200 cfs, which is equaled or exceeded 84 percent of the time (Fig. 7). These exceedence frequencies are based upon mean daily discharges. The fact that the berm is partially inundated at discharges that are exceeded 84 percent of the time indicates that the deposition on riprap may be highly transient. Without repeat surveys and observations, it is difficult to evaluate the transience of the berm. During the field investigation of April 1989, the deposition was observed to be failing, as desiccation cracks formed during waning flows following a peak discharge of 26,693 cfs at Wilkens Slough in March, suggesting that at least a portion of the sediment is semi-permanent.

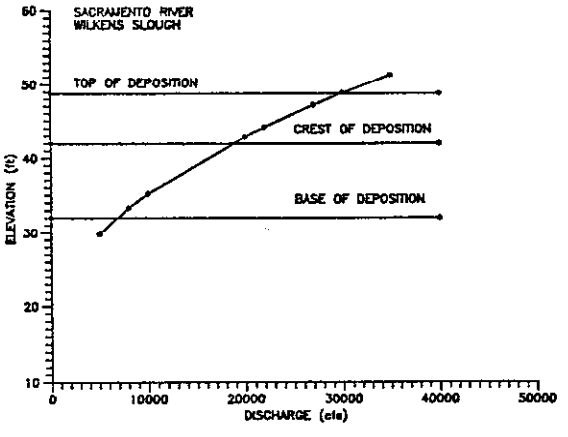

Figure 6. Rating curve for Cross Section #4, showing elevations of primary geomorphic features

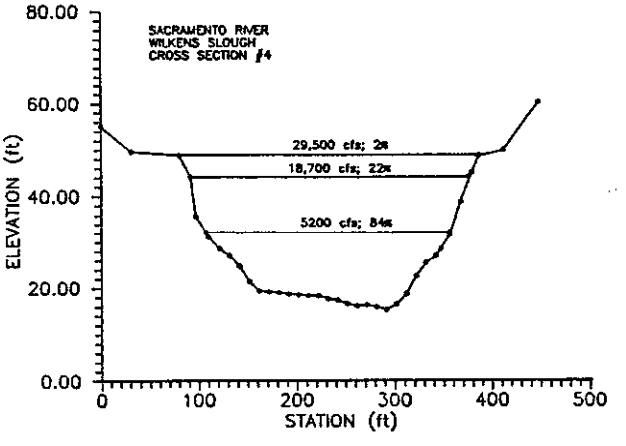

Figure 7. Relationship between top, crest and base of deposition to flow duration.

Approximately 3 percent of the cross section area at RM 117.7 has been lost due to deposition since 1966. A loss in channel area will result in an increase in specific gage height if hydraulic conveyance does not increase as a result of other compensatory changes in cross section variables. The specific gage plot for Wilkens Slough (8,000 cfs) shows an increase in gage height of approximately 1.5 feet from 1967-1986 (Fig.

8). The increasing gage height observed from 1971-1986 is accompanied by a slight decrease in mean velocity. This relationship suggests that the trend observed in the specific gage plot is not due solely to aggradation of the channel bed; rather, it may be due at least in part to a gradual increase since 1971 in channel roughness at Wilkens Slough at relatively low discharges. At 20,000 cfs, no general trends are present (Fig. 9). Although a range in the data is present, average values of gage height and velocity are maintained reasonably well from 1970 to 1988. Consequently, the changes in channel roughness observed at relatively low flows (8,000 cfs) do not appear to affect conveyance at higher discharges (20,000 cfs).

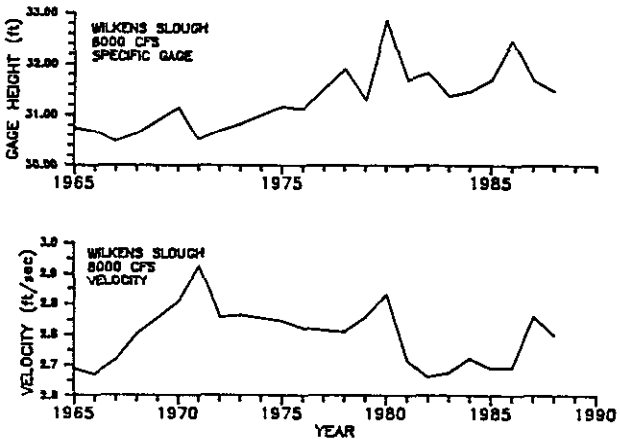

Figure 8. Specific gage and specific velocity at Wilkens Slough at 8,000 cfs.

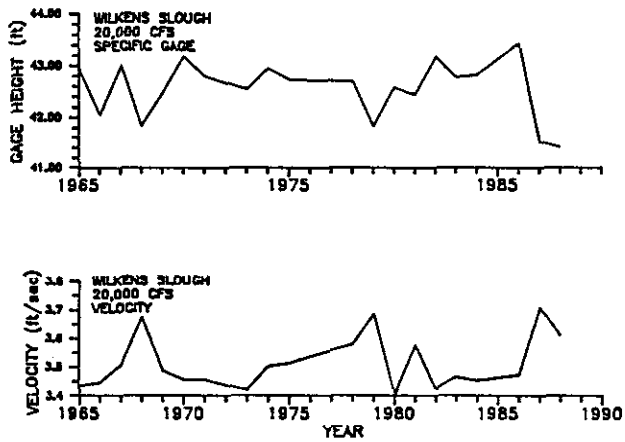

Figure 9. Specific gage and specific velocity at Wilkens Slough at 20,000 cfs.

VEGETATION

The distribution of established vegetation within the berm is highly variable. At several locations, annual grasses constitute the total growth; at the other locations, large cottonwood stands have become established on the revetment and extend up through the berm, where adventitious roots record rates of berm sedimentation (WET, 1990; Hook and Brown, 1973; Harvey, Pitlick and Laird, 1987; Simon and Hupp, 1987). The presence or absence of vegetation on the berm is evidently controlled by maintenance practices, as sites that display aggressive colonization may be directly adjacent to geomorphically identical sites that are entirely void of growth.

Deposition in revetment is not necessary for vegetative growth in rock; however, large woody riparian species have been observed to flourish on riprap that is buried by the laterally accreted berms. The presence of established riparian vegetation on the berm may add cohesion and allow accretion to form bank angles steeper than 2H:1V. The effects of the presence of large woody vegetation on the sedimentation rate of the berm, berm stability and hydraulic characteristics of the channel are important when considering the general consequences of revetment. Highly variable combinations of revetment age, bank angle, location and vegetation density are present on the Sacramento River between Colusa and Verona; the reach is, therefore, optimal for a detailed study of the hydraulic and aesthetic implications of berm development.

The progressive loss of riparian habitat on the Sacramento River has been a great concern for many years. Revetment is generally considered to be harmful to vegetation, as the most widely used form of revetment, rock riprap, requires bank shaping and associated removal of topbank vegetation. It is ironic, however, that the remaining stands of mature riparian vegetation located in levee setback subreaches are threatened by natural bank erosion. Hence, the future of the vegetation is inherently uncertain. Observations of vegetation

and deposition on revetment on the Sacramento River suggest that if maintenance standards are relaxed and vegetation is allowed to establish, a significant proportion of the riparian habitat lost by bank shaping can be regained on the revetted bank itself. In other words, the revetted site can provide a measure of self-mitigation. If the banks are laid back at an angle of 2H:1V, approximately 87 percent of the acreage removed from top bank is available on the revetment (Fig. 10). On banks this steep, however, sediment deposition appears minimal and vegetative colonization may be limited. On banks of 3H:1V, approximately 81 percent of the topbank area lost will be regained as riparian habitat on the bank. At this angle, sediment deposition is extensive and habitat quality, therefore, may be greater than on a 2H:1V bank. If the generation of quality riparian habitat in conjunction with effective bank stabilization is desired, an intermediate bank angle (approximately 2.5H:1V) is suggested, although further detailed study is highly recommended.

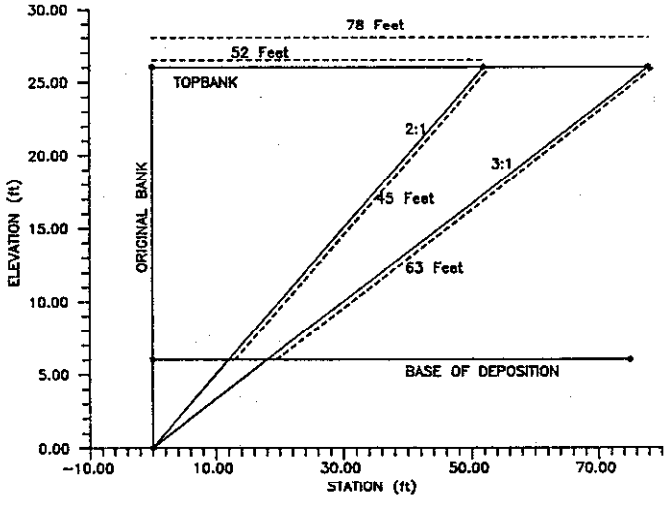

Figure 10. Surface area loss due to bank shaping at angles of 2H:1V and 3H:1V showing potential recovery of riparian habitat area on revetted bank.

CONCLUSIONS

Extensive deposition onto rock and river cobble riprap was observed on the Sacramento River downstream of Colusa. This deposition was surveyed at several cross sections; incorporation of one of the sections (Wilkens Slough) into a HEC-2 deck allowed the determination of the hydrogeomorphic character of the depositional berm. It appears that lateral accretion onto the revetment has affected channel roughness so that hydraulic conveyance has decreased for low flows at the cross section. This reduction in conveyance is not observed at high flows. The persistence and geotechnical stability of the berms are not clear. An understanding of the depositional history of the sediment would aid in the determination of general sediment transport and storage characteristics of the leveed reach.

In addition to sediment deposition, riparian vegetation is common on the revetment within the leveed reach. The vegetation ranges from grasses to young willows and alders to large stands of cottonwood. The presence of large stands of riparian vegetation atop rock revetment indicates a potential for riparian habitat on revetted banks. The relationship between lateral sediment accretion onto revetment and vegetative colonization onto revetment is unclear and should be evaluated in detail. It is clear, however, that deposition onto riprap is dependent on bank angle; if growth of riparian vegetation is enhanced by the presence of accreted sediment, a bank angle less than 2H:1V and somewhat greater than 3H:1V would optimize the recovery of habitat lost due to bank shaping.

ACKNOWLEDGEMENTS

Portions of the analyses in this paper were conducted under Contract No. DACW05-88-D-0044 for the U.S. Army Corps of Engineers. The views expressed herein are those of the authors and not necessarily those of the U.S. Army Corps of Engineers.

REFERENCES

Harvey, M.D., Pitlick, J., and Laird, J.R.,1987, Temporal and spatial variability of sediment storage and erosion in Ash Creek, Arizona, IAHS, Publ. No. 165, p. 281-282.

Harvey, M.D. and Watson, C.C., 1988, Channel response to grade control structures on Muddy Creek, Mississippi: Regulated Rivers Research and Management, v. 2, p. 79-92.

Hook, D.D. and Brown, C.L., 1973, Root adaptations and relative flood tolerance of five hardwood species, Forest Science, v. 19 (3), 225-229.

Schumm, S.A., 1960, The effect of sediment type on the shape and stratification of some modern fluvial deposits: American Journal of Science, v. 258, p. 177-184.

Simon, A. and Hupp, C.R., 1987, Geomorphic and vegetative recovery processes along modified Tennessee streams: An interdisciplinary approach to disturbed fluvial systems, IAHS - IASH Publ. No. 165, p. 251-262.

Taylor, G. and Woodyear, K.D., 1978, Bank deposition in suspended-load streams, IN: Fluvial Sedimentology, A.D. Miall, ed., Canadian Society of Petroleum Geologists Memoirs, p. 257-276.

Water Engineering & Technology, Inc., 1990, Geomorphic analysis and bank protection alternatives report for Sacramento River (RM 78-194) and Feather River (RM 0-28). Report prepared for Sacramento District, U.S. Army Corps of Engineers, Contract No. DACW05-88-D-0044, Delivery Order 5, 278 p.

SIZE DISTRIBUTION OF NONUNIFORM BED MATERIAL IN TRANSPORT

By Chih Ted Yang,
U.S. Bureau of Reclamation, Denver, Colorado; and
Shenggan Wan,
Nanjing Hydraulic Research Institute, Nanjing, China

ABSTRACT

The total bed material load formulas developed by Einstein, Laursen, Toffaleti, and Yang can be used to compute bed material transport by size fraction. These four formulas can also be used to predict the size distribution of bed material in transport. Three hundred five sets of laboratory data published by Guy, et al, are used to determine the accuracies of these formulas in predicting the median particle size of bed materials in transport. This study indicates that the accuracy of formulas in descending order are those developed by Yang, Laursen, Toffaleti, and Einstein.

INTRODUCTION

The size distribution of sediment particles in transport is important to our understanding of movement of pollutants attached to sediment particles, reservoir sediment distribution, and river engineering. Most sediment transport equations emphasize the estimation of total rate of sediment transport. Among the commonly used bed material load formulas, those developed by Einstein (1944), Laursen (1958), Toffaleti (1968), and Yang (1973, 1979, 1984) can be used to compute bed material transport by size fraction. These formulas are used in this paper to determine the particle size distribution of bed material in transport. Laboratory-measured bed material size distribution in alluvial beds and in transport are used to determine the accuracies of these formulas in predicting bed material size distribution in transport.

FORMULAS

The total bed material load formulas developed by Einstein (1944), Laursen (1958), Toffaleti (1968), and Yang (1973, 1979, 1984) were published in the literature and will not be elaborated here. The formulas by Einstein, Laursen, and Toffaleti can be used to compute total bed material load or concentration by size fraction directly. The three formulas proposed by Yang were originally developed for estimating total bed material concentration using the median particle diameter as the representative particle size. Yang's 1973, 1979, and 1984 formulas were developed for sand transport, sand transport with concentration greater than 20 ppm by weight, and gravel transport, respectively. Yang (1988) suggested that these formulas can also be used in conjuction with the following equation to predict total bed-material concentration of nonuniform materials:

$$C = \sum_{i=i}^{j} p_i C_i \qquad (1)$$

where C_i is the sediment concentration in parts per million by weight for size fraction i; j is the total number of size fractions used in the computation; and p_i is the percentage of material in size i. Among the three formulas proposed by Yang, only his 1973 formula in conjunction with equation (1) is used in this paper due to the range of data available for comparison.

VERIFICATION OF ACCURACY

The computer programs published by Stevens and Yang (1989) are used to compare the accuracies of total bed material load formulas in predicting the median particle size of bed materials in transport. Let us define the discrepancy ratio γ_1 as the ratio between median particle size d_c in transport computed by a formula and actually measured median particle size d_m in transport; that is,

$$\gamma_1 = \frac{d_c}{d_m} \tag{2}$$

Let us also define the discrepancy ratio γ_2 as the ratio between the median particle size d_c in transport computed by a formula and the median particle size d_{50} of the original bed materials on the alluvial bed; that is,

$$\gamma_2 = \frac{d_c}{d_{50}} \tag{3}$$

γ_1 should give us an indication of the average accuracy of a formula in predicting the size distribution of bed materials in transport. γ_2 should give us an indication of the reasonableness of a formula to describe the sorting process or the reduction of average particle size in the transport process.

The 305 sets of data published by Guy et al (1966) include information on size distributions of bed materials on the bed and bed materials in transport. The results shown in table 1 indicate that Yang's 1973 fraction formula has the best overall discrepancy ratio of 0.95. The results shown in table 1 and figure 1 also show that the γ_1 value of Yang's 1973 formula, when applied by size fraction, is not very sensitive to the variation of Froude number. These results suggest that Yang's 1973 equation, when applied by size fraction, can be used with accuracy to predict size distribution of bed materials in transport. Our study also indicates that the median sizes of bed materials in transportation predicted by Laursen (1958) and Toffaleti (1968) are too small, while those predicted by Einstein (1950) are too large.

Table 2 and figure 2 indicate that, with the exception of the Einstein formula, bed materials in transport computed by Laursen (1958), Yang (1973), and Toffaleti (1968) are finer than the original bed materials on the bed, which is consistent with the sorting phenomena. This sorting process explains why bed material size should decrease in the downstream direction. The measured γ_2 value of 0.77 shown in table 2 is the average value for all data. This value is very close to the average value of 0.75 computed by Yang's 1973 formula by size fraction. The γ_2 values of the Einstein (1950) formula are greater than one for all flow conditions, which means the materials in transport computed by the Einstein formula are coarser than the original bed materials, and the bed material size would increase in the downstream direction. This unreasonable result may stem from the use of the hiding correction factor and lifting correction factor by Einstein.

The total bed material load computed by the Einstein formula is directly related to bedload. In order to reflect the influence of nonuniform bed material size distribution and lift force, Einstein introduced the hiding factor ξ and lifting factor Y. The values of ξ and Y vary from 1 to 100 and from 0.25 to 0.85, respectively. The combined effect of ξY on a finer particle could be as high as 300 times the effect on a larger particle where the finer particle is hiding

behind the larger one. This effect is especially pronounced when the Froude number is small. This may be why the values of γ_1, and γ_2 in tables 1 and 2 decrease with increasing value of Froude number F_r.

SUMMARY AND CONCLUSIONS

Laboratory data with measured particle size distribution of bed material in alluvial bed and in transport are used to compare the accuracies of four total bed material load formulas in predicting the median size of bed material in transport. Our comparisons indicate that the accuracy of formulas in descending order are the Yang, Laursen, Toffaleti, and Einstein formulas. With the exception of the Einstein formula, computed bed material size in transport is finer than that in the original alluvial bed, which is consistent with the sorting phenomenon. Our study results suggest that Einstein's hiding and lifting correction factors overcorrected the effect of nonuniform size distribution of bed material on total bed material load transport, especially for flows with a low Froude number.

REFERENCES

Einstein, H. A., 1944, "Bed-Load Transportation in Mountain Creek," U.S. Department of Agriculture, Soil conservation Service Technical Paper 55.

Guy, H. P., Simons, D. B., and Richardson, E. V., 1966, "Summary of Alluvial Channel Data From Flume Experiment, 1956-1961," U.S. Geological Survey Professional Paper 426-I, 96 p.

Laursen, E. L., 1958, "The Total Sediment Load of Streams," ASCE Journal of the Hydraulics Division, Vol. 84, No. HY1, pp. 1-36.

Stevens, H. H., Jr., and Yang, C. T., 1989, "Summary and Use of Selected Fluvial Sediment-Discharge Formulas," U.S. Geological Survey Water Resources Investigations Report No. 89-4026, Denver, Colorado.

Toffaleti, F. B., 1968, "A Procedure for Computation of the Total River Sand Discharge and Detailed Distribution, Bed to Surface," Technical Report No. 5, Committee on Channel Stabilization, U.S. Army Corps of Engineers Waterways Experiment Station, Vicksburg, Mississippi, 177 p.

Yang, C. T., 1973, "Incipient Motion and Sediment Transport," ASCE Journal of the Hydraulics Division, Vol. 99, No. HY10, pp. 1679-1704.

Yang, C. T., 1979, "Unit Stream Power Equations for Total Load," Journal of Hydrology, Vol. 40, Elsevier Scientific Publishing Co., the Netherlands, pp. 123-138.

Yang, C. T., 1984, "Unit Stream Power Equation for Gravel," Journal of Hydraulic Engineering, ASCE, Vol. 110, No. 12, pp. 1783-1797.

Yang, C. T., 1988, "Sediment Transport and Unit Stream Power," Vol. 5, Chapter 8, Civil Engineering Practice, Edited by Cheremisinoff, P. N., Cheremisinoff, N. P., and Cheng, S. L., Technomic Publishing Co., Lancaster, Pennsylvania, pp. 265-289.

Table 1. - Comparison between computed and measured bed materials size in transport

Author of formula	Discrepancy ratio, γ_1					Number of data sets
	Mean	Percent of data in the range			Standard deviation	
		0.75-1.25	0.5-1.5	0.25-1.75		
			F_r = 0.20-0.30			
Laursen	0.86	79	100	100	0.15	19
Yang	1.09	79	100	100	0.18	19
Einstein	2.64	0	0	0	0.84	19
Toffaleti	0.77	42	100	100	0.19	19
			F_r = 0.30-0.50			
Laursen	0.82	60	97	100	0.19	117
Yang	1.03	85	93	100	0.21	117
Einstein	1.94	22	43	50	0.86	117
Toffaleti	0.61	32	59	85	0.28	117
			F_r = 0.50-1.00			
Laursen	0.78	60	88	95	0.23	86
Yang	0.91	80	92	99	0.25	86
Einstein	1.41	55	77	84	0.64	86
Toffaleti	0.55	22	51	83	0.27	86
			F_r = 1.00-2.00			
Laursen	0.73	48	89	100	0.16	83
Yang	0.85	66	99	100	0.18	83
Einstein	0.99	86	99	100	0.18	83
Toffaleti	0.53	22	47	94	0.23	83
			All data			
Laursen	0.79	58	92	99	0.19	305
Yang	0.95	78	95	100	0.21	305
Einstein	1.58	47	65	70	0.61	305
Toffaleti	0.58	27	65	87	0.26	305

Table 2. - Comparison between computed bed material size in transport and measured original bed material size

Author of formula	Discrepancy ratio, γ_2					Number of data sets
	Mean	Percent of data in the range			Standard deviation	
		0.75-1.25	0.5-1.5	0.25-1.75		
			F_r = 0.20-0.30			
Laursen	0.66	26	84	100	0.14	19
Yang	0.81	89	100	100	0.08	19
Einstein	1.98	0	26	37	0.54	19
Toffaleti	0.59	26	74	100	0.16	19
Measured value	0.77	58	95	100	0.10	19
			F_r = 0.30-0.50			
Laursen	0.61	17	87	91	0.16	117
Yang	0.76	80	91	91	0.18	117
Einstein	1.34	51	70	87	0.39	117
Toffaleti	0.43	8	40	79	0.20	117
Measured value	0.77	56	91	96	0.17	117
			F_r = 0.50-1.00			
Laursen	0.63	37	79	91	0.19	86
Yang	0.73	70	88	93	0.20	86
Einstein	1.06	90	97	100	0.17	86
Toffaleti	0.43	13	40	78	0.21	86
Measured value	0.77	79	91	99	0.17	86
			F_r = 1.00-2.00			
Laursen	0.65	17	93	100	0.10	83
Yang	0.76	61	100	100	0.08	83
Einstein	0.90	80	100	100	0.14	83
Toffaleti	0.46	5	36	94	0.15	83
Measured value	0.77	70	98	100	0.17	83
			All data			
Laursen	0.63	23	86	94	0.15	305
Yang	0.75	73	93	95	0.15	305
Einstein	1.18	67	83	91	0.27	305
Toffaleti	0.45	10	41	84	0.19	305
Measured value	0.77	66	93	98	0.17	305

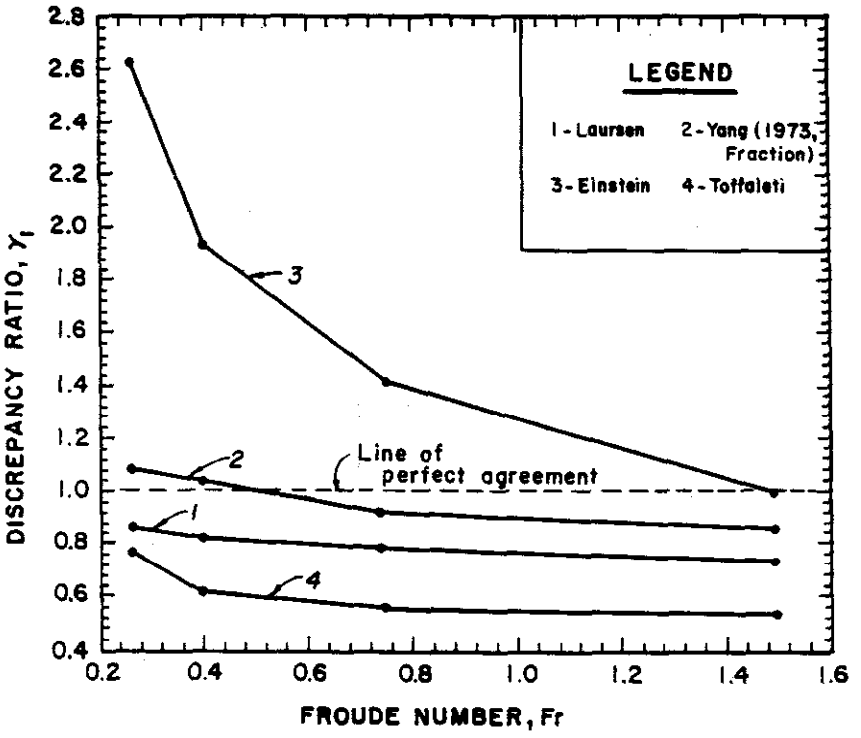

Figure 1. - Comparison between computed and measured particle size of bed material in transport.

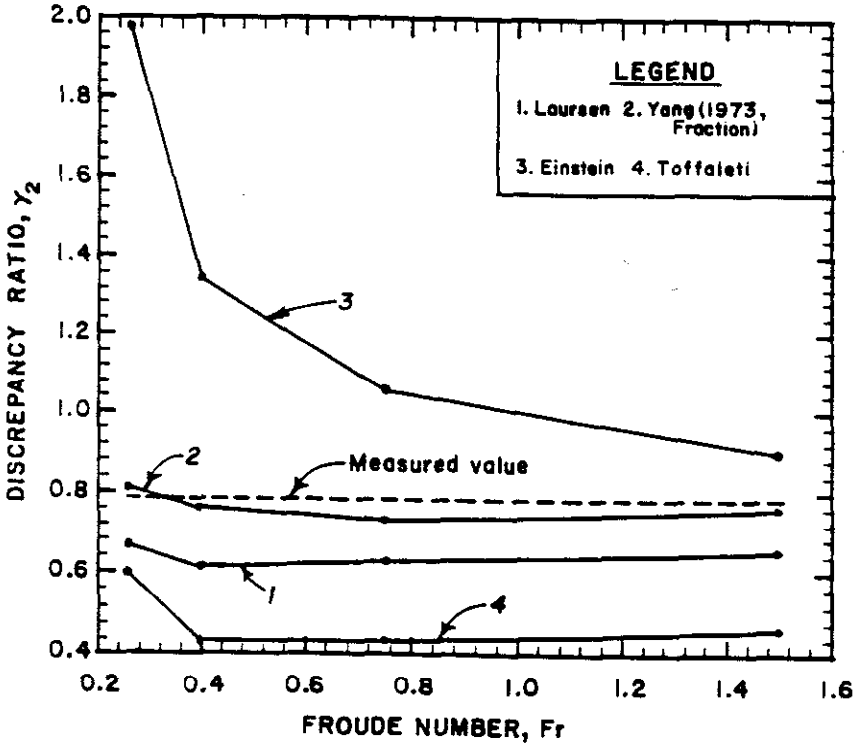

Figure 2. - Comparison between computed bed material size in transport and original bed material size.

CASE HISTORY:CHANNEL AGGRADATION ABOVE A RESERVOIR

By Christopher A. Gorbach, Hydraulic Engineer,
Bureau of Reclamation, Albuquerque, New Mexico

and Drew C. Baird, Chief, River Assessment Branch,
Bureau of Reclamation, Albuquerque, New Mexico,

ABSTRACT

The Bureau of Reclamation maintains facilities in the middle Rio Grande valley to provide efficient transport of water and sediment from Velarde, New Mexico to Elephant Butte and Caballo Reservoirs. Some 250 miles of the river valley are included in the Middle Rio Grande Project area. The major features of the project include a rectified floodway channel and the Low Flow Conveyance Channel.

The Low Flow Conveyance Channel was constructed in the 1950's, a period of prolonged drought and low reservoir levels, to carry flows up to 2000 cfs from San Acacia, New Mexico to Elephant Butte Reservoir. To maximize reservoir inflow the Low Flow Conveyance Channel was extended some 20 miles through then dry areas of the reservoir.

Between 1979 and 1987 flows in the Rio Grande were significantly above normal in eight of the nine years. Elephant Butte Reservoir filled for the first time since 1942 and the lower reaches of the Low Flow Conveyance Channel were inundated. Great quantities of sediment deposited in the upper reservoir and in the river reach affected by its backwater. Because the levee protecting the Low Flow Conveyance Channel confines the river to a narrow strip on the eastern side of the valley, much of the sediment deposition has been limited to a small portion of the floodplain. As a result, the river is now perched and threatens to breach or overtop the levee and destroy more of the Low Flow Conveyance Channel. This paper presents a case history of the development of the problem, its effects, and management responses to the changing conditions.

INTRODUCTION

Above Elephant Butte Reservoir the Rio Grande drains 25,923 square miles. Average annual flow (1961-1985) at San Marcial, which is just above the reservoir, is 485,000 acre feet. Peak discharge frequencies for the floodway are given in table 1. A total sediment concentration averaging roughly 20 tons per acre foot (15,000 mg/l) ranks the Rio Grande above Elephant Butte Reservoir among the more heavily sediment laden streams on earth. Near the head of the reservoir, mean diameter of river bed material is 0.2 millimeters. Virtually all sediments entering the reservoir are finer than 0.3 millimeters diameter. Clay materials from the

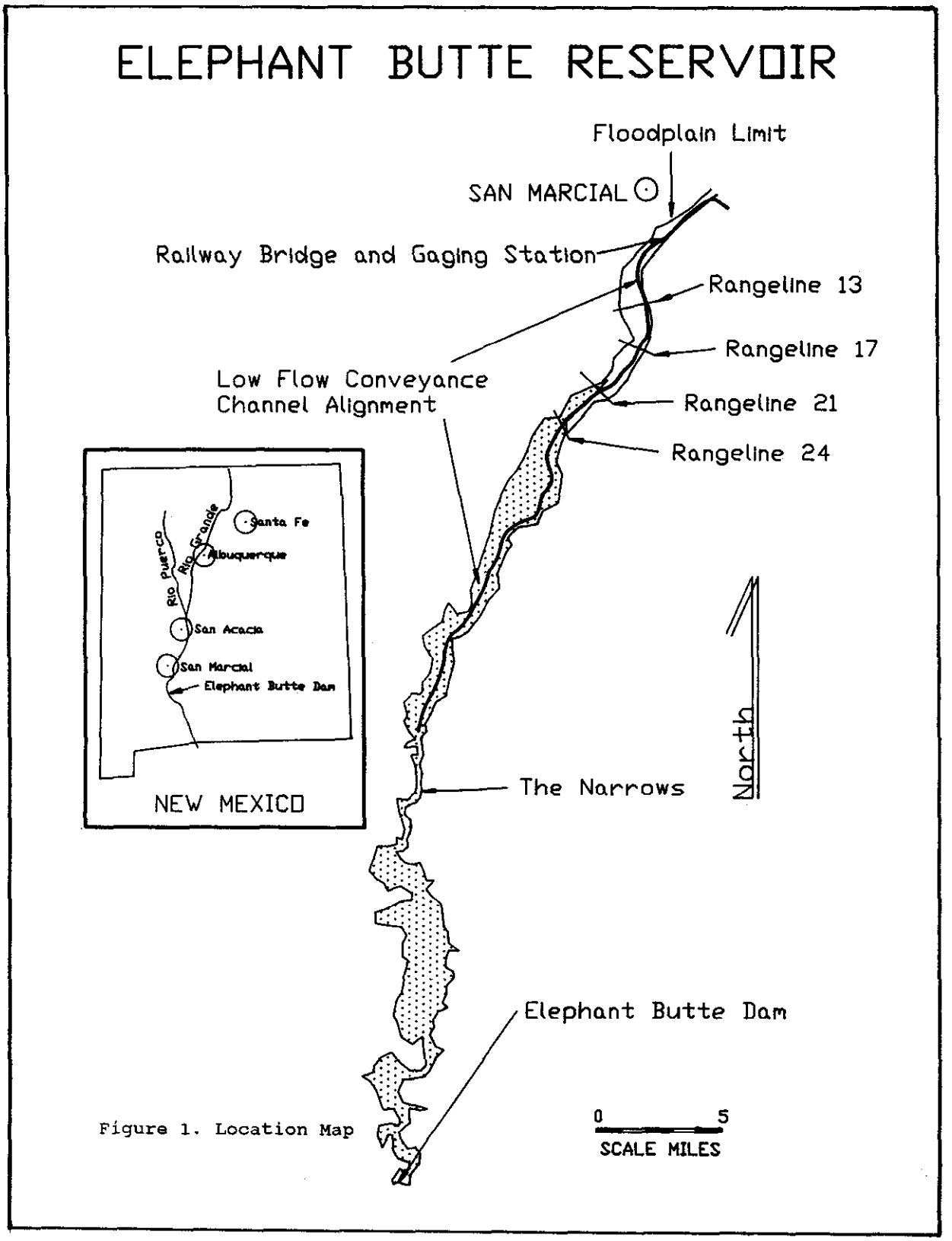

Figure 1. Location Map

tributary Rio Puerco make up a substantial portion of the total sediment load.

Table 1.

Rio Grande at San Marcial, New Mexico
Peak Discharge Frequency[1]

Return (years)	Peak Discharge (cfs)
2	7200
5	14400
10	20100
25	27900

[1]USGS data unadjusted for reservoir operations

The terms of the Rio Grande Compact require the State of New Mexico to deliver water to downstream users from Elephant Butte Reservoir. An international treaty also obligates the United States to deliver Rio Grande water to the Republic of Mexico. Maximizing the flow of water into Elephant Butte Reservoir is essential to meet these obligations.

Under authority granted by Congress in the Flood Control Acts of 1948 and 1950, the Bureau of Reclamation has constructed, operated, and maintained conveyance facilities in the Middle Rio Grande Valley to provide efficient transport of water and sediment through the valley and into the reservoir. Below San Marcial a floodway channel and the Low Flow Conveyance Channel (Conveyance Channel) are maintained for this purpose.

The Conveyance Channel is a man-made channel running approximately 70 miles from San Acacia, New Mexico to the reservoir. In normal operation, up to 2000 cfs can be diverted from the river at San Acacia and carried to the reservoir in the Conveyance Channel with a minimum of evaporation and infiltration loss. The floodway is essentially the natural river managed and maintained for passage of higher flows. Flow is divided between the Conveyance Channel and floodway according to Conveyance Channel capacity and other operational considerations. Flow in excess of Conveyance Channel capacity and irrigation demand is released into the floodway at San Acacia.

Two distinct basins exist in Elephant Butte Reservoir, the upper basin and the main pool. The two basins are connected by a narrow canyon known as The Narrows. Originally the Conveyance Channel extended through the upper basin, which was then dry, to The Narrows.

The Bureau of Reclamation began construction of conveyance facilities in the upper basin of Elephant Butte Reservoir in 1951. At that time the reservoir contained only 21,000 acre feet and the pool was far below The Narrows. Delta formations had completely obstructed the river channel in some places and the entire

floodplain was infested with dense growths of salt cedar (tamarisk). River flow ponded in marshes and swamps increasing the average annual conveyance loss between San Marcial and The Narrows to an estimated 143,000 acre feet per year[1]. The condition had worsened to a degree that severely limited New Mexico's ability meet Rio Grande Compact delivery requirements. Between 1943 and 1951 the state's water debit under the Compact had accrued to 331,800 acre feet[1].

In the construction of the Conveyance Channel, excavated material was spoiled to the east forming a levee that confines the river to a narrow strip on the eastern side of the floodplain. The levee is simply a spoil bank; no attempt was made to design, control, or otherwise improve the earthwork or foundation.

PROBLEM DEVELOPMENT AND MANAGEMENT RESPONSE

Figure 2 is a hydrograph showing the 10 year moving average of Rio Grande flow at San Marcial since 1905. The hydrograph drops sharply about 1950, remains low through the 1950's, 60's and 70's, and increases sharply about 1980. Other Rio Grande records show the same trend; flow was significantly above normal in all years 1979 through 1987 except 1981. Normal flow is considered to be the average of the previous 25 years. By June, 1985, the above normal flows filled Elephant Butte Reservoir for the first time since 1942. The lower 15 miles of the Low Flow Conveyance Channel were inundated and the river channel upstream of the reservoir rapidly aggraded.

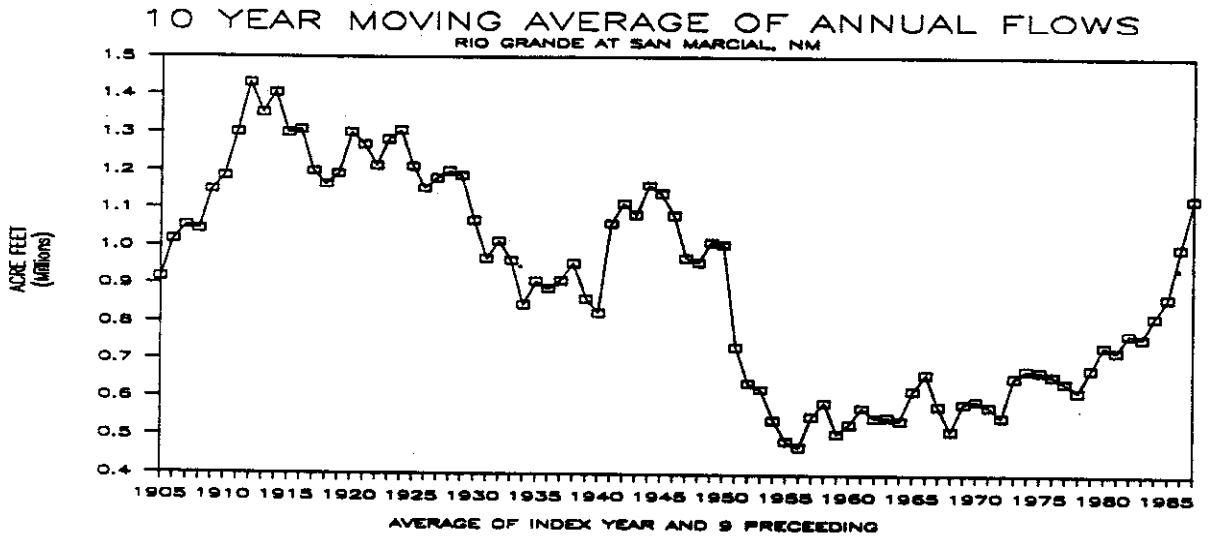

Figure 2. Hydrograph, 10 year moving average, Rio Grande at San Marcial, NM

Because the river channel was confined to the eastern side of the floodplain, aggradation caused the river to become perched in a narrow strip east of the levee. Gaging station records plotted in figure 3 show aggradation at San Marcial beginning in 1979 and amounting to about 10 feet by 1990. A cross section profile of Rangeline 21 (figure 4), which is 7 miles below the gage, illustrates the tendency of the river to become perched east of the levee.

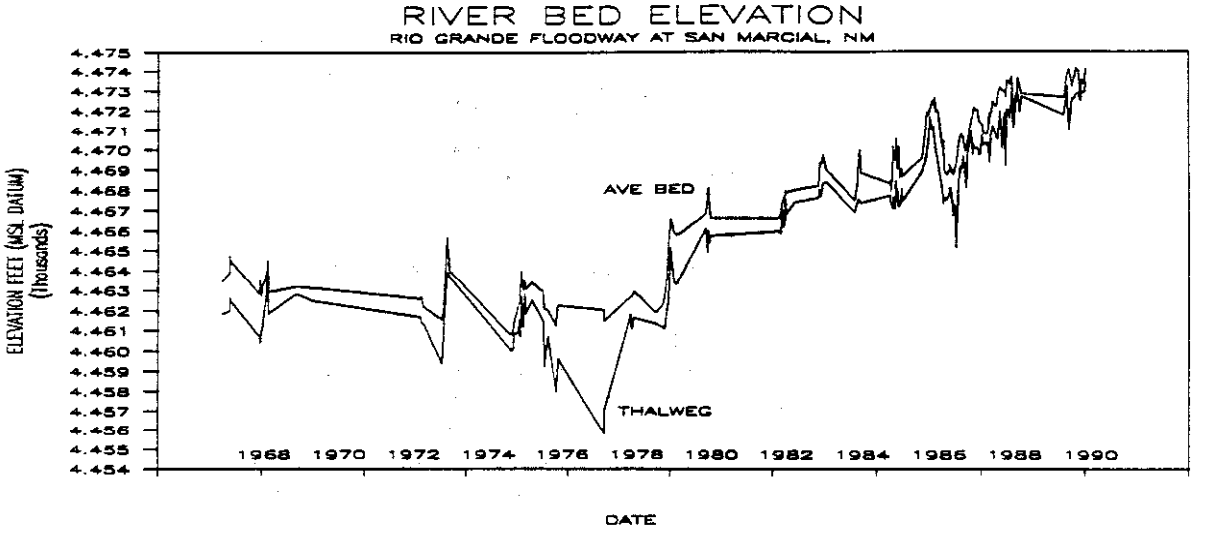

Figure 3. River bed elevation, Rio Grande Floodway at San Marcial, NM

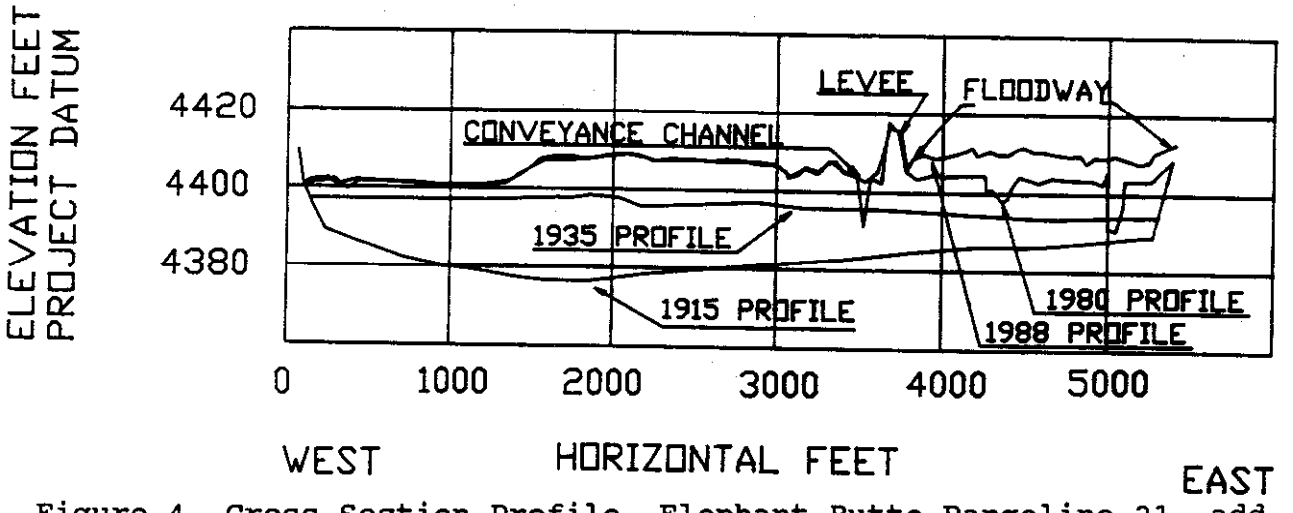

Figure 4. Cross Section Profile, Elephant Butte Rangeline 21, add 43.3 feet to project datum to correct to mean sea level.

Aggradation of the Rio Grande channel just above Elephant Butte Reservoir in the 1980's reduced channel capacity and caused shifting of the channel alignment. Water levels in the floodway became dangerously high, threatening to overtop or break through the levee at discharges less than 5,000 cfs. Original design capacity of the floodway was 25,000 cfs.[1]. Tendency of the river

to shift its course as existing channels became plugged with sand became a serious concern. While peak discharges were not remarkably high, unusually long flow durations exacerbated the problems caused by high river stages as water stored upstream was delivered to Elephant Butte Reservoir throughout the year.

The Albuquerque Projects Office of the Bureau of Reclamation has managed the river to protect and preserve as much as possible of the Conveyance Channel so that operation can be resumed when drier conditions return. Replacement cost of the Conveyance Channel is estimated to be $500,000 per mile. Because conditions of river flow and sediment movement were ever changing and unpredictable, responses were generally of a tactical rather than strategic nature. Resource limitations, environmental constraints, and inability to accomplish maintenance work because of the high water were also factors influencing management decisions.

The first washout of the levee caused by the rising reservoir occurred in July of 1979 approximately 2 miles above The Narrows. The reservoir continued to rise inundating the Conveyance Channel and levee. Successive breachings of the levee caused the river to deposit sand and sediments in the Conveyance Channel burying it many feet deep in some places. The latest breach occurred in 1987 near rangeline 24. Below this point all conveyance system facilities have been destroyed.

The outlet of the Low Flow Conveyance Channel was moved to a location near the top of the reservoir pool in 1983. Operation of the Conveyance Channel could not be continued, however, because rapid deposition of sediment prevented maintenance of a suitable outfall. Operation of the Conveyance Channel was discontinued in March, 1985.

Dredging to open and maintain a channel just above The Narrows was begun in April, 1983. This effort was abandoned when a storm overturned and sank the dredge in November, 1983.

A "paper spill" of the reservoir that counted some water still in upstream storage was declared on June 16, 1985. Some capacity was reserved for flood storage; the actual pool elevation was 1-1/2 feet below the spillway crest. Spilling of the reservoir cancelled all water debits under the Rio Grande Compact.

After the reservoir pool reached maximum elevation the river bed upstream continued to rise. In some areas freeboard on the levee diminished to less than a foot and low areas were raised to prevent overtopping. Head difference between the river on one side of the levee and the Conveyance Channel on the other was as much as 10 feet. Severe stress in the levee was manifest in piping of river water through the embankment and in the appearance of large cracks. The location of the most critical threat shifted with changes in river flow and sediment movement. Investigations were undertaken

to determine the safe limits of raising and reinforcing the levee. Levee raising activity continued throughout the period of high reservoir levels and into the subsequent period of recession.

Various plans to cut a breach through the levee were considered. The intent of these plans was to allow the river to flow to a lower elevation west of the levee and induce upstream headcutting. Protection of upper reaches of the Conveyance Channel would be bought at the price of the loss of a downstream reach. None of these plans was ever executed but temporary local relief of the aggradation was gained when breaches of the levee occurred naturally.

In the winter of 1985-1986 sand plugs formed in the channel at two locations below the railway bridge. Loss of flow over the bank upstream apparently reduced sediment carrying capacity in the old channel and caused the plugs to form.

One of the plugs was located below Rangeline 17 and caused a permanent change in channel alignment, forcing the river west within 50 feet of the levee. Steel Kellner jack units were installed during the summer of 1989 to stabilize the river in this new location and to diminish the threat of levee erosion.

The other plug formed near Rangeline 13. This plug also forced the river flow out of the main channel but because of heavy vegetation in the overbank areas a new channel was never formed. In February, 1987, during upstream flood storage releases, this plug washed out and the water surface upstream suddenly dropped 5 feet.

In the spring of 1986, near the right abutment of the railway bridge, the river breached the bank of a pilot channel that had been built in 1984. Scour holes around the bridge piers may have undermined the bank. The breach allowed 10 to 20 percent of the river discharge over 1500 cfs to flow west and north out of the main channel toward the levee. This water, combining with other flow forced out of the channel downstream, rose high along the levee causing a severe low freeboard condition. Low areas in a mile long reach of the levee were raised to prevent overtopping.

In addition to the overtopping threat, water flowing along the levee began scouring channels along its toe. Some of these channels eventually became up to 5 feet deep. Development of a main river channel right along the levee would have created a serious problem. Clearing of vegetation along the levee is thought to have contributed to the formation of these channels. To control the development of the new channels, gravel groins were built out from the levee in critical areas. Originally the groins were very short, approximately 40 feet, and were not effective in controlling the channel development. Extending the groins to 150 feet effectively controlled channel development by preventing complete drainage of the channel at low flow and causing deposition of

sediment. In some places Kellner jacks were placed in the developing channels but were less effective than the groins.

Runoff in the 1988 season was below normal for the first time since 1981. Nevertheless, water delivered to Elephant Butte Reservoir from upstream storage and unusually heavy summer rains kept the reservoir essentially full and threats to the levee continued.

Spring runoff in 1989 was again below normal. Dry conditions later in the year afforded the first opportunity to work out in the floodway since 1985. The breach in the pilot channel that had existed since 1986 was filled and heavily rip rapped. Another breach just downstream was also repaired. These actions diminished flow along the levee for about 3 miles downstream.

The below normal runoff in 1989 led to a lowering of the reservoir pool elevation. At the beginning of the season for irrigation releases in February, 1990 the pool stood approximately 10 feet below the spillway crest and the headwater of the reservoir had receded about 2 miles. Spring runoff (March through July) in 1990 was only 33 percent of normal at San Marcial. By November, 1990 the reservoir had dropped another 17 feet and receded another 2-1/2 miles.

Because all conveyance facilities below rangeline 24 have been destroyed, the means for efficient transport of water and sediment into the Elephant Butte Reservoir pool no longer exist. Above the reservoir, the decrease in channel capacity caused by aggradation of the river still threatens further destruction of the Conveyance Channel. Past management has caused the greatest deposition of sediment to occur on the east side of the floodplain and the river is now flowing to the west, dissipated in various small channels and sheet flow. A return to the condition of the early 1950's is feared and planning for the opening of a channel to the reservoir pool has begun. Action is needed to enable New Mexico to maximize water delivery into the reservoir and to provide efficient transport of sediment so that degradation of the river bed will be facilitated as the reservoir drops. Environmental compliance requirements and difficult site conditions are the principal constraints governing the channel restoration plan. Restoration of previously existing channels can be done under current environmental compliance documentation but the heavy deposition of sediment in the old channel areas makes alternative alignments running to the west more desirable. Newly deposited, saturated sediments are extremely soft and special equipment and methods will be required to accomplish the channel construction.

REFERENCE

[1] U.S. Department of the Interior, Bureau of Reclamation, Definite Plan Report, Initial Stage Channel Rectification, Middle Rio Grande Project, New Mexico. 1952.

MODELING SETTLING BASIN DEPOSITION AND SLUICING

By Ernest L. Pemberton, Consultant, 15 Abernathy Ct., Highlands Ranch, Colorado and Curtis J. Orvis, Hydraulic Engineer, Bureau of Reclamation, Denver, Colorado

ABSTRACT

Settling basins have been an integral part of water diversion schemes at Bureau of Reclamation facilities for a number of years. Recent demands for more efficient operating schemes both in the United States and other countries include the removal of sediment deposited in settling basins. This has produced a new look at the potential of designing basins with bottom slopes and sluicing capabilities. This paper describes the Sediment Transport and River Simulation (STARS) mathematical modeling efforts undertaken to study the deposition and sluicing capabilities of settling basins. Sediment transport equations were tested for applicability to both processes on the material in the sand and silt size ranges. Case studies are described in which the water requirements and time periods for sluicing were determined. The predicted versus experienced sediment deposition and transport is compared. This application of STARS model will be beneficial to future design of settling basins in any country encountering major sediment problems at diversions.

INTRODUCTION

The diversion of water from rivers carrying large quantities of sediment to irrigation projects usually requires a settling basin for trapping the coarser, sand-size sediment. Thus, problems such as reduced canal capacity or plugging of pipes in a distribution system can be avoided. Even with design features at a diversion for excluding the coarser sized sediment, sand-size sediments transported in suspension are diverted to the canal. A settling basin at the head of a canal isolates the coarser sediments and provides a more economical method for removing these sediments from the canal.

The design of settling basins by the Bureau of Reclamation was initially based upon settling velocity criteria by Vetter (1940). From studies initiated to design and maintain salmon fisheries by Einstein (1968), the technical approach was expanded by Pemberton and Lara (1971) to calculate by hand the dimensions of settling basins, trap efficiencies, and quantities of deposition for given inflow conditions. The SETSIZE model was developed by Randle (1984) for mainframe application to analyze operations of the settling basin and solve for an unknown basin dimension. Case studies on the application of the SETSIZE model to the Highline Canal and the Red Bluff settling basins were discussed by Strand (1986). The SETSIZE model was converted to the personal computer and additional case studies presented for the Crater Lakes basin (Orvis and Randle, 1989).

The STARS (Orvis and Randle, 1987) model described in this report for design of a settling basin has the advantage of a method based on transport of sediment rather than settling velocity. It is applicable for evaluating deposition in basins partially filled with sediment and can be used to determine if sediments can be hydraulically flushed from a basin.

OBJECTIVES

The STARS model was applied to design of a settling basin in four phases:

1. Check and verify the depositional characteristics of the STARS model against the SETSIZE model for two existing settling basins. Surveys of the two basins were available to compare with the results of the models.

2. Use the STARS and SETSIZE models on a future settling basin design problem for sediment removal.

3. Apply the STARS model to one of the existing settling basins and the future design problem to determine the volume of water and time required to flush the sediment from the basin.

4. Evaluate the depositional and sluicing capabilities of a basin with a sloping bottom.

PHASE 1

Socorro Main Canal Settling Basin

Construction of the settling basin on Socorro Main Canal was completed by March 1, 1956, and is located about 1.2 miles below the San Acacia Diversion on the Rio Grande in New Mexico. The basin is 2,400 feet in length with a bottom width of 90 feet and side slopes of 2:1. Flow and sediment data were collected upstream as well as downstream from the basin during a 112-day period from March 1, 1956, until June 21, 1956. For determining depositional volumes, a total of seven cross sections were surveyed before and after the study period. A plan view showing the layout of the cross sections is presented on figure 1. A set of 15 core samples for a grain size analysis were taken on June 21, 1956, along the five cross sections within the basin by driving a 10-foot plastic tube to the original basin floor.

Hydraulic and sediment data were sufficient for a thorough comparison and analysis of the Socorro Main Canal settling basin using both the SETSIZE and STARS models. A 7-day time step was selected for both models resulting in 16 computational intervals to model the 112 days. The results of these computations are given in table 1.

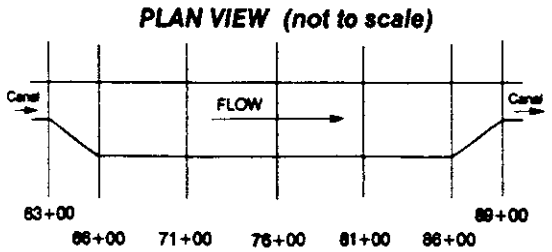

Figure 1. SOCORRO SETTLING BASIN

TABLE 1
SOCORRO MAIN CANAL SETTLING BASIN
(Units in Feet)

Section	Original Thalweg 3/1/56	Depths of Sediment Deposit: SETSIZE	STARS Model Vel.-Xi	STARS Model Yang	Survey 6/21/56
63+00 (Canal)	4660.0	0	0	0	1.3
66+00	4653.0	6.05	7.4	10.6	6.8
71+00	4653.0	6.05	7.0	10.9	6.5
76+00	4653.0	6.05	6.3	9.3	5.4
81+00	4653.0	6.05	4.7	3.5	5.1
86+00	4653.0	6.05	3.2	0	5.0
89+00 (Canal)	4658.2	0	0	0	-0.3
Volume (acre-feet)		34.04*	31.0**	35.0**	36.45

Inflow = 82 (acre-feet)

* - Density = >.062 mm @ 97 pounds/cubic foot
.062 mm to 004 mm @ 73 pounds/cubic foot
<.004 mm @ 60 pounds/cubic foot

** - Density = 97 pounds/cubic foot

It should be noted in the above comparison that the STARS model can utilize several of the different sediment transport equations. The two equations compared were the Bureau of Reclamation's, Velocity-Xi adjustment (Pemberton, 1972) to the original Einstein (1950) and the Yang equation (1973).

Red Bluff Settling Basin

The settling basin is located immediately below the Red Bluff Diversion on the Sacramento River in northern California. The dam was built in 1964; however, prior to about 1980, diversions had not reached their present day demand. The basin is 2,200 feet in length, 248-feet wide, and has riprapped banks with side slopes of 2:1. Dredging of the settling basin was first accomplished in 1980. The basin has been periodically dredged since 1980. The period selected for verification of the STARS and SETSIZE models was a 2-year period (1981 to 1983) between dredging. Cross section surveys were conducted in April of 1981 and 1983. The layout of the cross sections used in the analysis is given in figure 2.

The Red Bank Creek enters the Sacramento River immediately upstream from the diversion dam and the entrance to the settling basin. An assumption was made that Red Bank Creek discharge and corresponding sediment loads would be diverted directly into the settling basin and the remaining flows and sediment load would be from the Sacramento River.

Inflow data used in the models were the 1983 diversion schedule of flows applied to the 24 months from April 1981 through March 1983. The analysis by both models was done on monthly flow periods with 24 computational time steps during the 2-year period. The initial channel geometry for the STARS model was defined by the surveyed cross sections of April 1981. A representative bed-material size gradation used in the model was developed from a set of core samples of bottom sediments collected in March 1980. Results from the April 1983 survey are compared to the STARS and SETSIZE model computations in table 2.

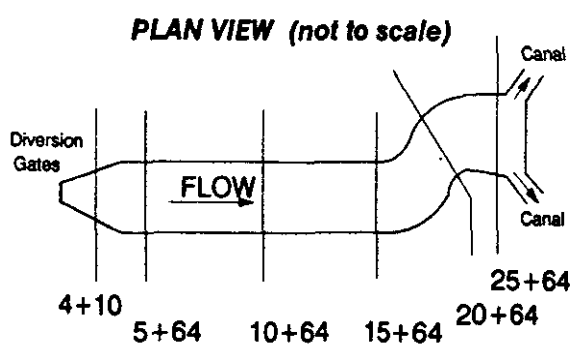

Figure 2. RED BLUFF SETTLING BASIN

TABLE 2
RED BLUFF SETTLING BASIN
(Units in Feet)

Section	Original Thalweg 4/14/81	Depths of Sediment Deposit SETSIZE	STARS Model Vel.-Xi	STARS Model Yang	Survey 4/6/83
4+10 (above)	231.0	0	0	0	-
5+64	229.3	3.2	4.0	3.8	5.5
10+64	228.2	3.2	4.6	3.8	5.3
15+64	228.7	3.2	5.5	4.5	4.1
20+64	228.7	3.2	4.9	6.8	3.3
25+64	228.2	3.2	0	0	2.5
Volume (acre-feet)		41.1*	55.0**	55.0**	51.5

Inflow = 115 (acre-feet)

* - Density = >.062 mm @ 97 pounds/cubic foot
.062 mm to .004 @ 73 pounds/cubic foot
<.004 mm @ 60 pounds/cubic foot

** - Density = 97 pounds/cubic foot

Summary of Phase 1

An examination of tables 1 and 2 shows that the STARS model provides a reasonable and more realistic sediment deposition pattern in the settling basin compared to the SETSIZE model. The volumes of deposition either by the SETSIZE or STARS models compared favorably with the survey results. Within the STARS model there can be considerable difference in the results associated with the selection of a sediment transport equation. Based on the two equations selected for comparison, the Velocity-Xi adjustment to Einstein gives the best comparison with survey results.

PHASE 2

On the Sunsari-Morang Irrigation II Project in Nepal, the Chatra Main Canal is experiencing severe sediment deposition problems. Large quantities of coarse sediment are being diverted into the canal from the Kosi River. A settling basin 6,234 feet (1,900 meters) long and 230 feet (70 meters) wide with side slopes of 2:1 is proposed to alleviate the problem.

The tests on use of the SETSIZE and STARS models were made with the assumed input data shown in table 3:

TABLE 3
CHATRA MAIN CANAL SETTLING BASIN
INPUT DATA

Diversions - 5 months, Q = 1,589 ft^3/s (45 m^3/s)
6 months, Q = 2,119 ft^3/s (60 m^3/s)
Sediment Concentration, Conc. = 800 Mg/L
Sediment Size Analysis -

Size	Percent Finer Than Suspended	Percent Finer Than Bed Material
0.031 mm	0	0
0.062 mm	3.0	0
0.125 mm	30.0	0.1
0.25 mm	64.0	1.2
0.50 mm	89.0	19.0
1.00 mm	98.5	48.0
2.00 mm	100.0	62.0
4.00 mm	100.0	72.0
8.00 mm	100.0	82.0
16.00 mm	100.0	91.0
32.00 mm	100.0	100.0

TABLE 4
CHATRA MAIN CANAL SETTLING BASIN
(Units in Feet)

Section	Original Thalweg	Depths of Sediment Deposit SETSIZE	Depths of Sediment Deposit STARS Model Vel.-Xi
0+00 (above)	352.8	0	0
2+66	347.8	17.1	19.2
5+00	347.8	17.1	18.8
25+00	347.8	17.1	15.7
45+00	347.8	17.1	12.9
65+00	347.8	17.1	10.4
67+00 (canal)	353.2	0	3.7
Volume (acre-feet) Inflow = 649 (acre-feet)		648*	506**

* - Density = >.062 mm @ 97 pounds/cubic foot
.062 mm to .004 @ 73 pounds/cubic foot
<.004 mm @ 60 pounds/cubic foot

** - Density = 97 pounds/cubic foot

A total of 11 monthly time steps were used in the analysis to compare the SETSIZE and STARS models for the proposed Chatra Main Canal settling basin. The results of this study are shown in table 4.

In table 4, the SETSIZE model shows that 99.8 percent of the inflow volume will be deposited because 97 percent of the suspended sediment inflow is sand or coarser material. Additional samples of the suspended sediment load may be needed to verify this size analysis.

Summary of Phase 2

The STARS model using the Velocity-Xi adjustment to Einstein, when compared with the SETSIZE model in the design of a settling basin, gives greater depths of deposits at the upper end of the settling basin. A recommended procedure

for the design of a settling basin is to obtain an initial size of the basin by use of the SETSIZE model and run the more sophisticated STARS model. In studies to develop dimensions for a settling basin, an upstream transitional cross section leading into the settling basin is required. The dimensions of this upstream section do not significantly change the volume of sediment deposited, but do have an effect on the depositional pattern.

PHASE 3

One feature of the STARS model is the capability to determine if the basin could be hydraulically flushed. This situation would normally apply to a concrete lined settling basin. During nonirrigation periods water could be routed through the basin and returned to the river for sluicing purposes. The flushing requires adequate hydraulic head to develop critical flow conditions at the downstream end of the basin. Scour initiated within the basin removes sediment in lieu of mechanical cleaning by dredge or dragline.

Another critical aspect of the potential for sluicing sediments is the environmental concerns of releasing higher concentrations of sediment into a downstream channel. In many countries or under special disposal conditions, the flushing may be possible. By use of the STARS model, the concentrations of sediment in the flushing flows could be determined for making an engineering evaluation of the process.

Socorro Main Canal Settling Basin - Flushing

The first test of the feasibility of flushing was conducted on the Socorro Main Canal settling basin. It was a hypothetical analysis. The assumption made in the flushing analysis was to convert the downstream canal section at 89+00 to a sluice gate with flow at critical discharge. The bed at section 89+00 was assumed to be nontransportable cobble material and the original bottom elevation of the settling basin was assumed to be large cobbles, simulating a concrete bottom. The initial deposits in the basin were made equal to the deposits computed by the STARS model using the Velocity-Xi adjustment to Einstein as shown in table 1.

Computations for sluicing were made with STARS using the Velocity-Xi sediment transport method and varying both the discharge and the incoming sediment concentration. The results of one computation are shown in table 5 of scour in feet at each cross section in the basin and total volume of sediment removed for a 28-day period with a discharge of 200 ft^3/s and incoming sediment concentration of zero.

All runs gave a scour pattern similar to that in table 5 with the highest rate in the first 7 days. Larger concentrations of sediment inflow caused a small decrease in the scouring rate. To remove all of the sediment from the basin in a 28-day period would take a discharge of about 1,000 ft^3/s.

TABLE 5
SOCORRO MAIN CANAL SETTLING BASIN - FLUSHING STUDY
(Units in Feet)

Section	Deposit Depth 112-Days	Scour Depths for Q = 200 ft³/s, Conc. = 0 7-Days	14-Days	21-Days	28-Days
63+00	0	0	0	0	0
66+00	7.4	4.1	5.4	5.9	6.2
71+00	7.0	3.6	4.7	5.1	5.4
76+00	6.3	3.1	3.9	4.3	4.5
81+00	4.7	2.0	2.5	2.8	2.9
86+00	3.2	1.1	1.5	1.8	2.1
89+00	0	0	0	0	0
Volume (acre-feet)					
Sediment	31	13	17	19	21
Water	31,000	2,780	5,550	8,330	11,100

Chatra Main Canal Settling Basin - Flushing

Sluicing of sediments from the proposed settling basin at Chatra in Nepal was studied by using the STARS model following the same procedure described for the Socorro Main Canal settling basin. The assumptions included the sediment deposits shown in table 4 and a sluice gate at the downstream end of the basin with an invert at elevation 347.8 feet. Cobble material was placed on the bed for the sluicing section 67+00 and underlying the deposited sediments within the basin.

In applying the STARS model with the Velocity-Xi transport equation, several discharges and sediment inflow concentrations were used to compute the sediment scoured by sluicing from the Chatra Main Canal settling basin. Because of the large depths of deposited sediment at the downstream end of the basin, the scour took place by the head cutting action. An example of the scour at each cross section and the volume of sediment removed from the basin by routing 3,530 ft^3/s (100 m^3/s) with zero sediment inflow concentration is shown in table 6.

TABLE 6
CHATRA MAIN CANAL SETTLING BASIN - FLUSHING STUDY
(Units in Feet)

Section	Deposit Depth 330-Days	Scour Depths for Q = 3,530 ft³/s, Conc. = 0 7-Days	14-Days	21-Days	30-Days
0+00	0	0	0	0	0
2+66	19.2	.3	.5	.6	.8
5+00	18.8	.2	.3	.4	.7
25+00	15.7	0	0	.1	.3
45+00	12.9	.1	1.4	2.3	3.0
65+00	10.4	7.7	8.5	8.8	9.1
67+00	0	0	0	0	0
Volume (acre-feet)					
Sediment	506	100	128	145	162
Water	1,230,000	42,000	98,000	147,000	210,000

Due to the large volume of deposited sediment in Chatra Main Canal settling basin, extremely high discharges would be required to remove all of the deposited sediments.

Summary of Phase 3

The two case studies on use of the STARS model for flushing sediment deposits from a settling basin identified the problems encountered by trying to sluice sediments by hydraulic action. The studies showed that by routing of extremely high discharges through the basin most of the deposited sediments can be removed. However, this may take considerable time and with the large volumes of water required is not feasible on irrigation projects. An alternative to the large discharges would be the splitting of a basin by construction of guide walls dividing the basin into two or three separate channels for analyzing the scouring potential by the STARS model.

The two case studies on sluicing show that the STARS model can predict the scour action by either downstream erosion or head cutting action. The type of erosion is dependent on the depth of deposits at the downstream end of the basin in relation to the critical discharge and associated velocities.

PHASE 4

The Socorro Main Canal settling basin was selected to determine if the STARS model could be applied to a sloping basin and result in any different depositional pattern. In the sloping basin study, the water and sediment inflow to the basin for computing sediment deposition were identical to the 112-day period under phases 1 and 3. The cross sections were changed to provide bottom slopes of .001 ft/ft and .005 ft/ft by leaving the thalweg at station 66+00 the same and progressively lowering each downstream cross section. Bed material with an underlying layer of cobble size sediment to control erosion along with a downstream sluice gate were the same as used in the phase 3 studies.

The STARS model with the velocity-Xi adjustment was used for computing deposition and sluicing capability for the settling basin with aforementioned changes. The results of these computation and the results from phase 3 studies for a basin with no slope are shown in table 7. The comparison of the results of sluicing a basin (slope = 0) from phase 3 with the basin having a slope = .001 ft/ft show almost identical results for the 28 days analyzed. For these two conditions, the size gradation of deposited sediments controlled the degradation. The extreme slope of .005 ft/ft showed greater sluicing capability, but this steep basin would not have a practical application on an irrigation project.

TABLE 7
SOCORRO MAIN CANAL SETTLING BASIN
SLOPING BOTTOM STUDY

Slope of Basin ft/ft	Sediment Deposit 112-Days acre-feet	Volume Removed by Q = 200 ft³/s, Conc. = 0 7-Days acre-feet	14-Days acre-feet	21-Days acre-feet	28-Days acre-feet
0 (Phase 3)	31	13	17	19	21
.001	35*	12	17	19	21
.005	35*	18	24	25	25
Volume Water (acre-feet)	31,000	2,780	5,550	8,330	11,100

*Basin was changed by starting from the upstream section and progressively lowering each downstream section, thus providing increased storage for sediment deposition.

SUMMARY AND CONCLUSIONS

The STARS and SETSIZE models provide reasonable results when checked against survey data for the Socorro and Red Bluff settling basins. Model results for the proposed Chatra Main Canal settling basin provided quantities of sediment deposits for use in evaluating basin dimensions and cleaning requirements.

The STARS model was able to simulate flushing of sediment for the hypothetical Socorro settling basin and the proposed Chatra basin configuration. Large quantities of clear water in combination with construction of guide walls for providing narrower move efficient sluiceways would be needed to flush either basin completely.

Tests for a sloping basin showed no change in flushing capabilities by increasing the bottom slope to 0.001, but by increasing the bottom slope to 0.005 the sluicing process was improved. The slope of 0.005 represents a slope greater than the natural river which makes it impractical for an irrigation project.

REFERENCES

Einstein, H. A., 1950, The Bed-Load Function for Sediment Transportation in Open Channel Flows, Soil Conservation Service Bulletin No. 1026.

Einstein, H. A., 1968, Deposition of Suspended Particles in a Gavel Bed, J. Hydraulics Division, American Society of Civil Engineers, Vol. 94, No. HY5, Proc. Paper 6102, pp 1197-1205.

Orvis, C. J., and Randle, T. J., 1987, STARS: Sediment Transport and River Simulation Model, Technical Guideline, Bureau of Reclamation

Orvis, C. J., and Randle, T. J., 1989, Settling Basin Model for the Personal Computer, American Society of Civil Engineers, Sediment Transport Modeling.

Pemberton, E. L., 1972, Einstein's Bedload Function Applied To Channel Design and Degradation, in Sedimentation, Symposium to Honor Professor H. A. Einstein, Edited and Published by H. W. Shen.

Pemberton, E. L., and Lara, J. M., 1971, A Procedure to Determine Sediment Deposition in a Settling Basin, Bureau of Reclamation.

Randle, T. J., 1984, User's Guide to Computer Modeling of Settling Basins, Bureau of Reclamation.

Strand, R. I., 1986, Sedimentation at Canal In-Line Structures, American Society of Civil Engineers, Water Forum '86.

Vetter, C. P., 1940, Technical Aspects of the Silt Problem on the Colorado River, Civil Engineering, Vol. 10, No. 11.

Yang, C. T., 1973, Incipient Motion and Sediment Transport, Journal of the Hydraulics Division, American Society of Civil Engineers, Vol. 99, No. HY10.

SAND TRANSPORT IN GOODWIN CREEK

By Joe C. Willis, Research Hydraulic Engineer, National Sedimentation Laboratory, USDA-ARS, Oxford, Mississippi

ABSTRACT

Stage frequency functions are developed for four consecutive water years for Goodwin Creek near Batesville, MS. These are used along with the average rating for the transport of sands to obtain estimates of the expected annual delivery of sands by the observed flows. Also, a shift factor to correct the rating for deviations of each ETR sample therefrom is used to obtain the best estimate of the ''measured'' sand delivery. The measured sand deliveries differ significantly from the expected for individual years. The differences in the average sand deliveries for the four years are primarily due to differences in the amount of rainfall.

The sand-load frequency tends to increase rapidly with increasing stage at low stages and to approach a constant value at higher stages. This suggests that the extreme, but infrequent, flow events constitute significant contributions to the sand load.

INTRODUCTION

The purpose of this investigation was to develop best estimates of the sand load delivered by Goodwin Creek on an annual basis. Measurements of the concentrations of sediment in transport are a crucial part of field investigations. The primary purpose of these measurements is to determine amounts of sediment delivered downstream and average sediment yields from the watershed above the point of measurement. Another related purpose of the transport data is to develop predictive relationships for the sediment load in terms of flow and channel variables that supposedly may be more readily measured than the concentration itself.

Unfortunately, variablity in transport data seems to be the rule rather than the exception. Several reasons for the variability may be cited. These include sampler error, sampling techniques that result in non-represenative samples, variations in the sediment supply, residual effects of upstream channel geometry, residual bed deposits from past flow events, migrating bedforms, flows originating from different source areas, and sporadic flow events. The stochastic nature of transport processes has been recognized for some time. Comparisons of sediment loads predicted by several transport formula were shown to differ by an order of magnitude. (Vanoni, et al; 1961). Even in laboratory flumes under steady, controlled conditions, the standard deviation of the concentration of the sand in transport was found to be on the order of the mean concentration itself (Willis and Bolton, 1979). Hamamori (1962) suggested a probability function for bed load deviations in one of the first theoretical treatments of fluctuating bed load. This was later generalized by Carey (1985). A probability approach has also been applied to the calibration of bed-load samplers (Hubble et al., 1985).

The analyses of Hamamori and Carey indicate that the variations in measurement of the bed load are large relative to the mean transport rate.

The implication is that dunes are the main cause of variation under controlled laboratory conditions. The bed load certainly changes from near zero at dune trough to a maximum value of about twice the average transport rate at the next crest. If the effects of other factors mentioned above are also considered, the expected variability of field data becomes very large indeed.

GOODWIN CREEK

The Goodwin Creek Watershed near Batesville, Mississippi, has been operated by the National Sedimentation Laboratory, Oxford, Mississippi, since about 1980. This watershed and the associated data collection program have been described previously (Bowie and Sansom, 1986). Since about 1983 an intensive sediment sampling program has been conducted at Station 2 of that watershed which represents the outflow from a seven-square-mile subwatershed. Fine sediments have been sampled reliabily by an automatic pump sampler, and sands have been determined by ETR (equal transit rate) samples through the entire depth of flow at the outfall of the supercritical flow structure with a boom-mounted DH-48 sampler. One of the purposes of the structure was to provide a stable flow rating and a deposition-free boundary to facilitate sediment sampling. Stage is the primary variable for relating flow and transport through the structure.

The stream above Station 2 is a relatively straight channel for 600 feet with relatively high but stable banks, a slope of about 0.003 and a bed width of about 35 feet. The bed material is a mixture of sand and gravel with a median diameter of about 4 mm. The sand fraction (less than 2 mm) of the bed material constitutes about 34 percent of the total and has a median diameter of about 0.63 mm and a geometric standard deviation of 1.83.

STAGE FREQUENCY

Data for the water years October 1984 through October 1987 were used to develop transport and flow relationships. The annual rainfall was highly variable during this period. It varied from 34.72 in. for the 1985/86 water year to 61.11 in. for the 1984/85 water year. Figure 1 depicts the temporal distribution of flow stages for the 4 years. The flow in the channel is essentially ephemeral with a low base flow on the order of 0.1-0.2 ft in the supercritical-depth structure. Flow events may occur throughout a year, but events with a stage greater than 5 feet occur very infrequently. Significant differences in the occurence of extreme events can be seen for the four years. The year 84/85 was the wettest of the four years and also had a larger number of extreme events. The year 85/86 was the driest, with no stage over 6 feet.

Figure 1 essentially represents the stage range for each day, since the resolution of the figure is on the order of a day and finer details are obscured. The stage data were analyzed in terms of time frequency, ie., the fraction of the time the flow is within an increment of stage per increment of stage. This frequency or probability function of stage is obtained by accumulating the time the stage remains within each increment of stage and dividing by the total time and the stage increment. A stage increment of 0.1 ft was used for this analysis. The resulting stage probability functions for each of the four years are shown in Figure 2 along with sand

load frequencies that will be discussed in the next section. The frequency functions are depicted in logarithmic coordinates to reveal the details of the low frequencies of the extreme flow events.

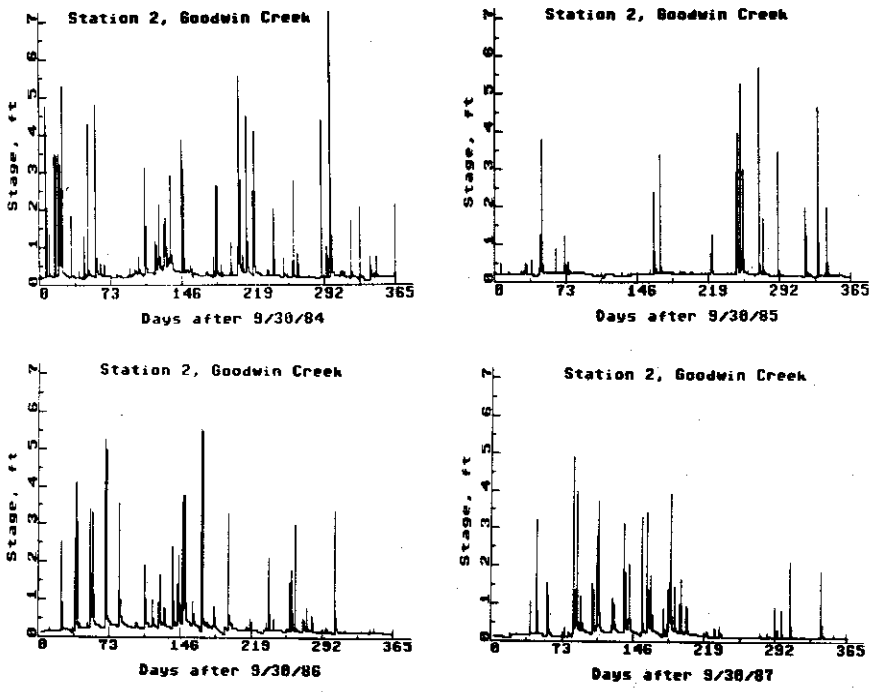

Figure 1. Flow Stages in Supercritical Flume No. 2, Goodwin Creek

The area under each stage frequency function (in arithmetic coordinates) is unity. The peak frequency occurring at about 0.16 ft. represents the stage existing most of the time. This may be regarded as the stage of base flow.

Since the stage frequency function is equivalent to the usual statistical probability function, all the attributes of probability density functions are applicable. As an example, the first moment is given by:

$$\bar{s} = \int_0^\infty s\ f(s)\ ds \qquad (1)$$

where $\bar{s}$ denotes the average stage, s is a particular stage, and f(s) is the frequency for that stage. Also, the average value of any function of stage is given by the integral of the product of that function and f(s) over all contributing s.

Flow discharge rate in the Goodwin Creek channel is a function of the stage in the supercritical structure.

$$Q = Q(s) \qquad (2)$$

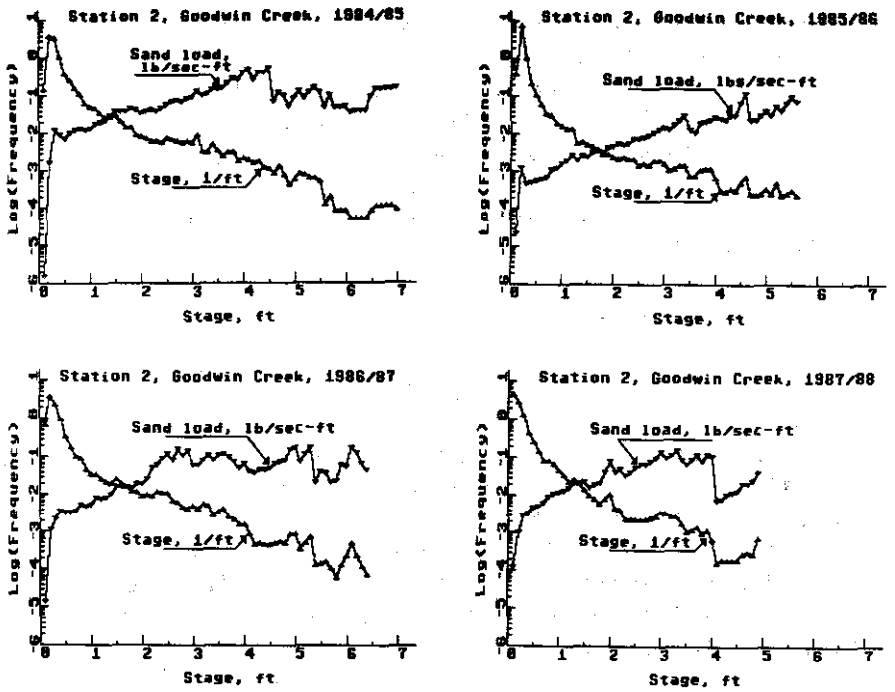

Figure 2. Stage and Sand-Load Frequencies, Goodwin Creek.

The function Q(s) is approximated by power functions for four stage segments.

$$
\begin{aligned}
Q(s) &= 46.94\ s^{2.58}, \quad s < 0.18 \text{ ft} \\
&= 36.65\ s^{2.431}, \quad 0.18 < s < 0.328 \\
&= 31.92\ s^{2.297}, \quad 0.328 < s < 4.108 \\
&= 47.98\ s^{2.025}, \quad s > 4.108
\end{aligned}
\tag{3}
$$

wherein Q(s) is the flow rate in ft^3/sec at stage s in ft. The ratings of Eq. 3 are based on the theoretical ratings of the structure as modified by in-situ flow discharge measurements.

In terms of the frequency functions, the average flow rate $\overline{Q}$ is given by:

$$\overline{Q} = \int_0^\infty Q(s)\ f(s)\ ds \tag{4}$$

The product Q(s)f(s) is the flow frequency and is directly related to the usual flow duration method of analysis of watershed data.

TRANSPORT FREQUENCY

The concentration of sediment in transport can also be related to stage; however, the relationship is not unique. A rather large range of concentrations are observed at any given stage, so only long term averages can be considered to be functions of stage alone. A preponderance of the measurements of sediment concentration are for flow events with lower stages, so to give equal weight in an average concentration-stage relationship, average concentrations and stages for each quarter-foot stage increment were calculated and a regression relative to stage was applied to these averages. The resulting sand rating for the period of record (after 1980) for station 2 of Goodwin Creek is:

$$c(s) = 52.4\ e^{0.675\ s}\ ,\ s > 1.22\ \text{ft.} \qquad (5)$$

$$= 97.6\ s\ ,\ s <= 1.22\ \text{ft.} \qquad (6)$$

where c(s) denote the concentrations of sand in parts per million by weight for stage s measured in feet. Figure 3 presents a graphical depiction of this sediment rating. Each of the data points represents an average of concentrations from between 18 and 325 composite crossection samples obtained with the DH-48 depth integrating sampler. The standard deviations of the individual samples within a depth interval were on the order of the average concentration for that interval.

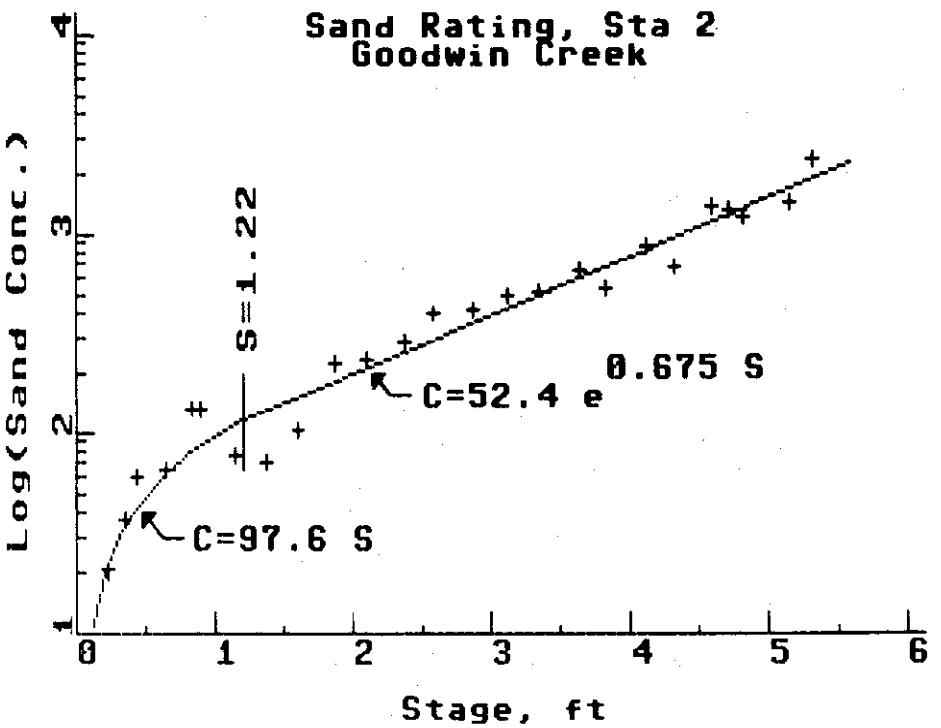

Figure 3. Sand-Load Rating, Station 2, Goodwin Creek

The transport rate of sediment at a given stage is given by

$$G(s) = 10^{-6} \gamma c(s) Q(s) \tag{7}$$

where γ denotes the unit weight of water (62.4 lb/cu ft).

Here again the product of G(s) and f(s) represents the rate of contribution to the average transport rate with stage. This product or load Frequency for the four water years is depicted in Figure 2 for the sand fraction of the sediment load for c(s) given by Eqs. 5 and 6. Although f(s) is a rapidly decreasing function at higher stages, the product Q(s)c(s) increases about equally as fast suggesting an almost constant load frequency at high stages. The variations in the load frequency at high stages about this ''constant'' level probability reflects the small number of extreme events. The load frequency increases sharply at low stages and indicates that the extreme, but infrequent, events make significant, if not dominant, contributions to the sand load.

The average transport rate is the area under the arithmic load frequency curve for contributing stages:

$$\bar{G} = \int_0^\infty G(s)\ f(s)\ ds \tag{8}$$

Column 3 of Table 1 depicts the annual sand loads based on the average transport rates from Eq. (8) for the four water years 1984-87. The loads for the four years differ significantly and appear to be highly correlated with the highest observed stage for a given year. If the load frequencies do become nearly constant at high stages, then the effect of a higher peak stage is to provide a longer stage base for integration under the load frequency curves of Figure 2.

Table 1. Calculated Annual Sand Loads - Goodwin Creek, Station 2

Water Year	Rainfall inches	Calculated Sand Load tons	
		Eq. 8	Eq. 10
1984/85	61.11	5170	11800
85/86	34.72	1550	1790
86/87	51.32	4090	6020
87/88	43.04	1370	3570

Although these calculations indicate significant differences in transport rates for different years, they only reflect the effects of variations in flow between the different years. They may also be somewhat low due to attenuation of the high deviations by the log transforms of Eq. 5 and Figure 3. The variations of the individual observed concentrations from the average curve can cause even greater deviations. The concentrations used in defining Eq. 5 exhibited standard deviations for each stage increment on the order of the average concentration itself. Furthermore, the deviations of

measured concentrations from the average values seemed to be rather consistent over significant time periods.

To account for these deviations, a shift factor K was defined as a ratio of the observed concentration to that predicted by the average curve. The K factor was then defined as a function of time with linear interpolations over time applied between samples. The product of K and the value of c(s) from the average curve then corresponded to the measured concentrations at the times samples were taken. The best estimate of the transport rate at time t and stage s is then taken as:

$$G(s,t) = 10^{-6} \gamma K(t) c(s) Q(s) \qquad (9)$$

wherein the concentration and flow rate are also taken as a function of time t. The index t has been added to G to distinguish it as a multivariate function.

To remove the time dependency of the load, the average value of G(s,t) for each increment of stage was computed. This is identical to the procedure used in establishing Eq. 2 except that the interval averages were used in the load computations rather than the regression curve. These averages $\overline{G}(s)$ were then only a function of stage and could be used in Eq. 8 to define the average transport rates

$$\overline{G} = \int_0^\infty \overline{G}(s) f(s) ds \qquad (10)$$

wherein the integrand is the frequency function of the transport rate. The load frequencies defined by Eq. (10) depicted similar curves to those of Eq. 8 except for somewhat higher frequencies for stages around 4 feet.

The annual loads based on the average transport rates from Eq. 10 are shown in column 4 of Table 1. The values in columns 3 and 4 differ significantly, with the higher values in column 4 reflecting high K(t) values for significant transport events. The values from Eq. 8 represent the expected long-term sand transport rates for the observed flows. Those from Eq. 10 represent the best available estimates of the annual sand loads when enough depth-integrated samples are available. The transport rates computed by Eq. 9 are rather insensitive to the form of the average load rating. With the addition of the shift factor K(t), Eq. 5 becomes primarily an interpolation scheme between samples.

CONCLUSIONS

Stage frequency functions, which represent the fraction of the total time that the flow is within an interval of stage per unit interval of stage, can be used to determine the observed or expected delivery of sand-sized sediments. The product of the average concentration at a particular stage, the flow rate, and the stage frequency defines a load frequency as the rate of contribution to the average transport rate with stage. The area under

the product of the stage frequency and any function of stage represents the average value of that function over contributing stages.

The stage frequency function is highly skewed to low stages and decreases rapidly as stage increases. The sediment transport rate increases with stage so that the product of transport rate and stage frequency tends toward a constant value at higher stages. This suggests that extreme, but infrequent, flow events maintain a significant contribution to the annual delivery of sands.

Computations of the annual yields of sand by Goodwin Creek near Batesville, MS, reveal significant differences between the expected yield for observed flow events and yields based on ETR sediment samples. The sand concentrations differ apppreciably from the average relationship with stage for time periods longer than a storm event.

REFERENCES

Bowie, A. J. and Sansom, O. W., 1986, Innovative Techniques for Collecting Hydrologic Data, Proceedings, Fourth Federal Interagency Sedimentation Conference, Vol. 1, p. 1-59 - 1-69.

Carey, W. P., 1985, Variability in Measured Bedload-Transport Rates, American Water Resources Association, Water Resources Bulletin, Vol. 21, No. 1.

Hamamori, A, 1962, A Theoretical Investigation of the Fluctuations of Bed-Load Transport, Rept. R4, Delft Hydraulics Laboratories, 22 P.

Hubble, D. W., Stevens, H. H., Jr., Skinner, J. V., And Beverage, J. P., 1985, New Approach to Calibrating Bed Load Samplers, ASCE Journal of Hydraulic Engineering, Vol. 111, No. HY4, p. 677-694.

Vanoni, V. A., Brooks, N. H., and Kennedy, J. F. 1961, Lecture Notes on Sediment Transport and Channel Stability, W. M. Keck Laboratory Rept. KH-R-1, P. 1-1 - 10-23.

Willis, J. C. and Bolton, G., 1979, Statistical Analyses of Concentration Records, ASCE Journal of the Hydraulics Division, Vol. 105, No. HY1, p. 1-15.

BED LOAD TRANSPORT ON TWO SMALL STREAMS

By Roger A. Kuhnle, Research Geologist, U. S. Department of Agriculture, Agricultural Research Service, National Sedimentation Laboratory, Oxford, Mississippi.

ABSTRACT

Bed load transport has been sampled on two small tributaries of Goodwin Creek using automatic continuously-recording box samplers. The watersheds of the two gravel-bed streams are adjacent to each other and bed material size distributions and average bed slope of the two channels are similar. Since November of 1988 more than 2000 bed load transport samples have been analyzed on each of the two streams. This data was used to calculate relations between mean bed load transport rate and mean boundary shear stress for the two streams. The transport relations show that one of the streams has a higher rate of dimensionless bed load transport for a given dimensionless bed shear stress. Several possible reasons for this difference are explored.

INTRODUCTION

Accurate determinations of the rates of transport of bed material sediment in alluvial channels is important for several reasons. An accurate determination of the rate of bed sediment in transport is essential for calculating the sediment yield from upstream areas, and also for assessing the effects of the sediment transported downstream. The transport processes of the bed material may also in some cases cause bank erosion problems. Yet published transport relations are not general enough to be of use in many instances (Parker et al., 1982) and the variable nature of the flow and bed load transport make the collection of reliable data difficult.

The bed load transport data used in this study were collected on two small streams using the same sampling technique for the same runoff events. In this study the resulting bed load transport relations of the two streams were compared to each other and potential causes of the differences between the two were identified.

FORMULATION OF THE PROBLEM

The accurate prediction of the rates of bed load transport of sand and gravel sediment by flowing water is a difficult task. The flow of water over a sand and gravel bed affects the size distribution of the bed material which in turn affects the flow. Superimposed on this process are bed forms which interact in complicated ways with the bed surface size distribution and cause the transport of the sediment to be variable even if the flow is steady and uniform. Adding unsteady and non-uniform flow to the problem increases the complexity further.

To simplify the situation somewhat the assumption can be made that all sediment sizes in the bed material of a gravel-bed stream are equally mobile (Parker et al., (1982). This yields the following important variables which control the sediment transport process:

$$q_b = F(\tau_0, d, \rho, \mu, \rho_s, g, D_{50}) \qquad (1)$$

where q_b = the bed load transport rate in mass per time per unit width, $\tau_0 = \rho g R S_0$ = boundary shear stress, d = mean flow depth, ρ = density of the water, μ = dynamic viscosity of the water, ρ_s = density of the sediment, g = acceleration of gravity, D_{50} = the median grain diameter of the sediment, R = hydraulic radius, S_0 = slope of the energy grade line, and F symbolizes a functional relationship. These eight variables can be represented by five dimensionless groups:

$$\frac{((\rho_s/\rho)-1)gq_b}{\rho_s\ (\tau_0/\rho)^{3/2}} = F\left[\ \frac{\tau_0}{(\rho_s-\rho)gD_{50}},\ \frac{d}{D_{50}},\ \frac{g^{1/3}\ D_{50}}{\nu^{2/3}},\ \frac{\rho_s}{\rho}\ \right] \tag{2}$$

where $\nu = \mu/\rho$. Equation 2 can be referred to in short-hand notation:

$$W^* = F(\tau_{50}{}^*, d^*, D_{50}{}^*, \rho_s/\rho) \tag{3}$$

For some gravel-bed streams the assumption of equal mobility is warranted (Parker et al., 1982), while in other cases it is not (Ashworth and Ferguson, 1989). For this study the assumption of equal mobility of the bed sediment is made. This implies that the sediment can be adequately represented by one grain size. Also it is assumed that

$$W^* = F(\tau_{50}{}^*) \tag{4}$$

and that the variables d^*, $D_{50}{}^*$, and ρ_s/ρ are equal in the two streams. This last assumption is warranted because the watersheds and channels of the two streams are approximately the same size. The bed material sediment size distributions also are very similar to each other and virtually all sediment in the two channels is of quartz density (2.65 g cm^{-3}).

STUDY AREA

The Goodwin Creek Research Watershed is a 21.4 km^2 instrumented watershed that is located in the bluff-line hills east of the Mississippi River flood plain in the north central part of the state of Mississippi. The watershed includes fourteen supercritical "V" shaped structures and data collecting stations located on 14 subwatersheds. The purpose of the watershed study as a whole is to relate upstream land use and watershed processes to sediment supply, transport in stream channels, and channel stability. The bed material of the channels in the watershed ranges from nearly pure sand with a median size of about 0.5 mm to 70% gravel with a median size of 8 mm. Bed material mixtures between these two extremes are also present. More details on the instrumentation and sediment sampling programs can be found in Bowie and Sansom (1986), Willis et al. (1986), and Kuhnle et al. (1988).

The focus of this study is on two subwatersheds of Goodwin Creek: number 13, with an area of 1.24 km^2, and number 14, with an area of 1.63 km^2. These two adjacent subwatersheds are small in area yet contribute a significant portion of the

coarse bed material delivered to the main channel. The channel bed at station 13 is 3.0 m wide with a bed slope of 0.010. At station 14 the channel bed is 3.4 wide with a bed slope of 0.008. Flow in the channels is ephemeral with both channels being dry for long periods during the summer and fall months. The intense rainfall necessary to generate significant runoff in the channels occurs most often in the winter and spring months. For the period 1982 - 1987, runoff events with a flow strong enough to move the bed material sediment occurred on average 15.6 and 15.0 times at 13 and 14 respectively.

SAMPLING

Equipment

The natural variability of the bed load transport process along with the flashy nature of the runoff of small streams makes collecting transport samples a difficult task. To deal with this problem two continuously-recording box samplers were used to collect the bed load transport data for this study. The box samplers, modified from a sampler design of Reid et al. (1980), were constructed of 0.64 cm aluminum plate and consist of 1.22 m x 0.61 m x 1.35 m high box buried in the channel bed with the top flush with the bed surface (Fig. 1). The sediment falls into three 0.56 x 0.37 x 1.22 m high inner boxes that are supported by a flexible pressure pillow filled with a mixture of 50% ethylene glycol and 50% water. The removable top of the box has three equal-sized openings each 0.38 m long in the streamwise direction and 0.33 m wide in the cross channel direction.

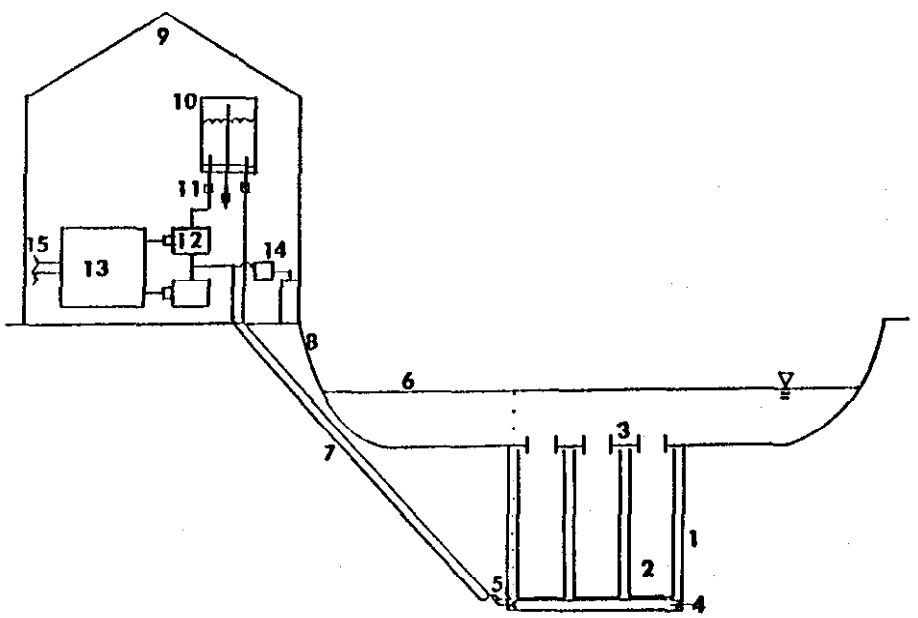

Fig. 1. Schematic cross section view of box sampler. 1.- outer box, 2.- inner box, 3.- slotted cover, 4.- pressure pillow, 5.- bubble tube outlet, 6.- water surface, 7.- tubes from bubbler and pillow, 8.- stream bank, 9.- instrument house, 10.- air trap, 11.- valves, 12.- pressure transducer, 13.- power supply, 14.- bubble gauge, 15.- wires to remote telemetry system.

Determining the rate of sediment accumulation into the box is accomplished by measuring the pressure due to the submerged weight of the sediment on the pressure pillow. A differential pressure transducer, with one side connected to the pressure pillow through a thick wall plastic tube filled with the ethylene glycol solution and the other side to a U.S. Geological Survey bubble gauge, gives a voltage that is proportional to the dry weight of the sediment in the boxes. The bubble gauge discharges into the outer box to compensate for the pressure on the pillow due to the depth of water in the channel. Another pressure transducer connected to the bubble gauge provides a voltage proportional to the depth of water over the box. The samplers were calibrated by placing weighed amounts of sediment into the inner boxes and recording the voltage change of the pressure transducer. A linear relation between dry sediment weight and voltage change was obtained.

Elevation of the water surface was measured 30.5 m upstream from the boxes using a bubble gauge and pressure transducer. The upstream and box bubble gauges allow the slope of the water surface to be calculated continuously. The pressure transducer connected to the bed load sampler and the two pressure transducers connected to the bubble gauges were sampled at one minute intervals and stored for 30 minute intervals in the mini-computer located at the station site. The data was radioed every 30 minutes to the laboratory main-frame computer using the remote telemetry system of the Goodwin Creek Watershed.

Techniques

The samplers were serviced after each transport event when flow depths in the channels were less than 0.1 m. Servicing of the samplers consisted of removing the slotted top and hoisting the inner boxes out of the outer box for emptying. Before emptying the center box was capped, laid horizontal, and one side was removed. The accumulated sediment was then sampled at 0.15 m vertical intervals for sediment size analysis.

Each time the boxes were serviced samples of the bed material sediment were collected. These samples were taken in the center of the channel 7.6 m upstream of the boxes. Two types of samples were collected: one of the bed surface layer sampled at a thickness equal to the largest sized grains (64 mm) and one of the bed sub-surface taken directly below the surface sample.

DATA

Bed Material

The bed material surface and sub-surface size distributions (each is a mean of 12 samples) are shown in Figure 2. The median sizes of the bed surface and bed sub-surface are 5.10, and 4.26 mm respectively for 13, and 8.51 and 5.86 mm, respectively for 14. All bed material samples have modes at 22.63 and 0.42 mm sizes and standard deviations of between 2.4 - 2.5 ϕ units (where $\phi = -\log_2(d_{mm})$). The median size of the bed sub-surface size distribution will be used here as the characteristic size for both streams.

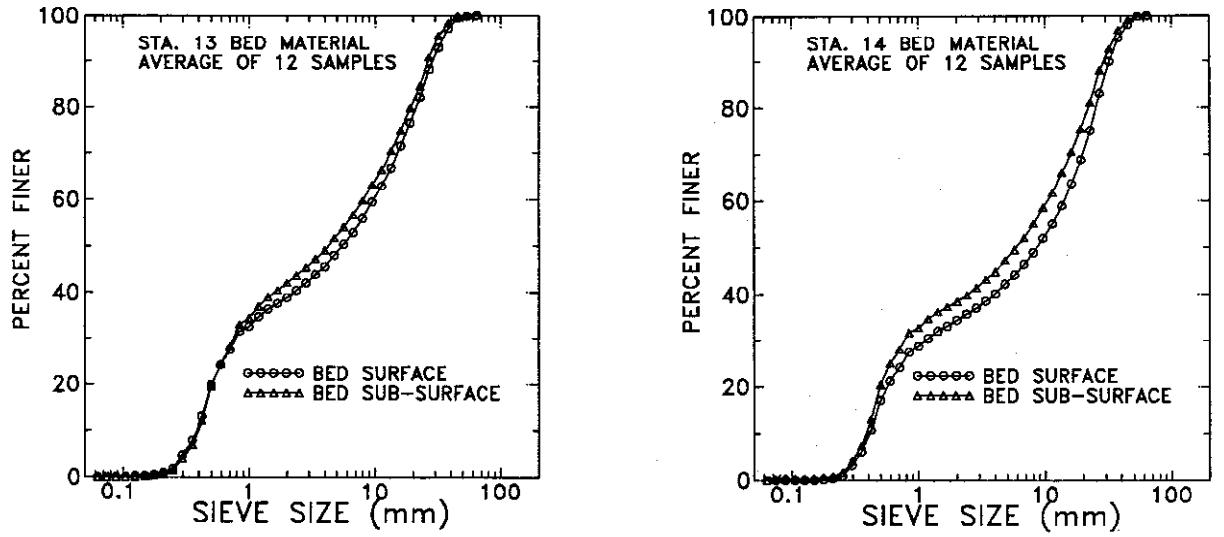

Fig. 2. Bed material size distributions for the two streams.

Bed Load Samples

The two samplers have been in operation at stations 13 and 14 from November of 1988 to the present. Data have been analyzed from 18 transport events which yielded a total of 2255 and 2682 samples from stations 13 and 14 respectively. Each sample is actually a record of each time the voltage of the pressure transducer connected to the box samplers is read and stored by the computer. Although the total number of samples is large most are concentrated at lower flows with a lack of samples at higher flows at both stations (Fig. 3). The variability of transport rates shown in Figure 3 is comparable with that shown for other studies of bed load transport in gravel-bed streams (e.g. Hubbell, 1987; Kuhnle and Southard, 1988; Kuhnle et al., 1989; Whiting et al., 1988). This large short term variability requires many samples at each flow strength in order for accurate estimates of the mean bed load transport rate to be calculated (Kuhnle and Southard, 1988). Due to the shortage of samples collected at flows greater than 3 $m^3 s^{-1}$ (Fig. 3) mean transport rates calculated for flows above 3 $m^3 s^{-1}$ are probably less accurate than those calculated for lower flows.

Transport Relations

In order to compare the bed load transport rates from streams 13 and 14 directly, a transport relation for each stream was calculated. Dimensionless bed load transport rate (W^*) was related to dimensionless bed shear stress (τ_{50}^*). Due to problems with the upstream bubble gauge at station 13 water surface slopes were not available to calculate bed shear stresses. In order to compare the bed load transport data from the two streams to each other the mean bed surface slope was used as an estimate of the slope of the energy grade line. It is recognized that bed surface slope is not always a good estimator of the energy grade line.

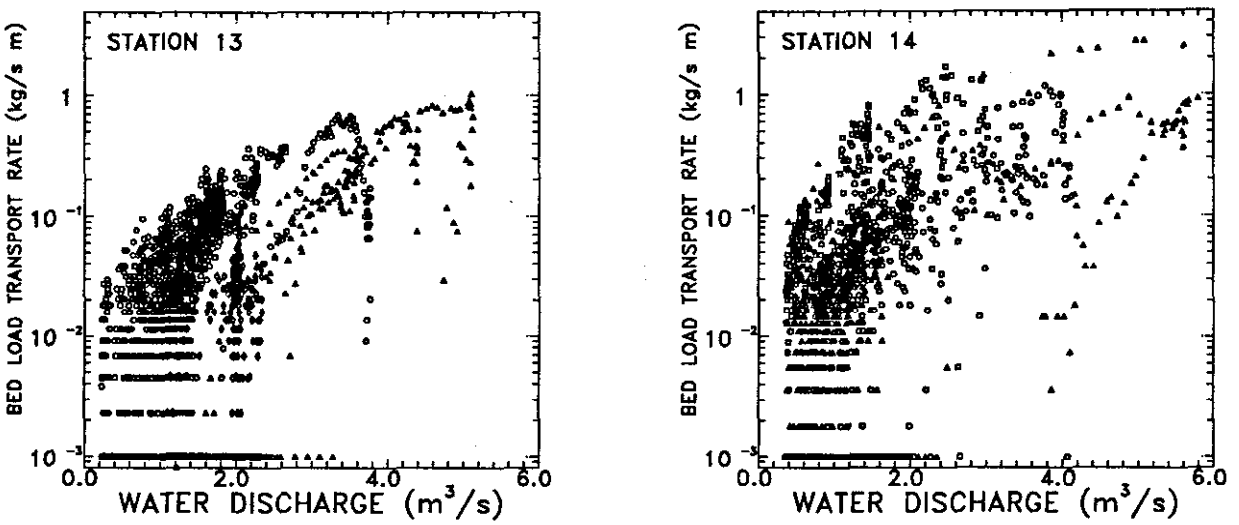

Fig. 3. Bed load transport rate vs. flow discharge. Zero values plotted as 10^{-3}.

The means of all the transport samples in each 5 N m^{-2} interval of bed shear stress were calculated for both streams 13 and 14. This averaging technique was used before fitting equations to the data due to the unevenness of the distribution of the samples. From these average values Figure 4 was plotted. Figure 4A shows the bed load transport relations of the two streams. A comparison between the two transport relations can be facilitated by removing the differences in the critical bed shear stresses of the bed material for the two streams. To accomplish this a reference bed shear stress was defined as: $\tau_r^* = \tau_{50}^*$, when $W^* = 0.002$. The value of τ_{50}^* at this low transport rate is

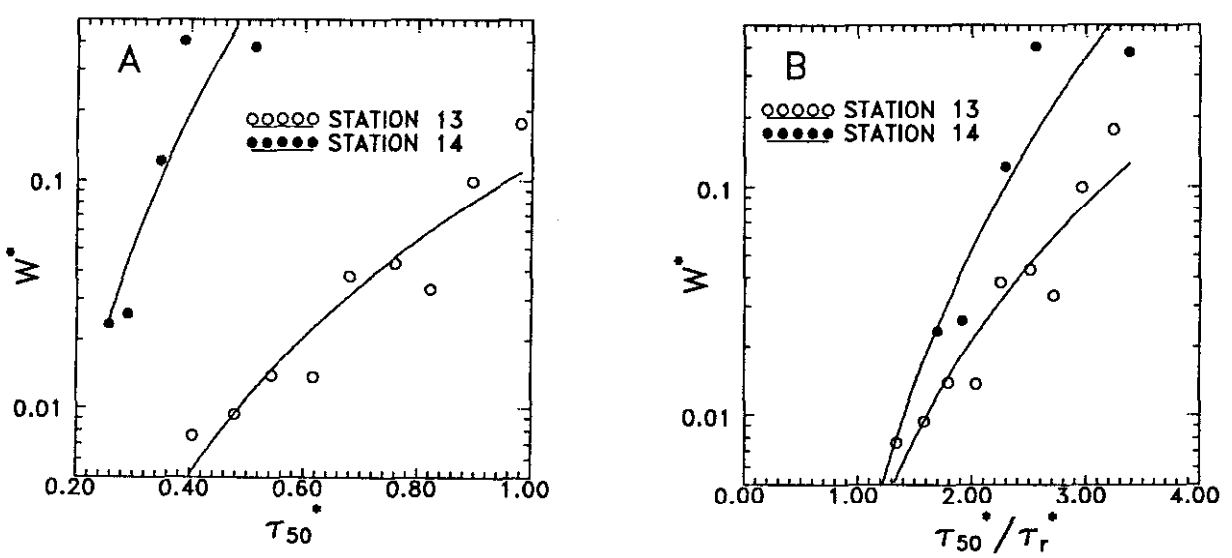

Fig. 4. Bed load transport relations. A - W^* vs. τ_{50}^*; B - W^* vs. τ_{50}^*/τ_r^*.

essentially a surrogate for critical bed shear stress for movement of the bed material (Parker et al., 1982). Reference bed shear stresses (τ_r^*) were 0.152 and 0.303 for stations 13 and 14 respectively. These values were calculated by fitting power functions using a least squares technique to the transport data of 13 and 14 and solving for the reference bed shear stress. Bed load transport rate versus the ratio of bed shear stress to reference bed shear stress is shown in Figure 4B. The slopes of the two relations are seen to be different in Figure 4B.

DISCUSSION AND SUMMARY

The differences shown in Figure 4B may be due to a variety of factors. If we assume that the differences are real the response of the two watersheds to a given amount of rainfall may explain the differences. When flow in the channels at stations 13 and 14 is strong enough to transport the bed material it is almost never steady. Hydrographs of the two streams have a variety of shapes depending on rainfall patterns and the antecedent conditions in the watershed. It has been recognized that the rising side of the hydrograph at station 14 is consistently steeper than that at station 13 for the same runoff event. The effects of unsteady and non-uniform flow on the transport of bed load sediment are poorly known. It is possible that differences in the time scale of the unsteadiness of the two channels is the major cause of the observed difference in bed load transport relations of the two channels (Fig. 4).

Another possibility is that the differences shown in Figure 4 were caused by imperfections in the data collection technique. It has already been mentioned that the amount of data collected at high flows was much less than that collected at low flows. It is possible that at high flows not enough samples have been collected to obtain an unbiased average rate. Also the use of the mean bed slope in the calculation of bed shear stress is known to only be an approximation. The mean bed slope of a channel presumably represents some long-term average of the slopes of the energy grade line. It is not known how the energy slope deviates from the bed slope with different flow strengths for the two channels. The deviations may be different for the two channels.

In summary differences in reference bed shear stress and bed load transport relations have been identified for two similar small gravel-bed streams in the Goodwin Creek Watershed. At the present time the cause of the differences is not known. Future planned improvements in the collection of bed load transport data at these two watersheds are expected to shed more light on the causes of the differences of the transport relations of these two streams.

REFERENCES

Ashworth, P. J. and Ferguson, R. I., 1989, Size-selective entrainment of bed load in gravel bed streams. Water Resources Research 25, 627-634.

Bowie, A. J., and Sansom, O. W., 1986, Innovative techniques for collecting hydrologic data. Proceedings of the 4th Federal Interagency Sedimentation Conference, Las Vegas, Nevada, 1-5 -1-69.

Hubbell, D. W., 1987, Bed load sampling and analysis. In Sediment Transport in Gravel-Bed Rivers, edited by C. R. Thorne, J. C. Bathhurst, and R. D. Hey, John Wiley, New York, 89-118.

Kuhnle, R. A., Willis, J. C., and Bowie, A. J., 1988, Measurement of bed load transport on Goodwin Creek, northern Mississippi. Proceedings of the Eighteenth Mississippi Water Resources Conference, edited by E. J. Hawkins, Jackson, Mississippi, 57-60.

Kuhnle, R. A. Willis, J. C., and Bowie, A. J., 1989, Variations in the transport of bed load sediment in a gravel-bed stream, Goodwin Creek, northern Mississippi, U.S.A.. Proceedings Fourth International Symposium on River Sedimentation, Beijing, China, 539-546.

Kuhnle, R. A., and Southard, J. B., 1988, Bed load transport fluctuations in a gravel-bed laboratory channel. Water Resources Research 24, 247-260.

Parker, G., Klingeman, P. C., and McLean, D. G., 1982, Bedload and size distribution in paved gravel-bed streams. Proceedings A.S.C.E. Journal Hydraulics Division 108, 544-571.

Reid, I., Layman, J. T., and Frostick, L. E., 1980, The continuous measurement of bedload discharge. Journal of Hydraulic Research 18, 243-249.

Whiting, P. J., Dietrich, W. E., Leopold, L. B., Drake, T. G., and Shreve, R. L., 1988, Bedload sheets in heterogeneous sediments. Geology 16, 105-108.

Willis, J. C., Darden, R. W., and Bowie, A. J., 1986, Sediment transport in Goodwin Creek. Proceedings 4th Federal Interagency Sedimentation Conference, Las Vegas, Nevada, 4-30 - 4-39.

SEDIMENT TRACING IN STEP-POOL GRANITIC STREAMS IN IDAHO

By Gary L. Ketcheson, Hydrologist, U.S. Forest Service, Sawtooth National Forest, Twin Falls, Idaho and Walter F. Megahan, Research Hydrologist, U.S. Forest Service, Forestry Sciences Laboratory, Boise, Idaho.

ABSTRACT

Sediment tracer studies were conducted on four, first- and second-order channels in the Silver Creek Study Area in south-central Idaho. The channels have a typical step-pool profile and are representative of the granitic terrain found in the Idaho batholith. Test reaches extend from 46 to 76 meters directly upstream from sediment catch basins and recording stream gages and range between 3.8 and 9.7 percent gradient. Sediment sizes of 0.25-0.5 mm, 0.5-1.0 mm, 1.0-2.0 mm, and 2.0-4.0 mm were tagged with four fluorescent dye colors dissolved in vinyl plastic and used as a sediment tracer. Detailed surveys of test reaches include profiles, cross sections, and plan maps showing bank overhangs, thalweg positions and locations of logs and rocks. A single slug of tracer particles was placed at the head of each reach just prior to spring snowmelt. After snowmelt runoff, samples of bed material were collected from all discrete deposits within the test reaches including bed forms and accumulations behind natural channel obstructions. In addition, sediment cores were taken from the sediment catch basins. From 91 to 99 percent of the 0.25-0.5 mm particles and 71 to 98 percent of the 2.0-4.0 mm particles moved through the test reaches. About two-thirds of the tracer material remaining in the reaches was deposited behind natural organic debris in the channel, while one-third was evenly divided among deposition in point bars, pools, and random bed and bank locations. Transport of tracer through the reaches was directly proportional to channel gradient and flow rate.

INTRODUCTION

Purpose and Scope

Earlier studies (Megahan, 1982) showed that steep, first- and second-order streams draining forested, granitic watersheds in Idaho store an average of 15 times more sediment behind natural channel obstructions than is yielded to the watershed outlets each year. We suspected that the sediment is retained behind channel obstructions for considerable periods of time and moves as masses when organic debris deteriorates and fails; however, we had not documented this process. This study was designed to explore the question of sediment residence time in step-pool channels and what stream morphological characteristics affect the amount and timing of sediment delivery downstream. Vinyl coated sediment particles tagged with flourescent dyes were chosen as a tracer.

Description of the Study Area

The Silver Creek Study Area is located in south-central Idaho in the Middle Fork Payette River drainage. The dominant bedrock is moderately to well weathered quartz monzonite characteristic of the Idaho Batholith. The non-cohesive soils are described as gravelly, coarse textured loamy sands and sandy loams (Clayton, et al, 1979) and are highly erodible. Hillslopes are generally steep, with gradients ranging from 22 to 36 degrees. Annual precipitation ranges from 90 to 130 cm, with about 65 percent falling as snow. High-intensity summer thunderstorms can be significant and are responsible for most of the erosion on disturbed soils (Megahan, 1978).

The test reaches are located in four small watersheds; D, Eggers, Ditch and Cabin; that range in size from 102 to 129 hectares. The D and Eggers watersheds were undisturbed; however road construction had occurred in the Ditch and Cabin Creek watersheds. Bedload sediment accounts for 60 to 70 percent of the total annual sediment yield from the study watersheds (Ketcheson, 1986). Streamflow and sediment production exhibit marked seasonal variation with both peaking during spring snowmelt.

The test reaches exhibit an array of characteristics (Table 1). All are high gradient mountain streams characterized as step-pool systems with steps formed by large organic debris and rocks (Figure 1). When the accumulated heights of the steps are subtracted from the total vertical drop, the resultant "effective" gradient is generally less than half the overall gradient.

Table 1. Test reach characteristics.

Watershed Name	Watershed Area (ha)	Test Reach: Length (m)	Test Reach: Gradient (%) Overall	Test Reach: Gradient (%) Effective[1]	Flow: Spring Runoff (cm)	Flow: Max. Peak[II] (m^3/s)
D	118	56.4	9.7	8.2	41.0	0.26
Eggers	129	57.3	7.1	3.1	36.8	0.25
Ditch	102	70.4	5.9	1.7	30.0	0.17
Cabin	110	76.2	4.2	2.1	31.9	0.16

[1]Effective gradient is the stream gradient after subtracting the vertical drops over obstructions from the total vertical drop of the reach.

[II]Sum of the runoff for the months of April and May.

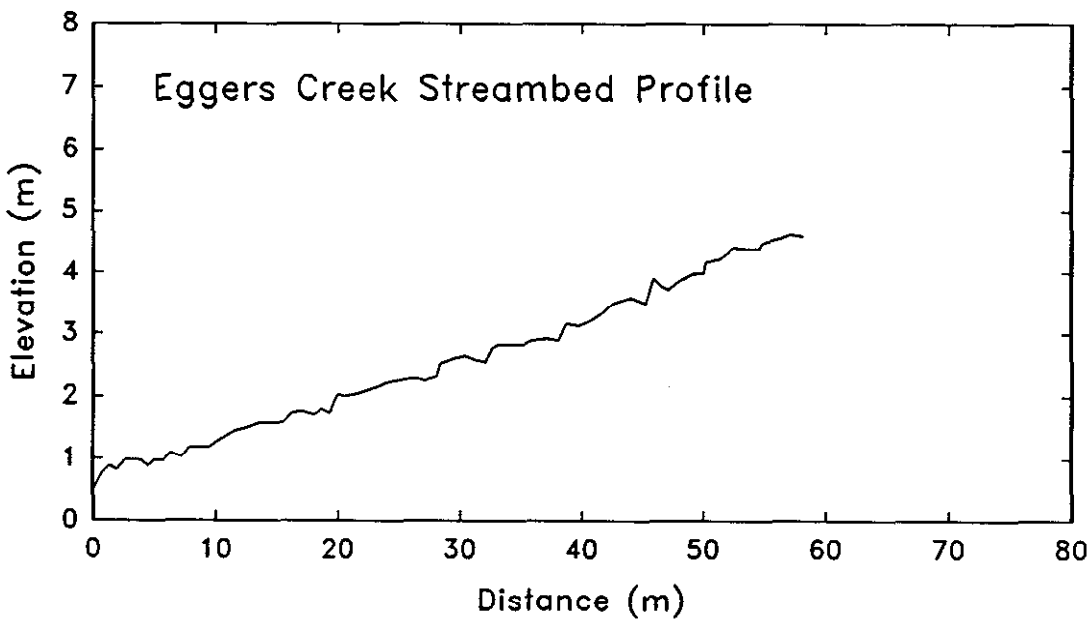

Figure 1. Typical Step-Pool Profile of Test Reaches

PROCEDURES

Preparation of Tracer Material

Four representative particle size classes from two-year old road fill slope samples were chosen as tracer material: 0.25-0.5 mm, 0.5-1.0 mm, 1.0-2.0 mm, 2.0-4.0 mm. Fluorescent dye (Day-Glow fluorescent pigment) was dissolved in a mixture of vinyl plastic VMCH blend 118 (a plastic hardener) and acetone. The particles were rotated in a cement mixer while being sprayed with the mixture. The particles were tumbled until well coated and dry. (Rathbun and Nordin, 1968).

Rathbun and Nordin suggested that enough tracer be used to have 400 particles of each size class in each sediment core taken in the test reach. Cores of 0.002 cubic meter capacity (12.7 cm diameter, 12.7 cm deep) were to be taken at least every three meters. Based on this, samples of 7.125 kg were prepared for each test reach with the following particle breakdown:

Size Class (mm)	Color	Number of Particles
0.25-0.5	Red	1,246,000
0.5-1.0	Blue	595,000
1.0-2.0	Green	236,000
2.0-4.0	Yellow	158,000

In April, 1982, prior to the snowmelt period, tracer samples were mixed with stream water in a bucket and slowly dumped across the channel section approximately 60 meters upstream from the sediment catch basins. Injection points were marked to establish the upper end of the test reaches.

Channel Mapping

The following August, each test reach was surveyed in detail. Channel profiles, cross-sections, and maps at a scale of one inch equals five feet were prepared from the data. The maps show channel bed and banks, the thalweg, and channel obstructions such as large organic material and rocks (Figure 2). Core sample and cross-section locations were also recorded. The total volume of sediment in deposits was determined using average length, width, and depth measurements following Megahan (1982).

Tracer Particle Recovery

Sediment core samples were taken every three meters along each channel, in all sediment deposits in the test reaches, and on a square meter grid in the sediment catch basins, to determine the distribution of tracer particles. The full depth of the core or sediment deposit, whichever was less, was sampled. From 45 to 60 channel sediment cores and 22 to 33 sediment catch basin cores were taken for each test reach.

Tracer particles in core samples were manually counted under black lights, using magnifiers for the smaller size classes. Large core samples were subsampled into 100 gram samples until at least 10 percent of the mass was sampled.

The total number of tracer particles deposited within the test reaches was estimated by extrapolating the tracer counts in the core volume to the total volume of deposits from which cores were taken. Core samples from the sediment catch basins were prorated to a square meter column to determine the amount of tracer in the catch basins. We assumed none of the particle sizes used for tracing would pass through the sediment basins.

RESULTS AND DISCUSSION

Complete recovery of tracer is indicated by the extrapolation of tracer counts in core samples to the sediment deposits. In fact, the results suggest the extrapolation over-estimates the number of tracer particles. Estimated total

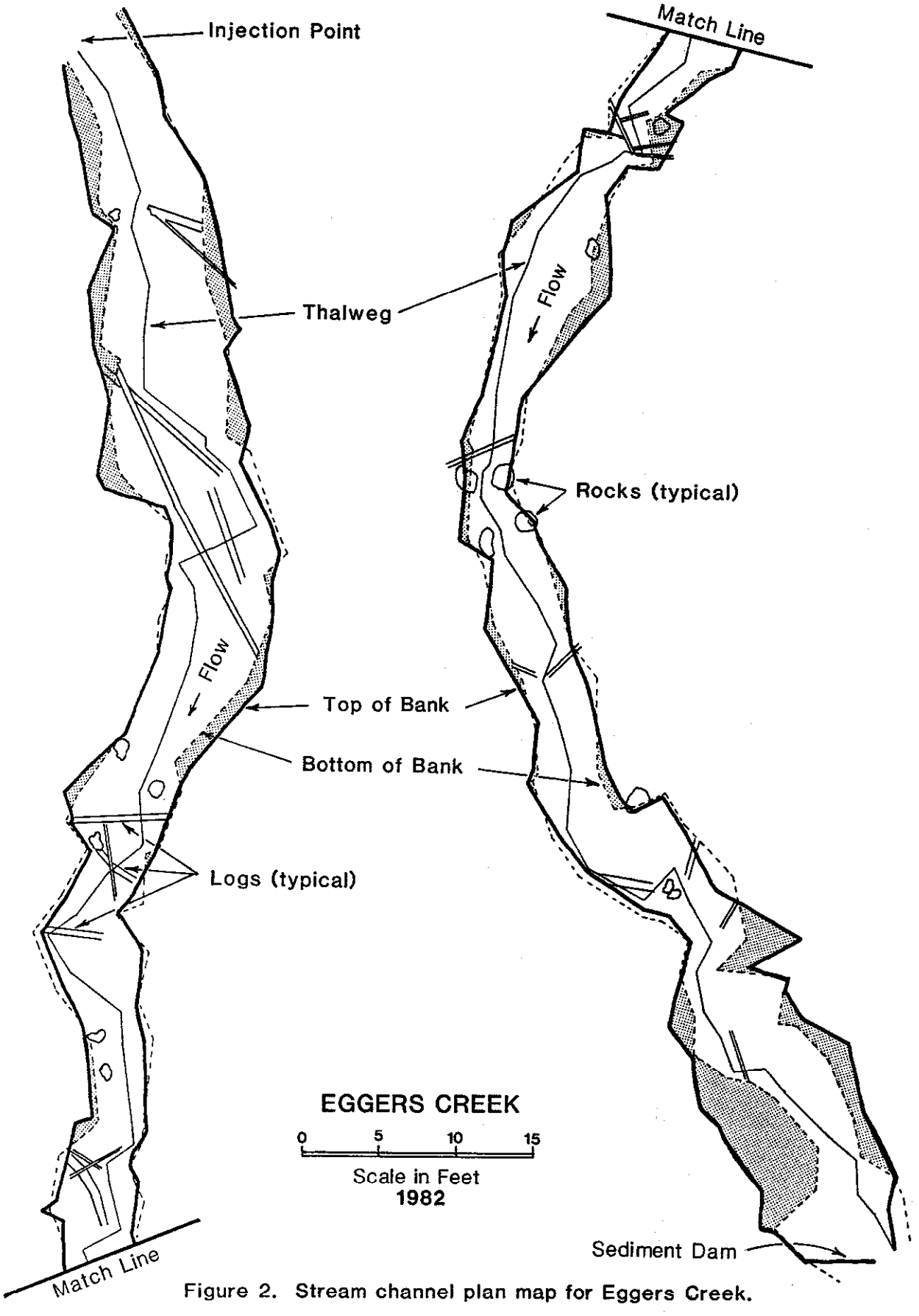

Figure 2. Stream channel plan map for Eggers Creek.

recovery, including both stream and sediment catch basin deposits, ranged from 106 percent for D Creek to 135 percent for Ditch Creek. The 1.0-2.0 mm and 2.0-4.0 mm size classes were over-estimated (161 and 150 percent, respectively) more than the 0.5-1.0 mm size class (122 percent). Recovery of the 0.25-0.5 mm size class was estimated at 61 and 86 percent for D and Eggers Creeks, respectively; while in Cabin Creek recovery was 127 and 119 percent, respectively.

Sediment sampling of the overflow at the sediment catch basins was conducted during snowmelt runoff. While no detailed analysis was conducted on these samples, sieving and weighing activities detected a few tracer particles in the 0.25-0.5 mm and 0.5-1.0 mm size classes. We are confident that very small tracer quantities were lost over the catch basin spillways.

Catch basin core samples were extrapolated over large volumes compared with the stream sediment core samples. The coring technique did not stratify the tracer counts by depth. We feel in-channel tracer estimates are more accurate because of fewer extrapolation errors.

Most of the tracer moved through the test reaches during the study period. As expected, travel distance tended to be inversely proportional to particle size (Figure 3a-d). An evaluation of the 1982 spring snowmelt runoff shows the relative magnitude of the total volume of spring runoff and maximum instantaneous peak flow rates. Spring runoff volume was indexed by summing the flows for the months of April and May (Table 1). A frequency of occurrence analysis for the volume of spring snowmelt values based on at least 23 years of record showed exceedence probabilities ranging from 0.08 to 0.17 for the four streams. Annual maximum instantaneous streamflow peaks in the study area always occur during snowmelt. Exceedence probabilities for instantaneous snowmelt peaks ranged from 0.10 to 0.27. Thus, high flow rates undoubtedly accounted for the high sediment transport rates. Even so, we were surprised by magnitude of the transport of the tracer through these step-pool channels.

Each test reach showed distinct properties that influence the transport of tracer material. D Creek had the steepest channel gradient, the fewest obstructions, and the highest snowmelt runoff (Table 2). Only two percent of the tracer material was retained in the test reach, with less than three percent of any size class (Figure 3a). Approximately 1.1 cubic meters of sediment were stored in the test reach, with 65 percent stored behind organic debris, 17 percent behind rocks, and the rest in bed forms; mostly pools (Table 2). Of the tracer deposited in the test reach, nearly half was trapped behind rocks with the other half split between organic debris and bed forms.

Eggers Creek, the channel with the second highest gradient and snowmelt runoff, but with considerable large organic debris, retained about six percent of the tracer in the test reach (Table 2). Less than ten percent of any size class was retained in the reach (Figure 3b). A total of 1.3 cubic meters of sediment was stored in the test reach, with 69 percent located behind organic debris, only four percent behind rocks, and the rest in bed forms; mostly pools. The tracer deposited in the test reach was evenly distributed between deposits trapped by bed forms and organic debris. Only three percent was trapped behind rocks.

The Ditch Creek test reach had a lower snowmelt runoff and gradient; with many obstructions. However, only one and a half percent of the tracer remained in the test reach (Table 2). No more than 2.5 percent of any size class was retained (Figure 3c). Approximately 1.6 cubic meters of sediment were stored in the test reach, with 62 percent stored behind organic debris and only three percent behind rocks. The remaining 0.6 cubic meter of sediment was present mostly as channel deposits with no apparent association with obstructions. Of the tracer deposited in the test reach, 60 percent was trapped behind organic obstructions and 38 percent in bed form deposits.

Cabin Creek, the lowest gradient channel with relatively few organic obstructions, transported far less tracer through the reach. Approximately 14 percent of the tracer particles were retained (Table 2), with up to 29 percent of the

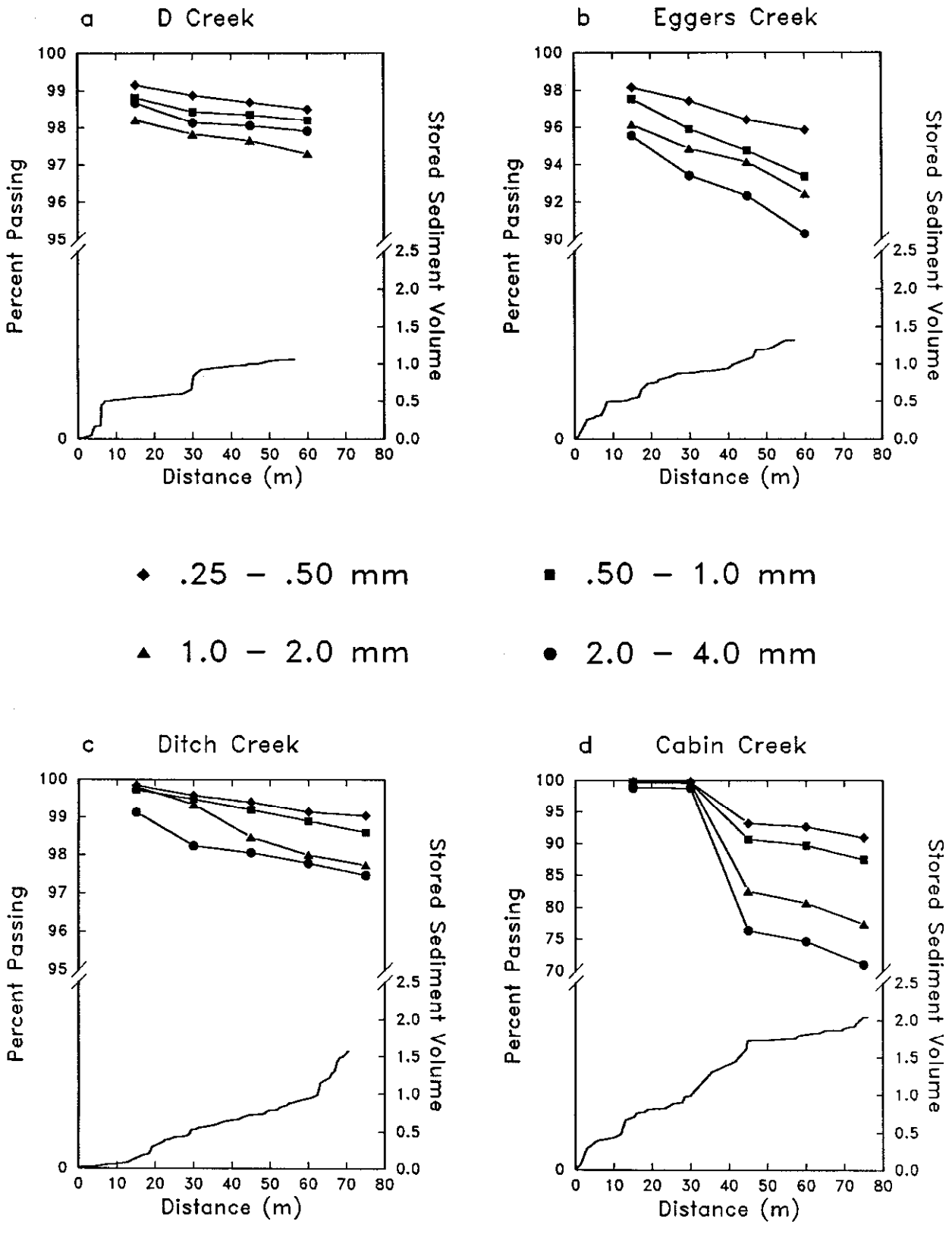

Figure 3. Cumulative Stored Sediment and Percent of Tracer Particles Passing Through Each Test Reach.

2.0-4.0 mm size class remaining in the reach (Figure 3d). Nearly all the tracer was transported through the first half of the reach. Just downstream from that point a number of log obstructions trap large quantities of sediment and reduce the effective channel gradient to only 1.3 percent. Approximately 2.0 cubic meters of sediment are stored in the test reach, with nearly half stored behind organic debris, less than one percent behind rocks, and the other half in bed forms; mostly point bars. Point bars are a significant feature of this test reach due to more meandering of the channel. Of the tracer deposited in the test reach, nearly half was trapped behind organic debris and slightly over half behind bed forms.

Table 2. Distribution of sediment and tracer particles in Silver Creek test reaches.

	%	% of total stored volume			% of tracer particles		
	Tracer		Obstructions			Obstructions	
Stream	Retained	Bed Forms	Rock	Organic	Bed Forms	Rock	Organic
'D'	2	17	17	65	28	45	27
Eggers	6	28	4	69	41	3	56
Ditch	2	35	3	62	38	2	60
Cabin	14	52	0	48	55	0	45
Mean	6	33	6	61	40	12	47

As expected, tracer movement appears to be proportional to channel gradient, and more specifically to effective channel gradient, and to differences in flow rates (Table 1). The greatest amount of deposition occurred in Cabin Creek, the lowest overall gradient test reach and lowest effective gradient; at least in the lower half of the test reach where much of the deposition occurred. The next greatest deposition occurred in Eggers Creek, which has a high overall gradient and runoff, but relatively low effective gradient. Ditch Creek was an anomoly, considering that it had the lowest overall effective gradient and snowmelt runoff. We have no explanation for the lack of tracer deposition except possibly that the channel had more of its storage capacity occupied by sediments derived from road construction within the watershed. Megahan et al (1986) measured 13 cubic meters of sediment storage in the Ditch Creek channel, in 1981, as a result of road construction using minimal erosion control measures. No increased sediment storage was detected in the Cabin Creek channel where extraordinary erosion control measures had been used.

Obstructions are a key factor affecting sediment deposition. Sixty-seven percent of the channel sediment is stored behind obstructions (rock and organic). Fifty-nine percent of the tracer deposited in the test reaches was found behind obstructions. Bed forms were more significant in Cabin Creek where channel meanders are more pronounced.

This tracer technique has great potential for small streams. Longer test reaches should be studied over additional flow events to answer questions about residence time.

REFERENCES

Clayton, James L., Megahan, Walter F., and Hampton, Delon, 1979, Soil and bedrock properties: weathering and alteration products and processes in the Idaho Batholith. USDA Forest Service, Intermountain For. and Range Expt. Sta., Ogden, UT, Research Paper INT-237, pp. 35.

Ketcheson, Gary, L. 1986, Sediment rating equations: an evaluation for streams in the Idaho batholith. USDA Forest Service, Gen. Tech. Rpt. INT-123, Intermountain Research Station, Ogden, UT; 12 p.

Megahan, Walter F., 1978, Erosion processes on steep granitic road fills in central Idaho. Soil Sci. Soc. Am. J. 42(2), 350-357.

Megahan, Walter F., 1982, Channel sediment storage behind obstructions in forested drainage basins drianing the granitic bedrock of the Idaho Batholith. USDA Forest Service, Gen. Tech. Rpt.PNW-141, Pacific Northwest For. and Range Expt. Sta., Portland, OR; p. 114-121.

Megahan, Walter F., Seyedbagheri, Kathleen A., Mosko, Timothy L., and Ketcheson, Gary L. 1986. Construction phase sediment budget for forest roads on granitic slopes in Idaho. In: Hadley, Richard F., Ed. Drainage basin sediment delivery: Proceedings; 1986 August 4-8; Albuquerque , NM. Intl. Assoc. of Scientific Hydrology Publ. No. 159. Wallingford, Ozon, United Kingdom; 1986: 31-39.

Rathbun, R.E. and Nordin, Carl F., 1968, Fluorescent tracer techniques in sediment transport studies. Progress Report No. 1, Background and procedures. U.S. Geological Survey informal report, pp. 72.

SEDIMENT TRANSPORT IN HEADWATER CHANNELS IN IDAHO

by

Kent R. Johnejack, Graduate Student, Department of Hydrology and Water Resources, University of Arizona, Tucson, Arizona.

and

Walter F. Megahan, Research Hydrologist, Forestry Sciences Laboratory, Boise, Idaho.

ABSTRACT

Prediction of sediment transport in steep, headwater channels is complicated by step-pool profiles and large scale roughness from boulders, logs, and brush. A study to evaluate four common sediment transport equations on such channels was conducted on four watersheds at the Silver Creek Study Area in south-central Idaho. Study reaches ranging from 150 to 250 feet long at the mouth of each watershed were used to develop hydraulic and sediment data for input to the Yang, Meyer-Peter Mueller, Laursen, and Einstein equations. Predicted transport rates exceeded measured rates by up to three orders of magnitude when using the valley slope. Use of an "effective" slope, which removed all vertical drops from the profile, reduced the valley slope from an average of 6.4% to 1.0%, and more accurately modeled the energy slope in the pools. The Laursen and Einstein equations then predicted transport within one order of magnitude, but the threshold of incipient motion was not exceeded with the Yang and Meyer-Peter Mueller equations. Neither the Laursen Relation nor the Einstein Equation correctly predicted the gradation of the transported material, or the percentages traveling as bed and suspended load. Although the agreement between predicted and measured transport rates was encouraging, it did not necessarily indicate that physical processes were correctly modeled.

INTRODUCTION

Purpose

Most sediment transport equations are based on conditions in alluvial channels or flumes -- conditions very different from steep, headwater channels with frequent pools, steps, and riffles. Because of this step-pool configuration, overall stream characteristics are not useful for predicting sediment transport, and pools and riffles must be modeled separately. The purpose of this study was two-fold: 1) to apply four common sediment transport equations by Yang (1972), Meyer-Peter Mueller (1948), Laursen (1958), and Einstein (1950) to steep, headwater channels, and 2) to use the equations to test the hypothesis that pools rather than riffles or steps, control sediment transport.

Description of Study Site

Four first and second order watersheds of the Silver Creek study area in central Idaho provided data for this investigation. D, Eggers, Ditch, and Cabin Creeks are each approximately 250 acres in area with southeast aspects and elevations from 4500 to 7000 feet. The area is representative of the Idaho Batholith with granitic parent material, frequent outcrops, and shallow, coarse textured soils. Vegetation is predominantly Douglas fir, Grand fir, and Ponderosa pine, with willows and mountain ash common in the riparian zones.

Average annual precipitation at Silver Creek is 33.8 inches with most coming as snow from cyclonic winter storms and minor amounts falling as rain during summer thunderstorms. Annual streamflow is dominated by snowmelt runoff in May and June, although rain on snow events can produce peak flows any time during winter. Spring runoff produces 90% of the annual sediment yield (Megahan, 1982).

DATA AND PROCEDURES

The four sediment transport equations required a variety of input, but common to all were the hydraulic parameters of velocity, roughness, wetted perimeter, area, top width, and bottom width. In addition, all of the equations needed a description of the bed material by either a particle size distribution or a representative size (D_{50} or D_{90}). Modeling was limited to spring runoff because little sediment transport occurred outside this period.

Detailed channel surveys provided cross section geometry at 8 to 11 locations in a 150 to 250 foot reach on each of the four creeks, as well as plan and profile showing overhangs, vertical drops, and thalweg. Rating curves of hydraulic parameters were developed with this field data using a method proposed by H.A. Einstein (1950). Four or five core samples were taken in the riffles of each study reach to provide bed material gradations.

In order to evaluate results from the equations, field data on instantaneous transport rates were needed, as well as gradations of the transported material and percentages traveling as bed and suspended load. Field data from DH-48 and Helley-Smith samplers provided instantaneous rates and percentages of bed and suspended loads. Core samples from deposits in sediment detention basins at the downstream end of each channel provided particle size distributions for the transported material.

Discharge was measured continuously in Parshall flumes just below each study reach. A limited number of instantaneous discharge measurements verified flume rating curves, and provided field velocity data for comparison to predicted velocities.

RESULTS AND ANALYSIS

The concept of an effective slope recognizes that the valley slope does not adequately describe hydraulic conditions in a step-pool channel. By subtracting vertical and near vertical drops from the total fall of a reach, the fall through pools was estimated. This fall divided by the total reach length provided the effective slope. Under assumptions of normal, subcritical flow, the effective slope became the energy slope in the sediment transport equations. Table 1 shows the valley and effective slopes based on field data from the four creeks.

TABLE 1

Valley and Effective Slopes

Creek	Reach Length (feet)	Total Fall (feet)	Valley Slope (ft./ft.)	Height of Drops (feet)	Effective Fall (feet)	Effective Slope (feet)
D	185.2	18.0	0.097	15.8	2.2	0.012
Eggers	190.5	13.6	0.071	11.1	2.5	0.013
Ditch	239.3	14.0	0.059	12.3	1.7	0.007
Cabin	248.1	9.5	0.031	7.5	2.0	0.008

Unfortunately, the field data was not detailed enough to separate the fall of the riffles from that of the pools. Thus the effective slopes in Table 1 may over estimate the energy slope of the pools alone. Another deficiency in the field data was the lack of bed material samples from pools.

To further explore the notion that pools control sediment transport, a hypothetical pool was created by arbitrarily reducing the effective slope to as mild a slope as possible without predicting unrealistic flow depths and velocities. This new slope was a more accurate estimate of the energy slope in the pools alone, again noting that flow was assumed normal and subcritical. To complete this picture of a hypothetical pool, a bed material sample was interpolated between the logical limits of the riffle bed material and the material deposited behind sediment dams. The valley and effective slopes of Table 1 were used with all four equations and all four creeks. Only the Laursen Relation and the Einstein Equation were used with D Creek to simulate the hypothetical pool. Because D Creek was representative of all four creeks, only the results from D Creek are detailed in this paper.

Predicted hydraulic conditions, particularly depth and velocity, were compared to field measurements. Results from the sediment transport equations were judged against field data by three criteria: instantaneous transport rates, particle size distributions, and mode of transport. An equation must predict all

three correctly to be reliable, for correct rates without correct gradations and mode of transport may be coincidental.

Hydraulic Conditions

Predicted velocities using the effective slopes of Table 1 ranged from 0.21 feet per second (fps) for 0.046 cubic feet per second (cfs) to 2.72 fps for 8.478 cfs, and matched field measurements within 10% at high discharges where most transport occurred. The assumed slope of the hypothetical pool (0.4%) produced slightly lower velocities for D Creek that ranged from 0.21 fps to 1.71 fps for 0.046 cfs and 8.478 cfs, respectively. Unrealistically low velocities were produced by assumed slopes less than 0.4%. Bankfull depths based on 8.478 cfs and effective slopes were approximately 1.0 feet on all four creeks, which closely matched the measured range of 0.7 to 1.4 feet. The hypothetical pool on D Creek had a slightly greater bankfull depth at 1.27 feet, but was still within the measured range.

Instantaneous Transport Rates

As expected, predicted transport rates were too high by two to three orders of magnitude when using the valley slope and riffle bed material as input to the four equations. Using the effective slopes and riffle bed material over predicted rates by one order of magnitude with the Laursen Relation, and under predicted rates by one order of magnitude with the Einstein Equation. Because flow depths and velocities were insufficient to exceed the threshold of incipient motion in Yang's Equation and the Meyer-Peter Mueller Formula these two equations predicted no sediment movement with the effective slope. Measured and predicted rates for D Creek are shown in Figure 1.

Predicted rates through the hypothetical pool on D Creek also are included on Figure 1. The Laursen Relation, which over predicted rates by only 20% to 30%, performed better than the order of magnitude accuracy produced by the Einstein Equation under these conditions.

Gradations of the Transported Material

Of the four equations, only the Laursen Relation and Einstein Equation predicted the gradation of the transported material. Using D Creek as an example, Table 2 shows predicted gradations (based on the effective slope and riffle bed material), as well as the measured gradations of the riffle bed and sediment dam material. The Laursen Relation incorrectly predicted a fine gradation composed largely of sand; the Einstein Equation predicted too coarse a gradation of gravel and larger particles.

TABLE 2

Predicted and Measured Gradation on D Creek
(Based on Effective Slope and Riffle Bed Material)

Particle (mm)	Riffle %	Sed. Dam %	Laursen %	Einstein %
Gravel and larger (>7.9)	46	4	0	98
Gravel (2.0 - 7.9)	22	34	2	2
Sand (0.05 - 2.0)	32	62	98	0

Predicted gradations became finer with the milder slope and finer bed material of the hypothetical pool. With the Laursen Relation, transported material became slightly finer and was composed completely of sand. The Einstein Equation still predicted too coarse a gradation, but changed significantly from 98% gravel and larger to 94% gravel and 6% sand. Results are complied in Table 3.

TABLE 3

Predicted and Measured Gradations on D Creek
(Based on the Hypothetical Pool)

Particle (mm)	Pool Bed %	Sed. Dam %	Laursen %	Einstein %
Gravel and Larger (7.9)	15	4	0	0
Gravel (2.0 - 7.9)	33	34	0	94
Sand (0.05 - 2.0)	52	62	100	6

Mode of Transport

Neither the Laursen Relation nor the Einstein Equation correctly matched the percentages of material moving as bed or suspended load on any of the four creeks. Whether the effective slope and riffle bed material were used, or the assumed slope and bed material of the hypothetical pool, the Laursen Relation predicted too much suspended load and the Einstein Equation predicted too much bed load. Table 4 compares measured and predicted values on D Creek.

TABLE 4

Measured and Predicted Mode of Transport on D Creek

	Laursen		Einstein	
Condition	Bed Load %	Sus. Load %	Bed Load %	Sus. Load %
Measured	73	27	73	27
Eff. slope and riffle bed	10	90	100	0
Hypothetical pool	8	92	100	0

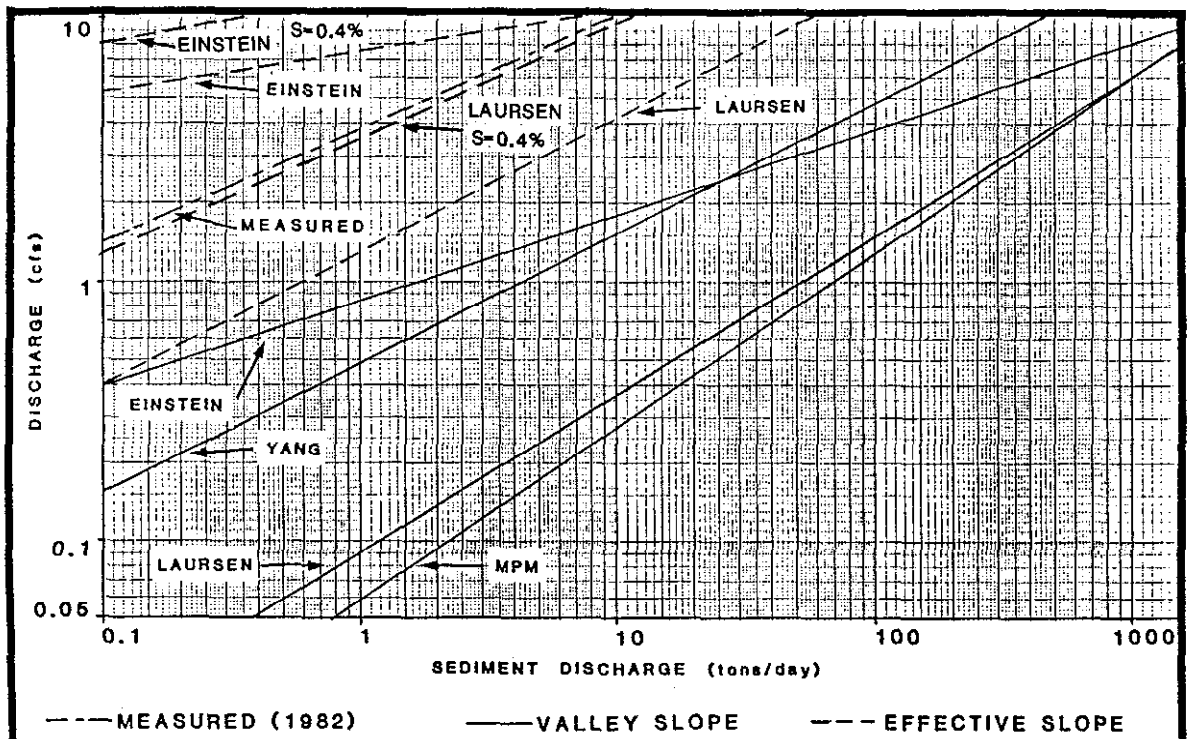

FIGURE 1
INSTANTANEOUS SEDIMENT DISCHARGE FOR D CREEK

CONCLUSIONS

Only two of the four equations,the Laursen Relation and the Einstein Equation, predicted sediment transport to within an order of magnitude of measured values, and then only by the use of an effective slope as a surrogate for the energy slope in the pools. All four equations over predicted transport by up to three orders of magnitude when using the valley slope. The Yang and Meyer-Peter Mueller Equations predicted no movement with the effective slope because their incipient motion terms were not exceeded. Agreement within 20% of measured transported rates was achieved with the Laursen Relation and a hypothetical pool that assumed a 0.4% energy slope and a fine bed material. Under all variations of slope and bed material, the Laursen Relation predicted too fine a load with too high a percentage moving in suspension. The Einstein Equation was equally inaccurate with too coarse a load and too high a percentage moving as bedload. Because neither the Laursen Relation nor the Einstein Equation correctly matched measured gradations or mode of transport, accurate prediction of rates is not conclusive evidence that physical processes are correctly modeled.

REFERENCES

Einstein, A. H., 1950, The Bed Load Function for Sediment Transport in Open Channels, Technical Bulletin 1026, U.S. Dept. of Agriculture, Soil Cons. Ser. Washington, D.C.

Johnejack, K. R., 1987, Report on Additional Modeling for Sediment Transport in Step-Pool Mountain Streams, Unpublished report on file, U.S. Department of Agriculture Forest Service, Intermountain Research Sciences Laboratory, Boise, Idaho.

Johnejack, K. R., 1986, Sediment Transport in Step-Pool Mountain Streams, M.S. Thesis, Dept. of Civ. Eng., Univ. of Arizona, Tucson, Arizona.

Laursen, E. M., 1958, The Total Sediment Load of Streams, J. Hyd. Div., Am. Soc. of Civ. Eng., 54, 1-36.

Megahan, W. F., 1982, Channel Sediment Storage Behind Obstructions in Forested Drainage Basins Draining the Granitic Bedrock of the Idaho Baholith, U.S. Dept. of Agriculture, Forest Ser., Pacific Northwest For. and Range Exp. Sta., General Technical Report PNW-141, Portland, Oregon., 114-121.

Meyer-Peter E. and Mueller, R., 1948, Formulas for Bed Load Transport, Report on Second Meeting of Int. Assoc. for Hyraulic Research, Stockholm, Sweden, 39-64.

Yang, C. T., Unit Stream Power and Sediment Transport, J. Hyd. Div., Am. Soc. of Civ. Eng., 98, 1805-1826.

TRANSPORT OF UNIFORM AND NONUNIFORM SEDIMENT SIZES

Hsieh Wen Shen and Chris Xudong Rao
Dept. of Civil Engineering, University of California, Berkeley

Abstract

This paper has three parts. The 1st part was to investigate the possibility of inserting a single representative sediment size into certain existing sediment transport models to obtain the sediment transport rate of nonuniform sediment sizes. In the 2nd part a new regression model was developed using mean sediment sizes. In the 3rd part a sediment gradation coefficient was inserted into a sediment transport model. It was found that the models developed here fitted the 1150 sets of available flume and river data well.

1. Source and Range of Collected Data.

Previously collected (1151 sets) flume and river sediment transport data (namely uniform and nonuniform sediment sizes) were used in this study. These data were collected by Guy et al (1966), Einstein (IRTCES Circular #2), Barton and Lin (1955), Einstein and Chien (1953), Mantz (1983), Samaga et al (1986 a, 1986 b), White and Day (1982), Proffitt and Sutherland (1983) and Karim & Kennedy (1983). These data cover wide ranges of hydraulic and sediment conditions. Sediment sizes (D_{50}) are in the range of 0.1 mm through 30 mm; sediment gradation coefficients (G) are in the range of 1 to 4; water depths (H) are in the range of 0.1 ft to 20 ft; flow velocities (U) are in the range of 1 ft/sec to 9 ft/sec; water surface slopes (S) are in the range of 0.0001 to 0.02 and sediment concentrations (C) are in the range of 2 ppm to 150000 ppm by weight. The sediment gradation coefficient is defined as:

$$G = \frac{1}{2}\left[\frac{D_{84}}{D_{50}} + \frac{D_{50}}{D_{16}}\right] \tag{1}$$

where D_p is the sediment size of which p percent of the total is less than that size by weight.

2. The Representative Size inserted in the Existing Sediment Transport Models.

This part was to investigate the possibility of inserting a single representative sediment size in certain existing sediment transport models to obtain the total sediment transport rate of nonuniform sediment sizes. The sediment transport models developed by Shen and Hung (1972), Ackers and White (1973), Bagnold (1973), Yang (1982), Rijn (1984 a, 1984 b) and Zhang (1959) were selected to be tested for the transport of non-uniform sediment sizes.

Sediment particles within a mixture were grouped into nine fractions, namely, D_{10}, D_{20} ... D_{90}. These sediment transport models were used to calculate the sediment concentrations C(D) with each of the selected sizes as the representative size. These C(D)'s were compared with the actual measured concentration C_o. A measure for the error between the C(D) and C_0 for N sets of data was defined as:

$$E_1 = N^{-1}\sum\left|(C_o - C(D))/C_o\right| \tag{2}$$

As shown in Figure 1 it was found that D_{50} was the best representative diameter to be inserted into all of these sediment transport models except the models by van Rijn and by Ackers and White. One reason for this result is that these sediment transport models were practically developed based on median sizes (D_{50}) of sediment and majority of the data point were obtained with nearly uniform sediment sizes.

From this section the following conclusion was made. Models by Ackers and White, Bagnold and van Rijn are more sensitive to the selection of representative size than the models by Shen, Yang, Zhang. The models by van Rijn and Ackers and white gave the minimum error between the calculated and measured concentrations when D_{90} and D_{70} were used respectively as the representative size. All other models gave the minimum errors when D_{50} used as the representative size. Since many data were collected with uniform sediment sizes, no conclusion can be drawn as the preferred sediment transport model.

The errors as defined in Equation (2) between the measured concentrations and the concentrations calculated by the existing models are in the range from 70 percent to 200 percent. The error in this range is not undesirable for prediction purposes.

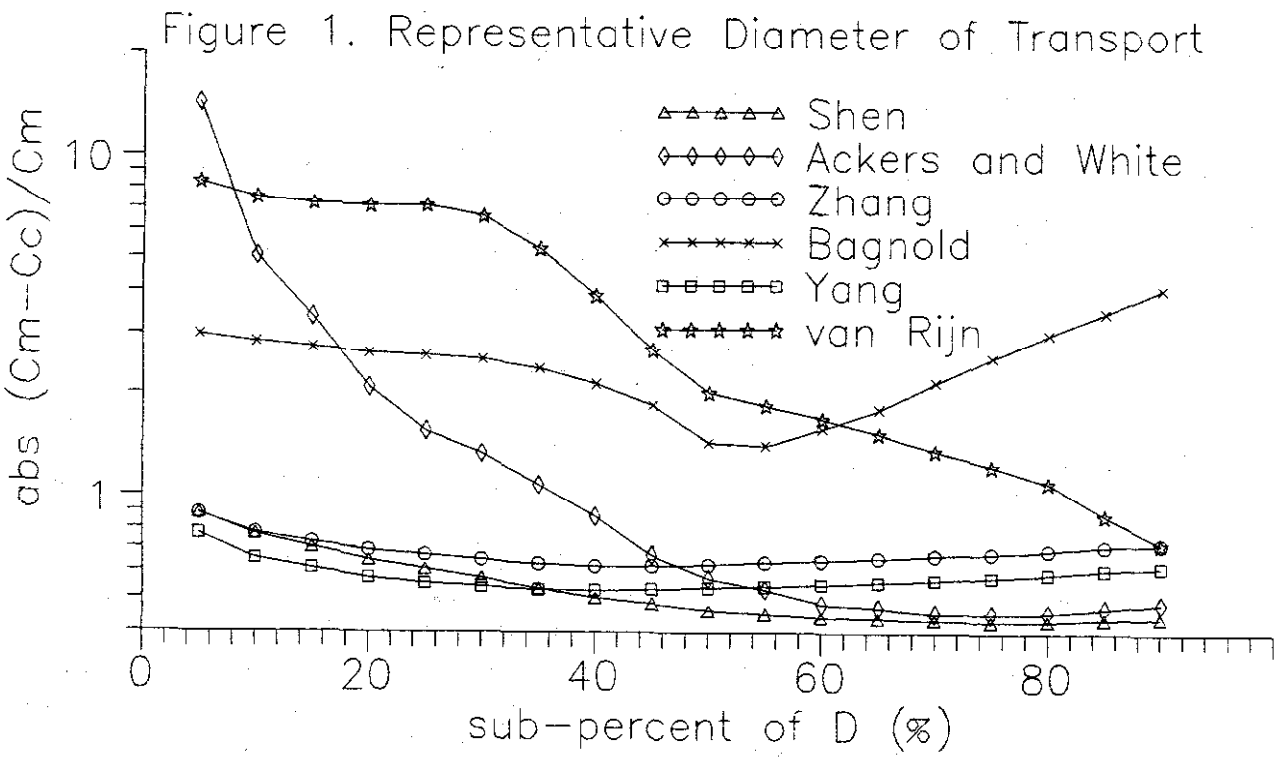

3. A Regression Model Using Mean Sediment Size.

Sediment transport rate is a function of flow condition and sediment characteristics. This function can be expressed in a dimension-less form as follows.

$$C = \phi\left[\frac{U^2}{gH}, \frac{U}{\omega}, a, \frac{UH}{\nu}, \frac{D}{H}, \frac{B}{H}\right] \tag{3}$$

where a = relative specific gravity of sediment particles (1.65 for natural sand), C = sediment concentration by weight, U = flow velocity, H = water depth, g = gravitational acceleration, ν = kinetic viscosity, ω = sediment particle fall velocity, D = sediment size, B = channel width.

It is still difficult at present to express the above equation explicitly and theoretically. For a wide channel with large B/H values, the influence of B/H on C may be dropped from Equation (3). Then the next two last terms UH/ν and D/H may be replaced by a boundary frictional coefficient f_0 as defined below.

$$f_0 = \Phi\left[\frac{UH}{\nu}, \frac{D}{H}\right] \tag{4}$$

Then Equation (3) becomes.

$$C = \Phi\left[\frac{U^3}{gH\omega}, f_0\right] \tag{5}$$

where $U^3/gH\omega$ is a product of U^2/gH and U/ω.

Many engineers from China and U.S.S.R. have found that (Chien, 1983).

$$C = \Phi\left[\frac{U^3}{gH\omega}\right] \tag{6}$$

$U^3/gH\omega$ can also be written as $8US/f\omega$ where f is defined as $f = 8gHS/U^2$. Then the following equation is obtained.

$$C = \Phi\left[\frac{US}{f\omega}\right] \tag{7}$$

Replacing f in the above equation with f_0, the equation becomes.

$$C = \Phi\left[\frac{US}{f_0\omega}\right] \tag{8}$$

If f in Equation (7) is considered as a constant, the following equation is obtained.

$$C = \Phi\left[\frac{US}{\omega}\right] \tag{9}$$

The expressions in Equation (9) was used by Yang and Molinas (1982) to developed their sediment transport models. It was found in this study that the form expressed in Equation (8) could fit the available data better than that defined in Equation (7) and (9). The error as defined in Equation (2) for an optimized Equation (8) is 62% and the errors for Equation (7) and (9) are respectively 96% and 87%. In the rest of this section the optimized results for all three form are obtained.

The functional relationship among sediment concentration and flow condition and

sediment characteristics is assumed to have the following form:

$$\log C = \sum_{n=0}^{3} a_n F_i^n \tag{10}$$

in which a_n = coefficients to be determined, F_i = parameters expressed as follows:

$$F_1 = \log\frac{US}{f_0\omega},\quad F_2 = \log\frac{US}{f\omega},\quad F_3 = \log\frac{US}{\omega} \tag{11}$$

The value f_o is calculated by the following equations as in Schlichting (1979).

$$\frac{1}{f_0^{1/2}} = -2\log\left[\frac{\epsilon/d}{3.7} + \frac{2.51}{Re f_0^{1/2}}\right] \tag{12}$$

where Re is the Reynolds number ($Re = 4UH/\nu$), $d = 4H$, ϵ = roughness height ($\epsilon = D_{50}$ is used in this study).

An approximate and explicit form for the above equation obtained by Haaland (1983) was used to simplify the calculation.

$$\frac{1}{f_0^{1/2}} = -1.8\log\left[\frac{6.9}{Re} + \left(\frac{\epsilon/d}{3.7}\right)^{1.11}\right] \tag{13}$$

Fall velocity of a sediment particle is calculated using Rubey (1933) equation:

$$\omega = \left[\left(\frac{6\nu}{D}\right)^2 + \frac{2agD}{3}\right]^{1/2} - \frac{6\nu}{D} \tag{14}$$

where D is the median size of sediment and the other are defined previously.

The function defined in Equation (10) can be obtained by minimizing the summation of all errors (E_2) which is defined as follows:

$$E_2 = \sum\left|\frac{\log C - \log C_0}{\log C_0}\right| \tag{15}$$

where C is the predicted sediment concentration and C_o is the observed sediment concentration.

By minimizing the error defined in Equation (15) with Rosenbrock (1960) technique, the coefficients for Equation (10) were obtained as follows. For the form defined in Equation (8) the coefficients are 2.82019, 1.28621, -0.208129, 0.0321417 with a mean absolute error [as defined in Equation (2)] of 62 percent. For the form defined in Equation (7) they are 2.74761, 1.15189, -0.0456634, -0.0135107 with a mean error of 96 percent. For the form defined in Equation (9) they are 4.58992, 0.906196, 0.0206441, 0.0459383 with a

mean error of 87 percent. For example, the form defined in Equation (8) the relationship among sediment concentration and flow condition and sediment characteristics is then expressed as:

$$\log C = 2.82019+1.28621F_1-0.208129F_1^2+0.0321417F_1^3 \tag{16}$$

The data points and the optimized relationship between log C and F_i are shown in Figure 2, Figure 3 and Figure 4. It can seen that the scatter in Figure 3 is less than that in Figure 2 and Figure 4.

It is concluded that the form defined in Equation (8) is the best one among the three forms defined in Equation (7), (8) and (9).

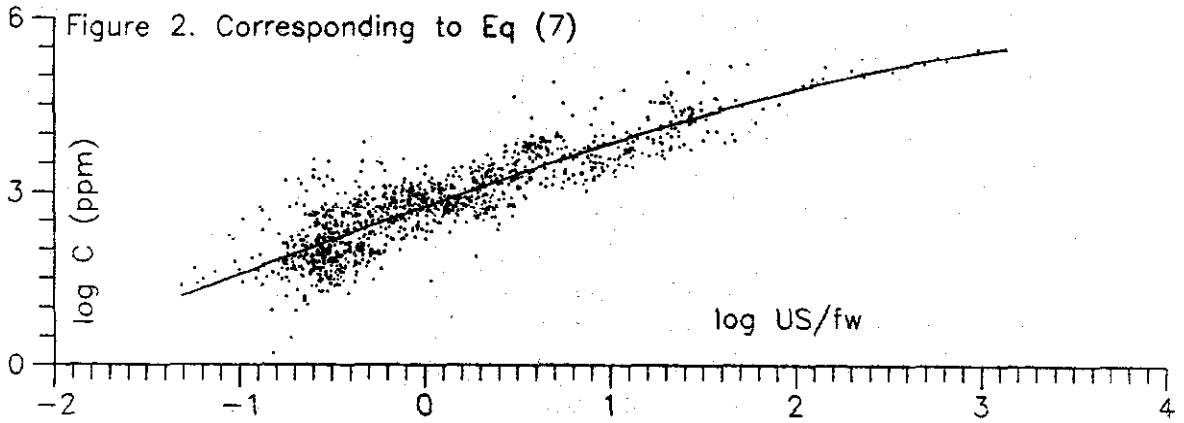

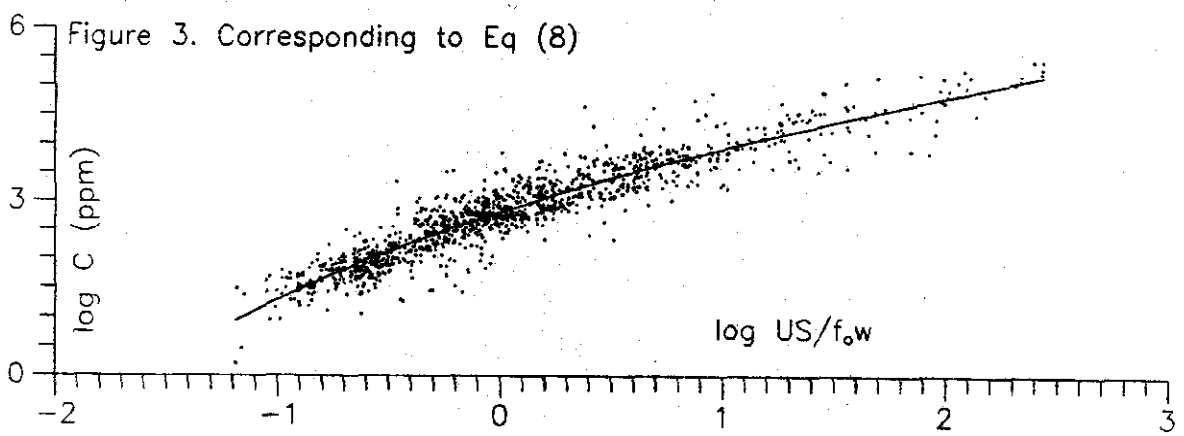

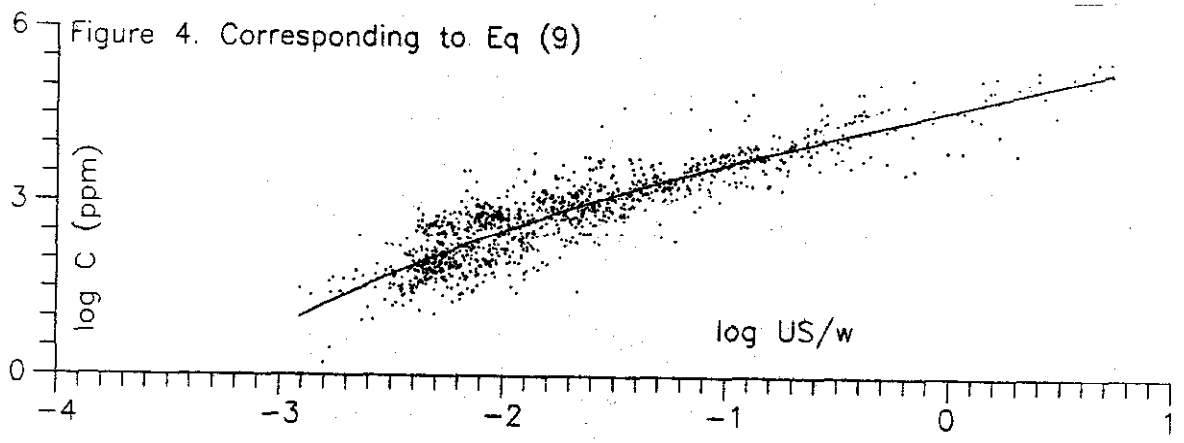

4. A Regression Model Using Mean Size and Gradation Coefficient.

It was believed that the sediment concentration was affected by flow conditions and different sediment gradation coefficients (G) as defined in Equation (1). The formulated relationship among sediment concentration and flow velocity (U), flow depth (H), water surface slope (S), sediment size (D_{50}), and sediment gradation coefficient (G) can be expressed as the following form:

$$C = \Phi\left[\left[(U/\omega)S^{c_1}G^{c_2}\right]^{c_3}\right] \tag{17}$$

$$\log C = \sum_{n=0}^{5} a_n (\log F)^n \tag{18}$$

where c_1 through c_3 and a_0 through a_5 are coefficients to be determined, F is the flow parameter defined as follows:

$$F = \left[(U/\omega)S^{c_1}G^{c_2}\right]^{c_3} \tag{19}$$

A measure for the error between the calculated sediment concentrations and the measured ones is defined as the summation of individual error for each set of data used.

$$E_3 = \sum \left[\log(C/C_0)\right]^2 \tag{20}$$

By minimizing the error defined in Equation (20) using Rosenbrock (1960) multidimensional minimizing method, these coefficients were obtained as: c_1 = 0.68985, c_2 = 0.12889, c_3 = 0.62831, a_0 = 3.9730, a_1 = 1.7656, a_2 = 0.39275, a_3 = 3.3128, a_4 = 2.5251, a_5 = 0.38090 with a mean absolute error [as defined in Equation (2)] of 51 percent.

The coefficients c_1, c_2 indicate that the sediment concentration is related to velocity with the first power, slope with the power of 0.69 and G with 0.13. The relationship between sediment concentration and flow parameter is plotted in Figure 5.

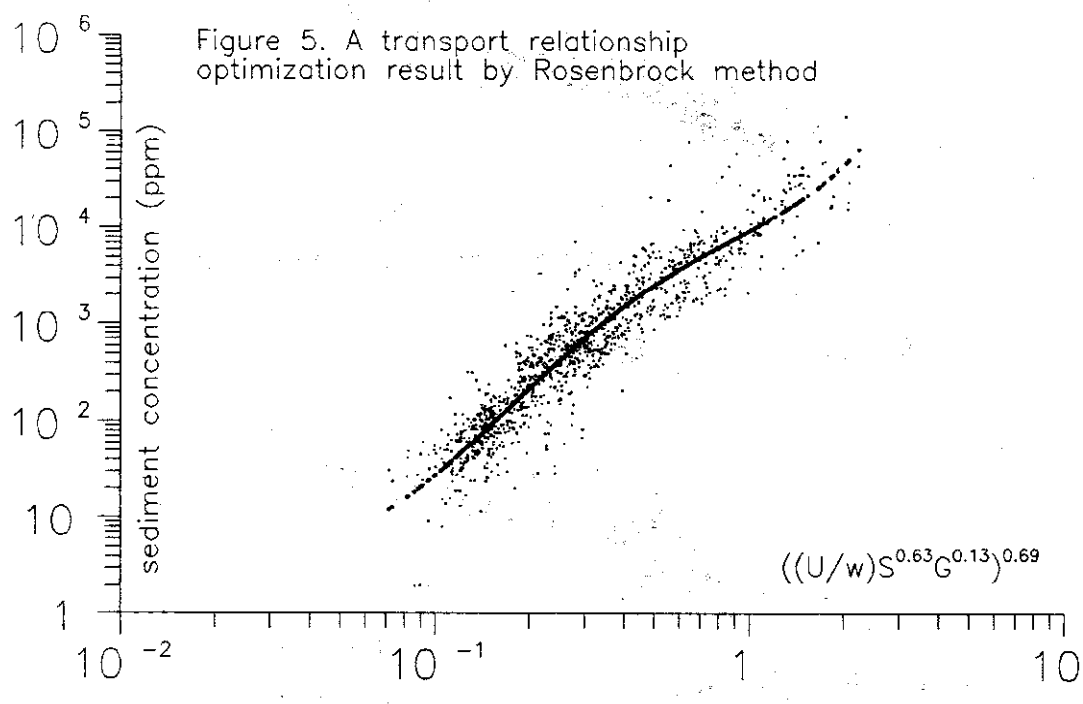

Figure 5. A transport relationship optimization result by Rosenbrock method

5. Conclusion.

The first part of the paper investigated the possibility of using a single representative size in certain existing sediment transport models through 1151 sets of flume and river data previously collected (uniform and nonuniform sediment sizes).

It was found that the newly developed models fitted the data well with mean absolute errors of 62 percent or 51 percent for the models without or with the sediment gradation coefficient in consideration.

Acknowledgement.

The work was partially supported by the U.S. Geological Survey. We would also like to thank the Hong Kong K. C. Wong Education Foundation for its financial support to the junior writer.

References.

Ackers, P. and White, W.R. (1973), "Sediment Transport, New Approach and Analysis", Journal of Hydraulics Division, Proc. ASCE., Vol. 99, No. 11, Nov. 1973, pp 2041-2060.

Bagnold, R.A. (1973), "The Nature of Saltation and of Bed Load Transport in Water", Proc. of the Royal Society, London, Series A, Vol. 332, 1973.

Barton, J.R. and P.N. Lin (1955), "A Study of Sediment Transport in Alluvial channels", Colorado A & M College, Fort Collins, Colorado, Report No. 55JRB2, 1955.

Einstein, H.A. and Chien N. (1953), Transport of Sediment Mixtures with Large Ranges of Grain Sizes, MRD Sediment Series No. 2, US Army Engineer Division, Missouri River, Corps of Engineers, Omaha, Neb., 1953.

Einstein (IRTCES Circular #2), Sediment Transport Data in Laboratorial Flumes, IRTCES Publication Circular No. 2, Beijing, China.

Guy, H.P., D.B. Simons and E.V. Richardson (1966), Summary of Alluvial Channel Data From Flume Experiments, 1956-61, Geological Survey Professional Paper 462-I, U.S. Government Printing Office, Washington, 1966.

Haaland, S.E., Simple and Explicit Formulas for Friction Factor in Turbulent Pipe Flow, J. of Fluids Eng., March 1983, pp 89-90.

Karim and Kennedy (1983), Missouri River Computer Based Predictors for Sediment Discharges, MRD sediment Series, 1983.

Mantz (1983), "Semi-Empirical Correlations for Fine and Coarse Cohesion-less Sediment Transport", Paper 8594, Proceedings of the Institution of Civil Engineers (Thomas Telford Ltd, London), Vol. 75, 1983.

Misri et al (1984), "Bed Load Transport of Coarse Non-Uniform Sediment", J. of Hydraulic Engineering, Vol. 110, No. 10, October 1984.

Proffitt, G. J. and Sutherland, A. J. (1983), "Transport of Nonuniform Sediment", Journal of Hydraulic Research, Proc. IAHR, Vol. 21, No. 1, 1983.

Qian, N. and Wan, Z. (1983), Mechanics of Sediment Transport, Scientific Publishing House, Beijing, China, 1983.

van Rijn, L.C. (1984 a), "Sediment Transport, Part I: Bed Load Transport", J. Hydraulic Eng., Vol. 110, No. 10, Oct. 1984.

van Rijn, L.C. (1984 b), "Sediment Transport, Part II: Suspended Load Transport", J. Hydraulic Eng., Vol. 110, No. 11, Nov. 1984.

Rosenbrock, H.H. (1960), "An Automatic Method for Finding the Greatest or Least Values of a Function", Computer Journal 3, pp 175-184.

Ruby, W.W. (1933), "Settling Velocities of Gravel, Sand, and Silt Particles", American Journal of Science, Vol. 25, No. 148, 1933, pp 325-338.

Samaga, B.R., Ranga Raju, K.G. and Grade, R.J. (1985), "Total Load Transport of Sediment Mixtures", J. of Central Board of Irrigation and Power, New Delhi, Vol. 42, No. 4, Oct. 1985.

Samaga, B.R., Ranga Raju, K.G. and Grade, R.J. (1986 a), "Bed Load Transport of Sediment Mixtures", J. Hydraulic Eng. ASCE, Vol. 112, No. 11, Nov. 1986

Samaga, B.R., Ranga Raju, K.G. and Grade, R.J. (1986 b), "Suspended Load Transport of Sediment Mixtures", J. Hydraulic Eng. ASCE, Vol. 112, No. 11, Nov. 1986

Schlichting, H. (1979), Boundary-Layer Theory, 7th Edition, McGraw-Hill, Inc., 1979, pp 615-626.

Shen, H.W. and Hung, C.S. (1972), "An Engineering Approach to Total Bed Material Load by Regression Analysis", Proc. of the Sedimentation Symposium, Chapter 14, 1972, pp 14.1-14.17.

Yang, C.T. and Molinas, A. (1982), "Sediment Transport and Unit Stream Power Function", J. Hydraulic Division, Proc. ASCE, Vol. 108, No. HY6, June 1982.

White, W.R. and Day, J.J. (1982), "Transport of Graded Gravel Bed Material", Gravel Bed Rivers, R. D. Hey, J. C. Bathurst and C. R. Thorne, Eds., John Wiley and Sons, New York, N.Y., 1982, pp181-223.

Zhang (1959), Sediment Research Group (Including Zhang et al), Wuhan Institute of Hydraulic and Electric Engineering, "Sediment Transport in the Yangtze River", Journal of Sediment Research, No. 2, 1959.

METHODS OF MEASURING INCIPIENT MOTION OF BED LOAD IN MOUNTAIN RIVERS

By Wojciech Bartnik, Wojciech Kopka Agricultural University Cracow Poland

ABSTRACT

The paper analyses the experiment data on incipient motion in mountain rivers. Studies on the incipient motion of bed load in rivers are of great importance for the majority of existing formulas used for calculating the bed load transport rate. This is done on the base of knowledge of the initial parameters of the motion's beginning. In these studies the natural armouring layer and the radioactive traser method of measuring incipient motion of bed load in mountain rivers were used to determine critical bed shear stresses.

The Radioactive Traser Method

The radioactive traser method of measuring incipient motion of bed load was adopted in some Polish mountain rivers /Table 1/. In the experiments the trasers were used [Jr-192 and Ta-182]. For the experiments about 30 grains of each chosen fractions were introduced into the nearby upstream region of each of the detectors. The detectors used were connected with the counting and recording system mounted in a field isotope lab. on a bus.
The depth at which 90% of the total amount of active grains moved and moved away from beneath the detector was considered as *critical depth*. Furthermore, the hydraulics measurements were carried out to define the mean velocities, slope under critical conditions of incipient motion of individual frictions of the bed material (Bartnik 89)

The parameters of rivers characteristics/Table 1/

parameters	*symbols*		*Wisloka river*	*Dunajec river*	Targaniczanka *river*
slope	J	%.	0.2-0.5	0.2-0.5	17
discharge	Q_{max}	m^3/s	750	730	50
depth of flow	h	m	1.0-3.1	1.0-4.7	0.3 - 1.0
width of flow	B	m	30.0	65.0	6.0
grain size	d_m	m	0.0031	0.0274	0.06 - 0.11
standard deviation of mixture diam.	δ	-	4.0	2.77	1.6 -4.5

The reletionship (Fig.1) between the *critical Froude number* for particles and and the *critical Reynolds number* for flow show that F_d decreases with the increase of R_e and it is a mistake to take the *Shields parameter* as a constant. After this the *critical shear stress* may be calculated

$$\tau_c = 0.039 \left(\frac{R_e}{10^5}\right) (\gamma_s - \gamma)\, d^{-0.48}$$

When the shear stress over the bed rivers exceeds its critical value, the motion of particles begins (Shen 76). In general, the observation and measuring critical conditions of particle motion are difficult in nature. The beginning of motion is not easily obtainable and difficult to define. In this paper we define that the motion is not local in character and that the movement occures in all parts of the river bed at the same time. Many experiments were conducted to develop and solve this problem. The Shields diagram is widely accepted as the equation $f_m = \tau_c / (\gamma - \gamma_s) d_m$. On the basis of it we do not exactly know how actually the Shields curve corresponds to the various grain size distribution curve. Recently, efforts have been directed towards the analysis of the behaviour of granular mixtures. In Poland, in some mountain rivers the radioactive traser method was adopted for measuring incipient motion of bed load (Bartnik 89). According to Egiazaroff in nonheterogenious material stability of grain size parameter increases when the grain size decreases as far as mean diameter is concerned. In Polish mountain rivers, i.e. for calculations of bed load transport, Meyer- Peter-Muller formula is most suitable (Gladki 81).

$$\gamma_s h J = k_i (\gamma_s - \gamma)\, d_i + 0.25 (\gamma/g)^{0.33} q_i^{0.66}$$

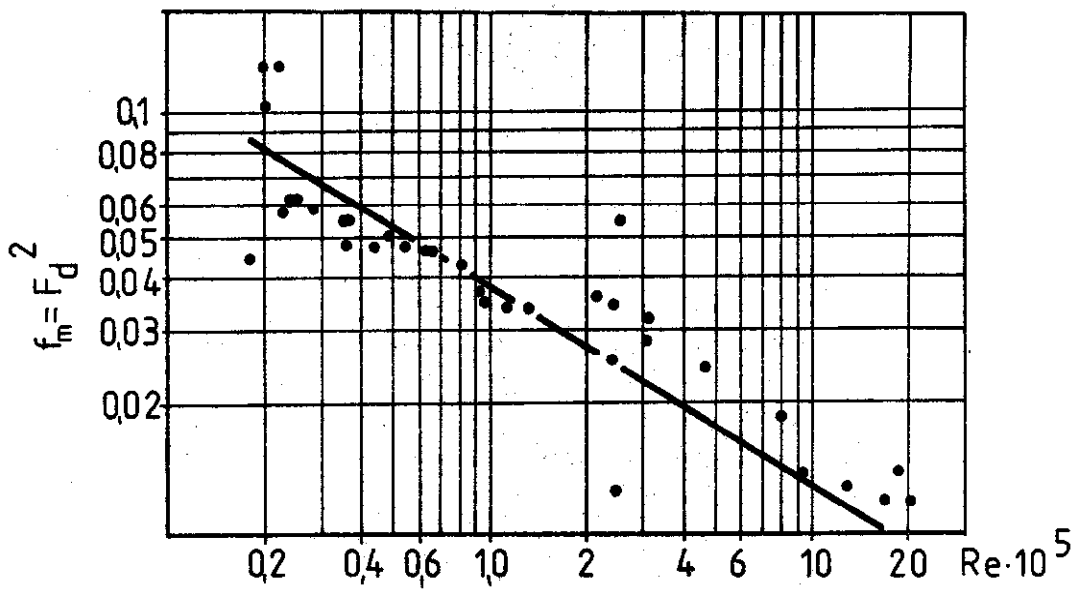

Fig.1.Relation between F_d and Re

FIG. 2 GRAIN SIZE DISTRIBUTION SIZE

The Targaniczanka river c.1.

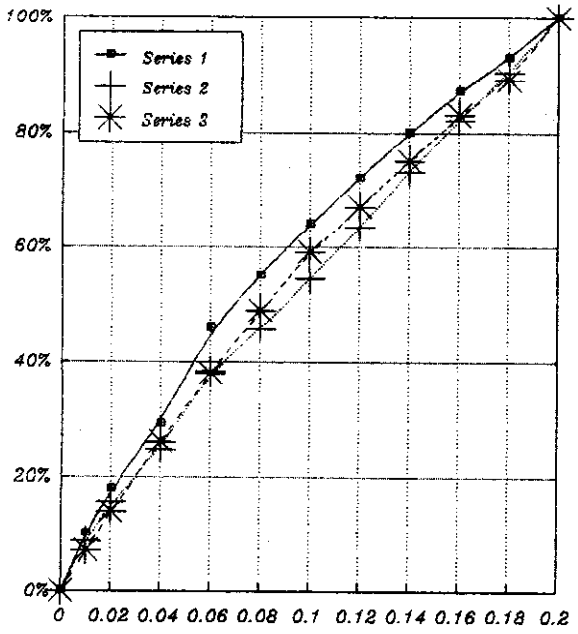

Series 1–before flood Series 2–prognosis
Series 3–after flood

The Targaniczanka river c.2.

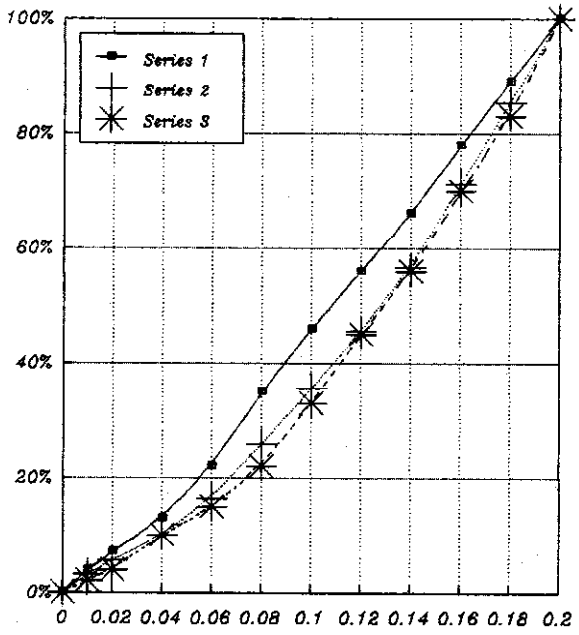

Series 1–before flood Series 2–prognosis
Series 3–after flood

The Targaniczanka river c.3.

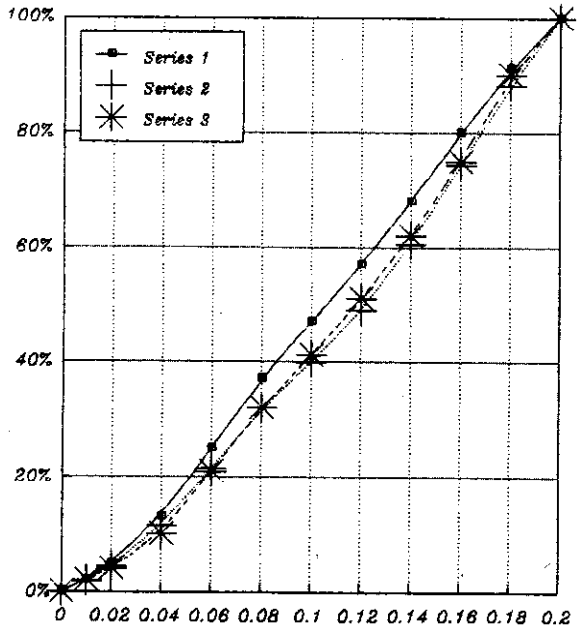

Series 1–before flood Series 2–prognosis
Series 3–after flood

The Targaniczanka river c.4.

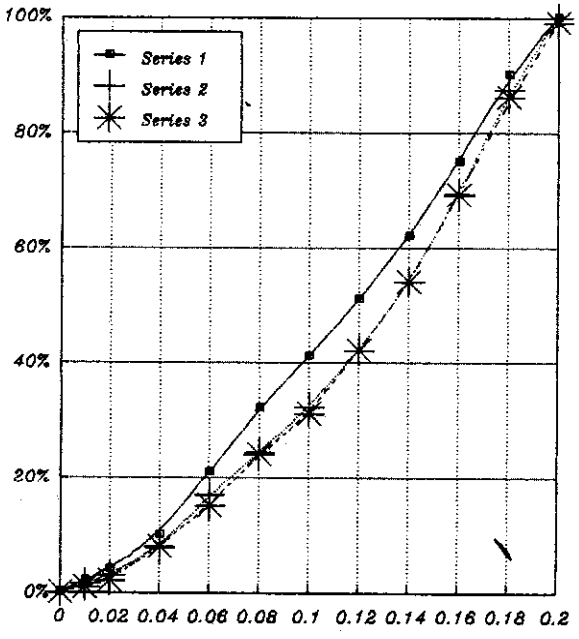

Series 1–before flood Series 2–prognosis
Series 3–after flood

where critical shear stress was calculated according to Wang

$$\tau_c = k_i (\gamma_s - \gamma) d_i \qquad \text{where}$$

$$k_i = \frac{f_m}{1.78 \, (d_i / d_m)^{0.947}} \qquad \text{for } d_i / d_m < 0.4 \quad \text{and}$$

$$k_i = \frac{f_m}{(d_i / d_m)^{0.314}} \qquad \text{for } d_i / d_m > 0.4$$

Armouring Layer Method

Because radioactive tracer method is very expensive in research, the stability parameter of bed f_m was determined on the basis of natural armouring layer, when standart deviation of mixture σ >1.3. The armour coat grain size distribution is given by Komura on a finite form of Gesslers equation (Simons77). The size curve was measured before and after flood (Fig.2).
In this case, a comparison of the curve size distribution after flood with the curve calculation according to the equation of Komura, was received with great accurancy for critical bed sher stress, where Shields parameter was f_m=0.023-0.075 for d_m. On its base f_m was determined as a function of standard deviation of mixture diameters (Fig.3).

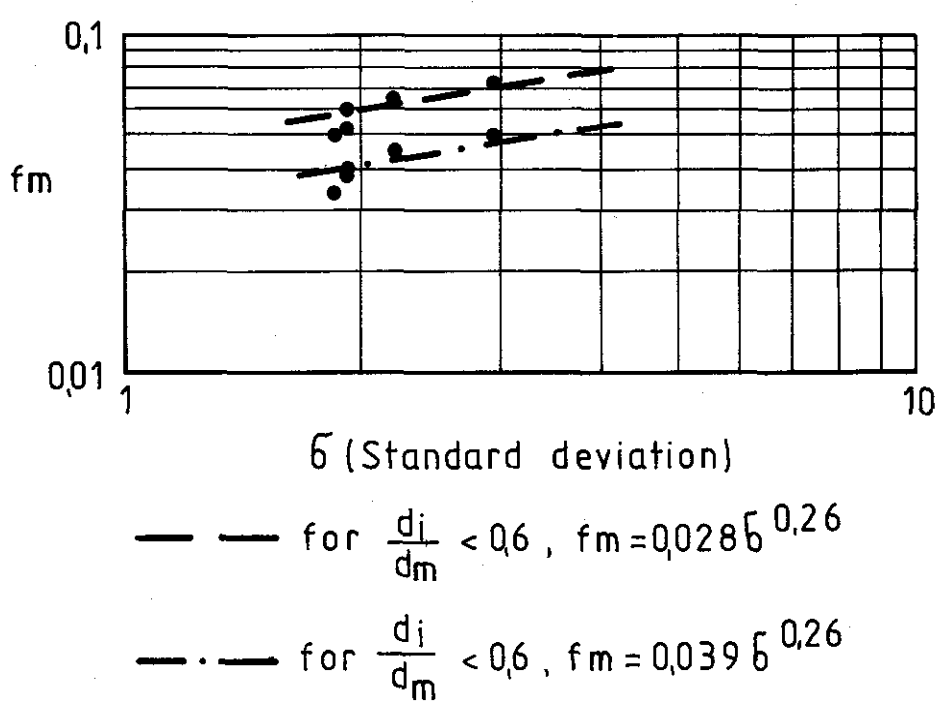

Fig.3. f_m vs. standard deviation σ

CONCLUSIONS

In the river beds composed of coarse materials the determination of the critical conditions using only one parameter is rather indefinite.There was no definite method to determine this phenomenon when the standart deviation of mixture diameters was high .The authors' opinions are that Shields curve is not sufficient to describe the beginning of bed load transport. Because movement influences much less shear stresses than it comes from the curve of Shields, to obtain a correct answer in this paper, the parameter of bed stability was determined as a function of standart deviation.

List of symbols

di	*-fraction diameter*
dm	*-typical grain size of mixture*
fm	*-parameter of bed stability for dm*
g	*-acceleration due to gravity*
ki	*-parameter of grain size stability*
Fd	*-Froude number for particles*
Re	*-Reynolds number for flow*
δ	*-standard deviation of mixture diameters* $(d_{84}/d_{16})^{1/2}$
γ_s	*- spesific weight of the grain*
γ	*-spesific weight of fluid*
τ_c	*-critical shear stress*

REFERENCE:

BARTNIK W. (1989) Determination of the Critical Conditions of Incipient Motion of Bed Load in Mountain Rivers.Workshop on Fluvial Hydraulics of Mountain Regions Trent, Italy.

GŁADKI H.,MICHALIK AL.,BARTNIK W. (1981) Measurement Bed Load Transport in Mountain Streams. IAHR WORKSHOP,Rappersville.

SIMONS B.,SENTURK F. (1977) Sediment Transport Technology, Colorado USA.

SHEN W. (1976) River Machanics USA.

POSTFIRE SUSPENDED SEDIMENT IN YELLOWSTONE PARK

By Jana Mohrman, Refuge Hydrologist, U.S. Fish and Wildlife Service, Denver, Colorado, and Roy Ewing, Research Scientist, National Park Service, Yellowstone National Park, Wyoming.

ABSTRACT

Prefire suspended-sediment transport in the Northern Yellowstone River Basin was documented in a study from 1985 through 1987. In the spring of 1989 the sediment study was reactivated to measure the effects of Yellowstone National Park's wildfires of 1988. Results of 1989 and 1990's snowmelt runoff are compared to prefire suspended-sediment conditions. Regional precipitation is presented for two pre- and post-fire years. The prefire year of 1986 had the highest runoff and sediment transport conditions of all years examined. From a preliminary analysis there were no major changes in sediment loading of Yellowstone Rivers as a result of the 1988 fires.

INTRODUCTION

During the summer of 1988 approximately 45% (400,000 ha) of Yellowstone National Park (YNP) was burned as a result of severe drought, high wind speeds and an abundance of fuels (Schullery, 1989). Heavy burning of watersheds may result in higher peak discharges, and accelerated erosion and sedimentation. Depending on factors such as fire intensity, slope steepness, and soil characteristics, erosional processes may vary from subtle sheet erosion to catastrophic debris flows. The maximum impact of these processes could occur in the first few years (White and Wells, 1981) or during several decades (Laid and Harvey, 1968).

In 1985 and 1986, an interagency study was conducted to determine baseline suspended sediment and turbidity conditions of the Yellowstone River and major tributaries from Yellowstone Lake Outlet, YNP, to Livingston, Montana. In 1989 and 1990 the same study (less several sites outside YNP) was repeated to investigate the impact of the wildfires of 1988. This report is a preliminary, abbreviated summary of the sediment study which is still being conducted in Yellowstone National Park.

METHODS

The suspended sediment data presented here was collected from two daily suspended-sediment stations, Yellowstone River at Corwin Springs, Montana (7 miles northwest of YNP's north entrance), and Lamar River at Tower Junction, YNP, Wyoming (28.25 river miles upstream from Corwin Springs). Sampling was done with a mounted depth-integrated sampler (D-49). Instantaneous suspended sediment and turbidity data was also collected at many other sites, but has not been thoroughly analyzed (Figure 1). Corwin Springs has had a U.S. Geological Survey (USGS) continuous-stream gage in operation since 1910. A USGS continuous gage was in operation on the Lamar River from

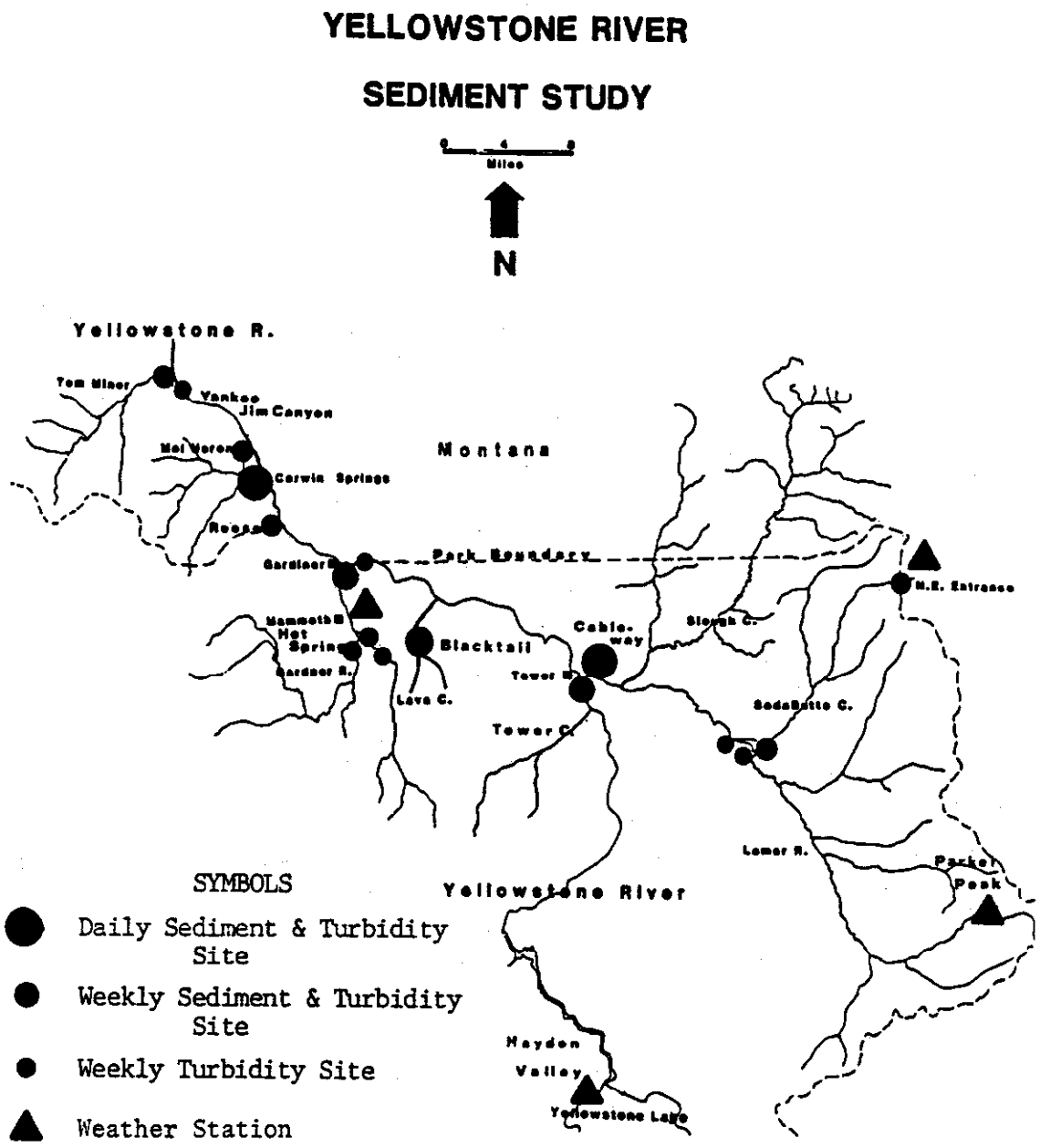

Figure 1. Postfire sample sites on the Yellowstone River and selected tributary watersheds for the Yellowstone River Suspended Sediment Study.

1923 to 1969. The prefire data were collected at the Lamar River using a USGS crest-stage and staff gage. Just after the fires a USGS continuous gage was again installed on the Lamar River. On Figure 1 the Lamar River site is labeled "cable way". Suspended-sediment concentrations were analyzed by the USGS, Water Resource Division lab in Helena, Montana

This report examines only the snowmelt period, or the rising limb of the annual hydrograph. This includes the first warming trend of each season, generally April through the beginning of June. In this report the rising limb of the hydrograph ends on the day of mean daily peak flow. Prefire years include 1985 and 1986 at both sites and 1987 was included at the Corwin Springs site since the data were available. Postfire data includes 1989 and 1990 for both sites.

RESULTS

Precipitation strongly influences trends in runoff and sediment transport. Seasonal precipitation at four weather stations in the study area (Figure 1) for water years 1985, 1986, 1989 and 1990 are presented in Table 1. Even though 1989 ranks the highest in precipitation during the study period, 1986 had the highest peak spring runoff due to unseasonably warm temperatures for two consecutive weeks in May (Table 2).

Table 1. Seasonal precipitation in inches at four weather stations in the study area.*

	Snowpack and Snowmelt Period October - June			
	1985	1986	1989	1990
Mammoth Hot Springs,YNP	7.89	9.70	12.41	10.81
Northeast Entrance, MT	14.30	18.70	20.40	19.80
Parker Peak, YNP	20.50	26.90	28.50	24.70
Lake Yellowstone, YNP	11.89	20.04	15.66	11.73
Study Area Averages	13.64	18.83	19.24	16.76

* Data is presented from water years, collected at Soil Conservation Service's Snow Survey pillow sites, and National Weather Service Climatological sites.

Table 2 presents the instantaneous mean and peak flow, and suspended-sediment concentrations for both sites. In 1986 at the Corwin Springs site, the instantaneous mean flow was less than in 1989, yet the instantaneous mean and peak suspended-sediment concentrations were larger. The standard deviation for both years for flow data was large, however, the peak flow for 1986 was 1.48 times as great as the peak flow for 1989. This is most likely the reason for the difference in sediment concentrations. The mean concentration in 1986 was 1.40 times greater than in 1989, while the peak concentration in 1986 was 2.55 times greater than in 1989. The rapid runoff and high peak flow in 1986 tended to overshadow any effects on suspended-sediment transport caused by the fires.

Lamar River at Tower Junction's instantaneous mean flows are very similar for 1985, 1986, and 1990. Yet, the sampled peak flow of 1986 is 1.4 times greater than both 1989 and 1990. There is even a greater difference in suspended-sediment concentration between those years. The 1986 mean concentration for snowmelt runoff is 1.95 times greater than both 1989 and 1990. The instantaneous peak concentration in 1986 is 2.22 and 1.54 times greater than 1989 and 1990. Again, the rapid runoff in 1986 tends to mask any effects of the fires.

Table 2. Instantaneous mean* and peak flow, and instantaneous mean, and peak suspended-sediment concentration of the rising limb data for Yellowstone River at Corwin Springs, MT, and Lamar River at Tower Junction, YNP, WY.

	FLOW (cfs)	STANDARD DEVIATION (cfs)	PEAK (cfs)	CONCENT-RATION (mg/l)	STANDARD DEVIATION (mg/l)	PEAK (mg/l)
Yellowstone River, Corwin Springs, MT						
1985	7578	(2674)	14660	164	(159)	677
1986	6953	(6573)	22290	203	(317)	2013
1987	3917	(2117)	7651	53	(50)	193
1989	6966	(4306)	14960	145	(170)	855
1990	4535	(2548)	13400	100	(132)	787
Lamar River, Tower Junction, YNP, WY						
1985	3412	(1364)	6120	160	(128)	463
1986	3323	(3163)	9630	249	(319)	1020
1989	2474	(1547)	6571	128	(128)	459
1990	3260	(1258)	6748	127	(141)	662

* Instantaneous mean flow presented here is the average of the flows at the time of sediment collection.

Figure 2 presents sediment rating curves for the Yellowstone River at Corwin Springs. These curves are least squares regressions of log-transformed values and are of the form $Y = aQ^b$, where Y = sediment concentration (mg/l) and Q = discharge (cfs). In 1988, 30.3% of the drainage area at the Yellowstone River at Corwin Springs burned, or 490 square miles of the 1617 total square miles. Upon examination of the pre- and post-fire sediment rating curves it appears that mean sediment concentrations decreased following the fire. Using the analysis of covariance, the slopes of the lines are significantly different at a .005 level of confidence. (Ponce, 1980). The near-flood runoff of 1986 resulted in exponentially higher sediment concentrations, which probably had the greatest impact on the slope of the prefire line. The slope of the postfire regression line approaches 1, indicating that the relationship between flow and sediment concentration is almost linear. It appears that more sediment is available for transport at lower flows than previously, and that the fire may have changed the relationship between discharge and sediment transport. Further monitoring would indicate the duration of this possible change.

FIG. 2 YELLOWSTONE RIVER, CORWIN SPRINGS, MT
SNOWMELT RUNOFF

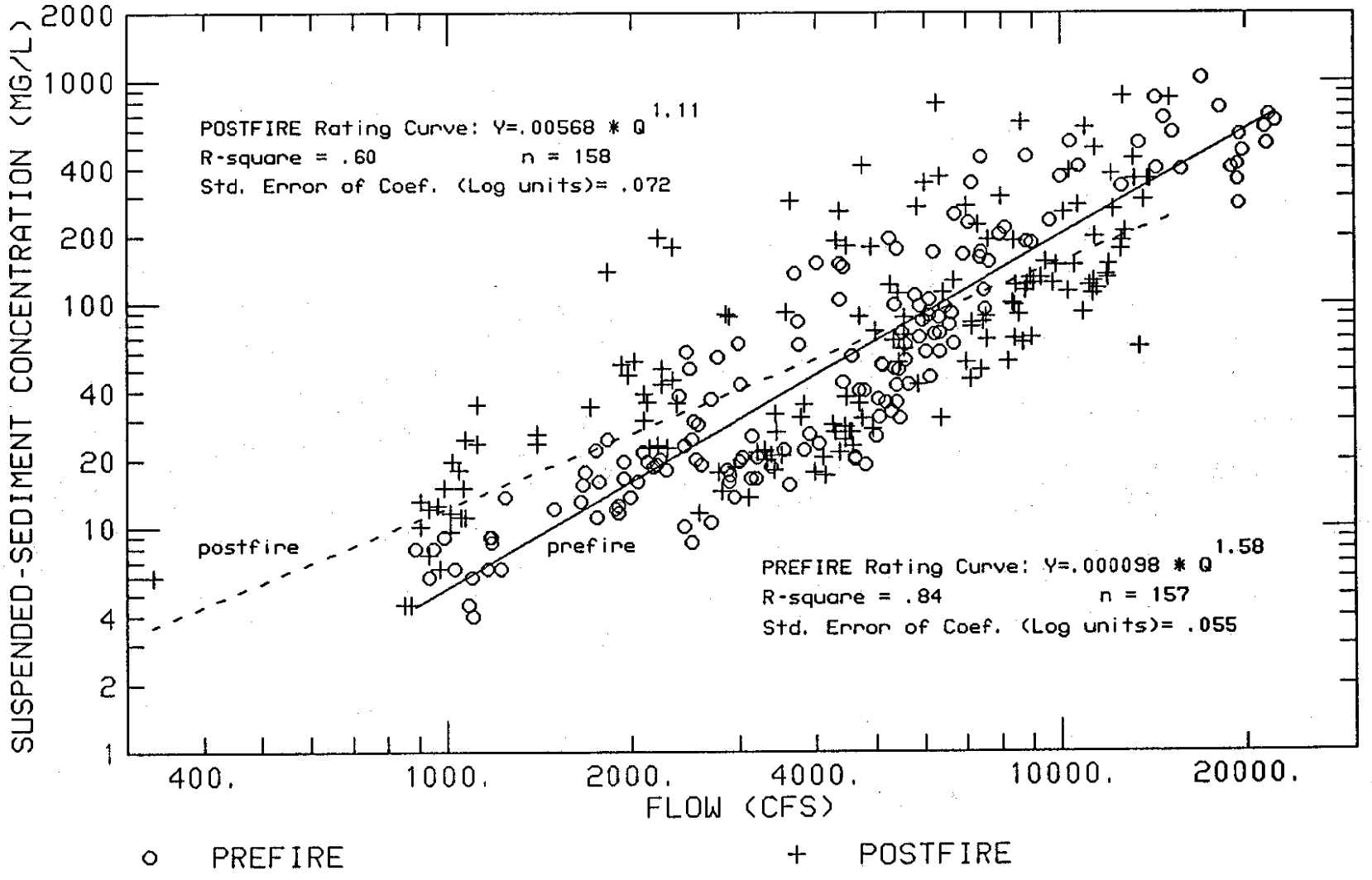

Figure 3 presents sediment rating curves for the Lamar River of the same form as presented in Figure 2. The Park's wildfires burned 38.3% of the drainage area at the Lamar River at Tower Junction, or 256 square miles of the 660 total square miles. The pre- and postfire rating curves are not significantly different at the .005 confidence level. The Lamar River drainage has a large percentage of steep erodible terrain (Ewing, 1988); these factors still seem to be the overriding control in sediment concentration at this site.

The data is widely scattered about the regression lines, but ranges of the coefficient of determination (r^2) between 0.60 and 0.85 are acceptable for water quality data (Ponce, 1985). The coefficients of determination for regression equations developed using prefire data were higher (greater that or equal to 0.84) than those developed using postfire data (less than or equal to 0.64) for both the Lamar and Yellowstone River sites. Sediment concentrations after the fire are more variable and less strongly related to discharge. Changes in vegetative cover would result in changes in both sediment availability, delivery, and surface runoff characteristics. Such changes could increase the variability evident in the postfire data.

The 1985 paper, "The Use of Suspended Sediment Load Measurements and Equations for Evaluation of Sediment Yield in the West", by Elliott Flaxman, contained a discussion of the exponent in log sediment concentration versus log discharge equations. He generalized that exponents ranging from 1.4 to 1.5 were characteristic of snowmelt dominated watersheds with a uniform response to runoff. Three of the four exponents, including both regressions for the Lamar River, have exponents greater than 1.5. However, the postfire regression exponent for the Corwin Springs site is 1.11. Flaxman contends that exponents ranging from 1.0 to 1.1 are indicative of watersheds where sediment concentrations rise in direct response to increases in flow. Such water sheds may be exposed to frequent and intense storms, or may have a greater availability of sediment at low flows due to exposed slopes or in-channel sources. The fire may have increased sediment availability at the Corwin Springs site, resulting in the change of slope of the regression line.

CONCLUSIONS

The data collected during this study cannot be used to reach any final conclusions about fires effects on sediment concentrations in the rivers draining Yellowstone National Park. Additional years of data, which hopefully will include peak flows comparable to 1986, will provide a better understanding of the effect of fires on suspended-sediment concentrations. However, it appears from the preliminary analysis presented here that there has been no major change in the sediment loading of Yellowstone Rivers as a result of the 1988 fires.

FIG. 3 LAMAR RIVER, TOWER JUNCTION, YNP, WY
SNOWMELT RUNOFF

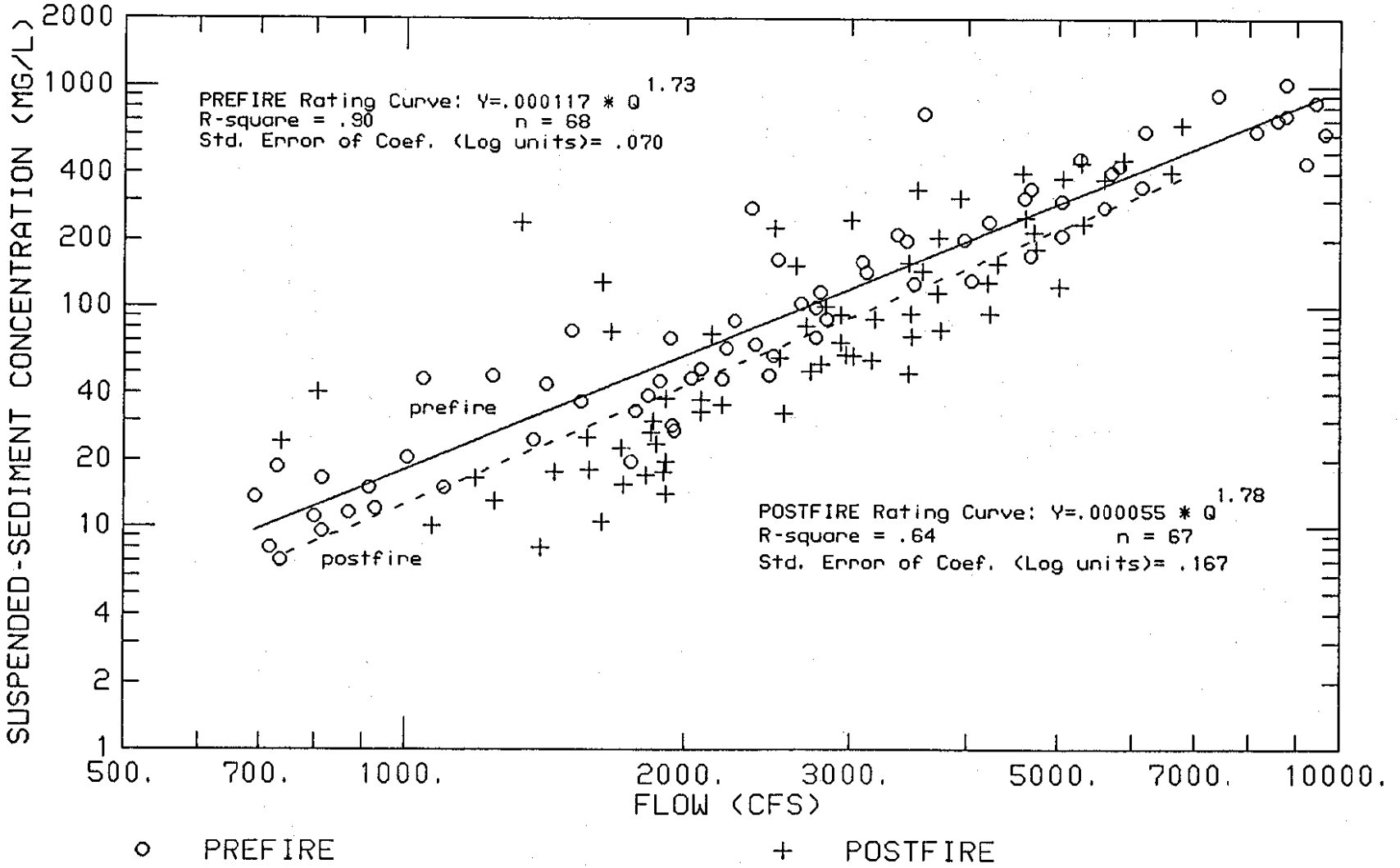

ACKNOWLEGEMENTS

We would like to acknowledge many organizatons (and special people) that through their funding and consultation made this research possible: U.S.Geological Survey, Water Resources Division, Helena, Montana; the Livingston Chapter of Trout Unlimited; Montana Fish, Wildlife, and Parks; Montana Water Quality Bureau; Park County, Conservation District; U.S. Soil Conservation Service, Snow Survey; Gallatin National Forest Service; U.S. Fish and Wildlife Service; and the National Park Service. Special thanks to Colleen Jorgensen for statistical interpretations, Megan Estep-Johnston, Mark Butler, and Robert Green, hydrologists with the U.S. Fish and Wildlife Service, Region 6, Denver Colorado, for technical and editorial advice.

REFERENCES

Ewing, R.E., and Mohrman, J.L., 1988 Suspended sediment and turbidity from Northern Yellowstone Park, Wyoming, 1985-1987. National AWRA 1988 Symposium Proceedings on Headwater Hydrology. 213-222.

Flaxman, E.M., 1975, The use of suspended-sediment load measurements and equations for evaluation of sediment yield in the West. Present and Prospective Technology for predicting Sediment Yields and Sources. Proceedings of the Sediment Yield Workshop, USDA Sedimentation Laboratory, Oxford, Mississippi. ARS-S-40. 46-56.

Laird, J.R., and Harvey, M.D., 1986, Complex response of chapparal drainage basin to fire. Drainage Basin Sediment Delivery. 165-184.

Ponce, S.L., 1980, Statistical methods commonly used in water quality data analysis WSDG Technical Paper WSDG-TP-00001. 51 pages.

Ponce, S.L., and Flug, M., 1985, The use of the paired basin technique for monitoring flow-related water quality trends in upland recreation areas. Westfornet Monthly Alert April Edition. Item #38, 15-31.

Schullery, P., 1989, The fires and fire policy. Bioscience. 39, 686-694.

White, W.D., and Wells S.G., 1981, Geomorphic effects of La Mesa fire. La Mesa Fire Symposium. Los Almos National Laboratory LA-9236-NERP. 73-90.

MOVEMENT OF BED MATERIAL CLASTS IN MOUNTAIN STREAMS

BY
Luna B. Leopold, Professor Emeritus
University of California, Berkeley, CA
David C. Rosgen, Consulting Hydrologist
Pagosa Springs, CO

ABSTRACT

The growth in observational data shows that it generally is true in gravel streams that the material on the immediate surface is coarser than that which lies below. Unfortunately, this has led to the use of the word armored or paved. The use of those words has given the impression to those who do not work directly with gravel bed streams that the bed material of the stream does not move with ordinary discharges.

In nine mountain streams in Colorado rocks chosen from the bed surface to represent sizes D_{35}, D_{50}, and D_{84} were collected, painted, and placed in straight lines across the channel. A total of 30 such lines comprising 769 rocks ranging in size from 39 mm to 250 mm were observed during the snowmelt runoff season of 1989. Stream discharge, depth, velocity, and water surface slope data were collected on a daily basis throughout the runoff period.

Of the total rocks placed, about 65% of all the rocks moved during the season, even though discharges in none of the streams reached the bankfull stage. The distance the rocks moved was relatively small during any one movement, generally less than a few meters. Some individual rocks moved more than once, and a few moved as many as four times during the season.

These observations represent one type of evidence that material of the bed surface moves at discharges equal to or less than bankfull, even though the movement is for a short distance and the resultant transport rate is small.

GENERAL STATEMENT

Field data show that the surface material comprising the bed of gravel rivers is coarser than the layer immediately below the surface. An early presentation of such data was in Leopold, Wolman, and Miller (1964) that also included a discussion of possible explanations. They have developed in the literature two terms to describe the phenomenon, "armoring" and "paving," both of which unfortunately leave the impression that this surface layer is immobile except in extreme flood events.

Bray and Church (1980) suggested definitions for these words. They used "armour" to describe surface layers coarser than the rest of the bed resulting from winnowing of the fines. The word "pavement" was used to describe the surface layer coarser than the material below that layer, and the movement of this pavement occurred only during extreme floods. We prefer the words "cover layer" suggested by Carson and Griffiths (1987) to describe the physical relation without inference as to origin or frequency of movement. Also in agreement with a recommendation by Carson and Griffiths (p. 60), the present paper is devoted to a description of how bed material moves and under what circumstances.

ORIGIN AND PURPOSE OF THE EXPERIMENT

Our field measurements have demonstrated that in gravel streams in the Rocky Mountains the bulk or greatest volume of the bedload is of sand size or very fine gravel, far smaller than the D_{50} of the bed material. The gravel to cobble size makes up the point bars, central bars, and the riffle reaches, yet constitutes only a minute fraction of the total bedload. In fact, this minute portion of total load forms the main morphologic features of gravel streams (Leopold, 1990).

The gravel clasts 32 to 90 mm or larger are seldom caught in a Helley-Smith sampler, partly because of the size of the sampler mouth but partly because they move infrequently. To obtain more information on the discharge needed for motion and to measure the distance moved in a single excursion, the following procedure was used. Nine gravel streams of various stream types were chosen in Colorado for detailed study during the snowmelt seasons of 1988 and 1989. At each stream measuring section, size distribution of the surface material of the bed was determined by pebble counting. Then from the streambed downstream of the study reaches, many rocks were collected of each of the sizes D_{84}, D_{50}, and D_{35}. These rocks were painted bright orange. At each stream two lines of painted rocks were placed by hand in the channel, a line of rocks D_{84} size and a line of D_{50} size. In four of the nine streams there was also a line of D_{35} size. The rocks on a line were placed at about 4 diameters apart, so there were more rocks in a D_{50} line than in a D_{84} line. The location in distance across the channel was recorded for each rock placed.

Every day during the runoff season, about May 20-July 30, each line was inspected. The downstream and/or lateral movement of any rock was measured daily. At each position where a rock moved, a measurement by current meter of the vertical distribution of velocity was obtained. Discharge of the river was recorded.

The design has the possible disadvantage that placement of a rock in the water by hand might result in the rock being on a spot somewhat above the general level of the adjoining rocks of the bed materials. However, because the number of rocks placed was large, 769 rocks, we felt that there was also the possibility that our hand-placed rocks were put in hollows or depressions. Therefore, on the average, the placed rocks were only slightly more exposed or more likely to move than those deposited by flowing water.

ROCK SIZES AND NUMBER MOVED

The D_{84} size ranged from 77 mm at Goose Creek #4 to 250 mm at Goose Creek #1. At the other sites the size was between 100 and 200 mm. The D_{50} sizes varied from 43 mm to 110 mm. Table 1 shows the number of rocks, their sizes, and the number that moved. The table includes some of the characteristics of each site, including bankfull discharge and channel slope.

There were 769 rocks placed, and of these, there were 500 movements. The percentage of placed rocks that moved varied from 57% to 69%, and interestingly, the D_{84} size had about the same percentage moved as did the smaller D_{35} size.

Bedload transport rate was measured nearly every day at each site. Every time a Helley-Smith sample was taken, the largest clast caught was recorded as well as the usual size distribution analyzed in the laboratory. Note that during the runoff season the sampler caught one rock of size either near the D_{50} but in some cases nearly as large as D_{84}. In some streams an HS sampler with a large mouth was used.

RELATION OF ROCK MOVEMENT TO DISCHARGE

The most significant result of the study was that the D_{84} size on the streambed was consistently moved by discharges far less than bankfull. Because bankfull in the streams has a recurrence interval of one to two years, as is usual for most streams, the coarse fraction of the bed material is moved by frequently occurring discharges. This confirms the results found by Andrews (1983) for other gravel bed rivers in the mountains.

Table 2 shows the number of rocks in the D_{84} rock lines moved by various discharges, the latter expressed as percentage of bankfull discharge. The table includes all D_{84} rock movements at five stream sites. At these sites the total number of rocks placed in D_{84} lines was 168, and the number of recorded movements was 137 in the 1989 runoff season. Note that 114 out of 137 movements were caused by discharges less than 80% bankfull. Twenty-three movements occurred in two days when the discharge of S. Fork Cache la Poudre was 84% of bankfull.

ROCKS THAT MOVED MORE THAN ONCE

There is concern that placement of rocks by hand might favor movement as compared with rocks coming to rest having been moved by water. Many rocks moved more than once. Table 3 presents data for three streams in which individual rocks were observed to move once or more than once.

The stream, S. Fork Cache la Poudre, had more D_{84} rocks moved more than once than the other sites for reasons unknown. The rock movement data appear to confirm the concept that rocks placed on the streambed by hand are, on the average, a reasonable sample of the rocks moved by flowing water from locations determined only by stream processes.

It should be obvious that the data in Tables 2, 3, and 4 deal with the D_{84} size because these rocks are among the largest clasts on the streambed. Rocks of smaller size are more likely to move.

DISTANCE MOVED BY INDIVIDUAL ROCKS

Though a large percentage of painted rocks placed on the streambed moved during the runoff season as indicated in Tables 1-3, the distance a rock moved in an individual excursion was surprisingly short. Table 4 records the average distance moved in a single hop or single excursion. These distances averaged less than two feet, regardless of the magnitude of the discharge that caused movement.

SUMMARY

Painted rocks placed in lines on the bed of gravel streams in the mountains of Colorado included three sizes, the sizes D_{84}, D_{50}, and D_{35} of the bed materials of the individual stream. Sixty-five percent of the largest rocks placed, the D_{84} size, moved during the runoff season of 1989. None of the nine streams reached bankfull discharge during that year. Therefore, the larger fraction of bed material on these streams moved at discharges less than bankfull. The distance moved was very small, only a few feet. Thus the transport rate of the larger clasts is very small.

The larger rocks of the bed material are plucked individually off the streambed and moved short distances at ordinary or frequent discharges. Not all rocks of a given size are moved, even when some of that size are moved.

The material on the bed of a gravel stream constitutes only a small part of the annual bedload volume, but it is the part of the sediment load responsible for the major morphologic features of the channel, the riffles, the bars, and the point bars.

ACKNOWLEDGMENT

The authors gratefully recognize the fine observations and measurements obtained by the numerous field personnel of the USDA Forest Service of the Rocky Mountain Region who participated in this study.

REFERENCES

Andrews, E. D., 1983, Entrainment of gravel from naturally sorted riverbed material: Bull. Geol. Soc. Amer., vol. 94, pp. 1225-1231.

Bray, D. I., and Church, M., 1982, Armoured versus paved gravel-beds: Jour. Hydr. Div. Amer. Soc. Civil Engineers, vol. 108, pp. 7727-7728.

Carson, M. A., and Griffiths, G. A., 1987, Bedload transport in gravel channels: Jour. Hydrology (New Zealand), vol. 26, No. 1, 151 pp.

Leopold, Luna B., 1990, The sediment size that determines channel morphology: Gravel Streams Conference, Florence, Italy, September, in press.

Authors cited in text (in order):
- Leopold, Wolman, and Miller (1964)
- Bray and Church (1980)
- Carson and Griffiths (1987)
- Leopold (1990)
- Andrews (1983)

Table 1. Painted rocks of three sizes, in several streams, Colorado, 1989

Stream	Left Hand	S. Fork Cache la Poudre	Upper Trap	Little Beaver	Goose #1	Goose #2	Goose #3	Goose #4	Middle Boulder
Drainage area (mi^2)	52	88	--	12	81	81	81	81	36
Bankfull discharge (cfs)	175	325	156	46	240	240	240	240	340
Slope	.035	.007	.06	.026	.012	.007	.005	.005	.013
Largest clast caught in HS sampler (mm)	113	43	136	45	30	81	--	41	98
D_{35}									
Size (mm)	42			39	70				57
No. rocks	51			52	35				64
No. movements	45			8	13				49
D_{50}									
Size (mm)	58	60	60	56	110	92	70	43	83
No. rocks	44	74	13	49	28	30	53	No data	71
No. movements	38	99	No data	6	8	14	15	No data	54
D_{84}									
Size (mm)	122	111	144	128	250	150	100	77	174
No. rocks	24	64	8	19	8	10	32	41	20
No. movements	21	84	No data	10	2	2	10	13	9

Total all sites:		% of rocks moved
D_{35}		
No. rocks	202	
No. movements	115	57
D_{50}		
No. rocks	349	
No. movements	234	67
D_{84}		
No. rocks	218	
No. movements	151	69
Total rocks placed	769	
Total rock movements	500	65

Table 2. Number of rocks of D_{84} size moved at discharges of different percentages of bankfull; data are for five sites that had a total of 168 rocks in the D_{84} lines.

Discharge in % of bankfull	Number of rocks moved
10-20	11
20-40	26
40-60	42
60-80	35
80-100	23
	137

Table 3. Number of rocks that moved once or more during runoff season, D_{84} size.

Stream	S. Fork, Cache la Poudre	Little Beaver	Left Hand
Number of D_{84} rocks placed	64	19	24
Number that did not move	16	14	0
Moved once	22	2	24
Moved twice	17	2	0
Moved thrice	7	0	0
Moved four times	2	1	0

Table 4. Distance in feet rocks of D_{84} size moved by discharges of various percentages of bankfull; data from five sites; total number of movements was 137.

Discharge in % of bankfull	Average distance of movement (ft)	Number of rocks moved out of observed reach
10-20	0.6	--
20-40	1.2	--
40-60	1.7	13
60-80	1.1	--
80-100	0.6	3